ROLE OF THE CAMP-PKA PATHWAY ON ADHESION AND PATHOGENICITY IN THE HUMAN FUNGAL PATHOGEN *CANDIDA GLABRATA*

Bea Timmermans

Supervisor:
Prof. P. Van Dijck

Members of the Examination Committee:
Prof. I. Castaño
Prof. J.M. Thevelein
Prof. J. Winderickx
Prof. G. Vande Velde
Prof. L. Moons
Dr. G. Van Zeebroeck

Dissertation presented in partial fulfilment of the requirements for the degree of Doctor of Science: Biochemistry and Biotechnology

September 2021

© 2021 KU Leuven, Science, Engineering & Technology
Uitgegeven in eigen beheer, Bea Timmermans, Leuven

Alle rechten voorbehouden. Niets uit deze uitgave mag worden vermenigvuldigd en/of openbaar gemaakt worden door middel van druk, fotokopie, microfilm, elektronisch of op welke andere wijze ook zonder voorafgaandelijke schriftelijke toestemming van de uitgever.

All rights reserved. No part of the publication may be reproduced in any form by print, photoprint, microfilm, electronic or any other means without written permission from the publisher.

Acknowledgements

The road to this PhD, what a journey! This was not possible without the help and support of many people:

First, thank you Professor Patrick Van Dijck for giving me the opportunity to be part of the *Candida* lab. I could really appreciate you as my supervisor, being always interested in scientific topics and other topics. Thank you for all the valuable input, feedback and encouragement, but also for valuing a good work atmosphere in the lab and during the travels.

I would also like to thank the members of the examination committee Prof. Irene Castaño, Prof. Johan Thevelein, Prof. Joris Winderickx, Prof. Greetje Vande Velde, Prof. Lieve Moons and Dr. Griet Van Zeebroeck for their critical reading, comments and contributions to improve the work of my PhD. Griet, thank you for introducing me into the world of yeasts and guidance during my master thesis. Because of this experience, I wanted to continue microbiology research.

Furthermore, I would like to thank all the technicians for their excellent lab support and help during experiments. Leni and Hilde, thank you for always helping with all technical issues and organizing the lab retreats! Special thanks to Nico for solving IT and printer issues, but also to be willing to listen when things didn't work like they should.

I would like to thank all present and former colleagues of the *Candida* lab, it has been a pleasure to work here! Also, I really enjoyed the efforts of being a group, going to Alma, kayaking, hiking or the *Candida* weekend. It was also very nice to be part of the MCB lab where so many cultures perfectly mixed in together, this is unique! I also want to show my appreciation to all students I have been guiding in these years.

Special thanks to all office mates! We were a mix of many people, but this place was always a nice environment for all kinds of (scientific/mom) topics.
Therefore, I should mention my fellow coffee drinkers Annelies and Stephen, Mieke and Stefanie and my neighbor-classmate-colleague-friend Winnie. You were all closely involved in my research, thanks for all input and support!

Graag wil ik mijn familie en vrienden bedanken om het leven buiten het labo zo aangenaam te maken. Ook ben ik heel dankbaar om in het fijne gezin van de Geeraerts-en te zijn beland! Bedankt om altijd klaar staan voor ons gezin, oma & opa, tantje Lies en nonkel Brecht!

Dikke merci mama/moeke en papa/bompa. Hoewel Leuven o-zo-ver-weg is van Lanklaar, doen jullie toch alles gemakkelijk en evident lijken, terwijl dit zeker niet altijd het geval is.

Save the best for last! Emiel en mijn twee zijprojectjes Arno en Tias

… tot aan de ☾ en terug

Bea

Summary

Candida glabrata is a human fungal pathogen that easily forms biofilms on medical devices, such as catheters and implants. These biofilms are difficult to treat, which often results in the necessity to physically remove the implant from the patient. Furthermore, *C. glabrata* is an important cause of invasive infections associated with high mortality rates, as it becomes easily resistant to the current antifungal drugs. Pathogens continuously encounter stress during the infection process. For instance, inside the human body the availability of nutrients is limited and the immune system is trying to eliminate the infection. Therefore, it is crucial for the pathogen to quickly adapt to the changing environment.

C. glabrata senses extracellular glucose, fructose and sucrose which elicits a fast intracellular response through the cAMP-PKA signaling pathway. These carbohydrates are sensed by the Gpr1-Gpa2 receptor complex causing an intracellular cAMP increase. cAMP activates the protein kinase A (PKA) and this in turn affects several cellular properties among which growth, the stress resistance properties of cells, the mobilization of reserve carbohydrates and adhesion.

In this thesis, we further investigated how the *C. glabrata* cAMP-PKA pathway affects trehalase activity and adhesion to polystyrene. Firstly, we showed that the trehalase activity of glycerol-grown wild type *C. glabrata* cells was very high and this was caused by the acid trehalase Ath1. A strain expressing only the neutral trehalase Nth1 showed a low basal trehalase activity and the Nth1 trehalase acitivity was activated rapidly by the cAMP-PKA pathway, similar to the situation in *S. cerevisiae*.

Secondly, we investigated adherence as a downstream target of the cAMP-PKA pathway. Adhesion to surfaces is the first step in biofilm formation and therefore represents an important *C. glabrata* virulence factor. We showed that *C. glabrata* adhesion to polystyrene is low in presence of glucose, fructose or sucrose. We verified that this reduced adherence is caused by signaling through the cAMP-PKA pathway using different pathway mutants. Next, we investigated which adhesin(s) are downstream of the pathway by looking into the glucose-induced transcriptome of predicted adhesins. The deletion of CAGL0J00253g or *AED2* resulted in strains with a similar adherence in presence of glucose and galactose, indicating that these genes are probably targets of the cAMP-PKA pathway, which needs to be further investigated. We also showed that both lab strains as well as clinical isolates have the

lower adherence in presence of glucose. Therefore, further investigation of molecules activating the cAMP-PKA pathway are potentially interesting to treat *C. glabrata*.
We also looked into the *C. glabrata* transcriptome after addition of glucose or galactose. Analysis of the RNA sequencing data provided a general overview of how the cells respond to the addition of these sugars: glucose induced the machinery for cell growth and fermentation, while the expression of genes involved in stress resistance was lowered, similar to the situation in *S. cerevisiae*. Unexpectedly, while *C. glabrata* is not able to use galactose, this sugar still affected the expression of a substantial number of genes among which genes involved in central metabolism.
Finally, we characterized the three *C. glabrata* trehalases. We showed that the acid trehalase Ath1 is necessary to grow on trehalose as a carbon source and is present in the periplasm or cell wall of the cells. The neutral trehalase Nth1 is located in the cytoplasm and affects the stress properties of the cells. Finally, the trehalase deletion strains were tested in two *in vivo* models: in a mouse model of systemic infection, the deletion of the trehalases did not affect virulence. On the other hand, the triple trehalase deletion strain was unable to stably colonize the mouse gastrointestinal tract.

Samenvatting

Candida glabrata is een fungus die gemakkelijk biofilms op medische hulpmiddelen zoals katheters en implantaten vormt. Deze biofilms zijn moeilijk behandelbaar waardoor een operatieve verwijdering vaak de enige oplossing is. Verder is *C. glabrata* een belangrijke oorzaak van invasieve infecties met een aanzienlijke sterftegraad, doordat het snel resistent wordt tegen de huidige antifungale drugs. Tijdens het infectieproces ondervindt een pathogeen constante stress: in het lichaam zijn er weinig nutriënten beschikbaar, het immuunsysteem tracht de infectie te elimineren, etc. Hierdoor is het cruciaal dat de pathogeen zich snel aanpast aan zijn omgeving. In *C. glabrata* veroorzaakt bijvoorbeeld extracellulair glucose, fructose en sucrose een snelle cellulaire respons via de cAMP-PKA signaalweg. Deze suikers worden waargenomen via het Gpr1-Gpa2 receptor complex waarna intracellulair cAMP geproduceerd wordt. Dit activeert het proteïne kinase A (PKA) waardoor verschillende eigenschappen van de cel beïnvloed worden waaronder de celcyclus, stressresistentie, opslag van reservesuikers en adhesie.

In deze thesis hebben we verder onderzocht hoe de cAMP-PKA signaalweg de cellulaire eigenschappen van *C. glabrata* beïnvloedt. Ten eerste vonden we dat trehalase geactiveerd wordt door de signaalweg, hoewel trehalase activiteit al erg hoog was in wild type *C. glabrata* cellen die gegroeid werden in glycerol. We toonden aan dat dit veroorzaakt werd door een hoge trehalase activiteit van het zure trehalase Ath1. Een stam die enkel het neutrale trehalase Nth1 tot expressie brengt, vertoonde ook een snelle trehalase activatie door de cAMP-PKA signaalweg, vergelijkbaar met de situatie in *S. cerevisiae*.

Ten tweede werd adhesie als een target van de cAMP-PKA signaalweg onderzocht. Adhesie aan een oppervlak is de eerste stap in de vorming van biofilms en dus een belangrijke virulentiefactor voor *C. glabrata.* We toonden aan dat adhesie van *C. glabrata* aan polystyreen laag is in aanwezigheid van glucose, fructose of sucrose. We verifieerden dat dit een effect is van de cAMP-PKA signaalweg door verschillende mutaties in de signaalweg te gebruiken. Vervolgens onderzochten we het glucose geïnduceerde transcriptoom om zo de adhesines verantwoordelijk voor het fenotype te vinden. Wanneer CAGL0J00253g of *AED2* gedeleteerd werden, was adhesie in aanwezigheid van glucose en galactose vergelijkbaar. Dit suggereert dat deze genen mogelijke targets zijn van de cAMP-PKA signaalweg, wat verder onderzocht dient te

worden. Zowel labostammen als klinische isolaten vertoonden de lagere adhesie door glucose. Verder onderzoek naar moleculen die de cAMP-PKA signaalweg activeren kunnen daarom mogelijk interessant zijn om *C. glabrata* te behandelen.

Ook onderzochten we het *C. glabrata* transcriptoom na toevoegen van glucose of galactose aan de cellen. Uit de RNA sequencing analyse werd enerzijds een algemeen beeld geschetst hoe de cellen zich aanpassen aan de veranderende omgeving: als reactie op het toevoegen van glucose starten de cellen alle machinerie om te groeien, wordt fermentatie gestart en vermindert de cel de expressie van stress resistentiegenen. Hoewel *C. glabrata* galactose niet kan gebruiken om te groeien, beïnvloed deze suiker de expressie van een aanzienlijke hoeveelheid genen, waaronder genen van het centrale metabolisme.

Verder karakteriseerden we de drie *C. glabrata* trehalase enzymen. Het zure trehalase Ath1 is nodig is om op trehalose als koolstofbron te groeien en is aanwezig in het periplasma van de cellen. Het neutrale trehalase Nth1 is gelokaliseerd in het cytoplasma en beïnvloedt de stresseigenschappen van de cellen. Vervolgens gingen we na of de trehalase genen belangrijk zijn *in vivo*, voor zowel kolonisatie in het gastro-intestinaal systeem als bij een systemische infectie. Er was geen verschil in virulentie tussen de wild type en verschillende trehalase deletiestammen in een systemische infectie. Maar een deletiestam van alle drie trehalasen kon de darmflora van muizen niet stabiel koloniseren.

List of abbreviations

ABC	ATP binding cassette
ADP	Adenosine diphosphate
ALS	Agglutinin-like sequence
AmB	Amphotericin B
AMP	Adenosine monophosphate
ATP	Adenosine triphosphate
cAMP	3',5'-cyclic adenosine monophosphate
CGD	*Candida* genome database
CFU	Colony forming unit
CSH	Cell surface hydrophobicity
CWP	Cell wall protein
DE	Differential expression
DHAP	Dihydroxyacetone-phosphate
DHN	Dihydroxynaphtalene
DIC	Differential interference contrast
EPA	Epithelial adhesion
FC	Fold change
FGM	Fermentable growth medium
Flo	Flocculin
FRT	Flippase recognition target
Fru-1,6-BisP	Fructose-1,6-bisphosphate
Fru6P	Fructose-6-phosphate
GA3P	Glyceraldehyde-3-phosphate
GAP	GTPase-activating protein
GDP	Guanosine diphosphate
GI-tract	Gastrointestinal tract
GlcNAc	N-Acetylglucosamine
Glu6P	Glucose-6-phosphate
GO	Gene ontology
GOF	Gain of function
GPCR	G protein-coupled receptor
GPI	Glycosylphosphatidylinositol
GTP	Guanosine triphosphate
GUT	Gastrointestinally induced transition
HWP	Hyphal wall protein
IC	Invasive candidiasis
ICU	Intensive care unit
IGV	Integrated genomics viewer
ISC	Iron sulfur cluster
IVET	*In vivo* expression technology
KRH	Kelch repeat homolog

MAPK	Mitogen-activated protein kinase
MDR	Multidrug resistance
MF	Major facilitator
MTSEA	2-aminoethyl-methanethiosulphonate
NAT	Nourseothricin
NCAC species	Non-*Candida albicans Candida* species
NLS	Nuclear localization signal
OPC	Oropharyngeal candidiasis
ORF	Open reading frame
PAMP	Pathogen-associated molecular pattern
PBS	Phosphate buffered saline
PCR	Polymerase chain reaction
PKA	Protein kinase A
PRR	Pattern-recognition receptor
PS	Polysaccharide
PWP	PA14 containing wall proteins
ROS	Reactive oxygen species
RP	Ribosomal protein
SAM	S-adenosyl methionine
SC	Synthetic complete
SCAM	Substituted cysteine accessibility method
SdmYg	Semi-defined yeast growth
SEM	Standard error of mean
T6P	Trehalose-6-phosphate
TCA	Tricarboxylic acid
TMD	Transmembrane domain
TOR	Target of rapamycin
TR	Tandem repeat
UDP	Uridine diphosphate
UPGMA	Unweighted pair method with arithmetic mean
UTI	Urinary tract infection
VVC	Vulvovaginal candidiasis
YFP	Yellow fluorescent protein

For clarification, we denote genes or proteins from other species than *C. glabrata* with the initials of the organism:

Af *Aspergillus fumigatus*
Ca *Candida albicans*
Cp *Candida parapsilosis*
Ct *Candida tropicalis*
Cn *Cryptococcus neoformans*
Mo *Magnaporthe oryzae*
Sc *Saccharomyces cerevisiae*
Um *Ustilago maydis*

Table of contents

Acknowledgements i

Summary iii

Samenvatting v

List of abbreviations vii

Table of contents ix

Chapter 1: Literature overview 1

1.1 Introduction 3
1.2 The genus *Candida* 3
1.2.1 *Candida* infections 4
1.2.2 Epidemiology of *Candida* 7
1.2.3 Genome and phylogeny 9
1.2.4 Virulence factors 12
1.2.4.1 Morphological switching 12
1.2.4.2 Adhesion and biofilm formation 13
1.2.4.2.1. *Candida glabrata* adhesins 14
1.2.4.2.2. *Candida albicans* adhesins 23
1.2.4.3 Adaptation to host environment 24
1.2.4.4 Resistance against antifungal drugs 25
1.3 The cAMP-PKA pathway 29
1.3.1 *Saccharomyces cerevisiae* 29
1.3.1.1 The second messenger cAMP and the protein kinase A 30
1.3.1.2 Extracellular glucose sensing activates *Sc*Gpr1-*Sc*Gpa2 31
1.3.1.3 Intracellular glucose sensing activates *Sc*Ras 34
1.3.1.4 PKA targets 36
1.3.2 The cAMP-PKA pathway regulates virulence factors in other pathogenic fungi 39
1.4 Nutrient signaling 44
1.4.1 Glucose signaling 44
1.4.2 Connections with other nutrient sensing pathways 47

Chapter 2: The *C. glabrata* cAMP-PKA pathway affects trehalase activity and adhesion 49

2.1 Introduction 51
2.2 Results 52
2.2.1 *C. glabrata* protein kinase A is activated by cAMP 52
2.2.2 The neutral trehalase Nth1 is a target of the cAMP-PKA pathway 55
2.2.3 The cAMP-PKA pathway lowers adhesion to polystyrene 59
2.2.4 The adherence phenotype is present in different *C. glabrata* background strains 64
2.2.5 Adhesion to catheters is not affected by the cAMP-PKA pathway 64
2.2.6 Epa1, Epa6 and Epa7 do not represent the adhesins downstream of the cAMP-PKA pathway affecting adhesion to polystyrene 65

2.3 Discussion 66
2.4 Materials and methods 72

Chapter 3: The *C. glabrata* transcriptome in response to glucose and galactose 79
3.1 Introduction 81
3.2 Results 81
3.2.1 RNA sequencing conditions 81
3.2.2 General transcriptional response 84
3.2.3 The glucose transcriptional response 87
3.2.4 cAMP-PKA pathway specific transcriptional response 91
3.2.5 The adhesin transcriptional response 93
3.2.6 Elucidation of adhesin(s) controlled by the cAMP-PKA pathway affecting adhesion to polystyrene 96
3.2.7 The galactose transcriptional response 100
3.3 Discussion 103
3.4 Materials and methods 112

Chapter 4: Characterization of *C. glabrata* trehalase enzymes 117
4.1 Introduction 119
4.2 Results 122
4.2.1 The *C. glabrata* trehalase enzymes are phylogenetically closely related to the *S. cerevisiae* trehalase enzymes 122
4.2.2 Ath1 is required for growth on trehalose as a carbon source 124
4.2.3 Nth1 is important for competition *in vitro* with other micro-organisms 131
4.2.4 The triple deletion strain is unable to stably colonize the gut 133
4.2.5 Nth1 is involved in regulation of *in vitro* oxidative stress resistance and survival in human macrophages 136
4.2.6 Trehalase plays a minor role in the virulence of *C. glabrata* in a mouse model of systemic infection 137
4.3 Discussion 139
4.4 Materials and methods 143

General discussion 151

References 159

Addendum 1: List of primers used in Chapter 2 181
Addendum 2: Overview of *C. glabrata* adhesins or adhesin-like genes described in literature 183
Addendum 3: List of primers used in Chapter 3 196
Addendum 4: Alignment of neutral trehalases and human trehalase 201
Addendum 5: List of primers used in Chapter 4 204

Chapter 1

Literature overview

Part of this introduction is based on and may contain text from:

Timmermans B., De Las Peñas A., Castaño I. and Van Dijck P. (2018). Adhesins in *Candida glabrata*. J Fungi (Basel) 4.

1.1 Introduction

Fungi are everywhere. They are eukaryotic organisms present outdoors, for example as macroscopic multicellular mushrooms or moulds on rotting fruits; indoors, as we are using unicellular yeasts to make bread or beer; but also in and on the human body. Fungi can be harmless or even beneficial, e.g. fungi present in the gut as part of the human microbiome or symbionts of plants. On the other hand, some fungi can cause disease and are classified as pathogens. The most common fungal diseases are asymptomatic-mild superficial infections of skin or nail, primarily caused by dermatophytes, affecting around 25% of the humans worldwide (Brown *et al.*, 2012). On the other hand, invasive fungal infections have a lower incidence but are of greater concern as they are potentially life-threatening. Annually, 1.5 million people die from an invasive fungal infection, mainly due to *Cryptococcus*, *Candida*, *Aspergillus* and *Pneumocystis* species (Brown *et al.*, 2012). In general, these fungi cause disease in people with a defective immune system, including HIV/AIDS patients. *Candida* species are the second most common cause of invasive fungal infections worldwide. In addition, the mortality rates associated with *Candida* infections are very high (46-75%) (Brown *et al.*, 2012). In this thesis, the connection between the cAMP-PKA pathway and virulence of the unicellular yeast *Candida glabrata* has been studied. Therefore, the next paragraph elaborates on the genus *Candida*, including an overview of the pathogenic *Candida* species, *Candida* infections, epidemiology and its virulence factors. Thereafter, an overview of the cAMP-PKA pathway is provided in different yeast species, starting with the yeast model *S. cerevisiae* (Section 1.3).

1.2 The genus *Candida*

The genus *Candida* contains approximately 150 species, of which only a subset is associated with colonization and disease in humans (Table 1.1) (Calderone and Clancy, 2012; Gabaldón and Carreté, 2016). Approximately 90% of *Candida* infections are caused by *C. albicans, C. glabrata*, *C. parapsilosis*, *C. tropicalis* and *C. krusei* (Pfaller *et al.*, 2010). Recently, *Candida auris* was discovered and gained major concern as it becomes easily multidrug resistant and *C. auris* infections are therefore associated with high mortality rates (Forsberg *et al.*, 2019; Lone and Ahmad, 2019).

Table 1.1: List of *Candida* species reported to cause infection, classified by incidence[a].

Incidence	Species
Common agents of candidiasis (5%-70%)	*C. albicans, C. glabrata, C. parapsilosis, C. tropicalis*
Rare but may be locally common (0.1%-3%)	*C. krusei* (*Pichia kudriavzevii*), *C. lusitanae* (*Clavispora lusitaniae*), *C. orthopsilosis*, *C.* metapsilosis, *C. guilliermondii* (*M. guilliermondii*), *C. kefyr* (*Kluyveromyces marxianus*), *C. inconspicua*, *C. famata* (*Debaryomyces hansenii*), *C. rugosa*, *C. dubliniensis*, *C. norvegensis* (*Pichia norvegensis*), *C. nivariensis*, *C. bracarensis*
Rarely reported (<0.1% including single case reports)	*C. pelliculosa* (*Wickerhamomyces anomalus*), *C. subhashii*, *C. lipolytica* (*Yarrowia lipolytica*), *C. sake*, *C. apicola*, *C. zeylanoides*, *C. valida* (*Pichia membranifaciens*), *C. intermedia*, *C. pulcherrima* (*Metschnikovia pulcherrima*), *C. haemulonii* (*C. heamulonis*), *C. stellatoidea*, *C. utilis* (*Cyberlindnera jardinii*), *C. humicola* (*Asterotremella humicola*), *C. lambica* (*Pichia fermentans*), *C. ciferrii* (*Trichomonascus ciferrii*), *C. colliculosa* (*Torulaspora delbrueckii*), *C. holmii* (*Kazachstania exigua*), *C. marina* (*Cryptococcus marinus*), *C. sphaerica* (*Kluyveromyces lactis*)

[a] Table adapted from Gabaldón and Carreté (2016), based on data of 10-year ARTEMIS study (Pfaller *et al.*, 2010).

1.2.1 *Candida* infections

Candida species are part of the human microbial flora, present in the gastrointestinal (GI) tract, oral cavity, skin and vaginal mucosa (Underhill and Iliev, 2014). As these body sites encompass various conditions, the genus *Candida* represents highly versatile organisms. Generally, opportunistic *Candida* species can cause infection when there is an imbalance in the host immune system, for example by disruption of the normal anatomical barriers or by a disturbed growth of the microbiota. Risk factors include patients receiving chemotherapy, the use of medical devices such as catheters and prosthetics, or the use of broad-spectrum antibiotics (Calderone and Clancy, 2012). *Candida* species can cause superficial infections, i.e. a local infection of the mucosa of a specific body part, or systemic infections, in which *Candida* cells reach

the bloodstream and disseminate throughout the human body. While superficial infections cause discomfort and reduce the quality of life, systemic infections are life-threatening to the patient (Calderone and Clancy, 2012; Guinea, 2014).

Superficial infection

The most common superficial *Candida* infections include vulvovaginal candidiasis (VVC) and oropharyngeal candidiasis (OPC) (Figure 1.1). As *Candida* is part of the microbial flora of the vaginal and oral mucosa, VVC and OPC are most often caused by endogenous *Candida* species (Drell *et al.*, 2013; Ghannoum *et al.*, 2010). VVC is characterized by vulvovaginal inflammation in presence of *Candida* species (Cauchie *et al.*, 2017). In contrast to other *Candida* infections which usually affect immunocompromised patients, VVC also commonly occurs in immunocompetent individuals. As many as 75% of all women in the reproductive age suffer from VVC at least once in their life, 45-50% will experience two or more episodes and 7-8% of all women suffer regular recurrent infections (Cauchie *et al.*, 2017). Fungal overgrowth is normally prevented by the host immune system, but a major role can also be attributed to the growth of *Lactobacillus* species which compete with *Candida* to grow and adhere to mucosa and lowering the pH by producing lactic acid (Peters *et al.*, 2014; Underhill and Iliev, 2014). *C. albicans* is the predominant species responsible for VVC (75-90%), followed by *C. glabrata* (7-16%) (Cauchie *et al.*, 2017).

OPC is characterized by painful red or white lesions of the oropharynx and altered taste (Patil *et al.*, 2018). Oral *Candida* infections are associated with underlying illness, e.g. OPC occurs in 7-48% of people with HIV infection and over 90% of HIV patients in an advanced state of disease. On the other hand, 65% of denture wearers encounter *Candida* denture stomatitis, independent of the immune status (Pankhurst, 2013). The biofilms associated with the dentures show mixed-species colonization and are generally more resistant to anti-fungal drugs. *C. albicans* (37-95%) is the most prevalent species causing OPC followed by *C. glabrata* (1-23%) and mixed colonization of different *Candida* species is seen in more than half of the patient samples (Patil *et al.*, 2018; Yano *et al.*, 2019).

Systemic infection

When *Candida* penetrates the epithelial barrier and enters the bloodstream, it can spread throughout the body. This is known as invasive candidiasis (IC) (Figure 1.1). The source of *Candida* can be exogenous, for instance by the use of medical intravascular devices or via parenteral nutrition, or endogenous from for instance the GI tract in patients with underlying conditions (Miranda *et al.*, 2009). This includes patients receiving long-term broad-spectrum antibiotics, which causes *Candida* overgrowth in the GI tract due to depletion of other gut microbiota. When fungal cells in the bloodstream survive and can escape into the surrounding tissue, they can disseminate to internal organs, such as liver and spleen. This condition is usually linked to patients receiving immunosuppressive agents, for instance by chemotherapy (Pappas *et al.*, 2018). The majority of invasive *Candida* infections are caused by *C. albicans* (over 60%), followed by *C. glabrata, C. tropicalis, C. parapsilosis* and *C. krusei.* The distribution of *Candida* species varies in studies carried out in different geographical areas: studies of most countries report *C. glabrata* as second most frequent cause of candidemia, except for Spain and Brazil, which show a higher incidence of *C. parapsilosis* cases (Guinea, 2014). Furthermore, the differences in the frequency of species depends on several other factors (eg. age and prior antibiotic use). For instance, *C. tropicalis* and *C. parapsilosis* are more prevalent in neonates than *C. glabrata*. Interestingly, the *C. glabrata* isolates of neonates are not resistant to antifungal drugs (Pfaller *et al.*, 2002). On the other hand, *C. glabrata* is the most frequent species in stem cell patients, probably due to the widespread use of azoles in this setting, promoting the azole-resistant species (Guinea, 2014).

Biofilms

Another type of infection is known as biofilm formation, which is defined by structured microbial communities attached to surfaces and encapsulated within a protective extracellular matrix (Costerton *et al.*, 1995). Fungal cells inside a biofilm behave very different from free-floating planktonic cells, including increased resistance to antifungal drugs and protection from host defenses (Ramage *et al.*, 2006). The biofilm substrate can be human tissue or abiotic surfaces, such as catheters and prostheses (Figure 1.1). Biofilm formation on medical devices has become an important problem in the past years, as catheters and implants are more frequently used due to the advances in medicine. Biofilms formed on implants are inherently difficult to treat and often result

in the necessity to physically remove the implant from the patient (Ramage *et al.*, 2009). Different *Candida* species can form biofilms, although the structure of the biofilm differs depend on their species-specific characteristics, such as morphology (Silva *et al.*, 2009). *C. albicans* and *C. glabrata* are the most frequent species forming biofilms. *C tropicalis* is associated with urinary tract infections, while *C. parapsilosis* (frequently found on the skin) is a frequent cause of catheter-related infections (Cavalheiro and Teixeira, 2018).

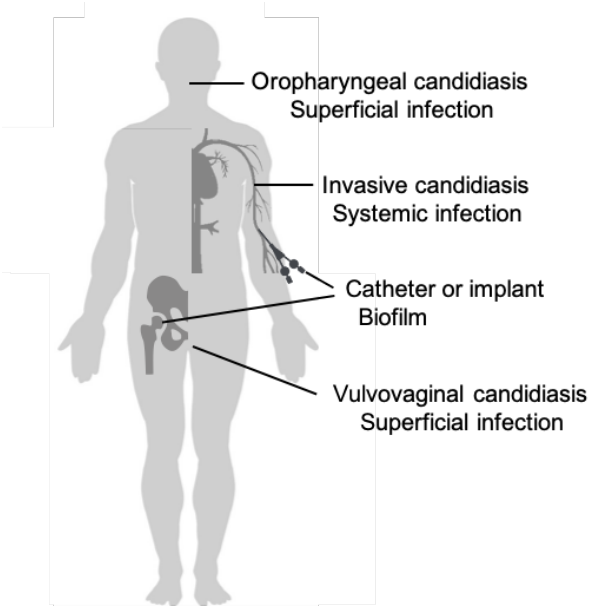

Figure 1.1: Overview of common *Candida* infection sites.

1.2.2 Epidemiology of *Candida*

Exact numbers of the incidence of fungal, and therefore *Candida* infections worldwide are hard to obtain due to misdiagnosis, lack of reporting, etc. Some studies report global estimations, based on surveillance studies: 1.7 billion people are estimated to have skin, nail and hair fungal infections, mainly caused by dermatophytes (Brown *et al.*, 2012). More than 150 million people have serious fungal diseases, mainly caused by *Candida*, *Aspergillus* and *Cryptococcus* species, which are associated with high mortality rates. *Candida* species are a common cause of invasive fungal infections worldwide, with estimations of around 750 000 cases per year and a mortality rate of 15-35% (Bongomin *et al.*, 2017; Guinea, 2014). Many of these serious infections are seen in patients at intensive care units (ICUs), as they often carry an underlying

disease or host factor, such as immune deficiencies that make them more prone to fungal overgrowth. The European Centre for disease prevention and control (ECDC) reports the incidence for the most frequent ICU infections in Europe: *Candida* species are the main fungal origin of pneumonia (8.6%), bloodstream infections (BSIs) (8.2%) and urinary tract infections (UTIs) (17.5%) (ECDC, 2018c).

As *Candida* infections are caused by multiple species, many studies focus on the incidence of individual *Candida* species. In a ten-year study of Pfaller *et al.* (2010), 31 different *Candida* species were identified from patients worldwide (Table 1.1). Overall, *C. albicans* was the most common *Candida* species isolated (65.3%), followed by *C. glabrata* (11.3%), *C. tropicalis* (7.2%), *C. parapsilosis* (6.0%) and *C. krusei* (2.4%). In Belgium, *C. albicans* is the most reported species (59%), followed by *C. glabrata* (22.4%), *C. parapsilosis* (8%), *C. tropicalis* (3%) and *C. krusei* (1.8%) (Goemaere *et al.*, 2018). These rates suggest that the incidence of *C. glabrata* in Belgium is very high compared to the global incidence. However, there are more examples of differences in the frequency of the *Candida* species in different geographical areas. For instance, *C. glabrata* was fourth in rank in Latin America (only 7.4%) and second in rank in North America (21.1%), while *C. tropicalis* was more prominent in Latin America (13.2%) than in other regions (4.9-7.3%) (Pfaller *et al.*, 2010). The cause for these differences is unknown but may be a consequence of climate, antifungal policy or different medical procedures. Also predisposing conditions of the patient, such as prior antifungal treatment in favor of non-*Candida albicans Candida* (NCAC) species can influence the frequency of *Candida* species (Guinea, 2014). Recently, *C. auris* was described as a newly emerging yeast which becomes easily resistant to antifungal drugs. Between 2013 and 2017, 620 cases of *C. auris* infections were reported in Europe, frequently associated with outbreaks in healthcare settings (ECDC, 2018a).

1.2.3 Genome and phylogeny

In 2004, the first complete genome sequences of *C. albicans* and *C. glabrata* were published (Dujon *et al.*, 2004; Jones *et al.*, 2004). *C. albicans* and *C. glabrata* are only distantly related: *C. albicans* together with some other frequently isolated *Candida* species are part of the CTG clade, while *C. glabrata* was found to be more closely related to the non-pathogenic yeast *S. cerevisiae* (Figure 1.2) (Butler *et al.*, 2009; Fitzpatrick *et al.*, 2006). In the past, species were assigned as '*Candida*' when there was no clearly defined sexual cycle at that time, although this did not imply a single evolutionary origin (Turner and Butler, 2014).

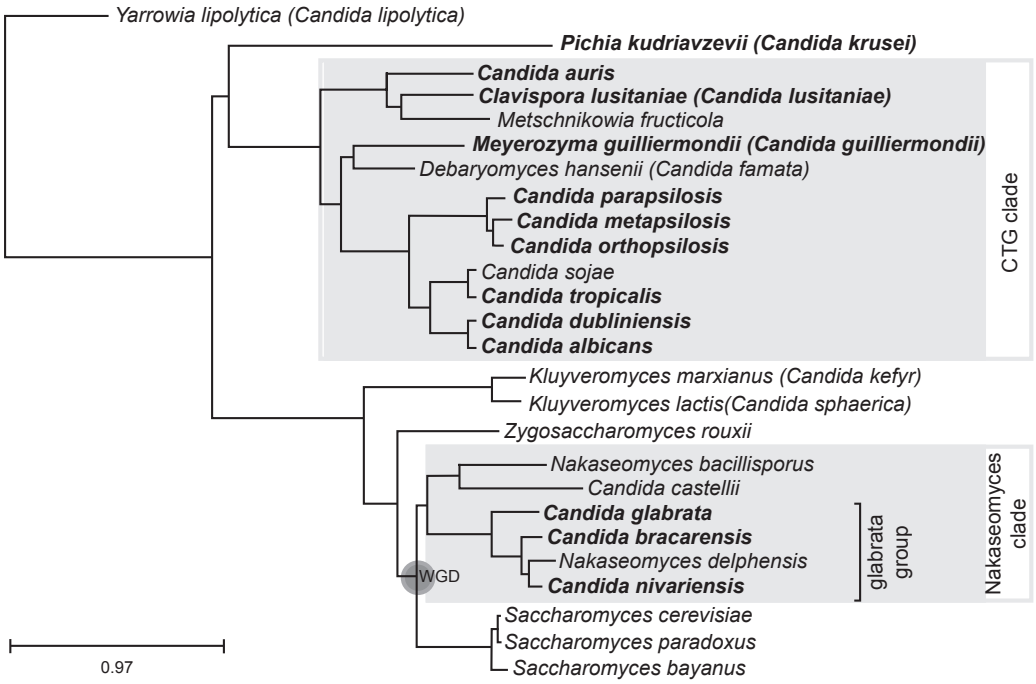

Figure 1.2: Phylogenetic relationship of several *Candida* species.
C. albicans belongs to the CTG clade, translating CUG to serine rather than leucine. *C. glabrata* is part of the *Nakaseomyces* clade, which is more closely related to *S. cerevisiae*. Pathogenic species are depicted in bold. Figure adapted from Gabaldón and Carreté (2016).

CTG clade

Butler *et al.* (2009) published the whole genome sequence of *C. albicans*, together with other closely related *Candida* species, including *C. parapsilosis* and *C. tropicalis*. These species belong to the CTG clade, translating the CUG codon as serine rather than leucine by the $tRNA_{CAG}^{Ser}$ for CUG codons and the $tRNA_{IAG}^{Leu}$ for CUA, CUC and CUU codons (Fitzpatrick *et al.*, 2006; Santos *et al.*, 1993). Alignment of genes

containing CUG codons in *S. cerevisiae* and *C. albicans* reveals functional replacement, as CUG codons in *C. albicans* almost never align to the CUG codons in *S. cerevisiae*: *C. albicans* CUG serine codons align primarily to *S. cerevisiae* serine (20%) or other hydrophilic residues (49%) and *S. cerevisiae* CUG leucine codons align primarily to *Candida* leucine (50%) or other hydrophobic residues (30%) (Butler *et al.*, 2009). In order to find genes involved in virulence, Butler *et al.* (2009) compared the genomes of several CTG-clade *Candida* pathogenic species with several non-pathogenic *Saccharomyces* species. 21 gene families were significantly enriched in the genomes of the pathogenic species, including the several cell wall families, as well as lipases and transmembrane transporters (Butler *et al.*, 2009).

C. glabrata clade

C. glabrata is a haploid yeast and encodes 5294 open reading frames (ORFs) (Skrzypek *et al.*, 2017). Dujon *et al.* (2004) compared the genomes of *S. cerevisiae* and *C. glabrata* in depth and reported that *C. glabrata* had lost many genes relative to *S. cerevisiae,* including several genes involved in galactose-, phosphate-, nitrogen- and sulphur metabolism. This suggests that genes were lost in a functionally coordinated manner. In 2013, the genome sequences of other species of the *Nakaseomyces* clade were published by Gabaldón *et al.* (2013), which provided new insights in how *C. glabrata* possibly became pathogenic. Previously, it was suggested that the gene losses by *C. glabrata* might be associated with its emergence as a pathogen. This seems not true as this event is not specific to *C. glabrata*, but is shared with all other species of the *Nakaseomyces* clade. This clade also contains the non-pathogenic species *C. castelli* and *N. bacillisporus*, it is more likely that pathogenesis emerged in the *glabrata* group. Interestingly, this study links the emergence to become a pathogen to the repertoire of genes encoding cell wall proteins mediating adhesion, also called adhesins, present in the *glabrata* group (Section 1.2.4.2.1). The study of Gabaldón *et al.* (2013) reported that *C. glabrata*, the most pathogenic species of the glabrata group, encodes 18 *EPA* adhesins, followed by 12 *EPA* genes in *C. bracarensis* and 9 in *C. nivarensis*. Furthermore, they report that the expansion of *EPA* genes in *C. glabrata* emerged from lineage-specific duplications, while the duplications of *EPA* genes in *C. bracarensis* and *C. nivariensis* are shared. Strikingly, *Nakaseomyces delphensis* encodes only a single *EPA* gene, which implies that this

species has lost *EPA* genes compared to its ancestor and therefore probably lost its pathogenicity (Gabaldón *et al.*, 2013).

Recently, a *de novo* genome assembly of the *C. glabrata* reference strain CBS138 was published (Xu *et al.*, 2020). While most ORFs of the new assembly were identical in the protein sequence compared to the reference genome (98.8% of the ORFs), 31 novel genes were found and 62 genes were removed. Furthermore, 21 genes contained structural variants in tandem repeat regions (Xu *et al.*, 2020). The quality of the previous genome assembly was especially variable in the telomeric regions. Because approximately half of the adhesins are located near the telomeres, many of the adhesins ORFs were corrected. The study predicts that there are 81 adhesin-like proteins present in the new assembly, among which 20 *EPA* genes (Figure 1.5B) (Xu *et al.*, 2020).

C. glabrata genome plasticity

Other studies focus on detecting more recent genome changes within different *C. glabrata* isolates. Earlier studies use karyotyping to detect chromosomal changes, such as larger segmental duplications, translocations of chromosomal arms, chromosomal fusions or even the presence of an additional minichromosome (Ahmad *et al.*, 2013; Muller *et al.*, 2009; Poláková *et al.*, 2009). With the advances in sequencing and the reduced costs of whole genome sequencing, more recent studies focus on whole genome sequencing of different *C. glabrata* isolates, with subsequent in-depth analysis (Carreté *et al.*, 2018; Vale-Silva *et al.*, 2017). All studies agree that there is an enormous genome plasticity in *C. glabrata.* For example, 33 *C. glabrata* strains in the study of Carreté *et al.* (2018) could be mapped into 7 subpopulations which had diverged in the past. Also, different isolates of the same patient show low sequence variability, indicating that the patient was colonized by a single strain which subsequently dispersed to different body sites. Comparison of these isolates with the reference strain CBS138 showed a high degree of chromosomal variation (Carreté *et al.*, 2018; Vale-Silva *et al.*, 2017). Interestingly, both these studies showed that many chromosomal changes involved genes encoding glycosylphosphatidylinositol (GPI)-anchored adhesin-like proteins, again indicating that adhesins play a major role in virulence. This genome plasticity also influences scientific research, as genome editing of the *C. glabrata* genome can be very challenging.

1.2.4 Virulence factors

1.2.4.1. Morphological switching

The most important virulence factor of *C. albicans* is morphological switching. *C. albicans* can grow as budding yeast, pseudohyphae (ellipsoid cells that are constricted at theid septa) or true hyphae (parallel-walled cells with no visible constrictions) (Figure 1.3) (Polke *et al.*, 2015). As *C. glabrata* only grows as a budding yeast, this paragraph will discuss morphological switching of *C. albicans*.

For many years, the yeast form was considered as the commensal cell type, while hyphae were associated with pathogenicity. As the morphological forms also display differences in gene expression, this makes the puzzle more complex than initially thought. Nowadays, the yeast and hyphal form are considered both important and complementary to each other. For instance, *C. albicans* yeast cells have been proposed to be important for dissemination via the bloodstream, while hyphal formation is associated with invasion of the surrounding tissue (Polke *et al.*, 2015). The morphological form is thought to reflect niche-specific conditions as the morphological switch is controlled by different signaling pathways, including the cyclic adenosine monophosphate – protein kinase A (cAMP-PKA) pathway and the mitogen-activated protein kinase (MAPK) pathway (Sudbery, 2011). Environmental factors inducing *C. albicans* hyphal formation include elevated temperature, presence of certain nutrients, serum, CO_2 and contact to physical surface.

Apart from the morphological forms, *C. albicans* also has few other different cell types: it exists as unicellular opaque cells which represents the mating-competent form in the cryptic mating cycle (Lohse and Johnson, 2009). In 2014, small unicellular smooth grey-colored cells were reported as the grey cell type (Tao *et al.*, 2014). Lastly, gastrointestinally induced transition (GUT) cells were discovered by screening of commensalism in the mammalian GI tract (Noble *et al.*, 2017; Pande *et al.*, 2013).

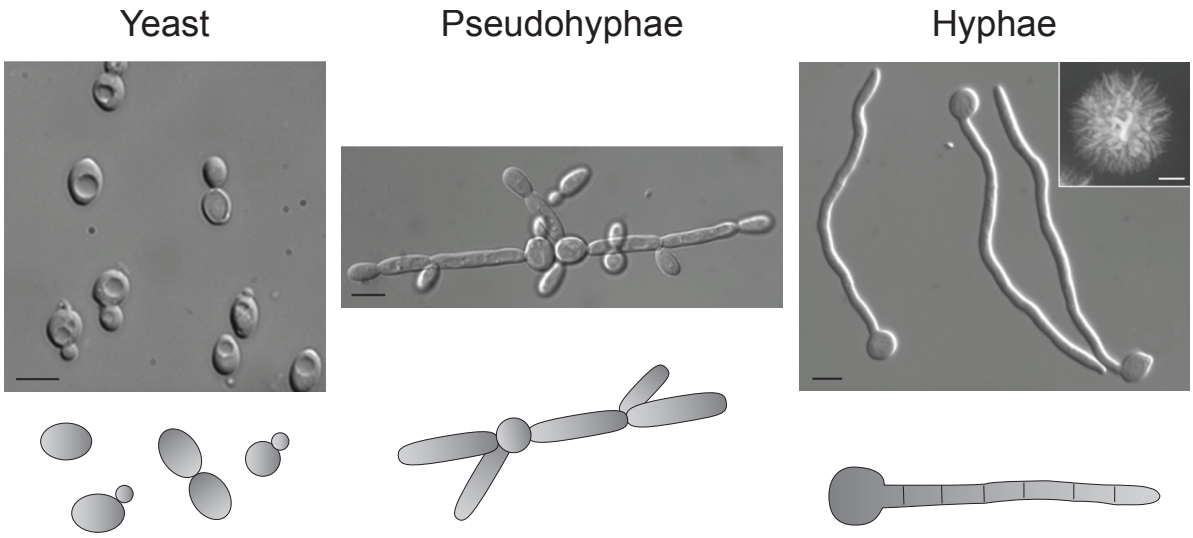

Figure 1.3: Morphological cell types of *C. albicans*.
Scale bars in the main panels represent 5 µm and in the inset on the hyphae panel 1 mm. Microscopy pictures from Sudbery (2011).

1.2.4.2. Adhesion and biofilm formation

Adhesion is the first step in the formation of a biofilm, which has been defined as a multi-layered structure consisting of a community of microorganisms attached to a surface, embedded in an exopolymeric matrix and exhibiting distinctive phenotypic properties (Donlan and Costerton, 2002). Biofilms are a major concern in hospitals as colonization on indwelling medical devices (e.g. urinary catheters) may require removal of the implant as other treatment options are often not available because of different physiology of the biofilm cells compared to planktonic cells, resulting in altered sensitivity towards antimicrobial drugs (Donlan and Costerton, 2002; ECDC, 2018b, d). These biofilms can be in the body for years or be life-threatening, depending on the microorganism and host environment (Vertes *et al.*, 2012). A main problem is that biofilms can serve as a reservoir for seeding infections.

A biofilm is formed in different stages (Figure 1.4) (Nobile *et al.*, 2012): first, yeast cells attach to a surface, which can be abiotic or biotic. Second, the adhered cells proliferate on the surface to form microcolonies after which extracellular matrix is produced. In the final stage, some cells will detach from the biofilm to disperse to other body sites. Because *C. glabrata* only grows by budding, *C. glabrata* mature biofilms are characterized by a dense network of yeast cells embedded in an extracellular matrix,

in contrast to *C. albicans*, which forms hyphae during the proliferation phase (Kucharíková *et al.*, 2015; Kuhn *et al.*, 2002; Nett *et al.*, 2007; Paulitsch *et al.*, 2009; Seneviratne *et al.*, 2010). This is also reflected in the thickness of the biofilms: mature *C. glabrata* biofilms are approximately half as thick (75-90 µm) as *C. albicans* biofilms (Kucharíková *et al.*, 2015).

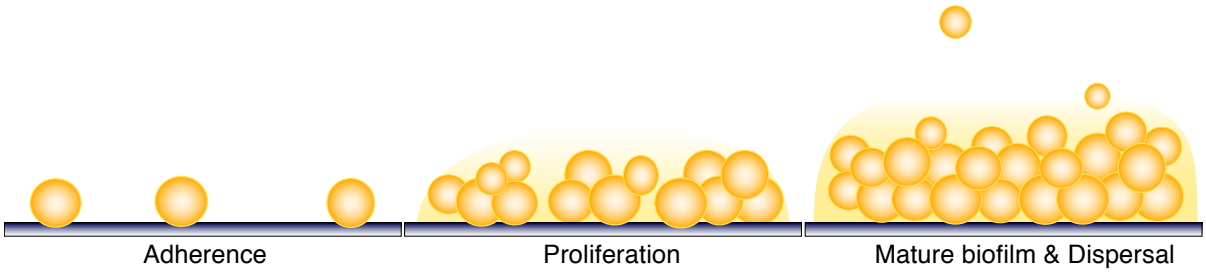

Figure 1.4: Schematic overview of the different stages of biofilm formation in *C. glabrata*.
To establish a biofilm, *C. glabrata* yeast cells first attach to a surface (left). Then, the cells proliferate to form microcolonies and the extracellular matrix is produced (central). Finally, some cells of the mature biofilm will detach and disperse to other body sites (right).

1.2.4.2.1. *Candida glabrata* adhesins

Identification of C. glabrata adhesins from genomic data

Since the complete genome sequences of different *Candida* species became available, several studies have been investigating differences between the genomes, with the main goal to identify genes responsible for pathogenesis (Butler *et al.*, 2009; Fitzpatrick *et al.*, 2006; Gabaldón *et al.*, 2013; Gabaldón *et al.*, 2016; Marcet-Houben and Gabaldon, 2009). *In silico* analysis revealed that *C. glabrata* contains a large number of genes encoding putative adhesins (51 or 67 genes) (de Groot *et al.*, 2008; Weig *et al.*, 2004). 44 out of these 67 adhesin-like encoding genes identified by de Groot *et al.* (2008) are located near the telomeres of all *C. glabrata* chromosomes (Figure 1.5A). Because these subtelomeric regions contain sequence repeats, they are prone to rearrangements or non-allelic homologous recombination, which could explain the expansion of the adhesin-encoding gene families. For some of these adhesins, it was already shown that their expression is under control of sub-telomeric silencing, mediated by Rap1, the Sir-complex and Ku70/80 (De Las Penas *et al.*, 2003;

Domergue *et al.*, 2005; Gallegos-García *et al.*, 2012; Halliwell *et al.*, 2012; Juárez-Reyes *et al.*, 2012).

Several adhesins also contain internal repetitive sequences (e.g. 'VSHITT' tandem repeats in *PWP7* and *AED1*), that may allow for local chromosomal rearrangements to occur, resulting in different variants of the adhesins (Desai *et al.*, 2011; Thierry *et al.*, 2008; Thierry *et al.*, 2010). For instance, an increase in the number of the repeats could result in an adhesin that may have its ligand binding domain projected further out of the cell wall, thereby improving adherence to specific substrates (Frieman *et al.*, 2002; Verstrepen *et al.*, 2005). In 2018 and 2020, the *C. glabrata* gene annotation was updated: some genes were removed, new genes were found and the sequence of some genes was corrected (Linde *et al.*, 2015; Xu *et al.*, 2020). The study of Xu *et al.* (2020) reports that there are 81 putative adhesin-like genes, among which 20 *EPA* genes (Figure 1.5B).

Since sequencing of fungal genomes became affordable, more studies have shown interest in comparing the genomes of clinical isolates with the genome of a reference lab strain (Ahmad *et al.*, 2013; Muller *et al.*, 2009; Poláková *et al.*, 2009; Vale-Silva *et al.*, 2017). All these studies show that the *C. glabrata* genome is highly dynamic. One study sequenced and analyzed the genomes of two *C. glabrata* isolates from one patient suffering from oropharyngeal candidiasis (Vale-Silva *et al.*, 2017): even between these two isolates, there was a difference of 1024 nucleotides. Further analysis showed that 6 adhesin-like genes of CBS138 were missing and interestingly, new predicted adhesin-like encoding genes were found exclusively in the clinical isolates. The two clinical isolates contained 101 and 107 adhesin-like genes, which is almost twice the number found in the CBS138 reference strain. Similar to the reference strain, half of the adhesin-like encoding genes were located close to the telomeres. A closer inspection of the predicted adhesin-like encoding genes identified a duplication of several *EPA* genes and also of *PWP* and *AWP* genes (Vale-Silva *et al.*, 2017). In this study, the number of adhesin-like encoding genes present in clinical isolates is significantly higher, which suggests again that adhesins play an important role in infection.

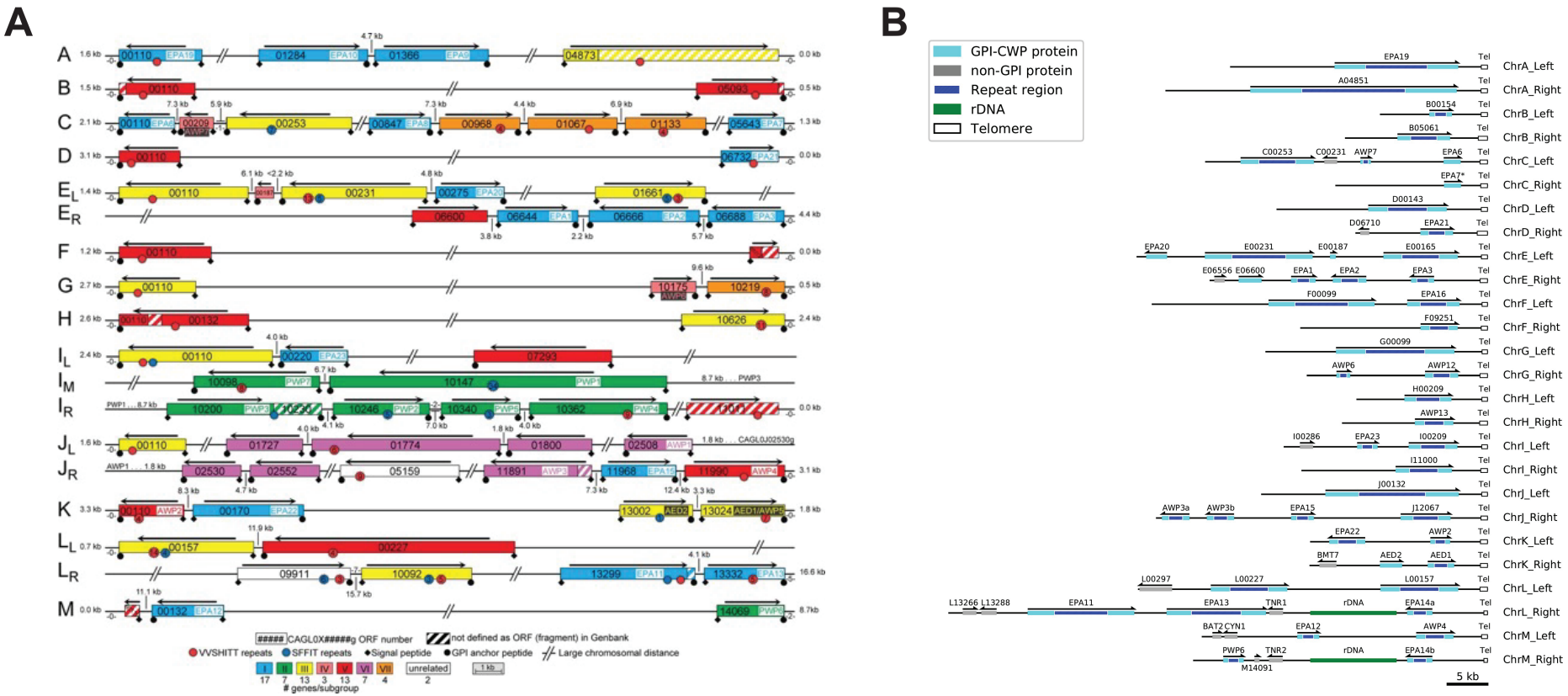

Figure 1.5: Genomic organization of predicted adhesin-like genes in *C. glabrata* strain CBS138 in 2008 by de Groot *et al.* (2008) (A) and a more recent update by Xu *et al.* (2020).

Panel A gives an overview of the predicted *C. glabrata* adhesins in 2008. More recently, the *C. glabrata* genome was reannotated which showed many differences in the predicted adhesin genes. Therefore, an update of the predicted adhesins by Xu *et al.* (2020) is shown in panel B. The ORFs are shown relative to each other on their respective chromosomal locations, the colors indicate the respective gene families. The figure from panel A originates from de Groot *et al.* (2008), panel B from Xu *et al.* (2020).

Adhesin families

The majority of *C. glabrata* cell wall proteins (CWPs) are GPI-anchored proteins cross-linked to 1,3-β-glucan, while a minority is bound to 1,6-β-glucan (de Groot *et al.*, 2008). GPI-CWPs have a modular structure with the N-terminal ligand binding domain followed by a low-complexity and usually highly repetitive region with a high percentage of serine and threonine residues that is heavily glycosylated (de Groot *et al.*, 2003). Based on their N-terminal substrate-binding domain, adhesins were classified into several subclasses or adhesin families: The first group includes the Epa protein family that contains a ligand binding domain of approximately 300 amino acids which was identified as the conserved anthrax protective antigen (PA14) domain, suggesting a carbohydrate-binding function (Rigden *et al.*, 2004). This N-terminal ligand binding domain is projected out of the cell through a long and highly glycosylated serine/threonine-rich region. This serine/threonine-rich region is essential for the adherence function of the Epa proteins (Frieman *et al.*, 2002; Ielasi *et al.*, 2012). A second subgroup also has a N-terminal PA14 domain and were therefore named Pwps (PA14 containing wall proteins). The remaining predicted adhesins were organized into five different subgroups, which have more distantly related ligand binding domains. These subgroups are poorly characterized, since most studies have focused on the Epa family of adhesins.

Ligand binding specificity

The ligand binding specificities of *C. glabrata* adhesins have been determined by modelling of the N-terminal ligand binding domain (Ielasi *et al.*, 2012), glycan interaction studies (Diderrich *et al.*, 2015; Ielasi *et al.*, 2016; Ielasi *et al.*, 2014; Zupancic *et al.*, 2008), mutagenesis (Ielasi *et al.*, 2014), inhibition experiments (Kuhn *et al.*, 2002; Zajac *et al.*, 2016) and atomic force microscopy (AFM) studies (El-Kirat-Chatel *et al.*, 2015; Valotteau *et al.*, 2019). These studies all focused on the Epa family of CWPs as they were the first *C. glabrata* adhesins characterized.

Already in 1999, Cormack and co-workers found that galactose, lactose (galactose β1-4 linked to glucose) and some other glycoconjugates were able to inhibit adhesion of *C. glabrata* to epithelial cells, suggesting a lectin binding function (Cormack, 1999). This theory was supported by the structural analysis of the N-terminal Epa1 binding domain (N-Epa1) co-crystallized with lactose (Ielasi *et al.*, 2012). Using a glycan

interaction assay with the N-Epa1 showed a strong preference of N-Epa1 to bind glycans containing a terminal galactose residue β1-3 or β1-4 linked to galactose, glucose, N-acetylgalactosamine or N-acetylglucosamine (Zupancic *et al.*, 2008). The same study investigated the N-terminal ligand binding domains of Epa6 and Epa7, which are highly homologous. It was shown that N-Epa7 has the narrowest ligand specificity, only binding to Galβ1-3Gal or Galβ1-4Glc, while Epa6 does not have any preference and binds to both α- and β-linked glycosides with a terminal galactose residue (Zupancic *et al.*, 2008). These interactions were later confirmed and extended in a study with all 17 Epa proteins of the CBS138 reference strain (Diderrich *et al.*, 2015). In the human body, these Epa proteins may interact with carbohydrates present on human cells. Indeed, N-Epa1 was found to bind to mucin (the main constituent of mucus and the glycocalyx), fibronectin (major component of blood plasma and extracellular matrix) and tumor necrosis factor (TNF-α) on peripheral blood mononuclear cells (PBMCs), and both Epa1 and Epa7 were found to interact with N-glycan structures of kidney and brain tissue, while in a competitive binding assay, Epa6 was found to bind to fibronectin (Ielasi *et al.*, 2016; Zajac *et al.*, 2016).

Surface hydrophobicity

C. glabrata can adhere to a diverse set of surfaces which can be biotic as well as abiotic. Adherence to abiotic surfaces is frequently tested *in vitro* using polystyrene or polypropylene multiwell plates because of the similarity to the CLSI susceptibility tests and because of the simple high throughput screening capacity (Krom and Willems, 2016). Other abiotic surfaces tested include more clinically relevant materials such as polyurethane catheter pieces, denture material or silicone pieces.

Plastic surfaces, as well as yeast cells, possess a negative surface charge, suggesting a repulsive force between them (Klotz *et al.*, 1985). However, *C. glabrata* was found to adhere well to abiotic surfaces. The adhesion force of *C. glabrata* cells is much lower towards a hydrophilic surface compared to a hydrophobic surface. Consistent with these results, several studies found a good correlation between an increased adherence capacity of *C. glabrata* cells to abiotic surfaces and a high cell surface hydrophobicity (CSH) (El-Kirat-Chatel *et al.*, 2015; Gómez-Molero *et al.*, 2015; Luo and Samaranayake, 2002). Thus, adherence to an inert material is mediated by hydrophobic interactions, also called London van der Waals forces (Klotz *et al.*, 1985).

The relative CSH of *C. glabrata* was found to be significantly higher than that of *C. albicans*, although both show intra-species variation (Hazen *et al.*, 1986; Luo and Samaranayake, 2002).

As CSH was found to be correlated to adherence to plastics, one would expect that this interaction is not mediated by specific receptor/adhesin ligand interactions. However, adherence to polystyrene was found to be significantly lower in an *epa6*Δ strain and the hydrophobic adhesion forces were also low in this strain (El-Kirat-Chatel *et al.*, 2015). This indicates that Epa6, which is rich in hydrophobic residues, is at least partially responsible for providing the CSH under the conditions tested.

A complex puzzle to be elucidated

Several studies have investigated the expression of *C. glabrata* adhesins at either transcriptional or protein level. However, it is difficult to compare between studies because of the variation in *C. glabrata* strains and the experimental conditions. For example, the growth medium used to grow the biofilms or even variations in the pH changed the expression of adhesins, thus affecting the biofilm morphology (Kraneveld *et al.*, 2011; Kucharíková *et al.*, 2011). Linde *et al.* (2015) even identified that some adhesins, among which *EPA3*, *EPA6* and *EPA20*, are expressed as different isoforms depending on the growth medium.

EPA1 (Epithelial adhesin 1) was the first *C. glabrata* CWP identified to be important for adhesion in an insertional mutant library screen (Cormack *et al.*, 1999). Epa1 was shown to be largely responsible for *in vitro* adherence of *C. glabrata* to epithelial cells, since *epa1*Δ strains showed a 95 percent reduced adherence while *S. cerevisiae* became highly adherent by heterologous expression of Epa1. The presence of Ca^{2+} was required for adhesion and adherence could be inhibited by addition of galactose or lactose. Epa1 is also involved in adherence to human macrophage-like cells: *C. glabrata* or *S. cerevisiae* cells expressing *EPA1* showed a great *in vitro* adherence to THP-1 cells and this interaction was inhibited by adding lactose (Kuhn and Vyas, 2012). A similar high adherence was seen with matured human PBMC derived macrophages but strikingly, this interaction could not be inhibited by addition of lactose. While the presence of Epa1 was sufficient for binding macrophage-like cells, *C. glabrata* was able to avoid subsequent phagocytosis whereas *S. cerevisiae* cells expressing Epa1 were phagocytosed by the macrophages after adhesion (Kuhn and Vyas, 2012). Vale-Silva *et al.* (2016) found that the transcription factor Pdr1, known to

control the expression of ABC transporters also regulates *EPA1* expression. Interestingly, several Pdr1 gain of function (GOF) mutants were found to adhere less to THP-1 macrophage-like cells and mouse BMDM macrophages, while adherence to epithelial cells *in vitro* was increased compared to the wild type strain (Vale-Silva *et al.*, 2013). A Pdr1 binding site was found in the *EPA1* promoter and the Pdr1^{L280F} GOF mutant leads to *EPA1* overexpression, which was eliminated by deletion of this Pdr1 binding site. Furthermore, introducing Pdr1 GOF mutations did not affect *in vitro* adherence to epithelial cells in an *epa1*Δ strain, indicating that Pdr1 regulates adherence through control of *EPA1* expression (Vale-Silva *et al.*, 2016).

In vivo, there was no difference in virulence between an *epa1*Δ or wild type strain in a murine vaginal model and in a gastrointestinal tract infection model (Cormack *et al.*, 1999). In a murine model of urinary tract infection (UTI), overexpression of *EPA1* leads to significantly elevated colonization of bladder and kidneys. Interestingly, deletion of *EPA1* alone caused a small decrease in organ colonization, but more repetitions are needed to confirm its significance (Vale-Silva *et al.*, 2016). This is probably due to the involvement of other adhesins, as it was shown by Domergue *et al.* (2005) that the triple mutant strain (*epa1*Δ *epa6*Δ *epa7*Δ) showed a significantly decreased colonization in the bladder in the murine UTI model. This study also showed that the expression of these adhesins was induced by removing nicotinic acid (NA) from the medium. Consistently, *in vitro* adherence to uroepithelial cells was significantly lower in presence of excess NA.

The insertional mutant library of Cormack and co-workers was used to search for aberrant *in vitro* biofilm formation in polystyrene multi-well plates. *epa6*Δ strains had significantly reduced biofilms, while *epa1-5*Δ strains were only slightly affected. The expression of *EPA6* and *EPA7* was also shown to be induced in biofilms (Iraqui *et al.*, 2005; Kucharíková *et al.*, 2011). *EPA6* and *EPA7* have a highly homologous sequence and are both located near the telomeres, where their expression is regulated by subtelomeric silencing (Castaño *et al.*, 2005). Other mutants that showed poor biofilms were deficient in genes encoding for the chromatin remodeling Swi/Snf complex and the protein kinase *YAK1*. The possible reason for the defect in biofilm formation in strains mutated for these genes is the fact that they are required for the expression of *EPA6* and *EPA7*, possibly by affecting subtelomeric silencing (Iraqui *et al.*, 2005; Riera *et al.*, 2012). On the other hand, overproducing biofilm strains were isolated: deletion of *CST6* resulted in a strain with strong biofilm formation capacity. Consistently, the

transcription factor Cst6 was shown to be a negative regulator of *EPA6* expression independent of subtelomeric silencing. Another overproducing biofilm strain had an insertion between the two *EPA*-like genes CAGL0I10147g (*PWP1*) and CAGL0I10200g (*PWP3*) (Riera *et al.*, 2012). Furthermore, the multidrug resistance transporter Tpo1_2 was also found to affect *in vitro* biofilm formation on polystyrene plates, as its deletion strain showed a 40 percent reduction in biofilm formation. The expression of several adhesins, including *EPA1*, was repressed in the *tpo1_2*Δ strain (Santos *et al.*, 2017).

C. glabrata biofilm formation on polystyrene was found to be significantly higher when *C. albicans* was present (Tati *et al.*, 2016). In dynamic flow conditions, *C. glabrata* is unable to form a biofilm unless *C. albicans* hyphae are present. Fluorescence microscopy pictures showed that the *C. glabrata* yeast cells were tightly associated along the *C. albicans* hyphae. This association was significantly reduced when the *C. albicans ALS1* and/or *ALS3* genes were deleted. The *C. glabrata* adhesins *EPA8*, *EPA19*, *AWP2*, *AWP7* and CAGL0F0018g were found to mediate this adherence and their expression was induced upon incubation with *C. albicans* hyphae (Tati *et al.*, 2016).

Furthermore, Pwp7 and Aed1 (adherence to endothelial cells) were found to play a role in adherence to endothelial cells *in vitro*, as their deletion strains show a significantly reduced adherence compared to the wild type strain (Desai *et al.*, 2011).

Other studies analyzed the expression of adhesins during biofilm formation. Santos *et al.* (2017) showed that the expression of *EPA1*, *EPA6/7*, *EAP1* and CAGL0G04125g was upregulated in a 24-hour *in vitro* biofilm compared to a 6-hour biofilm. Another study compared the adhesin expression of *in vitro* biofilm cells to planktonic grown cells: a unique peptide of Awp6 was found exclusively in biofilm cell walls, while peptides of Epa3 were found in the cell wall of biofilm cells and planktonic cells grown in semi-defined yeast growth (SdmYg) medium (Kraneveld *et al.*, 2011). At the transcriptional level, the expression of *AWP* adhesins was increased in biofilms compared to planktonic cells, except for *AWP2*. *EPA3* expression was elevated in YPD cultured biofilms, while *EPA7* expression was lower. The expression of *EPA1*, *EPA3*, *EPA7* and *EPA22* were only induced in SdmYg medium cultured biofilms (Kraneveld *et al.*, 2011). Gómez-Molero *et al.* (2015) compared the CWP profiles of two clinical isolates, which showed an increased *in vitro* adherence to polystyrene, silicone and denture material. Mass spectrometry of the isolated CWPs led to the

identification of 12 adhesin-like proteins, including Epa3, Epa6, Epa7 and several Awp adhesins of which 6 were newly identified. Most of the adhesins were shared between the two isolates.

Kucharíková *et al.* (2015) compared the expression of several adhesins in mature *in vitro* biofilms formed on polyurethane catheter pieces to mature biofilms isolated from a rat subcutaneous biofilm model. Major differences were found between the *in vitro* and *in vivo* biofilms, which could be expected since the growth conditions *in vitro* can be tightly controlled, while *in vivo* there is variation originating from the environment (different nutrient states, the state of the immune system, mouse variability etc.). The expression of *EPA3*, *EPA6*, *AWP2*, *AWP3* and *AWP5* was significantly higher under the *in vivo* conditions than in the *in vitro* biofilms, while there was no difference in *EPA1* expression (Kucharíková *et al.*, 2015).

To determine the expression of specific adhesin-encoding genes under *in vivo* conditions, Domergue *et al.* (2005) made use of recombinant *in vivo* expression technology (IVET). *C. glabrata* cells were engineered to become auxotroph for tryptophan and resistant to hygromycin when *EPA6* was expressed. In this way, the percentage of hygromycin resistant and tryptophan auxotroph colonies can be assessed for the *C. glabrata* recovered from *in vivo* models of infection. Using IVET, one can determine whether an adhesin was expressed in the tested condition, but it is not possible to address the specific moment of induction or expression. It was shown that *EPA6* was not expressed during *in vitro* growth or during intravenous infection of mice, while a significant portion of *C. glabrata* cells recovered from an *in vivo* UTI model was hygromycin resistant (Domergue *et al.*, 2005). Using IVET, *EPA2* was found to be expressed in a small but significant part of *C. glabrata* cells recovered from the liver in a murine model of systemic infection (Juárez-Cepeda *et al.*, 2015).

1.2.4.2.2. *Candida albicans* adhesins

In *C. albicans,* the initial adhesion likely occurs between yeast cells and epithelium, followed by the induction of hyphal formation. The hyphae express a distinct set of adhesins which are of major significance for further adhesion and cell-cell interactions (Höfs *et al.*, 2016).

The best characterized *C. albicans* adhesins belong to the agglutinin-like sequence (*ALS*) family of adhesins, consisting of eight similar cell surface glycoproteins (*Ca*Als1-*Ca*Als7 and *Ca*Als9). *CaALS* adhesins have a basic three-domain structure: a conserved N-terminal domain which is highly homologous to *S. cerevisiae* α-agglutinin, a cell-surface adhesive glycoprotein facilitating cell-cell contact during mating; a central domain of variable length consisting of a tandem repeat (TR) motif, which mediate hydrophobic interactions and facilitate aggregation; and a C-terminal domain consisting of a highly glycosylated serine/threonine-rich spacer region extending from the surface (de Groot *et al.*, 2013; Frank *et al.*, 2010; Hoyer *et al.*, 2008). *Ca*Als1-4 are specifically expressed on hyphae, while *Ca*Als5-7 and *Ca*Als9 can be found on yeast cells (Höfs *et al.*, 2016). Nobile *et al.* (2008) showed that *Ca*Als1 and *Ca*Als3 have critical but redundant roles in biofilm formation, as the double deletion strain showed no detectable adherence to catheters *in vivo*. *Ca*Als3 mediates attachment to epithelial and endothelial cells. *CaALS3* expression is upregulated during oral epithelial infection *in vitro* as well as in *in vivo* vaginal infection, suggesting it to play a role during infection (Naglik *et al.*, 2011). *Ca*Als3 plays many roles as it also functions as an invasin, inducing endocytosis into the host cell, but it also binds to host ferritin thereby enabling *C. albicans* to use the available iron (Liu and Filler, 2011). Furthermore, it was also found that *Ca*Als3 plays a major role in adherence of *Staphylococcus aureus* and *S. epidermidis*, bacteria regularly identified in co-infections with *C. albicans*, to *C. albicans* hyphae (Beaussart *et al.*, 2012; Peters *et al.*, 2012). Als adhesins are also present in other *Candida* species: in *C. dubliniensis* and *C. tropicalis*, three *ALS* genes were identified with a similar domain structure, but their sequences were extensively diversified (Hoyer *et al.*, 2001).

*Ca*Hwp1 is another important *C. albicans* adhesin and is predominantly expressed in hyphae. Hwp1 is involved in cell-cell aggregation and is required for biofilm formation. *Ca*Hwp1 and *Ca*Als1/3 are complementary in biofilm formation (Nobile *et al.*, 2008). Apart from being an adhesin, *Ca*Hwp1 is also a substrate for mammalian transglutaminase, resulting in stable attachments to epithelial cells (Staab *et al.*, 1999). Deletion of *CaHWP1* affects oropharyngeal candidiasis but does not play a direct role in systemic infection (Moyes *et al.*, 2015). Furthermore, *CaEAP1* was shown to mediate adhesion to polystyrene and epithelial cells *in vitro* as well as in an *in vivo* central venous catheter model (Li *et al.*, 2007).

1.2.4.3. Adaptation to host environment

Candida pathogens have evolved strategies to survive and proliferate within the human host. On the one hand, they are part of the microbiota, asymptomatically colonizing several niches including the oral cavity, gastrointestinal and urogenital tracts. On the other hand, as pathogens they can also be found in other parts of the body, for instance in the blood during systemic infection. Therefore, *Candida* species face many challenges as these niches have very different conditions, which can also change over time.

One major challenge is to adapt to the limited and changing availability of nutrients inside the host (metabolic adaptation), as this is critical for fungal growth (Kumamoto *et al.*, 2020). This includes the availability of sugars and amino acids, but also micronutrients including important cofactors of enzymes such as iron and zinc. The host limits the availability of free essential metals to counteract invading microorganisms, called nutritional immunity (Hood and Skaar, 2012). *Candida* cells also need to adapt to the constant stress they face due to the changing conditions and/or different niches including differences in pH, oxygen levels and concentrations of reactive oxygen species (ROS). In addition, the host innate immune system constantly surveys microbial pathogens to clear infection. Phagocytic cells have receptors (pattern-recognition receptors or PRRs) recognizing pathogen-associated molecular pattern (PAMPs), for instance specific fungal cell wall components. PAMP-PRR interactions trigger the induction of signaling pathways resulting in phagocytosis. These mechanisms were recently reviewed in depth by Alves *et al.* (2020).

1.2.4.4. Resistance against antifungal drugs

In the clinic, antifungal therapy options to treat systemic infections are restricted because only a few chemical classes are available as antifungal drugs (Table 1.2). Antifungal drugs are regularly used in immunocompromised patients, including treatment of fungal infections of HIV-positive patients but also as prophylactic treatment for ICU patients at higher risk for fungal infections. The widespread use of antifungal agents is presumed to be a factor promoting resistance. Antifungal drug resistance is on the rise and a major concern is the emergence of multidrug-resistant (MDR) strains. Therefore, there is a high need for new classes of antifungal drugs. The fungal cell wall is an ideal target for the development of new antifungal drugs, as mammalian cells do not have a cell wall.

Antifungal drugs either kill the fungus (fungicidal), e.g. causing leakage of cell contents, or prevent fungal cells from growing and reproducing (fungistatic). Isolates can be intrinsically resistant to antifungal drugs or become resistant following antifungal treatment (acquired resistance). The three common classes of antifungal drugs used are described in this paragraph together with the corresponding *Candida* resistance mechanisms (Table 1.2).

Azoles

Azoles (including ketoconazole, fluconazole and posaconazole) inhibit the fungal enzyme lanosterol-14α-demethylase, encoded by *ERG11* in *Candida* species, in the ergosterol biosynthesis pathway. Ergosterol is the major sterol of the fungal plasma membrane, analogous to cholesterol in mammalian cells, conferring membrane fluidity and integrity and is important for the function of membrane-bound enzymes (White *et al.*, 1998). Inhibition of ergosterol biosynthesis leads to the inhibition of *Candida* growth (fungistatic).

There are three main ways in which *Candida* species may become resistant to azoles: the first mechanism is the induction of multi-drug efflux pumps, resulting in reduced drug concentrations at the enzyme target inside the fungal cell. The *CDR* genes encode pumps belonging to the ATP binding cassette (ABC) superfamily and *CDR* overexpression is associated with resistance to azoles and other antifungals. *MDR* encoded efflux pumps belong to the major facilitator (MF) superfamily and confer resistance to fluconazole (Rogers, 2002; Sanguinetti *et al.*, 2015).

Secondly, the target enzyme of azoles is upregulated, leading to insufficient inhibition in presence of the azole drugs, or is mutated, reducing the binding of azoles to Erg11. The third mechanism involves the development of bypass pathways. The inhibition of Erg11 by azoles leads to the accumulation of the toxic 14-α-methyl-3,6-diol. When the fungal cell can prevent the formation of this toxic product and adapt to a functional cell membrane with alternative sterols, it circumvents the action of the azoles. For instance, loss-of-function mutations in *ERG3* have been reported for several *Candida* species to confer azole resistance (Pristov and Ghannoum, 2019; Sanguinetti *et al.*, 2015; Whaley *et al.*, 2016).

Fluconazole is the most widely used antifungal drug to treat *C. albicans* infections, because of its easy oral administration, high bio-activity, low toxicity and low cost (White *et al.*, 1998). *C. albicans*, *C. tropicalis* and *C. parapsilosis* are species which are generally susceptible to fluconazole, while an increased intrinsic resistance is present in *C. glabrata*, *C. krusei* and *C. auris* (Chowdhary *et al.*, 2018; Diekema *et al.*, 2012; Pfaller *et al.*, 2010; Toda *et al.*, 2019).

Polyenes

Polyenes are amphipathic molecules targeting fungal membranes, by interaction with ergosterol. They intercalate into the cell membrane, forming pores through which cellular components (including ions) leak out of the cell, causing cell death (fungicidal) (White *et al.*, 1998). An alternative theory proposes the formation of extra-membranous aggregates functioning as a sterol sponge, thereby perturbating ergosterol-dependent cellular processes (Carolus *et al.*, 2020). Resistance to polyenes is relatively rare (Carolus *et al.*, 2020; Toda *et al.*, 2019). Resistance is generally achieved by a reduction of the ergosterol content or by alterations in the sterol composition in the cell membrane reducing the affinity of the cell for polyenes (Rogers, 2002).

The polyene Amphotericin B (amB) has a good antifungal activity. However, its use was limited because the first formulation frequently caused nephrotoxicity, but this was reduced greatly with the development of a lipid-associated formulation. The polyene nystatin showed even a higher toxicity and its use is therefore restricted to topical administration (Rogers, 2002).

Echinocandins

Echinocandins (including caspofungin and anidulafungin) inhibit β(1,3)D-glucan synthase, an enzyme responsible for biosynthesis of β(1,3)D-glucan which is a key component of the fungal cell wall. The integrity of the fungal cell wall is critical for viability, as there is a constant delicate balance to be maintained between rigidity and flexibility during growth (Walker *et al.*, 2010). As inhibition of β(1,3)D-glucan synthesis leads to the formation of a defective fungal cell wall, this ultimately results in cell death in *Candida* species (fungicidal).

Resistance to echinocandins has been linked with point mutations in specific regions (so-called hot-spot regions) of genes encoding the *FKS* subunits of β(1,3)D-glucan synthase. These mutations lead to changes in the target site, inhibiting echinocandins (Pristov and Ghannoum, 2019; Sanguinetti *et al.*, 2015). Secondly, *Candida* species can overcome the cell wall defect in response to echinocandins by increasing chitin synthesis, by initiation of the adaptive stress response (Sanguinetti *et al.*, 2015). The increased use of echinocandins has been associated with the emergence of resistance to these drugs, affecting mainly *C. glabrata* and *C. albicans* (Coste *et al.*, 2020).

Table 1.2: Overview of *Candida* resistance mechanisms against antifungal drugs.

Antifungal class	**Mode of action**	**Basis for resistance**
Azoles	Inhibition of ergosterol biosynthesis (Erg11 enzyme)	Upregulation of *CDR1*, *CDR2* and *MDR1* encoded drug efflux pumps by point mutations in transcription factors
		Point mutations in *ERG11* decreasing binding of drug to target
		Upregulation of *ERG11* causing increased concentrations of target enzyme
		Point mutations in *ERG3* resulting in alternative sterol synthesis
Echinocandins	Inhibition of β(1,3)D-glucan synthesis	Point mutations in *FKS1* and *FKS2* decreasing binding of drug to target
		Increase chitin synthesis to reduce cell wall stress
Polyenes	Pore formation in fungal plasma membrane	Reduction of ergosterol results in reduced affinity
		Alterations in sterol content reducing affinity for polyenes

1.3 The cAMP-PKA pathway

In order to survive, yeast cells need to rapidly adapt to changes in the extracellular environment. Hence, nutrients do not only provide building blocks and energy necessary to grow, but also function as signaling molecules. One of the main nutrient-induced signaling pathways is the cAMP (3',5'-cyclic adenosine monophosphate)-protein kinase A (PKA) pathway. The cAMP-PKA pathway is well characterized in the model yeast *S. cerevisiae* (Section 1.3.1). In several pathogenic fungi, the cAMP-PKA pathway controls virulence factors and this is reviewed in section 1.3.2.

1.3.1 *Saccharomyces cerevisiae*

In *S. cerevisiae,* PKA plays a central role in the nutritional control of metabolism, stress resistance, cell cycle, growth and transcription (Rubio-Texeira *et al.*, 2010). Cells with a high PKA activity display low levels of storage carbohydrates trehalose and glycogen and have a low expression of stress resistance genes, resulting in low stress resistance. The activity of PKA is regulated by integration of different nutrient signals: the presence of a fermentable carbon source controls PKA activity via the cAMP-PKA pathway (overview of the pathway in Figure 1.6). Besides a fermentable carbon source, a complete growth medium is required to keep PKA active, which is mediated by the fermentable growth medium (FGM)-induced pathway (reviewed in Conrad *et al.* (2014)). The next sections give an overview of the cAMP-PKA pathway in *S. cerevisiae*, starting with the central components cAMP and PKA (Section 1.3.1.1), after which the two required routes of activation are discussed. The downstream targets of the pathway are reviewed in section 1.3.1.4.

1.3.1.1. The second messenger cAMP and the protein kinase A

The yeast adenylate cyclase, encoded by *ScCYR1*, converts adenosine triphosphate (ATP) into cAMP. Addition of glucose to glucose-deprived cells activates adenylate cyclase, resulting in a fast increase in cAMP levels; which acts as the second messenger of the pathway (Figure 1.6). The activation of adenylate cyclase requires a dual sensing system: a G protein-coupled receptor (GPCR) for extracellular sensing of sucrose or glucose and an intracellular system requiring glucose uptake and phosphorylation, discussed in Sections 1.3.1.2 and 1.3.1.3 respectively. Cytosolic cAMP is converted into adenosine monophosphate (AMP) by phosphodiesterase enzymes (Figure 1.6). *S. cerevisiae* contains a low-affinity and a high-affinity phosphodiesterase, encoded by *ScPDE1* and *ScPDE2* respectively (Nikawa *et al.*, 1987; Sass *et al.*, 1986). The low-affinity phosphodiesterase *Sc*Pde1 controls the glucose-induced cAMP increase, as the cAMP signal is much higher and longer-lived in a *Scpde1*Δ strain while a strain with *ScPDE2* deleted showed a wild type cAMP increase (Ma *et al.*, 1999). On the other hand, *Sc*Pde2 controls the basal cAMP level which was shown by *ScPDE2* overexpression increasing the resistance of cells to heat stress (Ma *et al.*, 1999). While adenylate cyclase is required for normal growth of *S. cerevisiae*, as a *Sccyr1*Δ strain arrests in the G1-phase, a strain deleted for both *ScPDE1* and *ScPDE2* is viable, but highly sensitive to stress (Matsumoto *et al.*, 1983; Nikawa *et al.*, 1987).

PKA is a heterotetrameric protein, consisting of two catalytic (encoded by *ScTPK1, ScTPK2 and ScTPK3*) and two regulatory subunits (encoded by *ScBCY1*) (Toda *et al.*, 1987a; Toda *et al.*, 1987b). The three *ScTPK* genes have a high amino acid sequence homology. None of the three *ScTPK* genes are essential, but the deletion of all three catalytic subunits is lethal (Toda *et al.*, 1987b). Disruption of *ScBCY1* renders the cells highly sensitive to heat shock and starvation (Toda *et al.*, 1987a). Binding of cAMP to the regulatory subunits causes dissociation of the catalytic subunits from the regulatory subunits and thereby PKA activation (Figure 1.6). PKA is a kinase which recognizes and phosphorylates the recognition sequence (R/K)(R/K)X(S/T) affecting different downstream targets, discussed in Section 1.3.1.4 (Kemp *et al.*, 1977). Upon activation by a cAMP increase, PKA also exerts a feedback down-regulation of the pathway by stimulating cAMP breakdown. For instance, PKA

phosphorylates the phosphodiesterases (Hu *et al.*, 2010; Ma *et al.*, 1999). In addition, PKA also controls feedback inhibition independent of the *Sc*Pde proteins as a strain lacking both phosphodiesterases shows only a modest increase in cAMP levels (Nikawa *et al.*, 1987). While several targets were investigated, none of these targets showed a comparable elevated cAMP level as a strain with attenuated PKA activity, so the precise target(s) of PKA feedback inhibition remains to be elucidated (reviewed in Vandamme *et al.* (2012)).

1.3.1.2. Extracellular glucose sensing activates *Sc*Gpr1-*Sc*Gpa2

G protein-coupled receptors (GPCRs) are a broadly conserved family of seven transmembrane receptors coupled to heterotrimeric G proteins. GPCRs are found in yeasts, but also in humans and have a broad diversity of ligands including different nutrients, pheromones and hormones. Binding of the ligand to the receptor leads to a conformational change, thereby promoting guanosine diphosphate (GDP) to guanosine triphosphate (GTP) exchange of the Gα protein and causing its dissociation from the Gβɣ subunits. A GTPase-activating protein (GAP) stimulates the hydrolysis of GTP into GDP, causing inactivation of the Gα protein and reassociation with the Gβɣ subunits. The GPCR upstream of adenylate cyclase in the cAMP-PKA pathway consists of *Sc*Gpr1 and *Sc*Gpa2, sensing extracellular glucose and sucrose.

The receptor ScGpr1

The C-terminus of *ScGPR1* was discovered in a yeast two-hybrid interaction screen using *ScGPA2* as a bait. *ScGPR1* encodes a protein of 961 amino acids with seven transmembrane domains, typical for GPCRs, a large third cytoplasmic loop and a large cytoplasmic tail (Kraakman *et al.*, 1999; Xue *et al.*, 1998). Addition of glucose causes an increase of cAMP in a wild type strain (Figure 1.6). This signal is largely abolished in a *Scgpr1*Δ strain indicating that *Sc*Gpr1 is a glucose receptor. The residual signal in the *Scgpr1*Δ strain was abolished by pre-addition of a small amount of glucose in advance to fulfil the second requirement (Section 1.3.1.3) (Kraakman *et al.*, 1999). In 2004, Lemaire and co-workers showed that *Sc*Gpr1 is not only a receptor for glucose (K_M of 20 mM), but also for sucrose (K_M of 0.5 mM). Furthermore, the ligand binding pocket was investigated, which involves transmembrane domains (TMDs) III, IV, V, VI

and VII in the typical structure of GPCRs, by substituted cysteine accessibility method (SCAM) analysis. This was done by substitution of the amino acids of TMD VI and the third extracellular loop one by one to cysteine and checking the cAMP increase after addition of glucose or sucrose. In addition, prior addition of 2-aminoethyl-methanethiosulphate (MTSEA), a reagent which covalently binds to cysteine residues in a polar water accessible environment, can provide further information about ligand binding as binding of MTSEA to cysteine can possibly physically hinder access to the sugar ligand. The results of this study showed that addition of MTSEA to wild type *S. cerevisiae* cells did not abolish cAMP signaling. The cysteine mutants were categorized in three classes: a first group contained mutants that were deficient in both glucose- and sucrose-induced cAMP induction and therefore are essential for ligand binding. The second group of mutants were neither affected in glucose- nor sucrose-induced signaling. Also, prior addition of MTSEA had no effect on sugar signaling. The third group of cysteine substitutions were deficient in glucose-induced signaling but still showed a cAMP increase after addition of sucrose. When MTSEA was given in advance, for two mutants also sucrose-induced cAMP signaling was abolished. Together, these results show that TMD VI is part of the glucose and sucrose binding pocket and specific residues contribute to the ligand specificity.

The Gα protein ScGpa2

The Gα protein *Sc*Gpa2 was discovered in a homology search with *Sc*Gpa1, the Gα protein involved in sensing of mating pheromones in *S. cerevisiae* (Nakafuku *et al.*, 1988). This study also showed that *Sc*Gpa2 regulates glucose-induced cAMP signaling. The abolished cAMP signaling upon addition of glucose to *Scgpr1*Δ cells was rescued by expression of a constitutively activated *ScGPA2*$^{VAL-132}$ allele, indicating *Sc*Gpa2 functions downstream of *Sc*Gpr1 (Figure 1.6) (Kraakman *et al.*, 1999). Peeters *et al.* (2006) reported physical binding of *Sc*Gpa2-GTP to adenylate cyclase *in vitro*, but not for GDP bound *Sc*Gpa2. As mentioned before, G proteins usually consist of three subunits. In the search for the Gβ subunit of *Sc*Gpa2, the kelch repeat homolog (Krh) proteins were proposed first but were later shown to act as downstream effectors instead (discussed in next paragraph). Instead, *Sc*Asc1 was identified as the Gβ subunit of *Sc*Gpa2 as this protein has the 7-WD domain structure, binds directly to GDP-*Sc*Gpa2 and inhibits *Sc*Gpa2 guanine nucleotide exchange

activity (Zeller *et al.*, 2007). Furthermore, *Sc*Asc1 binds to *Sc*Cyr1 resulting in a lowered cAMP production (Zeller *et al.*, 2007). *Sc*Rgs2 was found to be a negative regulator of *Sc*Gpa2 through direct GTPase activation (GAP) (Versele *et al.*, 1999). Together these results show that *Sc*Gpr1 and *Sc*Gpa2 form a GPCR complex sensing glucose and sucrose and thereby activating adenylate cyclase.

The kelch repeat protein bypass

Using yeast two-hybrid analysis, the kelch repeat proteins *Sc*Krh1 and *Sc*Krh2 were found to interact with *Sc*Gpa2 (Harashima and Heitman, 2002). Therefore, at first they were thought to function as alternative Gβ subunits of *Sc*Gpa2, based on structural similarities: the kelch repeat proteins lack the seven WD-40 repeats found in Gβ subunits, but instead contain seven kelch repeats which fold into a strikingly similar seven-bladed β propeller configuration (Harashima and Heitman, 2002). Later on, another group identified the amino acids important for the interaction between *Sc*Gpa2 and *Sc*Krh1, which did not resemble the typical binding of a Gα subunit to a Gβ subunit (Niranjan *et al.*, 2007). Instead, the *Sc*Krh proteins are downstream of *Sc*Gpa2 (Figure 1.6). Deletion of *ScKRH1* and/or *ScKRH2* increases PKA activity, independent of a cAMP increase (Lu and Hirsch, 2005). The *Sc*Krh proteins function as inhibitors of PKA: deletion of *ScKRH1/2* lowers the requirement of cAMP addition in the *Sccyr1*Δ *pde2*Δ strain. Furthermore, *Sc*Krh1 directly interacts with the catalytic subunits of PKA and promotes the association of the catalytic and regulatory PKA subunits *in vivo* (Peeters *et al.*, 2006). Therefore, the *Sc*Krh proteins form an adenylate cyclase bypass pathway from *Sc*Gpa2 directly towards PKA (Figure 1.6) (Peeters *et al.*, 2007).

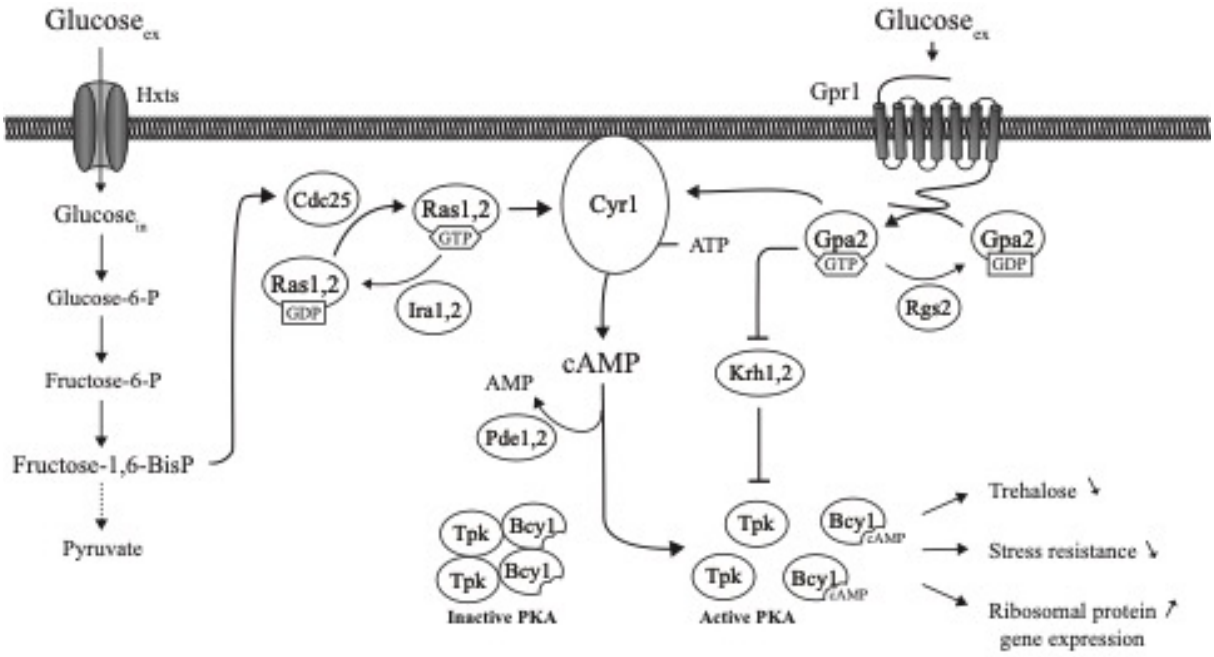

Figure 1.6: Overview of the cAMP-PKA pathway in *S. cerevisiae.*
Glucose activation of the cAMP-PKA pathway requires a two-fold sensing system: on the one hand, *Sc*Gpr1 and *Sc*Gpa2 form a GPCR sensing extracellular sucrose and glucose, resulting in activation of adenylate cyclase. Secondly, intracellular glucose sensing is required, based on its intermediate metabolic breakdown product fructose-1,6-bis phosphate, which activates the G protein Ras. Adenylate cyclase converts ATP into cAMP, the second messenger of the pathway, which in turn binds to and thereby activates PKA. The phosphodiesterases (ScPde1/2) hydrolyze cAMP in AMP. By phosphorylation of many targets, PKA changes the phenotypic properties of the cells. Additionally, a bypass was elucidated with direct inhibition of PKA by *Sc*Krh1 and *Sc*Krh2, independent of adenylate cyclase activity.

1.3.1.3. Intracellular glucose sensing activates *Sc*Ras

In addition to direct sensing of extracellular glucose, also intracellular glucose sensing is necessary for activation of the cAMP-PKA pathway in *S. cerevisiae*. In this way, glucose metabolism and signal transduction are intermingled. Therefore, the next paragraph first gives a brief overview of glucose metabolism in *S. cerevisiae* and how it is connected to the cAMP-PKA pathway.

Glucose uptake and metabolism

In *S. cerevisiae*, glucose transport occurs via facilitated diffusion by a set of glucose carriers of the *ScHXT* family (Figure 1.6). The low-affinity (15-20 mM) glucose transporters *Sc*Hxt1, *Sc*Hxt3 and *Sc*Hxt4 are constitutively expressed, while expression of the high-affinity (1-2 mM) glucose transporters *Sc*Hxt2, *Sc*Hxt6, *Sc*Hxt7 is induced by low levels of glucose and is repressed in presence of high glucose (Özcan and Johnston, 1999; Reifenberger *et al.*, 1997). The expression of the hexose transporters is regulated by the *Sc*Snf3/*Sc*Rgt2 signaling pathway with *Sc*Snf3 sensing low glucose levels and *Sc*Rgt2 detecting high levels of glucose (Kayikci and Nielsen, 2015). A strain with *ScHXT1-7* deleted (*Schxt* null mutant), is not able to grow on glucose as a carbon source (Reifenberger *et al.*, 1995). The galactose transporter *Sc*Gal2 can also transport glucose with high affinity (1-2 mM), but its expression is repressed by glucose (Özcan and Johnston, 1999; Reifenberger *et al.*, 1997).

Once imported, glucose is metabolized in the cytosol into pyruvate by glycolysis (Figure 1.6). Intracellular glucose is first phosphorylated to glucose-6-phosphate (Glu6P) by the glucokinase *Sc*Glk1 or one of the hexokinases *Sc*Hxk1 or *Sc*Hxk2. This step renders a low glucose level in the cytoplasm, promoting glucose uptake by the carriers. Then, Glu6P is converted into fructose-6-phosphate (Fru6P) by the phosphoglucose isomerase, which in turn is phosphorylated by the phosphofructokinase complex (*Sc*Pfk1 and *Sc*Pfk2) into fructose-1,6-bisphosphate (Fru-1,6-bisP). This molecule is cleaved by the *Sc*Fba1 aldolase into glyceraldehyde-3-phosphate (GA3P) and dihydroxyacetone phosphate (DHAP). These triose phosphates are then converted into pyruvate by a series of enzymatic reactions. Following glycolysis, pyruvate can be further oxidized in the Krebs cycle or fermented into ethanol.

Connecting glucose metabolism to activation of cAMP-PKA pathway

Evidence for a connection between glucose metabolism and cAMP signaling was reported by Beullens *et al.* (1988), as a strain in which the three sugar kinases were deleted did not show a glucose- nor fructose-induced cAMP increase. The presence of one kinase was sufficient to restore glucose-induced cAMP signaling (Beullens *et al.*, 1988). Prior to phosphorylation, glucose needs to be transported into the cells. Therefore, the addition of glucose to a *Schxt* strain does not induce cAMP signaling unless *Sc*Gal2 is constitutively expressed in this strain (Rolland *et al.*, 2000).

Mbonyi *et al.* (1988) showed that glucose-induced cAMP signaling is absent in a strain lacking functional *ScRAS* genes (in this strain *Scbcy1* is also deleted to suppress the lethality of *ScRAS* deficiency). These Ras proteins belong to a family of conserved small G proteins: for instance, *S. cerevisiae* Ras proteins can be functionally replaced by human Ras (Kataoka *et al.*, 1985). The activity of *Sc*Ras is controlled by *Sc*Cdc25/*Sc*Sdc25 (guanine nucleotide exchange factor, GEF) and *Sc*Ira1/ScIra2 (GAP) (Figure 1.6). In 2004, Colombo and coworkers showed that intracellular glucose phosphorylation induces a fast increase in GTP-bound *Sc*Ras protein. This glucose-induced GTP loading of *Sc*Ras is also present in *Scgpr1*Δ and *Scgpa2*Δ strains, but does require the presence of *ScCDC25* (Colombo *et al.*, 2004; van Aelst *et al.*, 1991). Addition of glycolytic metabolites to permeabilized spheroplasts revealed *Sc*Ras is activated by fructose-1,6-bisphosphate through *ScCDC25* (Peeters *et al.*, 2017) (Figure 1.6).

The two glucose sensing mechanisms necessary to activate the cAMP-PKA pathway can be separated from each other as exemplified by the study of Rolland and co-workers: the addition of maltose to glucose derepressed *Schxt* null cells can fulfil the intracellular glucose phosphorylation requirement, after which glucose can be given to fulfil the extracellular requirement via *Sc*Gpr1-*Sc*Gpa2 (Rolland *et al.*, 2000).

1.3.1.4. PKA targets

PKA affects a wide variety of targets in yeast cells. In general, it stimulates the phenotypic characteristics associated with rapid fermentative growth and suppresses properties associated with slow, respirative growth (Conrad *et al.*, 2014). This is achieved by PKA phosphorylation of many different targets including transcription factors and metabolic enzymes, discussed in this paragraph.

Stress resistance

The cAMP-PKA pathway also controls the stress resistance of *S. cerevisiae*. Cells with a high PKA activity, for instance a *Scbcy1*Δ strain, are very sensitive to heat shock (Shin *et al.*, 1987; Toda *et al.*, 1987a). Two homologous zinc finger proteins *Sc*Msn2 and *Sc*Msn4 function as transcriptional activators of several yeast genes, controlling a multi-stress response (Boy-Marcotte *et al.*, 1998; Martínez-Pastor *et al.*, 1996; Ruis

and Schüller, 1995). *Sc*Msn2/4 bind to stress responsive (STRE) elements (CCCCT) in the promoter of genes (Marchler *et al.*, 1993; Martínez-Pastor *et al.*, 1996). STRE-controlled genes include the cytosolic catalase T *ScCTT1*, heat shock protein *ScHSP12* and trehalose-6-phosphate phosphatase (*ScTPS2*) (Ruis and Schüller, 1995; Winderickx *et al.*, 1996). In response to stress or when PKA activity is low, *Sc*Msn2 translocates to the nucleus and induces transcription (Görner *et al.*, 1998; Smith *et al.*, 1998). The nuclear localization signal (NLS) of *Sc*Msn2 was found to be a direct target of PKA phosphorylation (Görner *et al.*, 2002). By PKA phosphorylation, the transcription factor is retained in the cytoplasm and is therefore unable to induce gene expression.

Ribosomal protein expression

S. cerevisiae ribosomal protein (RP) gene expression is regulated according to the growth rate of cells: rapidly growing cells require a high rate of protein synthesis and therefore transcription of RP genes. PKA controls ribosomal gene expression as their transcription is elevated in a *Scbcy1*Δ strain and cannot be induced in a strain with constitutively low PKA activity (Klein and Struhl, 1994). Nearly all RP genes contain a *Sc*Rap1 binding site in their promoter. These *Sc*Rap1 binding sites in RP promoters are required for PKA-mediated regulation of ribosomal gene expression (Klein and Struhl, 1994; Neuman-Silberberg *et al.*, 1995). *Sc*Rap1 is an abundant nuclear protein which either stimulates or inhibits transcription, likely mediated through interactions with other proteins (Klein and Struhl, 1994). For RP induction, *Sc*Rap1 interacts with the transcriptional activator *Sc*Gcr1 (Deminoff and Santangelo, 2001).

Pseudohyphal growth

Some diploid *S. cerevisiae* strains (Σ1278b and wild yeast strains) can form pseudohyphae in presence of abundant fermentable carbon source and nitrogen limitation (Lo and Dranginis, 1998). During filamentous growth, cells have an elongated morphology and switch to unipolar budding while remaining physically attached to each other (Lengeler *et al.*, 2000). Expression of *ScFLO11*, encoding a GPI-anchored cell wall flocculin, was shown to be critical for pseudohyphal formation (Lo and Dranginis, 1998). Pseudohyphal growth is a target of the cAMP-PKA pathway as *ScGPR1* or *ScGPA2* deletion strains show defective pseudohyphal growth, which can be reversed by addition of exogenous cAMP (Lorenz and Heitman, 1997; Tamaki

et al., 2000). While all three PKA catalytic subunit isoforms are redundant for viability, only *ScTPK2* is essential for pseudohyphal development (Robertson and Fink, 1998). The transcription factor *Sc*Sfl1 can be phosphorylated by *Sc*Tpk2, thereby controlling *ScFLO11* transcription (Conlan and Tzamarias, 2001; Robertson and Fink, 1998). Furthermore, cAMP-PKA-mediated pseudohyphal formation requires the transcription factor *Sc*Flo8 to induce *ScFLO11* expression (Rupp *et al.*, 1999). Van de Velde and Thevelein (2008) showed that sucrose is an even better inducer of pseudohyphal growth and this is dependent on the presence of *Sc*Gpr1. This reflects the higher affinity of *Sc*Gpr1 for sucrose (Ec_{50} = 0.5 mM) compared to glucose (Ec_{50} = 20 mM).

Trehalase

Trehalose (α-D-glucopyranosyl-1,1-α-D-glucopyranoside) is a reserve carbohydrate but also serves as a stress protectant molecule to yeast cells (Thevelein, 1984). In *S. cerevisiae*, trehalose is synthesized by the canonical pathway: trehalose-6-phosphate synthase (*Sc*Tps1) converts UDP-glucose and glucose-6-phosphate into UDP and trehalose-6-phosphate. The latter is converted into trehalose and free inorganic phosphate by the trehalose-6-phosphate phosphatase (*Sc*Tps2) (François and Parrou, 2001). The trehalose biosynthesis protein complex also includes the regulatory *Sc*Tps3 and *Sc*Tsl1 proteins (François and Parrou, 2001). On the other hand, trehalose is hydrolyzed into two glucose molecules by trehalase enzymes. Addition of glucose to derepressed cells results in a fast mobilization of trehalose, by activation of trehalase through the PKA pathway (Mbonyi *et al.*, 1990; Thevelein, 1984). Three trehalase enzymes are present in *S. cerevisiae*: *Sc*Ath1, *Sc*Nth1 and *Sc*Nth2. *Sc*Nth1 and *Sc*Nth2 are two cytosolic neutral trehalase enzymes (Kopp *et al.*, 1993; Nwaka *et al.*, 1995). Although the neutral trehalases have a high sequence identity, *Sc*Nth1 is mainly responsible for trehalose hydrolysis in the cytosol. *Sc*Nth1 activity is dependent on PKA phosphorylation, as glucose-induced neutral trehalase activation is largely abolished in a strain expressing only *ScTPK1* or *ScTPK3* (Mbonyi *et al.*, 1990). As neutral trehalase activity can be measured easily, it is often used as a read out for PKA activity of cells. Using phosphospecific antibodies, direct PKA phosphorylation could also be demonstrated, e.g. phosphorylation of *Sc*Nth1 Ser^{21} and Ser^{83} were shown *in vivo* upon addition of glucose (Schepers *et al.*, 2012). *Sc*Ath1 is an acid trehalase (pH optimum of 4.5) and is necessary for growth on trehalose as

a carbon source (Huang *et al.*, 2007). As *Sc*Ath1 is not a PKA target, it is not further discussed here.

1.3.2 The cAMP-PKA pathway regulates virulence factors in other pathogenic fungi

In several pathogenic fungi of both plants and humans, the cAMP-PKA pathway controls virulence factors including cellular morphology and resistance to host defenses. While the central components cAMP and PKA are conserved, upstream triggers of the pathway as well as downstream targets are more diverse, by rewiring during evolution. Therefore, in this paragraph some examples are described in both human and plant pathogens.

Human pathogenic fungi

In *Candida albicans*, the morphological transition between yeast and hyphae is the main virulence factor (Section 1.2.4.1). This yeast-to-hyphal transition is under control of multiple signaling pathways, of which the cAMP-PKA pathway plays a major role (Sudbery, 2011). A strain deleted for adenylate cyclase (*CaCYR1*) is unable to produce hyphae and is avirulent in a mouse model for systemic candidiasis (Bahn and Sundstrom, 2001). *C. albicans* PKA promotes the yeast-to-hyphal transition by phosphorylation of the transcription factor Efg1 (Figure 1.7). *Catpk1*Δ strains show a defective hyphal formation in solid medium, while *Catpk2*Δ strains cannot form hyphae in liquid medium (Bockmühl *et al.*, 2001). Several upstream signals activate the pathway including serum, high CO_2 levels, amino acids, high temperature and quorum sensing molecules (Figure 1.7) (Biswas *et al.*, 2007; Sudbery, 2011). Elevated temperature is sensed by heat shock protein 90 (*Ca*Hsp90), which regulates morphogenesis by repressing PKA signaling through *Ca*Ras (Shapiro *et al.*, 2009). Induction by methionine requires its uptake by the permease *Ca*Mup1 and metabolic conversion into S-adenosyl methionine (SAM) and subsequent decarboxylation by *Ca*Spe2 for intracellular activation of adenylate cyclase (Kraidlova *et al.*, 2016; Schrevens *et al.*, 2018). The receptor *Ca*Gpr1 and Gα protein *Ca*Gpa2 are orthologs of *Sc*Gpr1 and *Sc*Gpa2 and are also present upstream of the pathway in *C. albicans*. Maidan *et al.* (2005) showed that *Ca*Gpr1 is involved in amino acid signaling in

presence of glucose, while glucose-induced signaling is unaffected in the deletion strain. Strikingly, *Ca*Gpr1 also regulates another virulence factor: evasion of the host immune system. The study of Ballou *et al.* (2016) showed that lactate induces ß-glucan masking in a *Ca*Gpr1 dependent way (Figure 1.7, dashed line).
The cAMP-PKA pathway also controls filamentation and white-to-opaque switching in *C. tropicalis*: a deletion of *CtRAS1* or *CtCYR1* causes attenuated filamentation in presence of glucose or N-acetylglucosamine (GlcNAc), while deletion of phosphodiesterase *CtPDE2* enhances filamentous growth (Zhang *et al.*, 2016). An alkaline pH increases the cAMP level in *C. tropicalis*, thereby promoting the opaque phenotype, possibly through the Wor1 master regulator. Furthermore, overexpression of *CtTPK2* or deletion of *CtPDE2* promotes the opaque phenotype (Zheng *et al.*, 2017). The cAMP-PKA pathway is also present in *C. glabrata* and regulates its main virulence factor adhesion (unpublished research, therefore further described in section 2.1). *C. parapsilosis*, *C. dublienensis* and *C. auris* also encode homologs of adenylate cyclase and PKA, but these genes and their involvement in virulence have not been characterized up until now.

Aspergillus fumigatus is an important airborne human pathogen causing invasive aspergillosis associated with high mortality rates (Dagenais and Keller, 2009). The conidia can disperse easily through the air and by inhalation it can cause disease in the lungs of immunocompromised patients. The cAMP-PKA pathway is linked to *A. fumigatus* virulence, as mutants of adenylate cyclase (*AfacyA*∆) or the PKA catalytic subunit (*AfpkaC1*∆) show reduced growth and only form very few conidia *in vitro* (Figure 1.7) (Liebmann *et al.*, 2003; Liebmann *et al.*, 2004). Mutants of the PKA regulatory subunit (*AfpkaR*) grow slowly and the conidia show morphological abnormalities and germinate poorly *in vitro* (Zhao *et al.*, 2006). The *AfpkaC1*∆ strain is almost avirulent in a mouse infection model while the *AfpkaR* strain shows a reduced virulence, suggesting it is more harmful to have reduced PKA activity than unregulated activity for virulence (Liebmann *et al.*, 2004; Zhao *et al.*, 2006).
A. fumigatus conidia contain the pigment dihydroxynaphtalene (DHN) melanin, which serves as a stress protectant and is essential for survival inside phagocytes (Heinekamp *et al.*, 2012). PKA positively regulates the expression of polyketide synthase PksP, an essential enzyme for the production of DHN melanin (Figure 1.7) (Fuller *et al.*, 2009; Grosse *et al.*, 2008; Liebmann *et al.*, 2004). Consequently, deletion

of the catalytic PKA subunit rendered an almost avirulent strain in a murine inhalation model (Liebmann *et al.*, 2004). *A. fumigatus* is the most prevalent species causing invasive aspergillosis (up to 72% of the cases), followed by *A. flavus* (up to 17% of the cases) (Gregg and Kauffman, 2015). *A. flavus* produces the carcinogenic metabolite aflatoxin (AF), affecting both humans, animals and crops (e.g. maize). Deletion of adenylate cyclase in *A. flavus* causes defects in growth, sporulation, aflatoxin production and therefore virulence (Yang *et al.*, 2016).

Another important human fungal pathogen is *Cryptococcus neoformans*, causing cryptococcosis and meningoencephalitis in severe immunocompromised patients. Its virulence factors titan cell formation, polysaccharide capsule production and melanin biosynthesis are regulated by the cAMP-PKA pathway. Titan cells, identified as a subpopulation of enlarged cells, are characterized by a high resistance to oxidative or nitrosative stress and can escape phagocytosis as a mechanism to evade the host immune response and survive (Okagaki *et al.*, 2010; Zaragoza *et al.*, 2010). The polysaccharide (PS) capsule protects cells against stress and has antiphagocytic properties (Casadevall *et al.*, 2019). Strains defective in adenylate cyclase (*CnCAC1*) are mating defective, unable to form titan cells and do not produce melanin or a PS capsule, rendering it an avirulent strain (Figure 1.7) (Alspaugh *et al.*, 2002; Okagaki *et al.*, 2010; Zaragoza *et al.*, 2010). Similarly, when the catalytic PKA subunit was deleted, cells were sterile and failed to produce melanin or a PS capsule, while deletion of the regulatory PKA subunit produced an enlarged PS capsule, resulting in a hypervirulent strain (D'Souza *et al.*, 2001). The transcription factor *Cn*Nrg1 is directly controlled by PKA phosphorylation and controls capsule formation and mating (Figure 1.7) (Cramer *et al.*, 2006). Additionally, PKA also controls the localization and therefore the function of the transcription factor *Cn*Rim101 (O'Meara *et al.*, 2010). *Cn*Rim101 is required for capsule formation, but also regulates iron homeostasis (O'Meara *et al.*, 2010). The receptor *Cn*Gpr4 and Gα protein *Cn*Gpa1 were identified as upstream components of the cAMP-PKA pathway (Alspaugh *et al.*, 1997; Xue *et al.*, 2006). A *Cngpr4*Δ strain showed defective cAMP signaling for methionine, while glucose was still able to induce a cAMP increase (Figure 1.7) (Xue *et al.*, 2006). This indicates that possibly multiple receptors control the pathway.

Plant pathogenic fungi

The cAMP-PKA pathway also affects morphogenesis in *Ustilago maydis*: the unicellular budding yeast is non-pathogenic while fusion of compatible haploid yeast cells leads to the development of biotrophic and pathogenic dikaryotic hyphae (Mehrabi *et al.*, 2009). This morphological transition is regulated by a mitogen activated protein kinase (MAPK) signaling, involved in mycelial growth, and the cAMP-PKA pathway, involved in yeast development (Ruiz-Herrera *et al.*, 2020). Cells with high cAMP levels or PKA activity are budding, while low cAMP levels or PKA activity are associated with filamentous growth (Agarwal *et al.*, 2013; Dürrenberger *et al.*, 1998; Gold *et al.*, 1994). The pheromone response transcription factor *Um*Prf1 is controlled by both the MAPK and PKA pathway, thereby regulating the expression of the mating type genes (Figure 1.7) (Kaffarnik *et al.*, 2003). Furthermore, the expression of several genes involved in iron uptake are controlled by *Um*Adr1, probably by the *Um*Rim101 and *Um*Urbs1 transcription factors (Choi *et al.*, 2015; Eichhorn *et al.*, 2006). Among environmental signals inducing hyphal formation, plant-derived triacyl glycerides are linked to the cAMP-PKA pathway in *U. maydis* (Klosterman *et al.*, 2007). Furthermore, the Gα protein *Um*Gpa3 was found to be upstream of adenylate cyclase (Mehrabi *et al.*, 2009).

The rice blast pathogen *Magnaporthe oryzae* produces a specialized morphological structure called appressorium to physically penetrate the plant cuticle and cell wall. An adenylate cyclase deletion strain (*Momac1*Δ) shows reduced growth, is unable to form an appressorium and has a reduced conidial germination (Figure 1.7) (Choi and Dean, 1997). There are two catalytic PKA subunits: *Mo*CpkA is the major subunit and *Mo*Cpk2 (Li *et al.*, 2017; Mitchell and Dean, 1995). *MocpkA*Δ strains have a delayed appressorium formation and the resulting appressoria are smaller. This makes that the strain cannot infect healthy plants, although plants with wounds can still be successfully penetrated (Kang *et al.*, 1999). While the single *MoCPK2* deletion strain has no effect on growth, conidiation or appressorium formation, a strain lacking both catalytic PKA subunits is completely avirulent (Li *et al.*, 2017; Selvaraj *et al.*, 2017). The nine TMD receptor *Mo*Pth11 is linked to recognition of the hydrophobic plant surface. Addition of exogenous cAMP to *Mopth11*Δ mutants induces appressorium formation, suggesting that the receptor is upstream of the pathway (DeZwaan *et al.*, 1999).

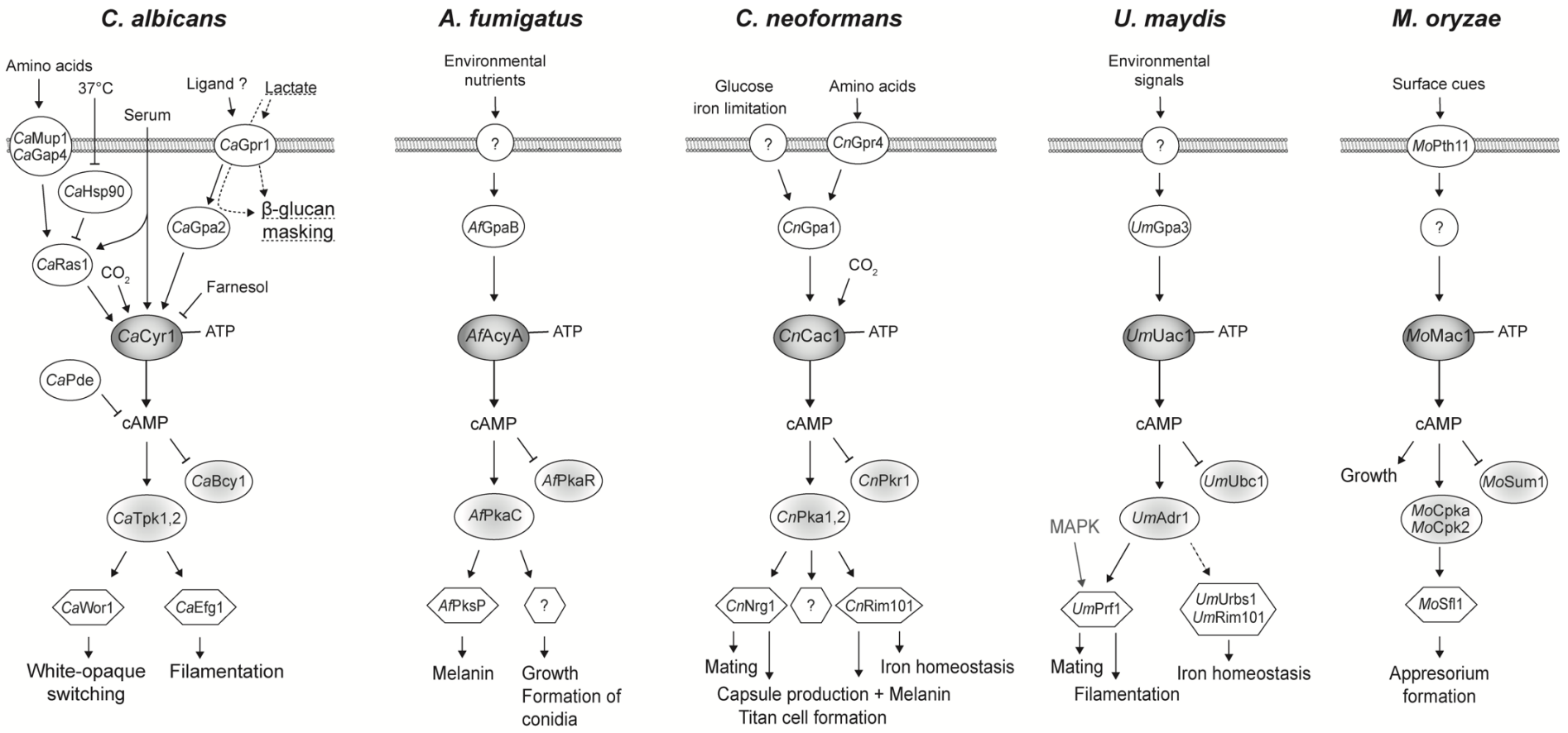

Figure 1.7: Overview of the cAMP-PKA pathway in the pathogens *C. albicans*, *A. fumigatus*, *C. neoformans*, *U. maydis* and *M. oryzae*.

The central components adenylate cyclase and PKA are conserved between species (marked in grey). While upstream signaling and downstream targets are more diverse, by evolutionary rewiring although morphology and virulence are general factors affected by the pathway. Transcription factors are depicted as hexagons.

1.4 Nutrient signaling

1.4.1 Glucose signaling

Besides being the preferred carbon source of *S. cerevisiae*, glucose also acts as a signaling molecule for several glucose specific signaling pathways. These include the Snf3/Rgt2 glucose sensing pathway, the glucose repression pathway and the cAMP-PKA pathway (Figure 1.8). Here, a general overview of the first two pathways is given (in depth reviews can be found by (Conrad *et al.*, 2014; Smets *et al.*, 2010; Van Ende *et al.*, 2019)), while the cAMP-PKA pathway was described in Section 1.3.

The Snf3/Rgt2 glucose sensing pathway

S. cerevisiae *Sc*Snf3 and *Sc*Rgt2 are a high-affinity and low-affinity glucose plasma membrane receptor, generating an intracellular signal for the induction of *ScHXT* gene expression (Özcan and Johnston, 1999). In the presence of glucose, the transcription factors *Sc*Std1 and *Sc*Mth1 are recruited to *Sc*Snf3/*Sc*Rgt2, where they are phosphorylated by the yeast casein kinase *Sc*Yck1. This leads to their ubiquitination by the *Sc*Grr1 ubiquitin ligase complex and subsequent degradation (Figure 1.8). As the repressor *Sc*Rgt1 requires *Sc*Mth1 and *Sc*Std1 for its activity, the presence of glucose relieves *Sc*Rgt1 repression of the *ScHXT* genes. In absence of glucose, *Sc*Mth1 and *Sc*Std1 are not degraded and therefore the *Sc*Rgt1-*Sc*Mth1/*Sc*Std1 repressor complex is formed at the promoters of the *HXT* genes (Figure 1.8) (Busti *et al.*, 2010; Conrad *et al.*, 2014; Van Ende *et al.*, 2019).

The glucose repression pathway

S. cerevisiae prefers glucose as a fermentable carbon source. Therefore, when glucose or another rapidly fermentable carbon source is present, the glucose repression pathway downregulates the utilization of alternative carbon sources (including gluconeogenesis, autophagy, the glyoxylate cycle) and respiration (Conrad *et al.*, 2014). The central protein of this pathway is the serine threonine protein kinase *Sc*Snf1. ScSnf1 is activated by phosphorylation in response to glucose limitation, by one of three upstream kinases (ScSak1, ScElm1 or ScTos3) (Figure 1.8). In presence of glucose, *Sc*Snf1 is inactivated by *Sc*Glc7-*Sc*Reg1 dephosphorylation (Figure 1.8). So far it is unclear how the glucose signal is transduced to *Sc*Snf1 (Busti *et al.*, 2010; Smets *et al.*, 2010).

Active *Sc*Snf1 inhibits the transcriptional repressor *Sc*Mig1 by phosphorylation, which promotes its nuclear export leading to the derepression of genes. When glucose becomes available, ScMig1 is dephosphorylated again, which makes it possible to translocate to the nucleus and subsequent repression of genes involved in the metabolism of alternative carbon sources. In absence of glucose, *Sc*Adr1, a transcription activator of genes involved in ethanol metabolism and fatty acid β-oxidation, is activated by *Sc*Snf1. The transcription activators *Sc*Cat8 and *Sc*Sip4, which control the expression of gluconeogenic genes, are activated by *Sc*Snf1 phosphorylation. *Sc*Snf1 also affects the activity of *Sc*Msn2/4 and *Sc*Gln3, thereby affecting their subcellular localization (Busti *et al.*, 2010; Conrad *et al.*, 2014; Kayikci and Nielsen, 2015; Smets *et al.*, 2010; Soontorngun *et al.*, 2007).

A glucose signaling network

While the paragraphs above give an overview of the separate glucose signaling pathways, the actual situation is more complex as several glucose signaling pathways have downstream effectors in common, which is visualized in Figure 1.8. One example is the transcription factor *Sc*Adr1, which is activated by the *Sc*Snf1 kinase of the glucose repression pathway in absence of glucose but is also negatively regulated by PKA in presence of glucose (Figure 1.8) (Busti *et al.*, 2010).

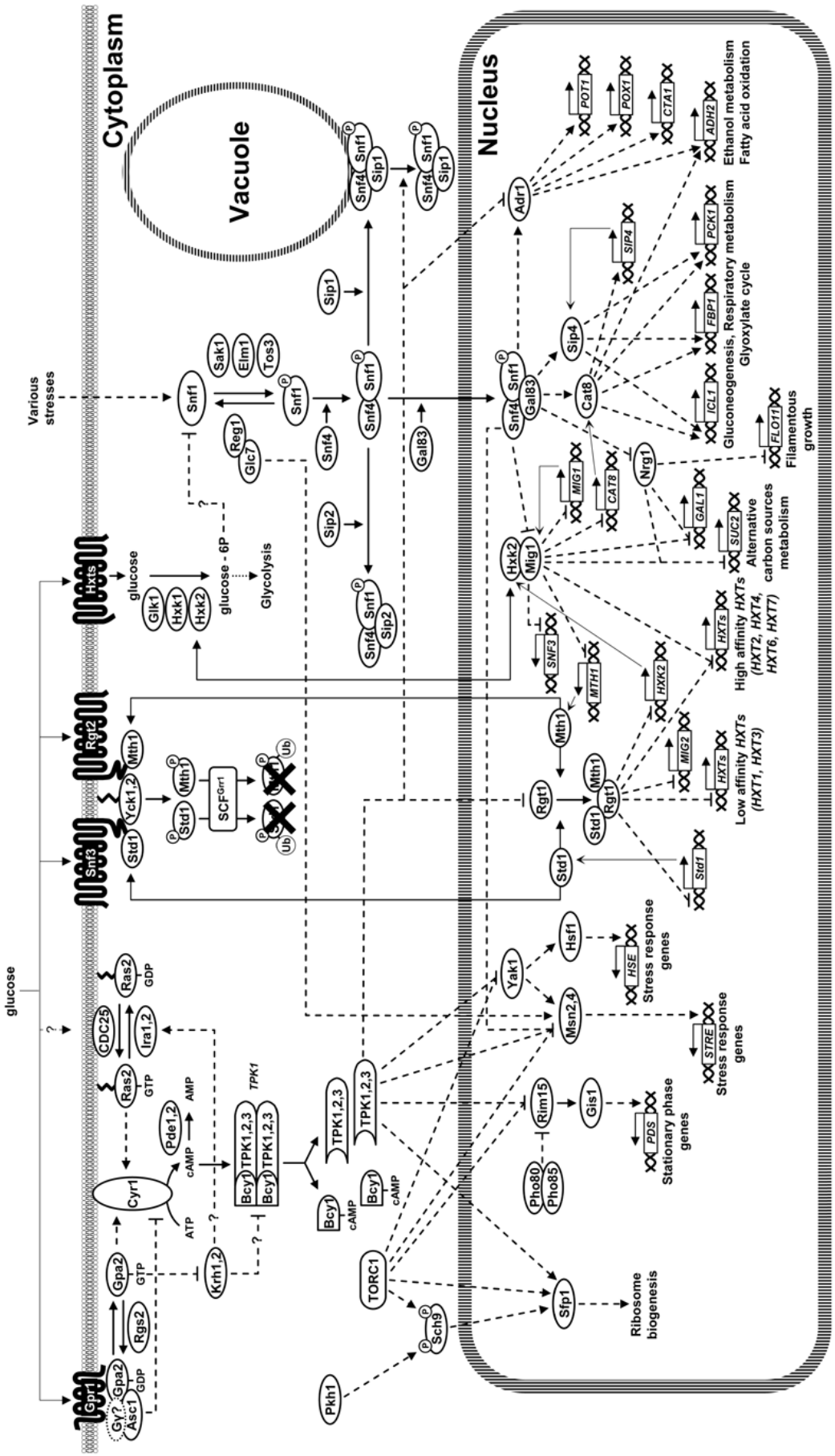

Figure 1.8: Overview of glucose signaling pathways in *S. cerevisiae*.
Schematic overview of the glucose repression pathway, the sugar receptor repressor pathway and the cAMP-PKA pathway. The interconnection with the TOR pathway is also indicated. Figure from Busti *et al.* (2010).

1.4.2 Connections with other nutrient sensing pathways

In vivo, not only glucose (and other sugars) triggers a signaling response, but also other nutrients including amino acids, nitrogen, phosphate etc. Therefore, this section describes two such integrative nutrient signaling pathways: the fermentable growth medium-induced pathway and the target of rapamycin (TOR) pathway.

The fermentable growth medium-induced pathway

When *S. cerevisiae* is starved for a single essential nutrient (e.g. nitrogen, phosphate, sulphate, iron or zinc) in the presence of a fermentative growth medium, cells display phenotypic properties associated with low PKA activity (high stress resistance, low trehalase activity). Upon re-addition of the missing nutrient, the phenotypes are rapidly reversed. This indicates that PKA is regulated by both the glucose-induced cAMP-PKA pathway and another nutrient-induced signaling pathway, which was therefore named the fermentable growth medium (FGM)-induced pathway (Thevelein, 1994).

The presence of the missing nutrient is sensed by transceptors, transporter(-like) proteins that also act as receptors (reviewed in Steyfkens *et al.* (2018) and Kriel *et al.* (2011)). For instance, the general amino acid permease *Sc*Gap1 mediates amino acid-induced signaling towards PKA (Donaton *et al.*, 2003; Van Zeebroeck *et al.*, 2009). The *Sc*Mep1 and *Sc*Mep2 ammonium permeases sense ammonium, inorganic phosphate-induced PKA signaling is dependent on the phosphate transporter *Sc*Pho84, *Sc*Sul1 and *Sc*Sul2 are sulphate transceptors, iron is sensed by the transceptor *Sc*Ftr1 and the zinc transporter *Sc*Zrt1 signals the presence of zinc in the medium (Giots *et al.*, 2003; Kankipati *et al.*, 2015; Popova *et al.*, 2010; Schothorst *et al.*, 2017; Van Nuland *et al.*, 2006).

In contrast to glucose-induced PKA activation, re-addition of the missing nutrient to the starved fermentable cells does not induce an intracellular cAMP increase, but still results in activation of PKA (Hirimburegama *et al.*, 1992; Van Zeebroeck *et al.*, 2020). Recently, direct interaction of *Sc*Gap1 with the catalytic PKA subunits was shown *in vitro* (Van Zeebroeck *et al.*, 2020). In addition, a common amino acid motive was found in the nutrient transceptors listed above as well as in the regulatory *Sc*Bcy1. Therefore a model to be further investigated is direct signaling from transceptor towards PKA (Van Zeebroeck *et al.*, 2020). To date, the exact mechanism by which the nutrient transceptors activate PKA remains to be elucidated.

The TOR pathway

Another major nutrient-responsive pathway in *S. cerevisiae* is the target of rapamycin (TOR) pathway regulating cell growth. The central protein of this pathway is the rapamycin-sensitive TORC1 kinase, consisting of the *Sc*Tor1 or *Sc*Tor2 protein kinase and the regulatory subunits *Sc*Lst8, *Sc*Tco89 and *Sc*Kog1 (Smets *et al.*, 2010). The TORC1 complex is regulated by intracellular amino acids: leucine and glutamine activate TORC1 through the EGO complex (EGOC) at the vacuolar membrane and form a scaffold for the Rag GTPases *Sc*Gtr1/2. When these amino acids are available in the cytoplasm, TORC1 is activated through this complex. High quality amino acids such as glutamine can also activate the TORC1 independent of EGOC, but the exact mechanism is not yet elucidated (Deprez *et al.*, 2018b). Apart from amino acids, also carbon availability activates the TORC1 complex through the vacuolar proton pump (V-ATPase) which activates *Sc*Gtr1. During fermentation, acetic acid is produced which dissociates inside the yeast cell causing intracellular acidification, counteracted by proton efflux through Pma1 and the V-ATPase-mediated vacuolar acidification (Deprez *et al.*, 2018a). Furthermore, in low glucose conditions, the *Sc*Snf1 protein kinase phosphorylates *Sc*Kog1 which reduces TORC1 activity.

TORC1 exerts most of its control via two branches: TORC1 activates the protein kinase *Sc*Sch9 by direct phosphorylation (Figure 1.8). In addition, *Sc*Sch9 can be phosphorylated by *Sc*Pkh1/2 and *Sc*Snf1. The protein kinase *Sc*Sch9 controls various cellular properties including cell cycle progression, cell size, autophagy, stress resistance through the protein kinase *Sc*Rim15, sphingolipid metabolism and protein synthesis (Deprez *et al.*, 2018b; Smets *et al.*, 2010). On the other hand, active TORC1 also phosphorylates *Sc*Tap42, which leads to inactive vacuolar membrane-associated complexes of *Sc*PP2A and *Sc*PP2A-like protein phosphate complexes. This downstream branch controls nitrogen and amino acid metabolism, the environmental stress response and autophagy (Conrad *et al.*, 2014; Deprez *et al.*, 2018b).

Chapter 2

The *C. glabrata* cAMP-PKA pathway affects trehalase activity and adhesion

2.1 Introduction

Previous work in our lab showed that the addition of glucose, fructose or sucrose to glucose-derepressed cells (glycerol as a carbon source) induces a cAMP increase in *C. glabrata* (Figure 2.1) (PhD thesis De Brucker, 2011). Based on the resemblance with *S. cerevisiae* cAMP signaling (described in Section 1.3.1), *C. glabrata* Gpr1 and Gpa2 were shown to be required for the sugar-induced cAMP increase. In addition, these proteins display the typical structural features of a transmembrane receptor and G protein and interact with one another, which was shown using a split-ubiquitin assay (unpublished results De Brucker, 2011). Furthermore, it was shown that the cAMP pathway rendered the cells more sensitive to heat stress and affected trehalose mobilization. The latter was delayed but not abolished in the *gpr1*Δ and *gpa2*Δ strains, indicating that the cAMP pathway is involved in the fast mobilization but is not required for the maintenance of phenotype. Subsequently, it was investigated if the cAMP-induced pathway also affects virulence or virulence factors, as this is true in several other pathogenic yeasts (described in Section 1.3.2). *C. glabrata* adhesion to polystyrene was indeed reduced in presence of the cAMP-inducing sugars and this effect depends on the presence of Gpr1. However, *in vivo*, the *gpr1*Δ strain did not show an altered virulence phenotype in a fly model of *C. glabrata* candidiasis (unpublished results, De Brucker, 2011) (Quintin *et al.*, 2013). Furthermore, De Brucker also showed that the *C. glabrata* Krh proteins form a similar bypass pathway as is the case in *S. cerevisiae*.

In this work, we aim to further elucidate the *C. glabrata* cAMP-PKA pathway. Firstly, we connected the intracellular levels of cAMP with *C. glabrata* PKA activity. Then, downstream targets were further investigated: as was shown that the fast trehalose mobilization is affected by the pathway, as a complementary argument we investigated the activation of trehalase. Finally, we further examined the role of the cAMP-PKA pathway in the control of the clinically relevant phenotype adhesion. We therefore aimed to prove that sugar signaling affects adherence and subsequently investigated which adhesin or adhesins are responsible for the observed phenotype.

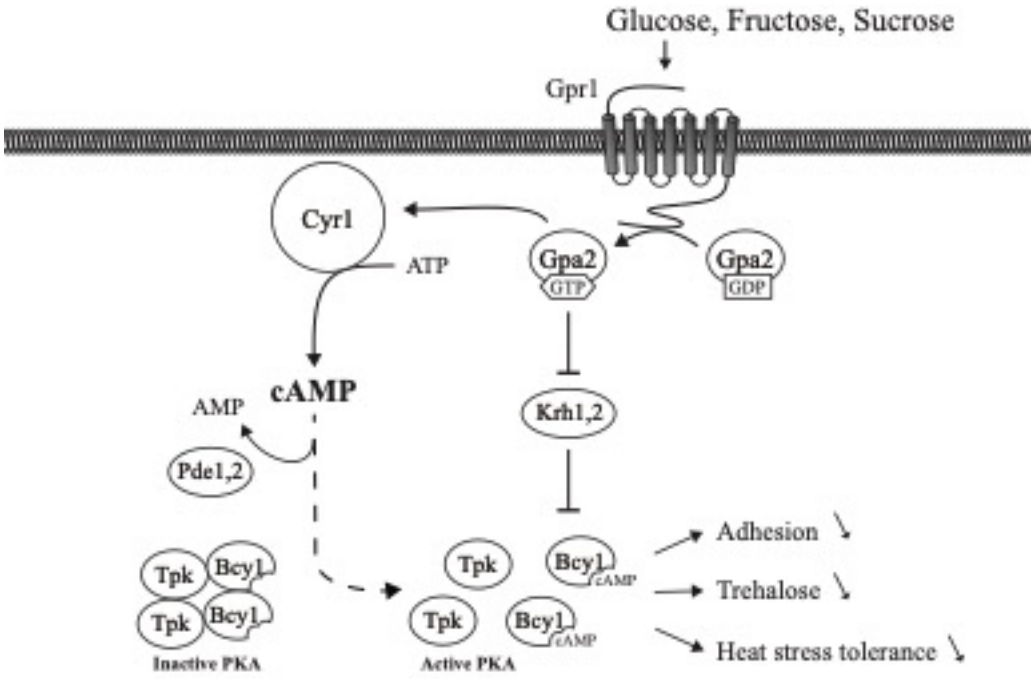

Figure 2.1: Overview of unpublished research on the *C. glabrata* cAMP-PKA pathway.
Glucose, fructose and sucrose induce a cAMP increase via Gpr1 and Gpa2. The Krh proteins function as negative regulators of PKA associated phenotypes. Activation of the cAMP-pathway results in the mobilization of trehalose and cells become more sensitive to heat stress. Addition of the cAMP-inducing sugars lowers adhesion to polystyrene and depends on the presence of Gpr1. The figure was made based on the unpublished results of the PhD thesis De Brucker (2011).

2.2 Results

2.2.1 *C. glabrata* protein kinase A is activated by cAMP

As mentioned in the introduction, De Brucker previously showed that the addition of glucose induces an intracellular cAMP increase. Therefore, we examined if cAMP activates protein kinase A (PKA) in *C. glabrata*. PKA is a heterotetrameric protein complex consisting of two regulatory and two catalytic subunits. When cAMP binds to the PKA regulatory subunits in *S. cerevisiae*, this causes the release and thereby activation of the PKA catalytic subunits (Toda *et al.*, 1987). The *C. glabrata* genome contains one homolog of the *S. cerevisiae* regulatory subunit *ScBCY1*, *BCY1* (CAGL0I05236g) and two homologs of the catalytic subunits: *TPK1* (CAGL0M08404g) and *TPK2* (CAGL0G09020g), homologous to *ScTPK3* and *ScTPK2* respectively

(Figure 2.2A). Inspection of the genomic loci of these genes also shows that there is no *C. glabrata* ortholog of *S. cerevisiae TPK1* (Figure 2.2B). To assess the PKA activity of the individual subunits, the *C. glabrata* single *TPK1* and *TPK2* deletion strains were constructed (described in Materials and methods).

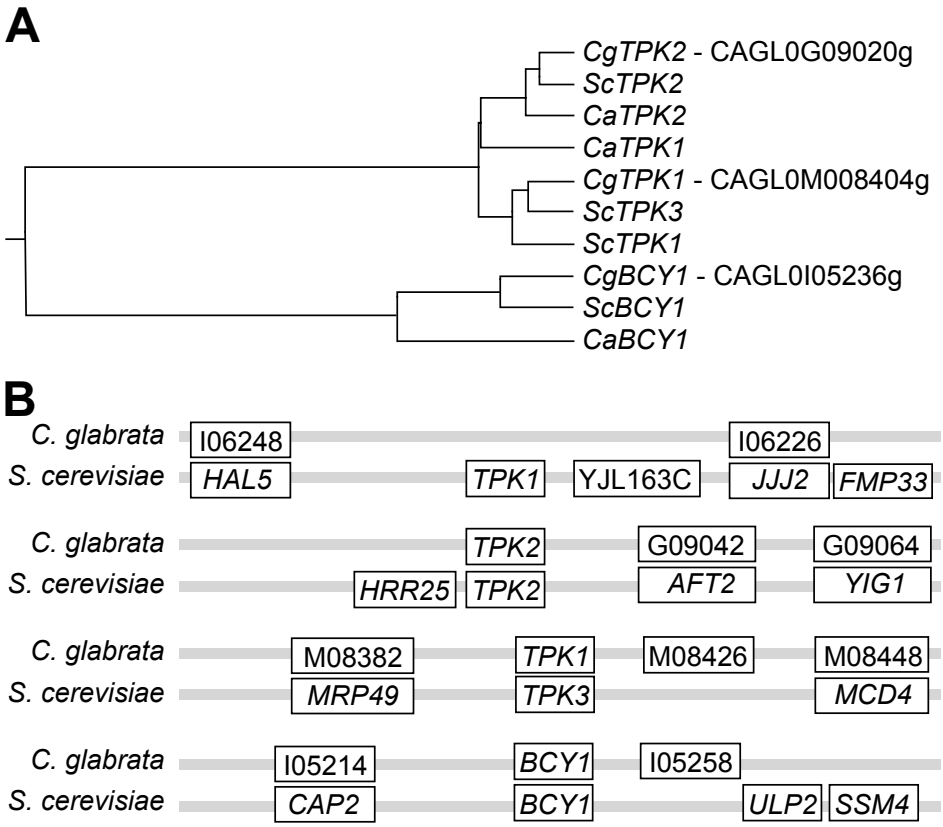

Figure 2.2: Phylogenetic tree of the PKA subunits (A) and synteny (B).
The *C. glabrata*, *S. cerevisiae* and *C. albicans* PKA subunit protein sequences were used to construct the phylogenetic tree. The unweighted pair method with arithmetic mean (UPGMA) was used for tree construction and the Kimura Protein model as a protein distance measure (A). Schematic representation of the *C. glabrata* and *S. cerevisiae* syntenic loci of the *TPK* and *BCY1* ORFs, based on the yeast gene order browser (Byrne and Wolfe, 2005) (B).

C. glabrata PKA activity was measured using different cAMP concentrations with the synthetic peptide kemptide (LRRASLG), which contains the PKA consensus sequence, as the substrate. In the wild type strain, PKA activity increased with elevating concentrations of cAMP (Figure 2.3A). The PKA activity of Tpk2 (*tpk1*Δ strain) also increased with rising cAMP concentrations, although in general its activity was lower compared to the wild type strain (Figure 2.3A). On the other hand, Tpk1

(*tpk2*Δ strain) showed a relatively constant PKA activity at all cAMP concentrations tested (Figure 2.3A). PKA activity of Tpk1 coincided with the basal PKA activity of the wild type strain (Figure 2.3B). The expression of the catalytic subunits in the single *TPK* deletion strains was checked to exclude that the difference in PKA activity in the two strains was caused by differences in transcript levels. There was no significant difference in expression of the catalytic subunits in single deletion strains compared to the wild type strain (Figure 2.4).

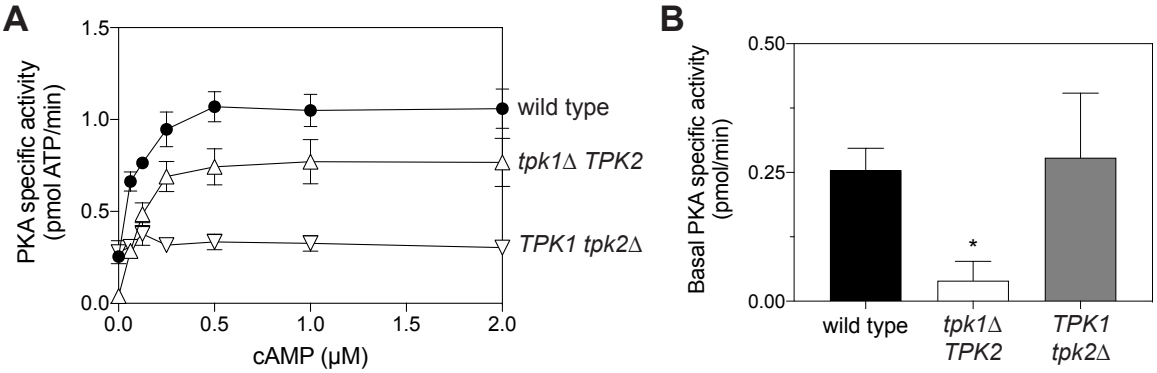

Figure 2.3: *C. glabrata* PKA activity increases with rising cAMP concentrations. The wild type (●), *tpk1*Δ *TPK2* (△) and *TPK1 tpk2*Δ (▽) strains were tested. Using the peptide kemptide and [γ-^{32}P] labeled ATP, PKA phosphorylation using whole cell extracts was measured at the indicated cAMP concentrations (as described in Materials and methods). Average PKA specific activity with standard error of mean (SEM) of two deletion strains and two independent experiments is shown as pmol ATP/min (A). Average basal PKA activity of the wild type strain and the two *TPK* deletion strains with standard error of mean (SEM) is shown (B). Statistical analysis was conducted by one-way ANOVA with Bonferroni correction, comparing the deletion strains to the wild type strain (*, P = 0.0189) (B).

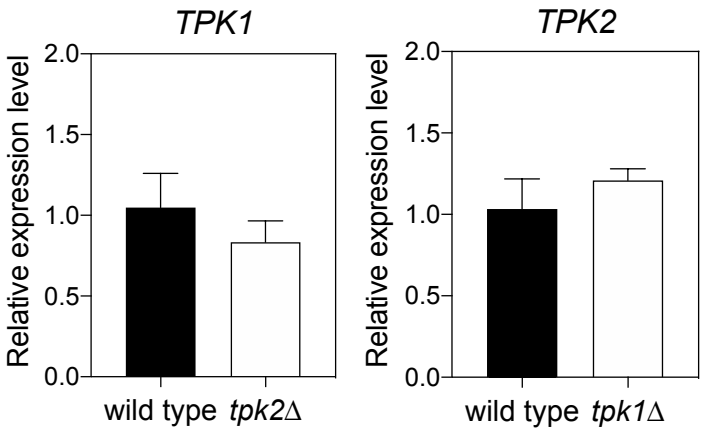

Figure 2.4: The expression of the catalytic subunits is not significantly different in the single *TPK* deletion strains compared to the wild type strain.
Using quantitative reverse transcriptase PCR, gene expression was analyzed of cells grown identically to the kemptide assay. Gene expression is shown relative to the wild type strain and the average of two independent transformants and three independent experiments with SEM is shown. Statistical analysis was conducted using an unpaired Student's t-test for each gene.

2.2.2 The neutral trehalase Nth1 is a target of the cAMP-PKA pathway

Previous work of De Brucker also showed that the cAMP-inducing sugars induce a rapid trehalose mobilization (PhD thesis De Brucker, 2011). Trehalose, a disaccharide of two glucose molecules joined by α,α-1,1-glycosidic bond, is a reserve carbohydrate and serves as a stress protectant in many organisms. In *S. cerevisiae*, trehalose accumulates in glucose-deprived cells and when conditions are favorable it is broken down into two glucose molecules by the cytosolic trehalase *Sc*Nth1, which depends on PKA phosphorylation of *Sc*Nth1 (Schepers *et al.*, 2012). Therefore, trehalase activation is commonly used in *S. cerevisiae* as a read-out of the PKA pathway. As we characterized the *C. glabrata* trehalase enzymes in this work (Chapter 4), we also investigated in this chapter if the cAMP-PKA pathway controls trehalase activity.
Therefore, cells were grown in glycerol as a carbon source, as such the cAMP-PKA pathway is not active, after which trehalase activity was measured at different timepoints before and after addition of glucose (activation of the pathway) or galactose (control) to the cells. In the wild type strain, trehalase activity increased upon addition of glucose but the trehalase activity before addition of the sugar was already very high (± 150 nmol glucose/min.mg protein) (Figure 2.5). To address this high basal trehalase

activity, we compared the trehalase activity of glycerol grown cells of the wild type to double trehalase deletion strains (Figure 2.5B), as there are three trehalases present in *C. glabrata*: Ath1, Nth1 and Nth2 (Chapter 4). Therefore, the individual contribution of each gene can be assessed using the different double trehalase deletion strains. Our results showed that the high trehalase activity was caused by the acid trehalase Ath1, as trehalase activity was significantly lower in the strains with *ATH1* deleted, while the *nth1*Δ *nth2*Δ strain showed a high trehalase activity, comparable to the wild type strain (Figure 2.5B).

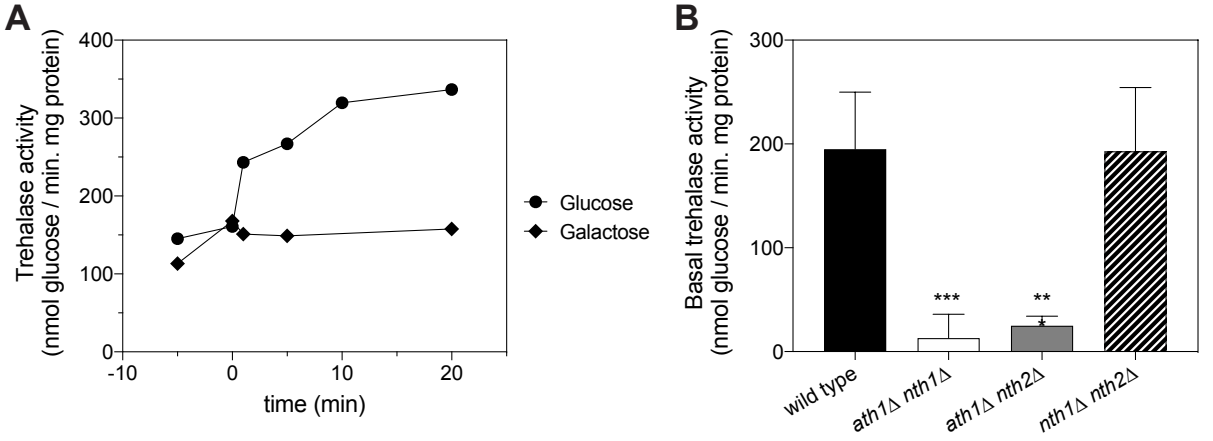

Figure 2.5: Wild type *C. glabrata* displays a high trehalase activity which further increases upon addition of glucose.
Cells were grown to exponential phase in glycerol, after which 100 mM of glucose or galactose was added to the cells at timepoint zero. Trehalase activity was measured at different timepoints, up to 20 min after addition of the sugar and is expressed as nmol glucose per min and per mg protein. Data of one representative time-course experiment is shown, but at least two independent experiments were conducted (A). Average basal trehalase activity of glycerol grown cells with SEM is shown of at least two independent experiments. Statistical analysis was conducted comparing the deletion strains to the wild type strain using one-way ANOVA with Bonferroni correction (**, $P < 0.01$; ****, $P < 0.0001$) (B).

To investigate which of the trehalase(s) is activated by glucose, we tested trehalase activity upon addition of glucose or galactose in the double trehalase deletion strains (Figure 2.6). The strains expressing only *ATH1* or *NTH2* showed a constant trehalase activity upon addition of glucose (Figure 2.6 B-C). In contrast, the strain expressing only the neutral trehalase *NTH1* showed a rapid increase in trehalase activity after addition of the cAMP-inducing sugars (Figure 2.6A). Subsequently, we deleted *GPR1*

or *GPA2* in the *ath1*Δ *NTH1 nth2*Δ strain (described in Materials and Methods). The glucose-induced activation of trehalase Nth1 was absent when *GPR1* or *GPA2* were deleted, indicating the cAMP-PKA pathway controls the glucose-induced activation of Nth1 (Figure 2.7).

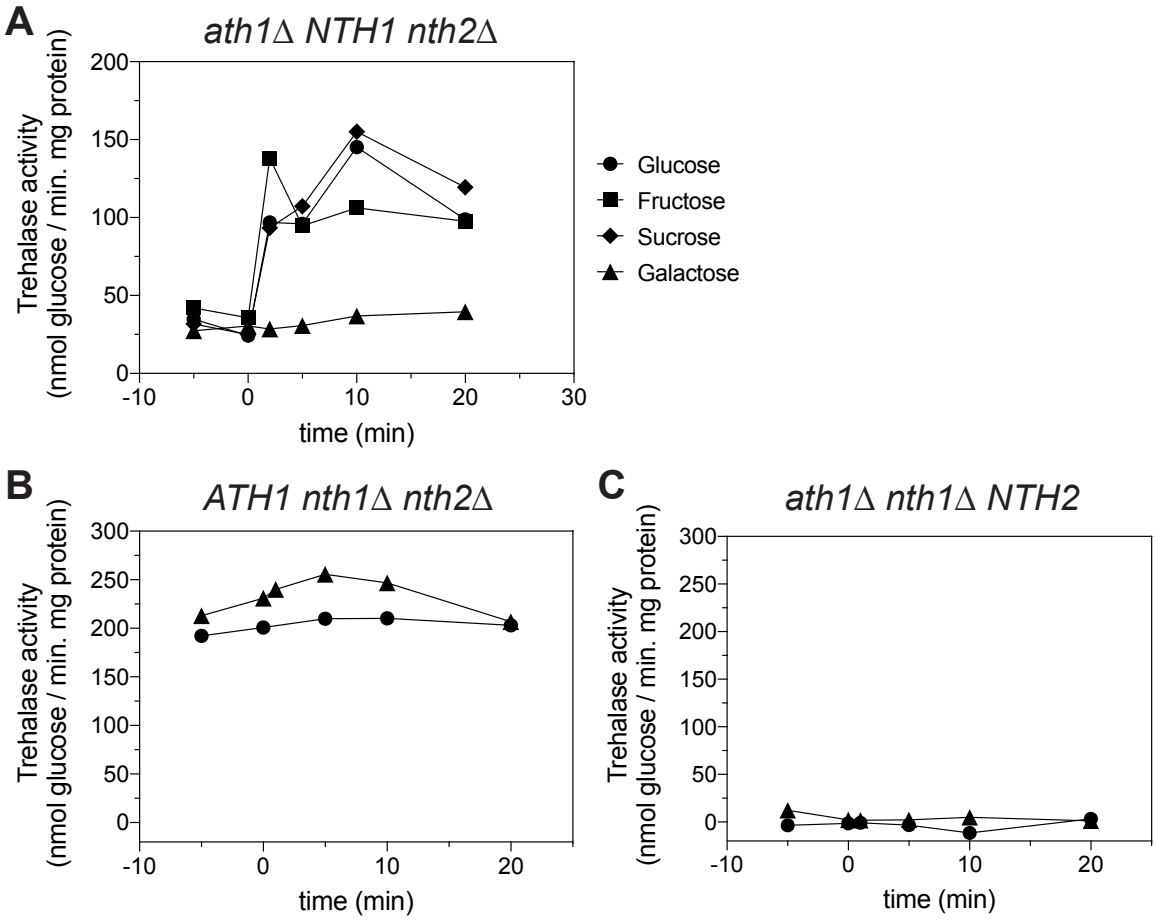

Figure 2.6: *C. glabrata* Nth1 trehalase activity increases upon addition of the cAMP-inducing sugars.

The strains were grown to exponential phase in glycerol and at timepoint zero, the indicated sugar (final concentration of 100 mM) was added to the cells. Trehalase activity was measured at different timepoints, up to 20 min after addition of the sugar and is expressed as nmol glucose per min and per mg protein. The *ath1*Δ *nth2*Δ strain (A), *nth1*Δ *nth2*Δ (B) and *ath1*Δ *nth1*Δ (C) strains were tested. Data of one representative time-course experiment is shown, but at least two independent experiments were conducted.

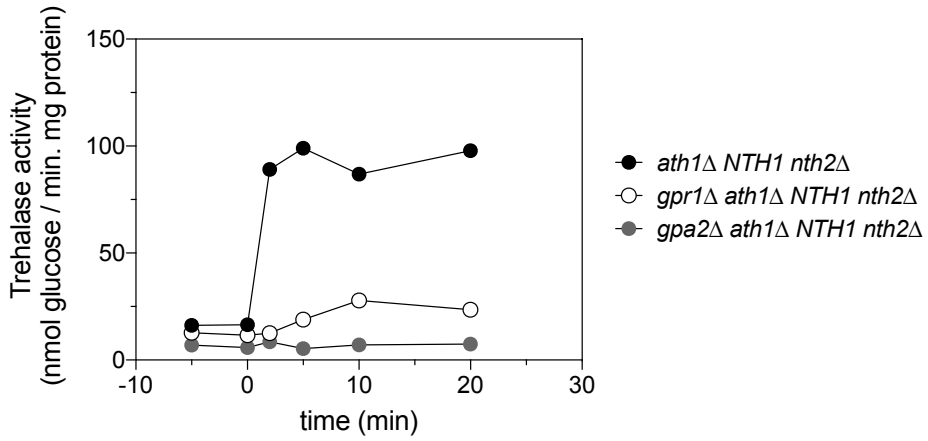

Figure 2.7: The glucose-induced Nth1 trehalase activation depends on the presence of Gpr1 and Gpa2.

Similar growth conditions and experimental procedures were used as Figure 2.6. Glucose was added to the indicated strains at timepoint zero. Trehalase activity is expressed as nmol glucose per min and per mg protein. Data of one representative time-course experiment is shown, but at least two independent experiments were conducted.

2.2.3 The cAMP-PKA pathway lowers adhesion to polystyrene

In *C. glabrata*, biofilm formation is the main virulence factor which is initiated by adherence of the yeast cells to a surface (Section 1.2.4.2). As the cAMP-PKA pathway controls different virulence factors in several pathogenic fungi (Section 1.3.2) and as previous work of De Brucker suggested that the cAMP-PKA pathway regulates adhesion in *C. glabrata*, we further investigated this phenotype.

Therefore, wild type *C. glabrata* was grown to exponential phase in glycerol (low PKA activity). The cells were subsequently resuspended in presence of glucose, sucrose, fructose, galactose or no sugar as a control. 10^6 cells were added to the polystyrene wells and incubated for 90 minutes (adhesion). Adhesion was indeed significantly reduced in presence of the cAMP-inducing sugars, while the addition of galactose showed a similar adherence compared to the no sugar condition (Figure 2.8).

As many *C. glabrata* adhesins contain a N-terminal carbohydrate-binding domain, it is necessary to demonstrate that the reduced adhesion is an effect of signaling and exclude direct binding of the carbohydrates in the medium to the adhesin in the *C. glabrata* cell wall, thereby affecting the adhesion phenotype. Therefore, we first tested adhesion in the *GPR1* and *GPA2* deletion strains, which did not show a significantly reduced adherence in presence of the cAMP-inducing sugars (Figure 2.8).

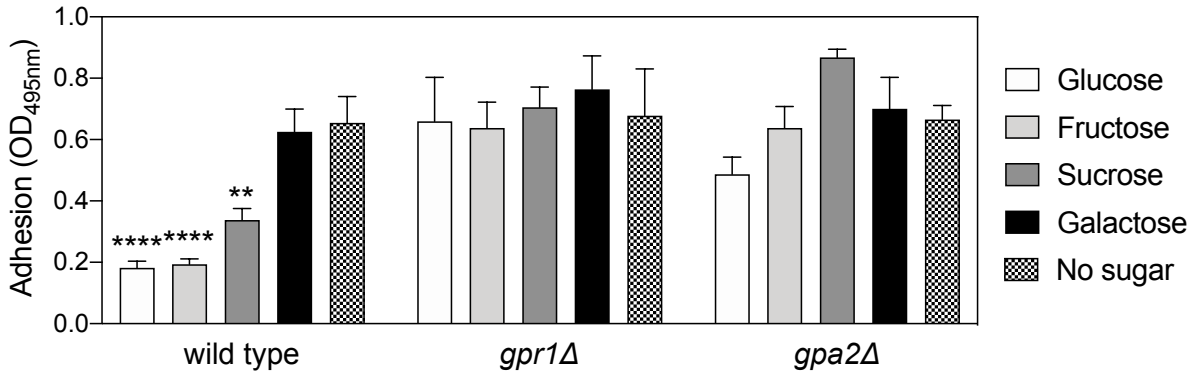

Figure 2.8: Adherence to polystyrene is lower in presence of the cAMP-inducing sugars and depends on the presence of the GPCR Gpr1 and Gpa2.

The strains were grown to exponential phase in glycerol (low PKA activity) and resuspended in medium containing the indicated sugar (2%). 10^6 cells were added to wells of a 96-well plate and incubated for 90 minutes. After washing, adhesion was read out by the XTT reduction assay. Average OD_{495nm} with SEM is shown of three independent experiments. Statistical analysis was conducted using two-way ANOVA with Bonferroni correction comparing the addition of each sugar to the no sugar condition for each strain (**, $P < 0.01$; ****, $P < 0.0001$).

Secondly, we introduced a single amino acid substitution in Gpa2 (Gln^{299} to Leu, in the conserved region common for G proteins), which rendered it a constitutively dominant active allele with reduced GTPase activity, based on literature (Harashima and Heitman, 2002). The constitutively active Gpa2 allele or wild type Gpa2 as a control were introduced in the *gpr1*Δ and *gpa2*Δ strains, after which the resulting strains were tested for adhesion. Introduction of wild type *GPA2* in the *gpa2*Δ strain restored the wild type adhesion phenotype, while in the *gpr1*Δ strain, the high adhesion was still present (Figure 2.9). However, when the constitutive active *GPA2*^{Q299L} allele was introduced in the *gpr1*Δ and *gpa2*Δ strains, both resulting strains showed a low adherence phenotype independent on the sugar in the medium (Figure 2.9). These results indicate that the cAMP-PKA signaling affects *C. glabrata* adhesion.

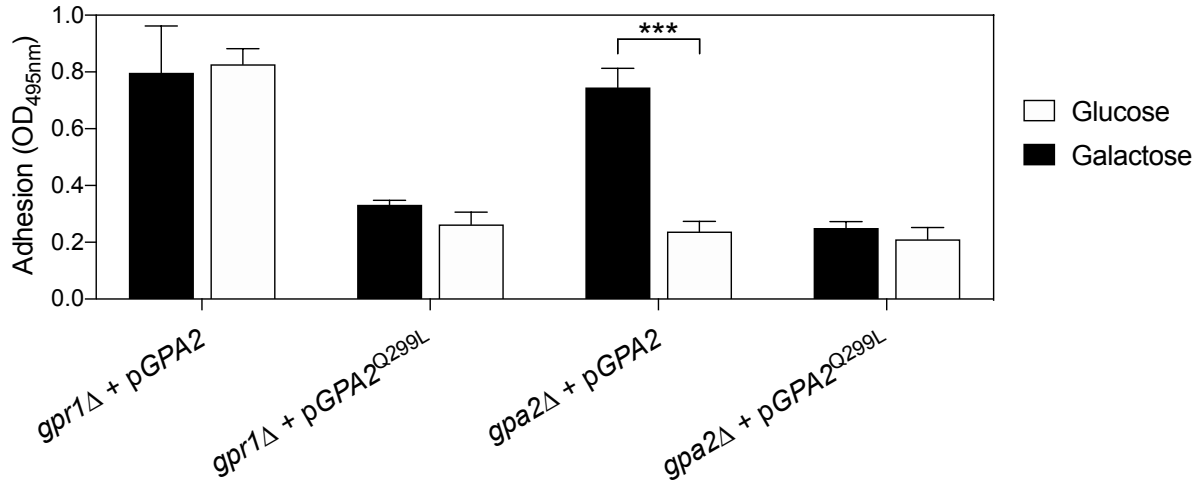

Figure 2.9: Introduction of the constitutive active *GPA2*^{Q299L} allele results in cells with a low adhesion phenotype independent of the sugar in the medium.
A centromeric *C. glabrata* plasmid containing wild type *GPA2* or the constitutive *GPA2* under the native *GPA2* promoter were introduced in the *gpr1*Δ strain and *gpa2*Δ strain. The indicated strains were grown to exponential phase in glycerol as a carbon source (low PKA activity) in complete medium minus tryptophan and resuspended in presence of glucose or galactose (2%). 10^6 cells were added to wells of a 96-well plate and incubated for 90 minutes. After washing, adhesion was read out by the XTT reduction assay. Average OD_{495nm} with SEM is shown of at least two independent experiments. Statistical analysis was conducted using two-way ANOVA with Bonferroni correction comparing the addition of glucose to galactose for each strain (***, $P < 0.001$).

We also tested adherence in presence of different sugar concentrations (Figure 2.10), to assess a correlation with the affinity of Gpr1 for the sugars (PhD thesis De Brucker, 2011). As expected, there was no drop in adhesion with elevating galactose concentrations (Figure 2.10). For both glucose and fructose, a similar reduction in adherence was present with increasing concentrations (Figure 2.10). In presence of sucrose, only the highest concentrations tested showed a modest reduction in adhesion (Figure 2.10).

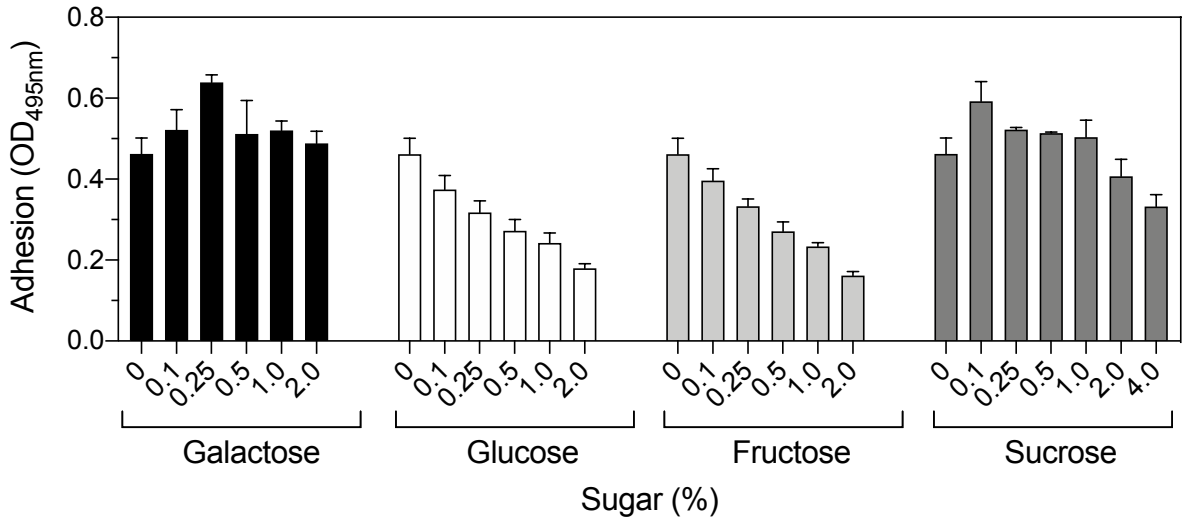

Figure 2.10: The reduction in adherence depends on the concentration of the cAMP-inducing sugar.
The strains were grown to exponential phase in glycerol as a carbon source (low PKA activity) and resuspended in presence of the indicated sugar at the indicated concentration. 10^6 cells were added to wells of a 96-well plate and incubated for 90 minutes. After washing, adhesion was read out by the XTT reduction assay. Average OD_{495nm} with SEM of three independent experiments is shown.

Finally, we wanted to demonstrate carbohydrate signaling through Gpr1, by testing adherence of strains with a single amino acid substitution in the Gpr1 ligand binding pocket. It was previously shown for *S. cerevisiae Sc*Gpr1 that transmembrane domain six and the third extracellular loop are involved in ligand binding (Lemaire et al., 2004). As glucose and sucrose are cAMP-inducing sugars in both *S. cerevisiae* and *C. glabrata*, we compared the ligand binding sequences of *Sc*Gpr1 to *C. glabrata* Gpr1, showing many identical amino acids (Figure 2.11). Based on the findings of Lemaire

et al. (2004) in *S. cerevisiae*, *C. glabrata* Gpr1 amino acids P572, A575, D576 and Q579 were selected for SCAM analysis.

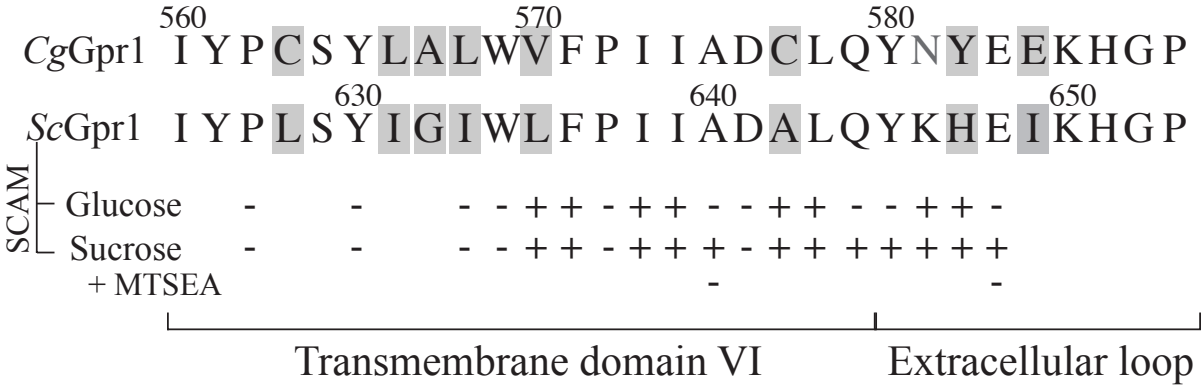

Figure 2.11: The ligand binding domain of *S. cerevisiae Sc*Gpr1 and *C. glabrata* Gpr1 share many identical amino acids.
Amino acid alignment of *S. cerevisiae Sc*Gpr1 TMD VI and the following extracellular loop to *C. glabrata* Gpr1. Non-identical amino acids are shaded in grey. For *Sc*Gpr1, the glucose- and sucrose-induced signaling from the SCAM analysis of Lemaire *et al.* (2004) is summarized below the *Sc*Gpr1 amino acid sequence: + indicates that substitution into cysteine did not affect signaling for the indicated sugar, while – indicates that signaling was deficient by substitution of the amino acid into cysteine. A pretreatment of MTSEA abolished sucrose signaling for allele A640C and E648C, as indicated in the figure.

Therefore, a plasmid containing Gpr1 with the indicated amino acid substitution was introduced in the *gpr1*Δ strain (described in Materials and methods). As control conditions, the wild type, *gpr1*Δ and *gpa2*Δ strains were included in the experiment. In presence of glucose, the P572C mutant showed a high adherence similar to the *gpr1*Δ strain, while the A575C and Q579C mutants showed a reduced adhesion similar to the wild type strain (Figure 2.12). In presence of fructose and sucrose, the P572C and D576C strains showed high adhesion, while A575C and Q579C did not give a conclusive result but rather an intermediate adhesion phenotype (Figure 2.12).

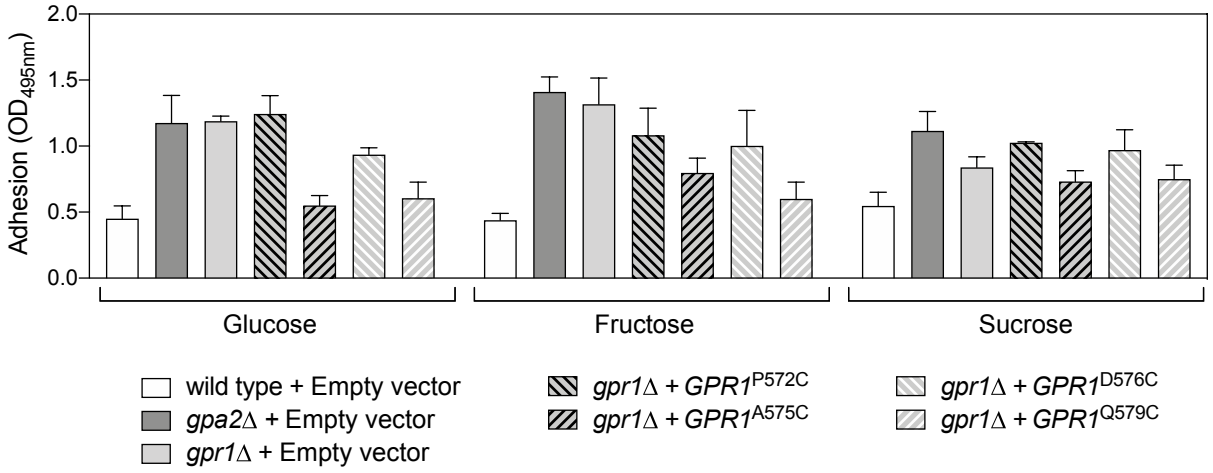

Figure 2.12: Adhesion of the Gpr1 SCAM strains.
The strains were grown to exponential phase in glycerol as a carbon source (low PKA activity) and resuspended in presence of the indicated sugar (2%). 10^6 cells were added to wells of a 96-well plate and incubated for 90 minutes. After washing, adhesion was read out by the XTT reduction assay. Average OD_{495nm} with SEM of three independent transformants of one experiment is shown.

2.2.4 The adherence phenotype is present in different *C. glabrata* background strains

As there is a lot of variability in the number of genes encoding for adhesins in different *C. glabrata* genomes (described in Section 1.2.4.2.1), we also tested if glucose was able to reduce adherence in several different background strains from our lab collection, including two clinical isolates. All strains showed a low adherence phenotype in presence of glucose, while adhesion was somewhat variable in presence of galactose (Figure 2.13). This indicates that the cAMP-PKA pathway controls adhesion in the variety of strains tested and is most likely common for all *C. glabrata* strains, including the clinical isolates.

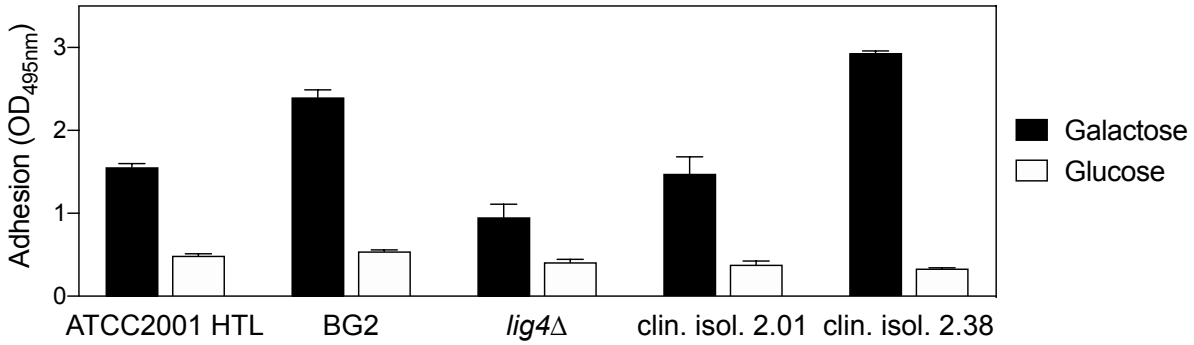

Figure 2.13: Different *C. glabrata* background strains show a reduced adherence to polystyrene in presence of glucose.
The strains were grown to exponential phase in glycerol as a carbon source (low PKA activity) and resuspended in medium containing glucose or galactose (2%). 10^6 cells were added to wells of a 96-well plate and incubated for 90 minutes. After washing, adhesion was read out by the XTT reduction assay. Average OD_{495nm} with SEM is shown of at least two independent experiments.

2.2.5 Adhesion to catheters is not affected by the cAMP-PKA pathway

Next, we tested the adherence phenotype to catheters, which represents another abiotic surface commonly tested in the lab for *Candida* adhesion and biofilm formation. In the commonly used protocol, catheters are coated with fetal bovine serum (FBS) overnight before addition of the *Candida* inoculum. To compare the results with the adherence to the uncoated polystyrene 96-well plates, we also included the untreated catheters in this assay. Therefore, the cells were grown in glycerol as a carbon source, as such the PKA pathway is not active. Then glucose (activation of PKA pathway) or

galactose (control) was added to the cells and incubated with the catheter pieces for 90 minutes. In both conditions, there was no significant difference between adherence in presence of glucose or galactose (Figure 2.14). Furthermore, it was also noticeable that *C. glabrata* prefers to adhere to the uncoated catheter pieces.

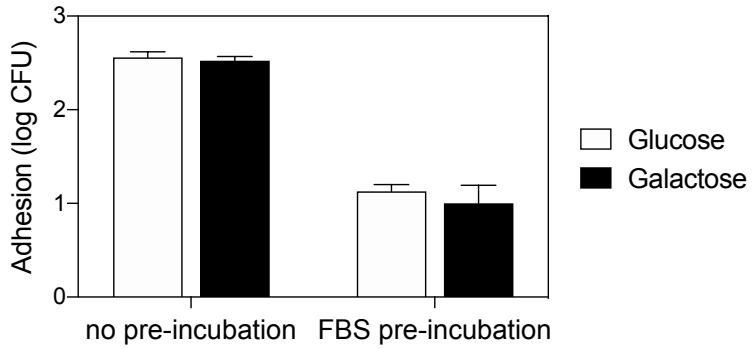

Figure 2.14: Adherence to catheters is not affected by the sugar present in the medium.
When indicated, catheters were coated overnight with FBS. Wild type *C. glabrata* was grown in glycerol and resuspended in medium containing glucose or galactose (2%). The catheters and 10^6 *C. glabrata* cells were incubated for 90 minutes, after which the catheters were washed and plated for CFU counting. Adhesion is shown as average log CFU with SEM of three independent experiments and three technical repeats. Statistical analysis was conducted comparing glucose to galactose using an unpaired Student's t-test.

2.2.6 Epa1, Epa6 and Epa7 do not represent the adhesins downstream of the cAMP-PKA pathway affecting adhesion to polystyrene

Recently, it was published that when sub-telomeric silencing is lost, Epa1, Epa6 and Epa7 at least partially mediate hydrophilic as well as hydrophobic interactions (Valotteau *et al.*, 2019). This study also reported that when silencing is intact, adhesion to abiotic surfaces is mediated by other unidentified proteins. As a first step in our search for putative downstream adhesins of the cAMP-PKA pathway, we investigated if the presence of these three *EPA* genes affected the adhesion phenotype observed in our conditions. Therefore, we tested adhesion of the BG2 wild type strain and the triple *epa1*Δ *epa6*Δ *epa7*Δ deletion strain. The triple *epa1*Δ *epa6*Δ *epa7*Δ deletion strain and the BG2 *ura3*Δ parent strain showed an identical adhesion profile (Figure 2.15), indicating these adhesins are not the responsible adhesins in our assay and therefore not downstream of the cAMP-PKA pathway.

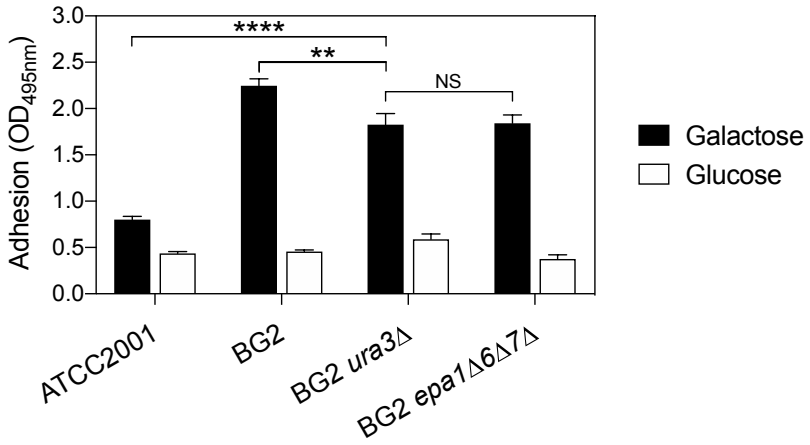

Figure 2.15: Adhesion is not affected in the *epa1*Δ *epa6*Δ *epa7*Δ strain.
The strains were grown to exponential phase in glycerol as a carbon source (low PKA activity) and resuspended in medium containing glucose or galactose (2%). 10^6 cells were added to wells of a 96-well plate and incubated for 90 minutes. After washing, adhesion was read out by the XTT reduction assay. Average OD_{495nm} with SEM is shown of at least two independent experiments. Statistical analysis was conducted using two-way ANOVA with Bonferroni correction for the sugar conditions separately, comparing the strains to the BG2 *ura3*Δ background strain (**, P < 0.01; ****, P < 0.0001). Adhesion was not significantly different in presence of glucose.

2.3 Discussion

In order to survive, microorganisms need to adapt quickly to changes in the environment. Therefore, sensing the extracellular status and transmission of the signals intracellularly through the appropriate pathways is crucial. In this chapter, we investigated the cAMP-PKA pathway in the opportunistic pathogen *C. glabrata*, continuing the work previously performed in our lab by PhD thesis De Brucker (2011). cAMP signaling in *C. glabrata* is induced by glucose, fructose and sucrose, in contrast to *C. albicans* (Biswas *et al.*, 2007; PhD thesis De Brucker, 2011). In the phylogenetically closely related *S. cerevisiae*, glucose and sucrose elicit a cAMP increase through the GPCR *Sc*Gpr1-*Sc*Gpa2 (Kraakman *et al.*, 1999; Lemaire *et al.*, 2004). Logically, the alignment of residues in the Gpr1 ligand binding pocket of *C. glabrata* and *S. cerevisiae* showed a high degree of conservation, supporting their similarities in ligand specificity. Yet, there are also some differences: *C. glabrata* Gpr1 functions as a receptor for fructose, which is not the case in *S. cerevisiae* (Lemaire *et al.*, 2004; PhD thesis De Brucker, 2011). Furthermore, the affinity for sucrose is the

lowest for *C. glabrata* cAMP induction, while sucrose is the preferred carbohydrate of *Sc*Gpr1 (Lemaire *et al.*, 2004). Despite the fact that sucrose cannot be utilized as a carbon source by *C. glabrata*, sucrose still is a ligand of Gpr1 (Dujon *et al.*, 2004). An explanation for this unexpected sucrose signaling is that *C. glabrata* has lost its sucrose metabolism, among which the invertase gene, in its reductive evolution and because Gpr1 not only signals sucrose but also glucose, *GPR1* was not lost during evolution.

Similar to other fungi, we showed that cAMP activates *C. glabrata* PKA (D'Souza *et al.*, 2001; Liebmann *et al.*, 2004; Lin *et al.*, 2018; Portela *et al.*, 2002; Souto *et al.*, 2006). In line with our results, Demuyser *et al.* (2018) reported both the induction of a cAMP signal as well as an increase in PKA activity *in vivo* after addition of glucose to glucose-starved wild type C. *glabrata* cells. Our findings indicate that Tpk1 activity coincides with the basal PKA activity, while Tpk2 activity increases with elevating cAMP concentrations. Yet, the *in vivo* role of different catalytic PKA subunits can have different effects on the cellular properties and this is not always straightforwardly connected to their activity. For instance, a *C. tropicalis Cttpk1*∆ strain shows a slight reduction in PKA activity, while *Ct*Tpk1 is shown to be important for antifungal resistance and *Ct*Tpk2 affects flocculation (Lin *et al.*, 2018; Zhang *et al.*, 2016). In *C. albicans*, *Ca*Tpk2 is responsible for the majority of PKA activity (Souto *et al.*, 2006). Still, both *Ca*Tpk subunits have distinct cellular roles: for example, hyphal formation on solid medium is mediated by *Ca*Tpk1 while *Ca*Tpk2 affects invasive growth and morphogenesis in liquid medium (Bockmühl *et al.*, 2001; Cloutier *et al.*, 2003). In *C. glabrata,* Tpk2 is involved in the feedback inhibition of the cAMP signal similar to *S. cerevisiae Sc*Tpk2 (Mbonyi *et al.*, 1990; PhD thesis De Brucker, 2011).

The activation of PKA leads to the phosphorylation of downstream targets, affecting multiple phenotypic properties of the cells (Thevelein and de Winde, 1999). In *S. cerevisiae*, the activation of trehalase is commonly used as a read out of PKA activity. As we characterized the *C. glabrata* trehalase enzymes (Chapter 4), the possibility of the cAMP-PKA pathway controlling trehalase activity was assessed. First of all, we observed a high trehalase activity of *C. glabrata* cells grown in glycerol (± 150 nmol glucose/min.mg protein) compared to glucose (± 5 nmol glucose/min.mg protein, data not shown) as well as compared to *S. cerevisiae* glycerol-grown cells (± 20 nmol

glucose/min.mg protein, data not shown). In the clinic, the rapid hydrolysis of trehalose is used to diagnose *C. glabrata* infections in a quick and cost-effective way, which is caused by a high Ath1 activity suggesting Ath1 causes the high basal activity seen in our experiment (Fraser *et al.*, 2012; Lopez *et al.*, 2001; Willinger *et al.*, 2005; Zilli *et al.*, 2015). This is indeed true, as a *C. glabrata* strain expressing only *ATH1* shows a comparable trehalase activity as the wild type strain. Furthermore, our results show that the neutral *C. glabrata* trehalase Nth1 is rapidly activated by the cAMP-PKA pathway, while the addition of glucose does not affect Ath1 or Nth2 activity. The rapid activation of Nth1 suggests post-translational activation by PKA phosphorylation, similar to *S. cerevisiae* in which Ser^{21} and Ser^{83} were shown to be phosphorylated after addition of glucose (Schepers *et al.*, 2012; van der Plaat, 1974). The regions containing these residues are highly conserved, supporting this hypothesis. Therefore, the phospho-specific antibodies used in *S. cerevisiae* are currently tested in our lab for use in *C. glabrata*. Furthermore, future work includes the generation of single amino acid substitutions of the homologous *C. glabrata* serine residues and subsequent measurement of trehalase activation after cAMP-PKA pathway activation. Nth1 affects the stress resistance properties of *C. glabrata* cells as the *nth1*Δ strain is more sensitive towards oxidative stress *in vitro* (Van Ende and Timmermans *et al.*, 2020). Cells deleted for *NTH1* are also less sensitive to heat stress and this coincided with higher levels of trehalose in the cells (Van Ende, unpublished results). Yet, our *in vivo* experiments (Chapter 4) show that the different trehalases combined rather than one specific trehalase affects colonization in the gastro-intestinal tract or virulence in a mouse model of systemic infection (Van Ende and Timmermans *et al.*, 2020).

Besides stress resistance, the cAMP-PKA pathway often controls important virulence factors in fungal pathogens (Biswas *et al.*, 2007; Grosse *et al.*, 2008; Kronstad *et al.*, 2011). Adhesion and subsequent biofilm formation are considered as crucial for virulence in *C. glabrata* (Galocha *et al.*, 2019; Kaur *et al.*, 2005). This is also apparent from the high number of predicted adhesin genes present in the *C. glabrata* genome (de Groot *et al.*, 2008; Timmermans *et al.*, 2018). We show that *C. glabrata* adherence to polystyrene is significantly lower in the presence of the cAMP-inducing sugars and depends on the presence of *GPR1*, suggesting that the cAMP-PKA pathway controls adhesion to polystyrene (PhD thesis De Brucker, 2011). As many adhesins, including the important *EPA* family, contain a carbohydrate-binding domain (Ielasi *et al.*, 2016;

Zupancic *et al.*, 2008), it is important to differentiate whether the reduced adherence phenotype is caused by sugar signaling via the cAMP-PKA pathway instead of direct binding of the carbohydrates to the cell wall adhesins. Therefore, we investigated signaling mutants: when either *GPR1* or *GPA2* was deleted, thereby eliminating the sugar GPCR system, the significant decrease in adhesion is absent. Secondly, the introduction of a dominant active allele of Gpa2 by a single amino acid substitution renders the cells almost non-adherent independent of the sugar present in the medium. Thirdly, based on the *S. cerevisiae* data of Lemaire *et al.* (2004) (Figure 2.11), we introduced single amino acid substitutions in the Gpr1 ligand binding pocket and tested these strains for adhesion in the presence of the cAMP-inducing sugars. A high adhesion phenotype is seen for Gpr1^{P572C} and Gpr1^{D576C} in the presence of glucose, fructose and sucrose, indicating signaling is impaired. While this in line with the results seen in *Sc*Gpr1, the result is not conclusive as it needs to be checked if the Gpr1 mutants are present in the membrane. On the other hand, in the presence of fructose and sucrose, the adhesion phenotype of the Gpr1^{A575C} and Gpr1^{Q579C} substitutions show an intermediate adhesion phenotype. Interestingly, glucose signaling is not abolished in the Gpr1^{A575C} and Gpr1^{Q579C} strains, in contrast to the homologous substitutions in *S. cerevisiae* (Lemaire *et al.*, 2004). Especially in the presence of sucrose, the adhesion phenotype of the mutants is weakly affected, probably because *C. glabrata* Gpr1 has a low affinity for sucrose compared to *S. cerevisiae* (PhD thesis De Brucker, 2011). While the 96-well format adhesion assay can be used to test several conditions (semi high-throughput), it is also a very delicate assay. We therefore propose to test the conditions with intermediate adhesion results in the strains in presence of the cAMP and PKA FRET (fluorescence resonance energy transfer) biosensors of Demuyser *et al.* (2018) as a follow-up experiment for clarity. Furthermore, we also tested adherence in the presence of different sugar concentrations in wild type *C. glabrata*. For glucose and fructose, a gradual decrease in adherence was seen with elevating concentrations, while this trend was less pronounced for sucrose. However, this can be explained as previous research showed that the affinity of Gpr1 for sucrose is lower than glucose and fructose (PhD thesis De Brucker, 2011).

Our results confirm that Gpa2 is acting downstream of Gpr1, in line with the split ubiquitin assay showing interaction between the Gpr1 C-terminus and Gpa2 (PhD

thesis De Brucker, 2011): introduction of wild type Gpa2 in the *gpr1*Δ strain does not affect adhesion, while introduction of the dominant active Gpa2 allele lowers adhesion. On the other hand, we tested if the reduction in adhesion in presence of glucose is present in different *C. glabrata* strains, as there is a high genomic variability between background strains and especially in genes encoding for adhesins (described in Section 1.2.4.2.1). Three lab strains and two clinical isolates all show the reduced adhesion in presence of glucose, indicating the phenotype is common. Noticeably, when the cAMP-PKA pathway is not active, there is some level of variability in adherence between the strains. This might be caused by the expression of a different set of adhesins between the strains, or by differences in expression of the responsible adhesins which can be due to a variable degree of sub-telomeric silencing (Martinez-Jimenez *et al.*, 2013).

We also investigated how the cAMP-PKA pathway causes the adhesion phenotype in *C. glabrata*. Adherence to abiotic surfaces is correlated with a high cell surface hydrophobicity (CSH) and is mediated by hydrophobic interactions rather than specific receptor-adhesin ligand interactions. The range of adhesins present at a given moment in the cell wall affects the CSH of the cells (Klotz *et al.*, 1985; Luo and Samaranayake, 2002). Evidence from literature shows that Epa6, which contains a high number of hydrophobic residues, at least partially mediates *in vitro* adhesion to polystyrene (El-Kirat-Chatel *et al.*, 2015). Furthermore, the same group recently published that Epa1, Epa6 and Epa7 affect both hydrophilic and hydrophobic interactions in absence of *C. glabrata* sub-telomeric silencing (Valotteau *et al.*, 2019). We therefore started our search for the adhesins downstream of the pathway by investigating the triple *EPA* deletion strain in our assay, which shows a wild type adhesion phenotype indicating other adhesin(s) are involved.
In *S. cerevisiae*, overexpression of flocculin (Flo) cell wall proteins increases the cell wall hydrophobicity (Van Mulders *et al.*, 2009). While *Sc*Flo1, *Sc*Flo5, *Sc*Flo9 and *Sc*Flo10 promote flocculation (cell-cell adhesion), *Sc*Flo11 mediates adhesion to agar and polystyrene (Reynolds and Fink, 2001; Verstrepen and Klis, 2006). Moreover, *ScFLO11* expression is controlled by protein kinase A via the transcriptional activator *Sc*Flo8 and repressor *Sc*Sfl1, which are directly phosphorylated by *Sc*Tpk2 (Conlan and Tzamarias, 2001; Pan and Heitman, 2002; Robertson and Fink, 1998). PKA phosphorylation inhibits *Sc*Sfl1 binding to the *ScFLO11* promoter, while

phosphorylated *Sc*Flo8 activates its binding *in vivo* (Pan and Heitman, 2002). Based on these findings, the *C. glabrata* homolog of *ScFLO11* would represent a relevant cell wall protein to investigate in our adhesion assay. However, the *ScFLO11* genomic region is not syntenic and also a protein blast search to the *C. glabrata* genome did not identify any significant homologous proteins.
Because of the high number of *C. glabrata* adhesins and as many of these genes are uncharacterized, we continued our search for the responsible adhesins in a genome-wide transcriptome study by RNA sequencing, described in the next chapter.

Changes in the expression of the adhesins responsible for adhesion can serve as an adaptation of the pathogen to nutritional signals encountered in the host. This strategy was already shown by Domergue *et al.* (2005) as the expression of *EPA6* depends on the levels of nicotinic acid in the host niche. In this case, a low concentration of nicotinic acid resulted in the inactivation of Sir2, which is part of the sub-telomeric silencing complex, resulting in the relief of silencing and expression of *EPA6* (Domergue *et al.*, 2005). In our assay, we show that the activation of the cAMP-PKA pathway reduces *C. glabrata* adhesion to polystyrene. At first sight, it might seem counterintuitive that when the environmental conditions become optimal (e.g. in presence of glucose), the cells lower adhesion. We hypothesize that when the conditions are favorable, *C. glabrata* cells prefer to disperse in the host to other environments, while in sub-optimal circumstances cells attach and subsequently form a protective environment by means of a biofilm. This hypothesis is supported by a study in *C. albicans* showing that glucose indeed affects the preference to either form a biofilm or disperse as planktonic cells (Uppuluri *et al.*, 2010).

2.4 Materials and methods

Yeast strains, plasmids and primers

Table 2.1: List of *C. glabrata* strains used in this chapter

Strain	Background / Genotype	Source
311	ATCC2001 *his3Δ:::FRT leuΔ:::FRT trp1Δ:::FRT*	(Schwarzmüller *et al.*, 2014)
315	BG2	(Cormack *et al.*, 1999)
317	BG2 *ura3Δ*	(Castaño *et al.*, 2005; Valotteau *et al.*, 2019)
804	Clinical isolate 2.01	Provided by Prof. K. Lagrou, Lab collection
8011	Clinical isolate 2.38	Provided by Prof. K. Lagrou, Lab collection
3884	ATCC2001 *lig4Δ::HIS3 leuΔ::FRT trp1Δ::FRT*	(Cen *et al.*, 2015)
3911	BG2 *epa1Δ epa6Δ epa7Δ*	(Castaño *et al.*, 2005; Valotteau *et al.*, 2019)
HT631	*gpr1Δ*::NatMX *his3Δ leuΔ trpΔ*	Lab collection
HT633	*gpa2Δ*::NatMX *his3Δ leuΔ trpΔ*	Lab collection
*Cg*B1	*tpk1Δ*::NatMX *his3Δ leuΔ trpΔ*	This work
*Cg*B2	tpk2Δ::NatMX *his3Δ leuΔ trpΔ*	This work
*Cg*BM4	*ath1Δ*::FRT *nth1Δ*::FRT *NTH2*	This work
*Cg*BM5	*ath1Δ*::FRT *NTH1 nth2Δ*::FRT	This work
*Cg*BM6	*ATH1 nth1Δ*::FRT *nth2Δ*::FRT	This work
*Cg*B3	*gpr1Δ*::NatMX *ath1Δ*::FRT *NTH1 nth2Δ*::FRT	This work
*Cg*B4	*gpa2Δ*::NatMX *ath1Δ*::FRT *NTH1 nth2Δ*::FRT	This work

Table 2.2: List of plasmids used in this chapter

Plasmid	Relevant genotype	Used for	Source
pYC44	NatMX cassette flanked by FRT sites	Construction of deletion cassette	(Yáñez-Carrillo *et al.*, 2015)
p*CgACT1*	*TRP1*	Centromeric expression vector for *C. glabrata*	(Miyazaki *et al.*, 2010)
p*CgACT1-GPA2*	*GPA2*^{WT}	Expression of wild type Gpa2	This work
p*CgACT1-GPA2*^{Q299L}	*GPA2*^{Q299L}	Expression of constitutive active Gpa2	This work
p*CgACT1*-Gpr1^{P572C}	*GPR1*^{P572C}	Expression of Gpr1 with amino acid substitution	This work
p*CgACT1*-Gpr1^{A575C}	*GPR1*^{A575C}	Expression of Gpr1 with amino acid substitution	This work
p*CgACT1*-Gpr1^{D576C}	*GPR1*^{D576C}	Expression of Gpr1 with amino acid substitution	This work
p*CgACT1*-Gpr1^{Q579C}	*GPR1*^{Q579C}	Expression of Gpr1 with amino acid substitution	This work

A list of primers used in this chapter can be found in Addendum 1.

Cultivating conditions

Yeast cells were grown in either YP (1% yeast extract, 2% bacteriological peptone) or synthetic complete (SC) medium (1.7 g/L Difco yeast nitrogen base without amino acids and without ammonium sulphate, 0.79 g/L complete supplement mixture [CSM; MP Biomedicals], 5 g/L ammonium sulphate). These media were supplemented with a carbon source as indicated in the experiment. For solid media, 15 g/L Difco agar granulated was added.

Construction of plasmids

p*Cg*ACT-Gpa2^{WT} was constructed by ligation of BamHI digested plasmid p*CgACT1* and BamHI digested PCR product containing the *GPA2* promoter, wild type *GPA2* and *GPA2* terminator (primers B3007 and B3008, Addendum 1). p*CgACT1*-Gpa2^{Q299L} was constructed by ligation of BamHI digested plasmid p*CgACT1* and BamHI digested fusion PCR product containing the *GPA2* promoter, *GPA2* ORF containing the desired point mutation and *GPA2* terminator (primers B3007 and B3009; B3008 and B3010). Correct insertion was checked by PCR using primers B4165 and B4166, after which the vector was verified by sequencing.

The p*CgACT1*-Gpr1 plasmids containing a single point mutation (P572C; A575C; D576C or Q579C) were constructed in SacI and SphI digested p*CgACT1*. For each plasmid, the insert containing the desired mutation was amplified in two pieces: a first part consisted of the *GPR1* promoter and beginning of *GPR1* ORF until the mutation, amplified using primers B6103 and 'Gpr1-mutation Rv' (Addendum 1). The second part consisted of *GPR1* ORF starting from the mutation and the *GPR1* terminator, amplified using primers B6279 and 'Gpr1-mutation Fw' (Addendum 1). Subsequently, the two inserts were inserted in the digested and dephosphorylated vector by Gibson assembly. Correct insertion of the two pieces was checked by PCR using primers 6973 plus B3074 and A2265 plus A4486 (Addendum 1). Finally, the correct mutations were all verified by sequencing the resulting plasmids.

Construction of C. glabrata strains

The strains generated in this study were generated in the wild type ATCC2001 HTL (*his3*Δ *leu2*Δ *trp1*Δ) background (Schwarzmüller *et al.*, 2014), using the dominant nourseothricin resistance marker (Reuß *et al.*, 2004; Yáñez-Carrillo *et al.*, 2015). Deletion constructs for *TPK1* and *TPK2* were made by fusion PCR of 500 bp

homologous upstream and downstream sequences flanking the target gene to the nourseothricin marker. First, the upstream and downstream flanking sequences were amplified by PCR (Addendum 1: primers 'ORF upstream' or 'ORF downstream'). The selectable nourseothricin marker was amplified from plasmid PYC44 using primers 9351 and 9356. Subsequently, the upstream and downstream sequence were used as primers for fusion PCR on the nourseothricin marker as template. The complete deletion construct was transformed by *C. glabrata* electroporation (Reuß *et al.*, 2004) and cells were plated on YPD agar containing nourseothricin (200 µg ml^{-1}). Transformants were checked by PCR using primers outside the region used for homologous recombination (Addendum 1 primers 'ORF control upstream Fw' with primer 9064 and 'ORF control downstream Fw' with primer 9065).
Plasmids based on the p*CgACT1* vector were transformed in the indicated strains by electroporation, after which colonies were plated on -TRP selective medium.

Determination of trehalase activity
C. glabrata was grown to mid-exponential phase in glycerol containing medium and at timepoint zero, the indicated carbon source was added to the cells. Samples of 50 mg cells were harvested at different time points. The cells were resuspended in 500 µL ice-cold extraction buffer (50 mM Mes/KOH pH 7.0, 50 µM CaCl2) and lysed by vigorous shaking (FastPrep). The lysates were centrifuged at 14 000 rpm for 5 min at 4°C, after which the lysates were dialyzed overnight at 4°C on dialysis membrane (SpectraPor) and dialysis buffer (10 mM Mes buffer pH 7.0, 50 µM CaCl2). Trehalase activity was determined as described in (Pernambuco *et al.*, 1996). In short, crude extracts were incubated with 50 µL trehalose buffer (250 µM trehalose, 62.5 mM Mes/KOH, pH 7.0, 125 µM CaCl2). After 30 minutes of incubation at 30°C, the reaction was terminated by boiling for 5 minutes at 90°C. The glucose liberated was determined by the glucose oxidase–peroxidase method. Protein levels were determined by the Lowry method. Trehalase specific activity is expressed as nmol of glucose released per min and mg of protein.

In vitro assay of PKA activity

The activity of PKA was measured in vitro using kemptide, a peptide (LRRASLG) containing the PKA consensus phosphorylation sequence RRXS/TY (Y tends to be hydrophobic). Using γ-labeled ^{32}P-ATP, phosphorylation of kemptide by the cell extracts was measured. The strains were grown to exponential phase in YPD at 37°C. The cells were harvested by centrifugation and washed in ice-cold water. Yeast extracts were prepared by vigorous shaking (FastPrep) in 500 µL ice-cold lysis buffer (PBS 1X, 1 mM DTT, 1 mM EDTA pH 8.0, 10% glycerol, 0.1 mM β-glycerophosphate, 2.5 mM $MgCl_2$, 10 mM NaF, 0.4 mM Na_3VO_4, 0.1% Triton X-100 and one tablet of protease inhibitor mix (complete, EDTA-free, Roche) per 10 mL of lysis buffer) in presence of glass beads. Cell lysates were centrifuged at 14 000 rpm at 4°C for 15 minutes. Protein concentrations were determined using Pierce™ 660nm protein assay (Thermofisher). The crude extracts were diluted to a final concentration of 250 µg/µL. The kinase reaction mixture consisted of 1 mg protein of cell extract, 300 µM kemptide (Innovagen), 5 µg bovine serum albumin (BSA), the cAMP concentration indicated, up to a total volume of 50 µL in kinase buffer (25 mM Tris pH 8.0, 1 mM β-glycerophosphate, 2 mM Na_3VO_4). PKA activity was measured as a function of the cAMP concentration (0, 0.125, 0.250, 0.5, 1, 2, and 5 µM cAMP). The kinase reaction was initiated by addition of [γ-32P] ATP (final concentration of 0.1 µCi/µL) in 0,1 mM ATP and 1.5 mM $Mg(CH_3COO)_2$. After 15 minutes of incubation at 30°C, the kinase reaction was terminated by spotting 10 µL on a phosphocellulose filter paper (Whatman P81). The filters were washed three times 20 min in phosphoric acid (0.5% v/v) and once in acetone. After drying, the radioactivity was measured using a scintillation counter (Hidex 300SL). A blanc measurement (reaction without crude protein extract) and specific activity (a sample of the radioactive ATP mixture directly) were also measured. The specific activity measurement (CPM/pmol ATP) was used to determine the phosphorylation of the kemptide substrate.

RNA extraction and gene expression analysis by qRT-PCR

The strains were grown to exponential phase in YPD at 37°C. The cells were harvested by centrifugation and washed in ice-cold water. The cells were resuspended in TRIzol (ThermoFisher) and broken using glass beads and a FastPrep machine. RNA was extracted by addition of chloroform and isopropanol. After three washes with

70% ethanol, the RNA was treated with deoxyribonuclease enzyme (DNase, New England Biolabs). The complementary DNA (cDNA) was prepared using the iScript cDNA synthesis kit (Bio-Rad). The qPCR reactions were done in the StepOnePlus Real-Time PCR device using the GoTaq polymerase (Promega). The resulting data were analyzed in qBasePlus (Biogazelle) and Graphpad Prism. *GAPDH*, *RPL10*, *RPL13A*, *RPL2A*, *UBC13* and *ACT1* were used as reference genes, after analysis by geNorm in the qBasePlus software (Biogazelle).

In vitro adhesion to polystyrene

Adhesion to polystyrene was tested as described in Ramage *et al.* (2001). In short, cells were washed twice in phosphate buffered saline (PBS) and diluted to 10^7 cells ml^{-1} in the desired medium. 10^6 cells were added to per well of a 96 well plate and incubated for 90 minutes at 37°C. Non-adherent cells were removed by washing twice with PBS. The quantification of adherent cells was measured using 2,3-bis(2-methoxy-4-nitro-5-sulphophenyl)-2*H*-tetrazolium-5-carboxanilide assay (XTT, Sigma). 100 µl of XTT (1 mg/ml) and 1 µM menadione (Sigma) was added to each well and incubated for one hour at 37°C, after which the optical density at 495 nm was measured.

In vitro adhesion to catheters

The polyurethane catheters were divided in pieces of 1 cm and incubated overnight in fetal bovine serum (FBS) at 37°C when indicated in the figure. *C. glabrata* cells were washed twice in phosphate buffered saline (PBS), after which a cell suspension of 10^6 cells/mL was prepared in the indicated medium. For adhesion, the individual catheter pieces were incubated in 1 mL inoculum at 37°C for 90 minutes. Subsequently, the catheters were washed twice with 1 mL of PBS and transferred to a new Eppendorf tube with 1 mL PBS. After sonication (10 min, 40 000 Hz) and 30 seconds of vortexing, serial dilution was plated on YPD agar. Afterwards, colony forming units (CFUs) were counted after incubation at 37°C. For each condition, at least three technical repeats (catheter pieces) were used.

Chapter 3

The *C. glabrata* transcriptome in response to glucose and galactose

3.1 Introduction

In Chapter 2, we showed that glucose, sucrose and fructose activate the cAMP-PKA pathway in *C. glabrata*, through the GPCR system Gpr1 and Gpa2. While the previous chapter focused on specific downstream targets, here we wanted to obtain a broad overview of the cellular processes in response to the addition of glucose and galactose. Therefore, we investigated the *C. glabrata* transcriptome in response to glucose and galactose using RNA sequencing. In the following sections, the genome-wide transcriptional response comparing glucose and galactose will be discussed, followed by the analysis of both carbohydrate responses separately. Furthermore, we will zoom in on the cAMP-PKA pathway transcriptional response and the adhesin glucose-induced transcriptome.

3.2 Results

3.2.1 RNA sequencing conditions

The RNA sequencing growth conditions were matched with the experiments performed in Chapter 2. Therefore, the cells were grown to exponential phase in presence of glycerol as a carbon source, so PKA activity is low, after which either glucose to induce activation of cAMP-PKA pathway or galactose as a control was added to the cells. These two carbohydrates were also always used in the experiments of chapter 2. Additionally, as *C. glabrata* can't use galactose, the addition of galactose to the cells only causes a signaling effect and possible interference of metabolism is absent.

A first sample was taken right before addition of the carbohydrate (timepoint 0) and two more samples were taken after 30 minutes and 60 minutes incubation with glucose or galactose. As we wanted to investigate which adhesin(s) are downstream of the cAMP-PKA pathway, we chose two timepoints within the 90 minutes of the adhesion phase. Because it was possible that the addition of a sugar would induce a transient transcriptional response, we chose two timepoints: 30 and 60 minutes.

The strains selected for investigation in this chapter are the wild type ATCC2001 HTL strain, the *gpr1*Δ strain in which the carbohydrate receptor of the cAMP-PKA pathway

is absent and the *GPA2*^{Q299L} strain which expresses the constitutively active Gpa2 allele. The RNA of all samples was isolated and sequenced at the VIB nucleomics core (as described in Materials and methods). The sequence reads were mapped to the *C. glabrata* reference sequence and can be visualized using the integrative genomics viewer (IGV), as shown in Figure 3.1 (Robinson *et al.*, 2017). For instance, zooming in on the *GPR1* locus (CAGL0K01507g) showed the absence of reads in the *gpr1*Δ strain as expected (Figure 3.1A), while closer inspection of the *GPA2* locus (CAGL0I08195g) showed the mutation CAG (Glutamine) to TTG (Leucine) present in the *GPA2*^{Q299L} strain (red line represents this mapping error against reference sequence in Figure 3.1B).

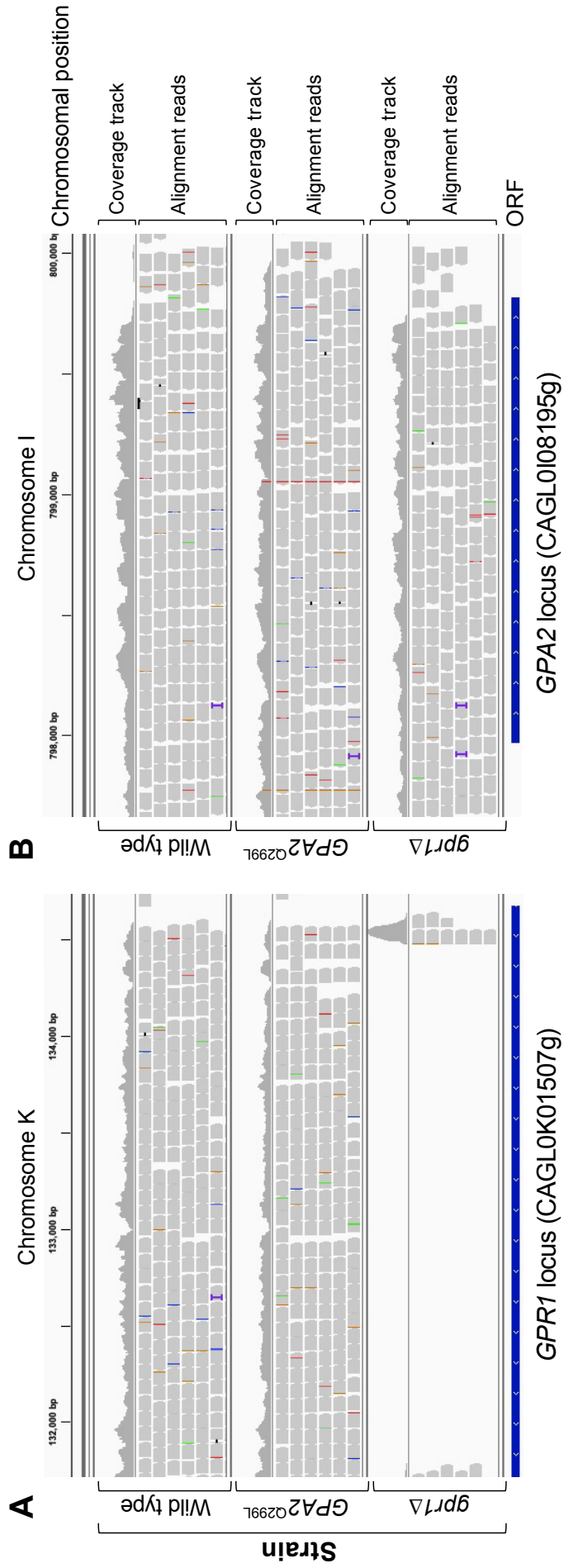

Figure 3.1: Visualization of the sequencing reads mapped to the *GPR1* locus (A) and *GPA2* locus (B) for the wild type strain (top), *GPA2*^{Q299L} strain (middle) and *gpr1*Δ strain (bottom).
Individual mapped reads are shown as grey arrows below the exact chromosomal position, which is indicated on top. Mapping errors are shown as colored lines in the grey arrows. For each strain, six rows of reads are shown because of visibility limits (indicated as alignment reads) and on top a visualization of the total coverage for each strain is shown (indicated as coverage track). The *GPR1* ORF (A) and *GPA2* ORF (B) are depicted as a blue bar at the bottom. The mapping was visualized using the integrative genomics viewer tool (IGV).

3.2.2 General transcriptional response

In a first step to investigate the *C. glabrata* transcriptional data after addition of glucose or galactose, we started with the comparison of the genome-wide transcriptome data of all tested strains. In our RNA sequencing analysis, genes were considered as significantly up- or downregulated when the Benjamini-Hochberg corrected p-value was <0.05. Upon addition of glucose to the wild type strain, the expression of 1817 genes changed significantly (Figure 3.2A), while 406 genes were differentially expressed (DE) when galactose was supplemented to the cells (Figure 3.2B). For both the addition of glucose and galactose, the number of DE ORFs was largely shared between the two sampling timepoints and for both sugars, only one gene was upregulated at 30 minutes while downregulated at 60 minutes. A comparison of the general transcriptional response induced by the two sugars in the wild type strain is depicted in Figure 3.2C. The majority of glucose DE genes were exclusive for glucose, while a smaller number of genes showed a similar or an opposite transcriptional response with the galactose DE genes.

We also generated a genome-wide heat map including all the strains and clustered both the conditions as well as the gene expression profiles (Figure 3.3). While this figure is not useful for in depth analysis of the transcriptome, it provides some general features regarding the samples: firstly, on top the two main clusters were composed by the glucose and galactose responses. The galactose cluster showed that the two timepoints of each strain were always clustered together, indicating that the transcriptome of the two timepoints was very similar. In the glucose cluster, the transcriptome of the *gpr1*Δ strain was more different from the transcriptome of the wild type and *GPA2*^{Q299L} strains and the samples of the latter two strains clustered together at both timepoints. On the left, the expression profile clusters showed that a large number of genes were not differentially expressed in the conditions tested.

In the next paragraphs, the transcriptional response is analyzed further in depth, discussing the galactose and glucose response separately.

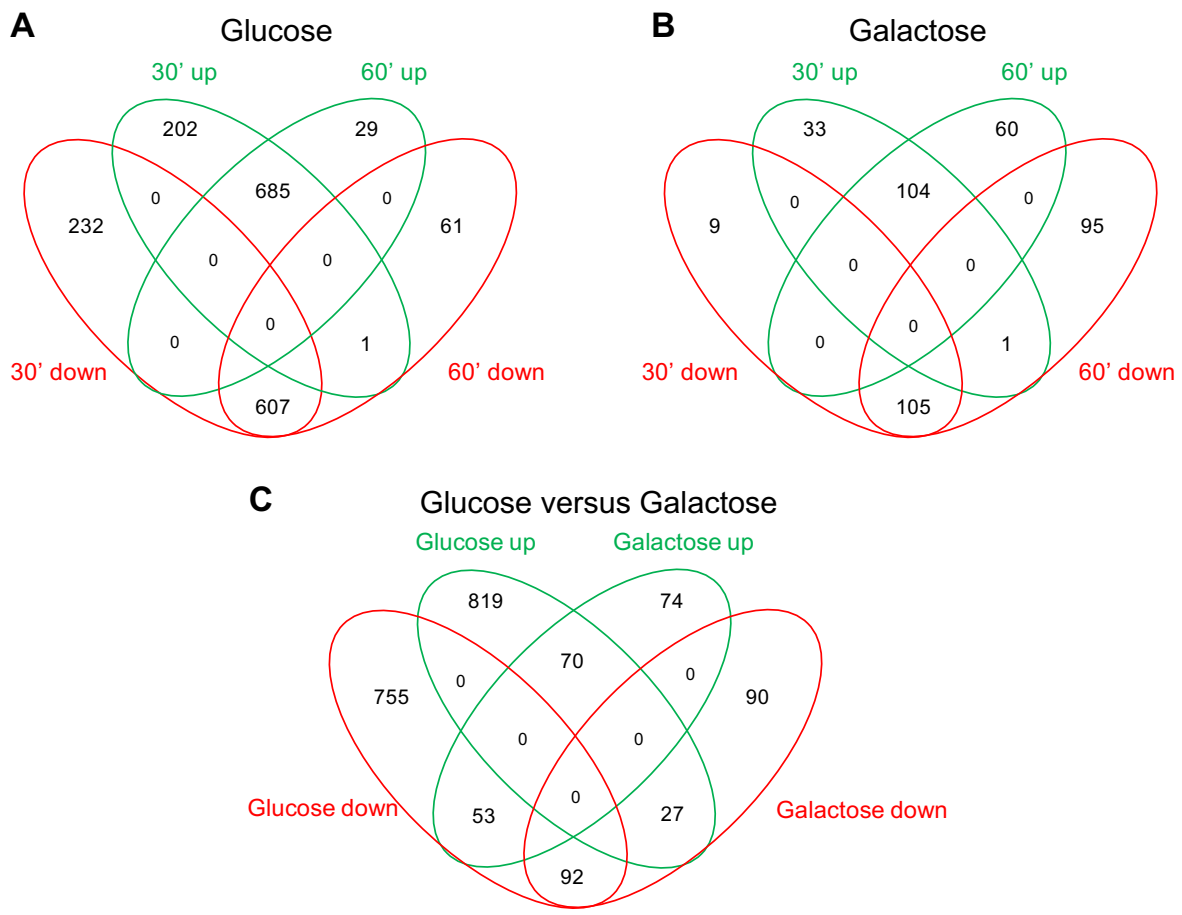

Figure 3.2: Schematic overview of the differentially up- (green) and downregulated (red) genes in the wild type strain.
The number of DE genes after addition of glucose (A) or galactose (B) for each timepoint is shown. The glucose DE response was also compared to the galactose DE response (C). The Venn diagrams were made using Venny 2.1.

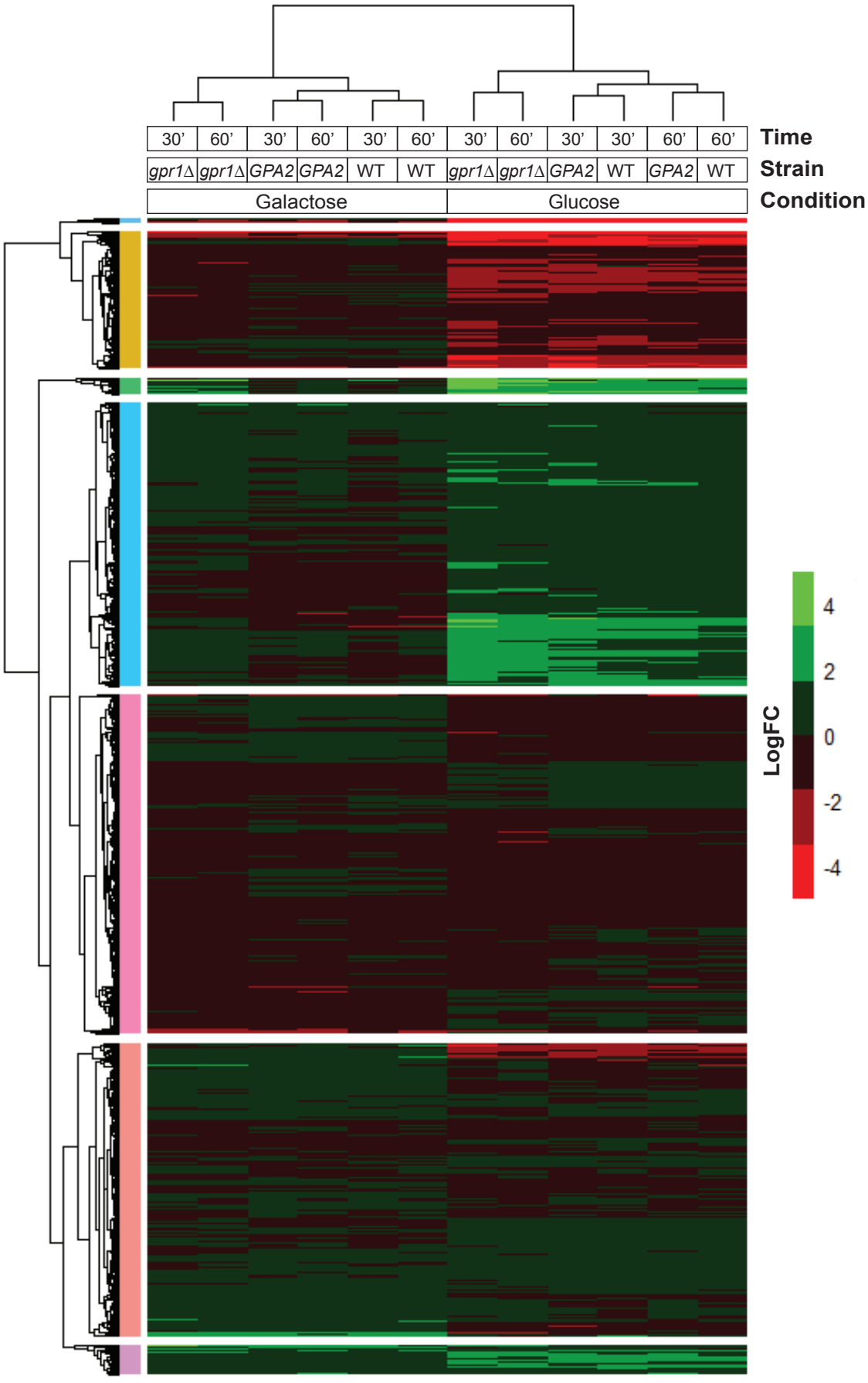
30’
60’
30’
60’
30’
60’
30’
60’
30’
30’
60’
60’
Time
gpr1Δ
gpr1Δ
GPA2
GPA2
WT
WT
gpr1Δ
gpr1Δ
GPA2
WT
GPA2
WT
Strain
Galactose
Glucose
Condition
4
2
0
-2
-4
LogFC

Figure 3.3: Genome-wide heatmap of the *C. glabrata* transcriptome.
Log fold change (Log FC) of each sample (time and sugar) versus the zero timepoint is shown. Both gene expression (vertical clustering with each cluster shown as a different color) and samples (horizontal clusters) were clustered hierarchically as described in Materials and methods.

3.2.3 The glucose transcriptional response

The addition of glucose caused a change in the expression of a large number of genes (1817 genes, Figure 3.2A). This transcriptional response is mediated by multiple glucose signaling pathways: in *S. cerevisiae*, the main glucose signaling pathways are the sugar receptor repressor pathway, the cAMP-PKA pathway and the glucose repression pathway (Conrad *et al.*, 2014). Therefore, investigation of the GO-enriched categories of differentially expressed genes after addition of glucose provides a general view on the cell status rather than the effect of one pathway. Using FungiFun2, we investigated significantly enriched GO categories of glucose up- and downregulated *C. glabrata* genes, summarized in Table 3.1 and Table 3.2.

Inspection of the glucose upregulated genes shows that the cells clearly start the translational machinery, as the different steps of ribosome biogenesis were strongly enriched, as well as tRNAs and nucleotides synthesis (Table 3.1). On the other hand, different genes involved in arginine biosynthesis (*CPA1/2*, *ORT1*, *ARG1*, *ARG3*, *ARG7* and *ARG8*) and several orthologs of *S. cerevisiae* genes involved in heme biosynthesis (*HEM1*, *HEM3*, *HEM4*, *HEM13*, *HEM14* and *HEM15*) were upregulated.

Investigating the glucose downregulated ORFs indicates that the addition of glucose also affects central metabolism: although not present as a significantly enriched category in Table 3.2, inspection of our RNA sequencing data showed transcriptional repression of genes involved in the glyoxylate cycle, gluconeogenesis and TCA cycle (Table 3.3). Furthermore, fatty acid catabolism (ß-oxidation *POX1*, *FOX2/3*), aerobic respiration and the pentose-phosphate shunt were enriched transcriptionally downregulated GO categories (Table 3.2). The *C. glabrata* downregulated genes were also significantly enriched in the GO categories of glycogen and trehalose metabolism as well as cellular response to starvation and oxidative stress (Table 3.2). Closer inspection of the genes in glycogen and trehalose metabolism revealed both genes of synthesis (*TPS2/3*, *TSL1*, *GSY1/2*, *GLC3*) and breakdown (*ATH1*, *NTH1/2*, *GDB1*, *GPH1*) were downregulated.

Furthermore, vesicle mediated transport (including autophagy and endocytosis), protein catabolism in the vacuole and proteolysis were downregulated. Eukaryotic cells generally induce autophagy under non-optimal conditions, sequestering portions of the cytoplasm to degrade the content by lysosomal or vacuolar hydrolases, which results in degradation products that can be reused by the cell (Cebollero and Reggiori, 2009). As glucose is a preferred carbon source, it is plausible that autophagy is repressed. Endocytosis involves the internalization of clathrin-coated vesicles from the plasma membrane towards endosomal compartments, which can be recycled back to the plasma membrane or be permanently removed in the lysosome (Laidlaw *et al.*, 2021).

Table 3.1: Gene Ontology (GO) enrichment of glucose upregulated genes

GO ID	**GO name**	**Adjusted P-value**	**# genes / category**
42254	Ribosome biogenesis	2,91 E-22	72 / 112
9303	rRNA transcription	2,20 E-04	16 / 31
6364	rRNA processing	3,46 E-09	44 / 74
154	rRNA modification	1,42 E-02	7 / 11
16075	rRNA catabolic process	4,09 E-04	15 / 29
42273	Ribosomal large subunit biogenesis	2,94 E-16	46 / 61
42274	Ribosomal small subunit biogenesis	2,20 E-04	16 / 31
22618	Ribonucleoprotein complex assembly	2,60 E-01	43 / 109
54	Ribosomal subunit export from nucleus	1,69 E-02	26 / 45
42255	Ribosome assembly	3,21 E-02	26 / 46
9304	tRNA synthesis		
42797	tRNA transcription from RNA polymerase III promoter	3,64 E-04	17 / 19
6400	tRNA modification	1,09 E-13	35 / 43
8033	tRNA processing	7,83 E-06	20 / 37
16078	tRNA catabolic process	2,33 E-05	11 / 14
9165	Nucleotide biosynthetic process	6,58 E-03	7 / 10
6526	Arginine biosynthetic process	1,42 E-02	7 / 11
42168	Heme metabolic process	2,20 E-02	6 / 9
398	mRNA splicing, via spliceosome	2,45 E-02	25 / 83

Table 3.2: Gene Ontology (GO) enrichment of glucose downregulated genes

GO ID	GO name	Adjusted P-value	# genes / category
9060	Aerobic respiration	1,80 E-04	25 / 59
22904	Respiratory electron transport chain	1,84 E-05	15 / 22
15986	ATP synthesis coupled proton transport	1,79 E-05	13 / 17
55114	Oxidation-reduction process	8,21 E-04	49 / 166
9062	Fatty acid catabolic process	3,66 E-04	11 / 16
6098	Pentose-phosphate shunt	1,88 E-02	7 / 11
16192	Vesicle-mediated transport	6,61 E-05	47 / 141
6897	Endocytosis	6,46 E-04	29 / 79
32940	Secretion by cell	3,11 E-03	15 / 32
46907	Intracellular transport	4,53 E-03	32 / 101
6914	Autophagy	2,25 E-02	23 / 72
7039	Protein catabolic process in the vacuole	2,25 E-02	4 / 4
6508	Proteolysis	1,68 E-03	27 / 75
5975	Carbohydrate metabolic process	1,45 E-02	15 / 37
5977	Glycogen metabolic process	6,61 E-05	12 / 16
5991	Trehalose metabolic process	2,52 E-04	10 / 13
19318	Hexose metabolic process	4,16 E-02	8 / 16
6111	Regulation of gluconeogenesis	3,00 E-02	7 / 12
9267	Cellular response to starvation	1,12 E-02	30 / 98
34599	Cellular response to oxidative stress	4,28 E-02	21 / 68

Table 3.3: Comparison of genes involved in central carbon metabolism displaying a differential gene expression in response to glucose in *S. cerevisiae* and *C. glabrata.*

	S. cerevisiae		***C. glabrata***	
Protein	**Gene**	**1% glucose[1]**	**Gene**	**2% glucose[2]**
Gluconeogenesis				
Fbp1	YLR377C	-3,28	CAGL0H04939g	-8.19
Pck1	YKR097W	-5,98	CAGL0H06633g	-3.76
Glyoxylate cycle				
Icl1	YER065C	-4,82	CAGL0J03058g	-1.39
Mls1	YNL117W	-3,29	CAGL0L03982g	-1.77
TCA cycle				
Cit1	YNR001C	-5,77	CAGL0H03993g	-2.35
Aco1	YLR304C	-8,85	CAGL0D06424g	-0.59
Idh2	YOR136W	-2,31	CAGL0I07227g	-0.67
Kgd1	YIL125	-3,55	CAGL0G08712g	-2.27
Kgd2	YDR148C	-2,69	CAGL0E01287g	-1.12
Lsc1	YOR142W	-1,63	CAGL0I07139g	-2.50
Lsc2	YGR244C	-2,66	CAGL0F08107g	-2.74
Sdh2	YLL041C	-2,71	CAGL0C03223g	-1.07
Sdh3	YKL141W	-2,47	CAGL0D01958g	0.69
Sdh4	YDR178W	-2,21	CAGL0F05863g	0.38
Fum1	YPL262W	-2,25	CAGL0A01045g	-1.27
Mdh1	YKL085W	-3,05	CAGL0L05236g	-2.40

[1] Differential expression (fold change) of exponential cells grown in YP lactate and 30 minutes after addition of 1% glucose. Data from (Yin *et al.*, 2003).

[2] Differential expression (log_2 fold change) of exponential cells grown in SC glycerol and 30 minutes after addition of 2% glucose.

3.2.4 cAMP-PKA pathway specific transcriptional response

The wild type transcriptional response discussed in the previous section results from the activity of several glucose-induced signaling pathways. To examine the cAMP-PKA pathway specifically, the *gpr1*Δ strain and the constitutive active *GPA2*^{Q299L} strain were also included in the RNA sequencing experiment. We hypothesized that when genes are controlled solely through activation of the GPCR system Gpr1 and Gpa2 towards PKA, the glucose-induced transcriptional response would be abrogated in the *gpr1*Δ strain. Filtering our data for these features revealed 114 induced and 115 repressed genes in the wild type strain, without any significantly enriched GO categories. We also visually compared the genome-wide transcriptional changes following glucose addition to the glycerol-grown cells of the wild type and the *gpr1*Δ strain (Figure 3.4A) or the wild type and *GPA2*^{Q299L} strain (Figure 3.4B). These figures show that the glucose-induced transcriptional responses are very similar for the strains, as the linear fit of the plot (red line) approaches the diagonal (blue line) in both cases. This indicates that several pathways redundantly mediate the glucose-induced transcriptional response.

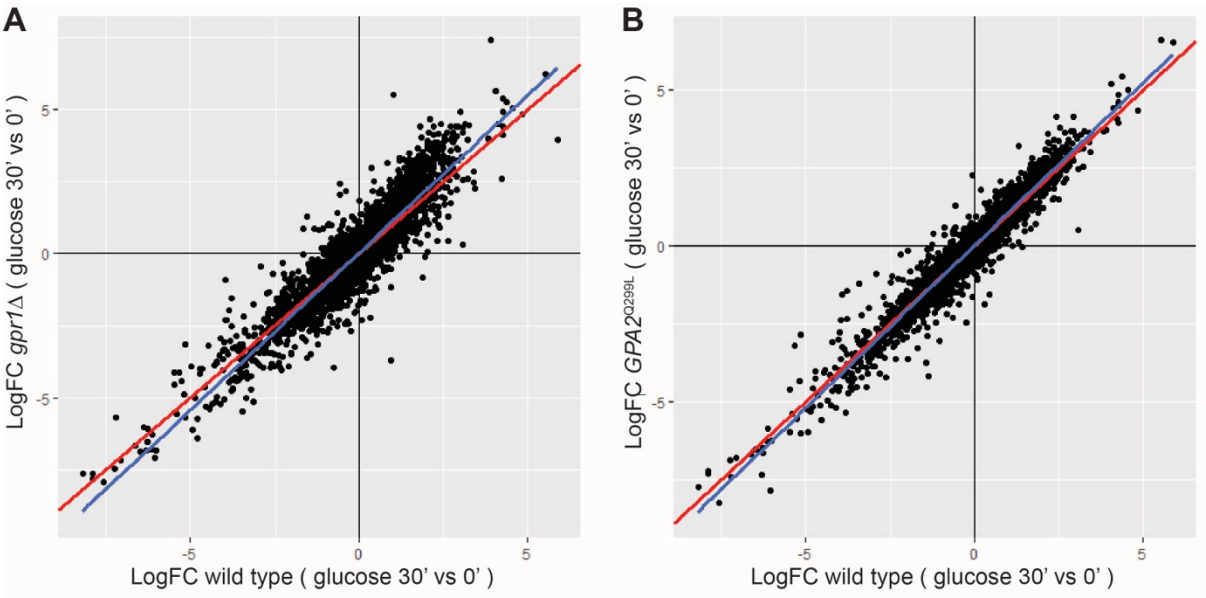

Figure 3.4: The genome wide glucose-induced transcriptional responses are very similar between wild type and mutant strains.
Scatter plot of the Log_2FC of glucose transcriptional response between the wild type and *gpr1*Δ strain (A) or the wild type and *GPA2*^{Q299L} strain (B). The blue line represents the diagonal, the red line represents the linear fit of the data.

The expression of genes typically controlled by the PKA pathway in *S. cerevisiae* include ribosomal protein genes and genes affecting stress resistance (including heat shock proteins, described in Section 1.3.1.4). We therefore listed the glucose-induced expression profile of the *C. glabrata* homologs in Table 3.4. Unexpectedly, these specific ribosomal protein genes were not significantly upregulated. Genes involved in the stress response were repressed, as is the case in *S. cerevisiae*. As mentioned before, genes involved in both glycogen and trehalose synthesis (*TPS1/2/3*, *TSL1*, *GSY1/2*, *GLC3*) and breakdown (*GDB1*, *GPH1*) were downregulated.

Table 3.4: Expression profile of the *C. glabrata* homologs of known *S. cerevisiae* PKA controlled genes.

		Glucose-induced change of gene expression[1]		
***S. cerevisiae* gene**	***C. glabrata* homolog**	**wild type**	***gpr1*Δ**	***GPA2*^{Q299L}**
Ribosomal protein genes				
RPL16A	CAGL0J10164g	0,98	1,67	0,90
RPL28	CAGL0J10384g	-0,06	-0,04	0,15
RPL29	CAGL0D05214g	1,06	1,50	1,23
RPS4	CAGL0F09031g	0,67	0,79	0,67
RPS13	CAGL0G05027g	0,37	0,55	0,52
Stress response genes				
DDR2	CAGL0H02563g	-2,25	-3,59	-2,67
HSP12	CAGL0J04202g	-5,32	-4,11	-3,20
HSP104	CAGL0G03883g	-4,55	-5,28	-5,58
SSA3	CAGL0G03289g	-3,35	-5,00	-4,22
UBI4	CAGL0D05082g	-0,09	-0,56	-0,16
Glycogen and trehalose metabolism genes				
GAC1	CAGL0H04037g	-1,98	-2,11	-1,96
GPH1	CAGL0F04895g	-4,88	-5,02	-5,30
GSY2	CAGL0F04719g	-4,81	-5,70	-5,16
TPS1	CAGL0J09812g	-2,74	-2,65	-3,00
TPS2	CAGL0G05335g	-1,60	-1,77	-1,89
TPS3	CAGL0J06468g	-2,70	-3,11	-3,03
TSL1	CAGL0J06468g	-2,70	-3,11	-3,03

[1]Change in gene expression is shown as $\log_2$ fold change at 30 minutes after addition of 2% glucose and timepoint zero.

3.2.5 The adhesin transcriptional response

In Chapter 2, we described that the *C. glabrata* cAMP-PKA pathway negatively controls adhesion to plastic. As mentioned in Chapter 1, *C. glabrata* encodes a large number of ORFs encoding predicted adhesins which are largely uncharacterized. Therefore, we decided to analyze the adhesin transcriptional response after glucose addition. As a first step, literature was checked to construct a comprehensive list of the ORFs which are described as or predicted to be adhesin(-like) genes (listed in Addendum 2). In 2015 and 2020, transcriptome studies of Linde *et al.* (2015) and Xu *et al.* (2020) changed the open reading frames of *C. glabrata* genes, among which a number of predicted adhesins. Some adhesins were split into two or more new ORFs and other genes were removed. At the time this analysis was performed, the reannotation of Xu *et al.* (2020) was not published yet. Therefore, as described in the materials and methods section, our mapping was performed on the previous reference sequence. As the study of Xu *et al.* (2020) shows that the annotation of several adhesins has changed, the wrongly annotated adhesins were removed from our list (Addendum 2, shown as strikethrough). As our reference map does not contain the novel ORF names, it was not possible to include the new predicted adhesin sequences (Addendum 2, shown in bold).

From the genome-wide transcriptome data, several putative adhesins showed less than 10 counts over all samples and were therefore considered as not expressed (Table 3.5). The genome update of Xu *et al.* (2020) removed most of these genes.

As phenotypically *C. glabrata* adhesion was reduced upon addition of glucose in the wild type strain and adherence remained high in the *gpr1*Δ strain, we focused on the glucose-induced transcriptional response. The list of adhesins were ordered from downregulated to upregulated and further divided into groups according to differences in the expression pattern between the strains as indicated (Figure 3.5). For many adhesins, the glucose-induced response was highly similar in the different strains: the adhesins were all differentially up- or downregulated or their expression did not significantly change upon addition of glucose.

Table 3.5: Overview of non-expressed adhesin-like genes.
Due to a recent update of the *C. glabrata* gene annotation (Xu *et al.*, 2020), several genes were removed: these are indicated as strikethrough.

Gene ID	Gene name or Alias	Max count	Description CGD
~~CAGL0A00105g~~	~~CAGL0A00110g.1~~	~~0~~	~~Protein of unknown function~~
CAGL0A00116g	CAGL0A00110g.2	0	Protein of unknown function
CAGL0B05126g	CAGL0B05093g.1	0	Protein of unknown function
CAGL0B05137g	CAGL0B05093g.3	0	Protein of unknown function
CAGL0B05148g	CAGL0B05093g.2	0	Protein of unknown function
~~CAGL0C01056g~~	~~CAGL0C01067g.1~~	~~0~~	~~Protein of unknown function~~
~~CAGL0C01078g~~	~~CAGL0C01067g.2~~	~~0~~	~~Protein of unknown function~~
~~CAGL0D00105g~~	~~CAGL0D00110g.2~~	~~0~~	~~Protein of unknown function~~
~~CAGL0D00116g~~	~~CAGL0D00110g.1~~	~~0~~	~~Protein of unknown function~~
~~CAGL0E00105g~~	~~CAGL0E00110g.1~~	~~0~~	~~Protein of unknown function~~
~~CAGL0E00116g~~	~~CAGL0E00110g.3~~	~~0~~	~~Protein of unknown function~~
~~CAGL0E00132g~~	~~CAGL0E00110g.2~~	~~0~~	~~Protein of unknown function~~
CAGL0E00187g		7	Putative adhesin-like protein; belongs to adhesin cluster IV
~~CAGL0F00116g~~	~~CAGL0F00110g.1~~	~~1~~	~~Protein of unknown function~~
~~CAGL0G00105g~~	~~CAGL0G00110g.2~~	~~0~~	~~Protein of unknown function~~
~~CAGL0G00121g~~	~~CAGL0G00110g.1~~	~~0~~	~~Protein of unknown function~~
~~CAGL0H00143g~~	~~CAGL0H00132g.2~~	~~0~~	~~Protein of unknown function~~
~~CAGL0I00105g~~	~~CAGL0I00110g.1~~	~~0~~	~~Protein of unknown function~~
~~CAGL0I00121g~~	~~CAGL0I00110g.4~~	~~0~~	~~Protein of unknown function~~
~~CAGL0I00143g~~	~~CAGL0I00110g.2~~	~~0~~	~~Protein of unknown function~~
~~CAGL0I11011g~~		~~9~~	~~Putative adhesin; belongs to adhesin cluster V~~
~~CAGL0J00105g~~	~~CAGL0J00110g.2~~	~~0~~	~~Protein of unknown function~~
~~CAGL0J00116g~~	~~CAGL0J00110g.1~~	~~0~~	~~Protein of unknown function~~
CAGL0J01727g		7	Putative adhesion protein; predicted GPI-anchor; belongs to adhesin cluster VI
CAGL0J02552g		5	Adhesin-like protein; predicted GPI anchor; belongs to adhesin cluster VI
~~CAGL0J11979g~~	~~*AWP4.1;* CAGL0J11990g.3~~	~~0~~	~~Protein of unknown function~~
~~CAGL0J12012g~~	~~*AWP4.2;* CAGL0J11990g.1~~	~~0~~	~~Protein of unknown function~~
~~CAGL0M00110g~~	~~*AWP11*~~	~~3~~	~~Putative adhesin-like protein; GPI-anchored; belongs to adhesin cluster V; ORF appears artificially broken into fragments due to sequencing errors but the gene is likely protein-coding based on mass spectrometry data~~

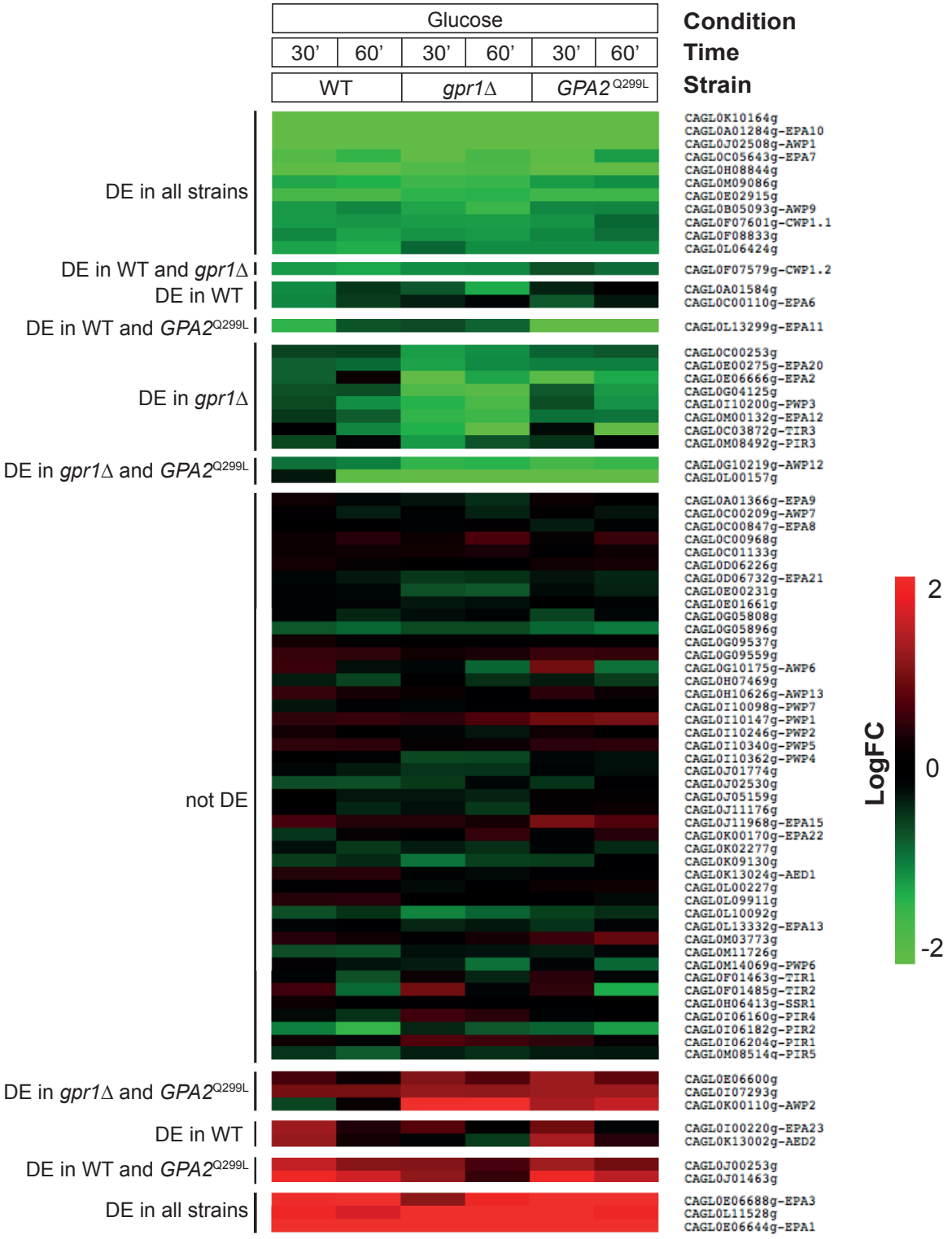

Figure 3.5: Overview of the glucose-induced adhesin transcriptional response. Log_2 FC of the indicated timepoint and the zero timepoint (before addition of the indicated sugar) of the strains is shown. The adhesins were sorted from downregulated to upregulated in response to glucose addition and divided into groups according to differences between strains.

Based on the adherence phenotype, we were particularly interested in adhesins showing a different glucose-induced response in the wild type compared to the *gpr1*Δ strain. As adherence was lowered by glucose in the wild type strain, we hypothesized that the expression of the responsible adhesin would be repressed in this condition, while not significantly repressed in the *gpr1*Δ strain. However, we did not want to exclude the possibility of the induction of an adhesin which lowers the affinity towards plastic, for instance by increasing the substrate specificity towards specific biotic surfaces. Therefore, we also included adhesins upregulated in the wild type strain and which did not show a significant differential expression in the *gpr1*Δ strain. Therefore, the adhesins of interest selected were CAGL0A01584g, *EPA6* and *EPA11* (downregulated in wild type) or *EPA23*, *AED2*, CAGL0J00253g and CAGL0J01463g (upregulated in wild type).

3.2.6 Elucidation of adhesin(s) controlled by the cAMP-PKA pathway affecting adhesion to polystyrene

To further investigate the selected adhesins, we tried to delete the genes. As a lot of adhesins are located near the telomeres and therefore possibly more difficult to modify, we first constructed the deletion cassettes of all selected adhesin ORFs in vectors. The cassettes consisted of the nourseothricin selection marker flanked by 500 bp sequences upstream and downstream of the target gene (described in Materials and methods). Despite many transformations using elevated concentrations of the deletion cassette, we were not able to retrieve any correct colonies in our ATCC2001 wild type strain. As it is known that homologous recombination works with poor efficiency in *C. glabrata*, we switched to the ATCC2001 *lig4*Δ strain created in our lab, thereby eliminating non-homologous end joining and increasing the chance for homologous recombination (Cen *et al.*, 2015). In this *lig4*Δ strain, we were able to successfully retrieve three independent transformants for eight of the selected adhesins (CAGL0A01584g, *EPA6*, *EPA11*, *AED2*, CAGL0J00253g and CAGL0J01463g).

We hypothesized that when an adhesin responsible for adherence is deleted, adhesion in presence of galactose would resemble the glucose condition. We subsequently tested the available deletion strains for adhesion in presence of glucose and galactose. The results are depicted in Figure 3.6 in two ways: panel A displays

the comparison of the glucose and galactose condition relative to each other, while panel B shows the adhesion in presence of both glucose and galactose for all strains. In Figure 3.6A, two adhesin deletion strains show a similar adherence in presence of galactose and glucose: *AED2* (ns, P = 0.0626) and CAGL0J00253g (P = 0.0054). A closer look at Figure 3.6B shows that when the predicted adhesin CAGL0J00253g was deleted, a similar reduced adherence in both conditions was present. In contrast, the *aed2*Δ strain showed a similarly high adhesion phenotype in the presence of both glucose and galactose (Figure 3.6B).

CAGL0J00253g is an *in silico* predicted adhesin-like protein of 497 amino acids (Chaudhuri *et al.*, 2011). Up until now, there are no publications characterizing this gene. Using the PROTTER algorithm, we predicted the CAGL0J00253g protein to contain a signal peptide and a single transmembrane domain (Omasits *et al.*, 2014). Furthermore, a region in the middle of the CAGL0J00253g protein is homologous to the *Sc*Mid2 Pfam domain of *S. cerevisiae ScMID2*, while the N- and C-terminal sequences do not show any sequence similarity to other proteins (Figure 3.7). *S. cerevisiae Sc*Mid2 is a cell wall sensor for cell integrity signaling, which contains an extracellular domain, the *Sc*Mid2 transmembrane domain and an intracellular domain (Rajavel *et al.*, 1999). Noticeably, the extracellular residues are rich in serine (46%) and threonine (9,6%) residues, frequently present in *C. glabrata* adhesins.

AED2 is predicted to be an adhesin of family III, lacking a PA14 protein domain (de Groot *et al.*, 2008). It encodes a GPI-anchored protein of 937 amino acids with no common protein domains. Although Aed2 shows some similarities to the Aed1 adhesin, it lacks the tandem repeats present in Aed1 (Desai *et al.*, 2011). While Aed1 mediates adherence to endothelial cells *in vitro*, this is not true for Aed2 (Desai *et al.*, 2011). Until now, there is no further evidence for Aed2 to mediate adhesion.

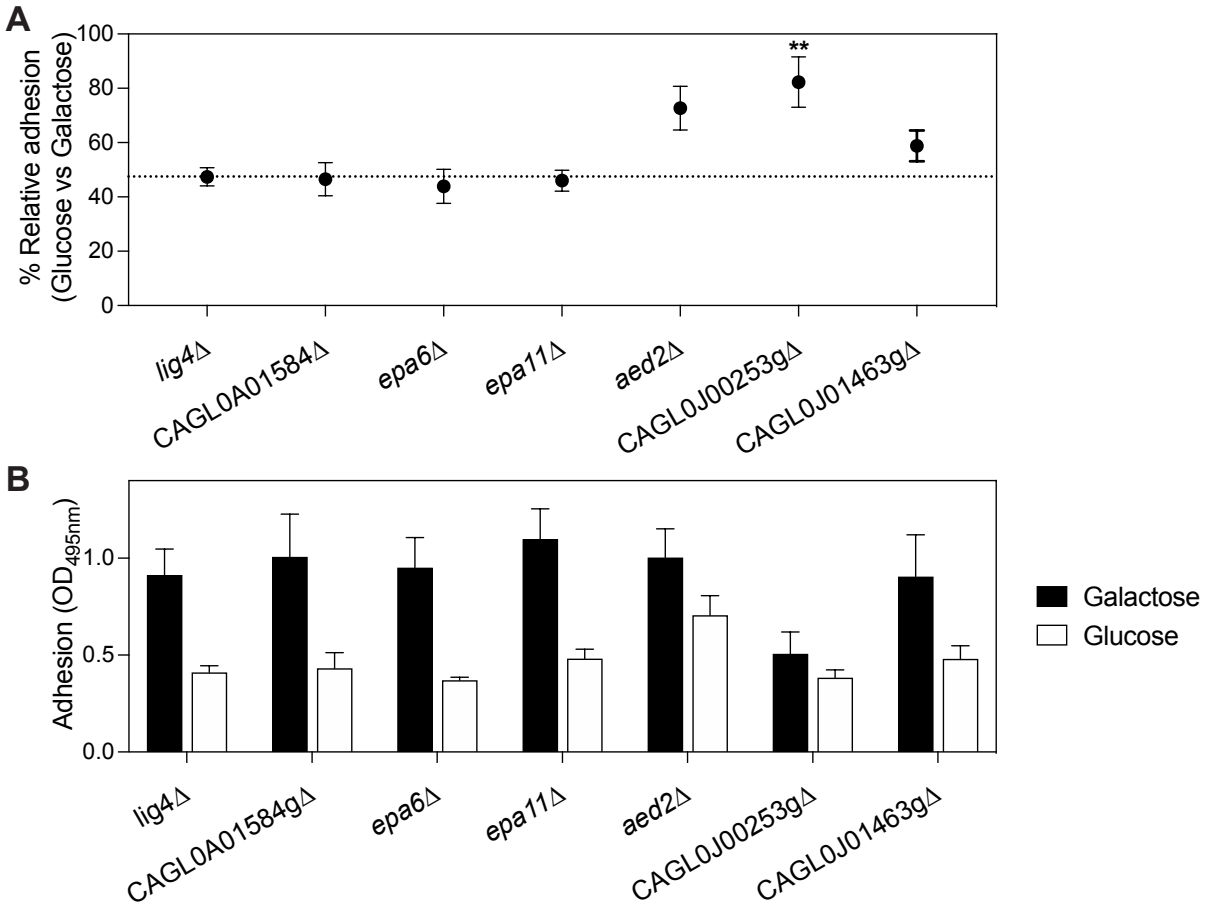

Figure 3.6: The CAGL0J00253g deletion strain shows a low adherence phenotype.
The strains were grown to exponential phase in glycerol and resuspended in glucose or galactose (2%). 10^6 cells were added to wells of a 96-well plate and incubated for 90 minutes. After washing, adhesion was read out by the XTT reduction assay. Adherence in presence of glucose compared to galactose is shown as the average percentage relative adhesion with SEM of three independent deletion strains and two experiments (A). Statistical analysis was conducted by one-way ANOVA with Bonferroni correction, comparing the deletion strains to the *lig4*Δ background strain (**, P = 0.0054) (A). Average OD_{495nm} with SEM for each strain and condition is shown (B).

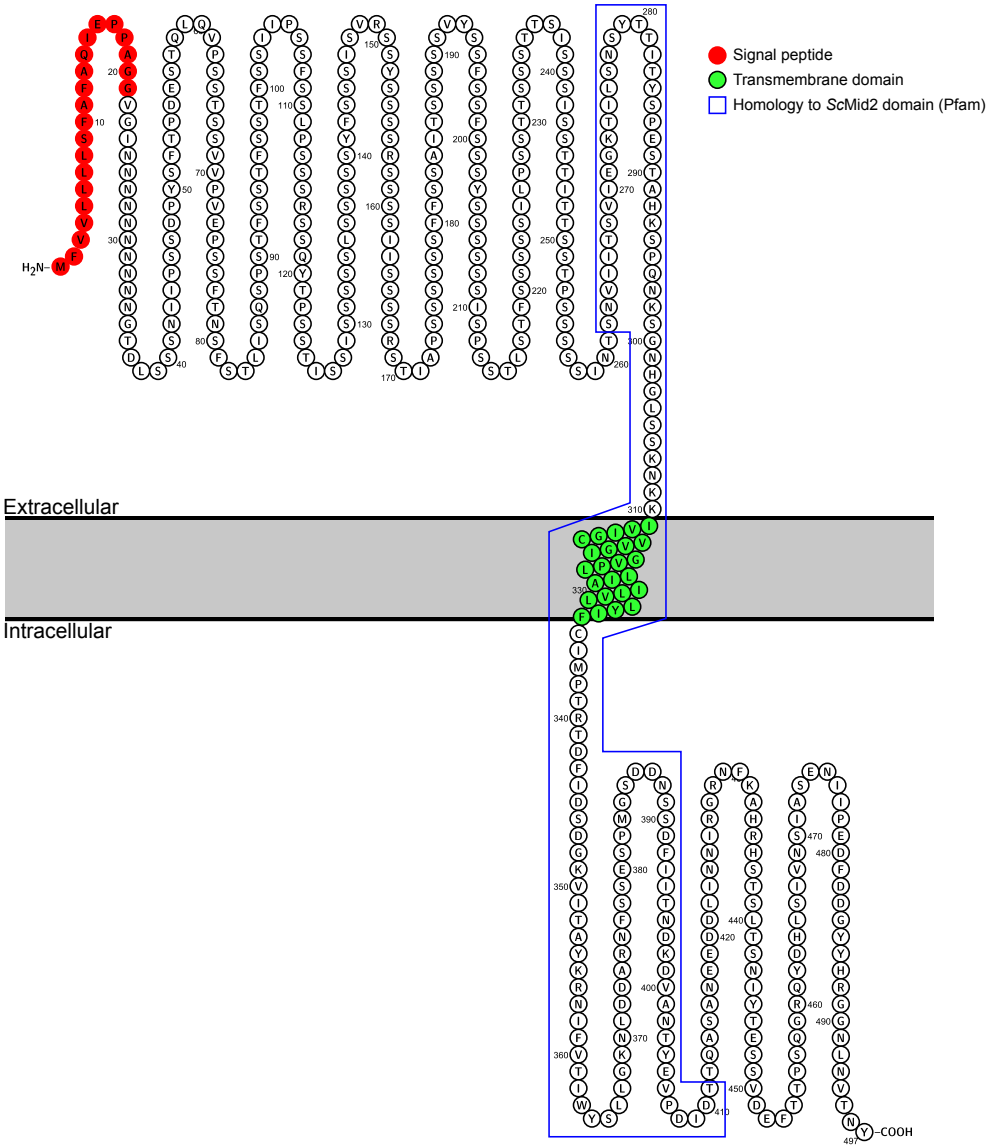

Figure 3.7: Predicted protein topology of CAGL0J00253g.
The signal peptide is coloured in red, transmembrane domain residues are shown in green and the Pfam domain showing homology to the *S.cerevisiae Sc*Mid2 domain is enclosed by the blue line. Protein topology was created using the PROTTER algorithm (Omasits *et al.*, 2014)

3.2.7 The galactose transcriptional response

In response to galactose, 198 genes were upregulated, and 210 genes were downregulated (Figure 3.2B). The number of DE genes is low compared to glucose, but can be explained by the fact that the genes specific for galactose metabolism are missing in *C. glabrata* including *ScGAL1, ScGAL7* and *ScGAL10* of the galactose catabolic pathway called the Leloir pathway as well as *ScGAL3* (Figure 3.8) (Dujon *et al.*, 2004). In *S. cerevisiae*, galactose is transported into the cells by the high affinity transporter *Sc*Gal2 and the high affinity maltose transporter *Sc*Mal11 (Timson, 2007). Intracellular galactose is sensed by the intracellular galactose sensor *Sc*Gal3p which then binds to *Sc*Gal80p, a transcriptional repressor, resulting in *Sc*Gal4p activation of transcription of many genes including genes of the Leloir pathway (Figure 3.8). The Leloir pathway converts galactose into glucose-6-phosphate, which can be further metabolized in glycolysis.

A search for homologs of the other *ScGAL* genes showed that *C. glabrata* does not have homologs of *ScGAL2*, *ScMal11*, *ScGAL4* or *ScGAL80*. *C. glabrata* does have a *ScGAL5* homolog (CAGL0K03421g), but this phosphoglucomutase is not specific for growth on galactose and is also used for growth on glucose (Bhat, 2008).

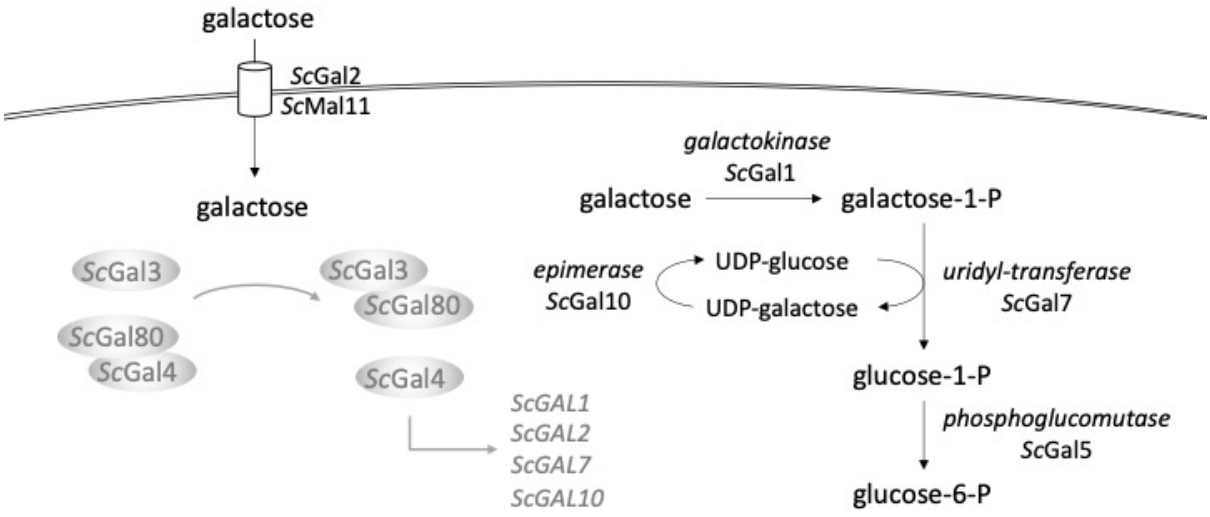

Figure 3.8: Overview of galactose uptake, galactose transcriptional control (grey) and the Leloir pathway (black) in *S. cerevisiae*.

We confirmed that *C. glabrata* is not able to use galactose as a carbon source by a growth curve and simultaneous measurement of the sugars in the medium: *C. glabrata* was able to grow on glucose and fructose, while galactose and sucrose were not consumed (Figure 3.9). The latter is due to the absence of a sucrose invertase homolog in *C. glabrata* (Dujon *et al.*, 2004). The concentration of galactose and sucrose in the medium also remained constant over time, confirming galactose metabolism is absent in *C. glabrata* (Figure 3.9).

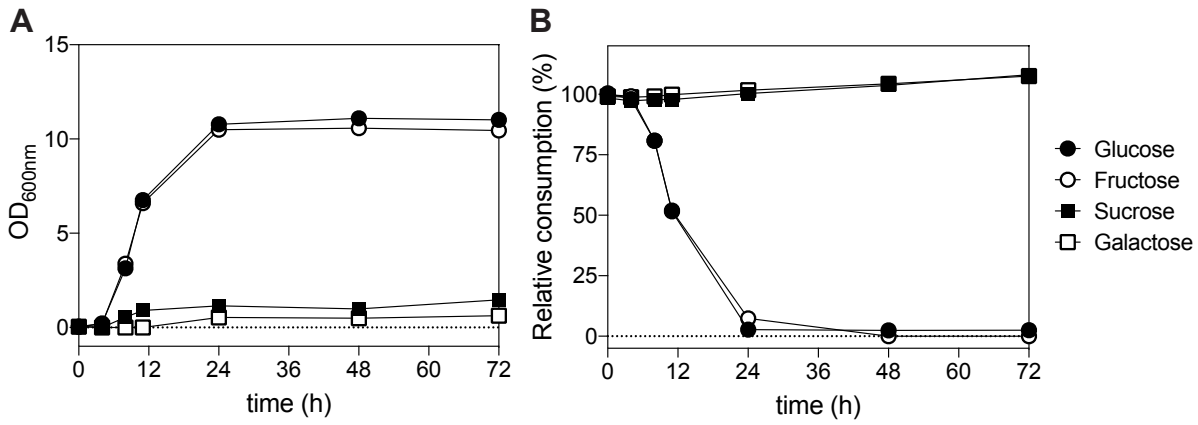

Figure 3.9: Growth of *C. glabrata* using different carbohydrates as a carbon source.
Wild type *C. glabrata* was grown in YNB supplemented with the indicated sugar (2%). Growth (OD_{600nm}) was followed in time (A) and simultaneously consumption of the carbohydrate in the growth medium was followed in time (B). Average results of three independent experiments are shown.

While the addition of galactose served as the non-inducible condition in our experiment and *C. glabrata* does not take up nor metabolizes galactose, still over 400 genes were differentially expressed upon addition of galactose. Therefore, we were interested in the galactose up- and downregulated genes and analyzed if there were GO enriched categories (Table 3.6 and Table 3.7). Unexpectedly, galactose affected the cellular metabolic response: several genes of the TCA cycle (including *CIT1*, *ACO1*) and electron transport chain (e.g. *NDI1*, *QCR6/9*, *CYC1*) were upregulated. Also, genes of heme biosynthesis (*HEM3/13/15*) and iron-sulfur cluster assembly (*ISA1/2* and *NFU1*) were upregulated as well as the expression of several genes of acetate metabolism (*ADY2*, *YAT1*, *ACH1*) and lipid biosynthesis (*HFA1*, *FAS1/2*, *CHO2*, *OPI3*, *INO1*) were upregulated. While not present as a GO category, key genes of the glyoxylate cycle and gluconeogenesis were induced by galactose: isocitrate lyase (*ICL1*), fructose 1,6-

bisphosphate 1-phosphatase (*FPB1*) and phosphoenolpyruvate carboxykinase (*PCK1*). On the other hand, genes of glycolysis (including *PFK2*, *TPI1*, *PGK1*, *ENO1*, *PYK1*) and two genes encoding for enzymes in the conversion of amino acids to alcohol (Ehrlich pathway: *PDC6, ADH1*) were downregulated. Genes encoding for different transmembrane transporters were up- (*MUP1/3*; *PHO84*; *PUT4*) and downregulated (*HXT1*; *HXT4*; *HXT6/7*; *HXT4/6/7*; *FET3/4*). Genes involved in cellular iron ion homeostasis (*AFT1*; *CCC2*) and nucleoside diphosphate metabolism (*RNR1/2/4*) were downregulated. Lastly, the cellular response to hydrogen peroxide (*GPX2*; *TSA1*; *CTA1*) was upregulated.

Table 3.6: Gene Ontology (GO) enrichment of galactose upregulated genes

GO ID	GO name	Adjusted P-value	# genes / category
9060	Aerobic respiration	1,88 E-06	14 / 59
6099	Tricarboxylic acid cycle	1,99 E-06	8 / 15
22904	Respiratory electron transport chain	4,88 E-04	7 / 22
16226	Iron-sulfur cluster assembly	4,88 E-04	7 / 22
6783	Heme biosynthetic process	2,29 E-02	4 / 13
6083	Acetate metabolic process	3,52 E-03	5 / 14
35433	Acetate transmembrane transport	2,57 E-02	2 / 2
8654	Phospholipid biosynthetic process	2,64 E-02	5 / 25
70301	Cellular response to hydrogen peroxide	3,20 E-02	4 / 16
15976	Carbon utilization	3,20 E-02	4 / 16
34220	Ion transmembrane transport	3,56 E-02	6 / 40
55114	Oxidation-reduction process	1,30 E-01	25 / 166

Table 3.7: Gene Ontology (GO) enrichment of galactose downregulated genes

GO ID	GO name	Adjusted P-value	# genes / category
6096	Glycolytic process	3,02 E-06	9 / 17
55114	Oxidation-reduction process	1,96 E-04	21 / 166
9132	Nucleoside diphosphate metabolic process	5,20 E-03	3 / 3
55085	Transmembrane transport	2,13 E-04	17 / 116
34755	Iron ion transmembrane transport	4,60 E-02	3 / 6
6879	Cellular iron ion homeostasis	1,46 E-02	6 / 24
947	Amino acid catabolic process to alcohol via Ehrlich pathway	4,60 E-02	3 / 6

3.3 Discussion

In this chapter, we investigated the *C. glabrata* transcriptome in response to the addition of glucose or galactose to glycerol grown cells. In general, nutrients can affect the cell in several ways: they can serve as signaling molecules of transduction pathways or can be metabolized by the cell and in turn, these metabolic intermediates can serve as signaling molecules. One study in *S. cerevisiae* investigated the glucose-induced transcriptome and considered 60 minutes post glucose addition with the cell adapting to the new conditions, as the transcriptional response at this timepoint often had an opposite polarity compared to earlier timepoints (Wang *et al.*, 2004). In our data, the number of differentially expressed genes at 30 minutes post glucose addition is also substantially higher than at 60 minutes, suggesting the possibility of adaptation to the new conditions at the later timepoint. As a control condition for our experiments, we chose to treat the cells with galactose, which does not induce the cAMP-PKA pathway and in addition cannot be metabolized by *C. glabrata* (Dujon *et al.*, 2004). Therefore, the galactose induced transcriptional response is an effect of signaling.

Glucose response

Upon addition of glucose, the expression of 34.3% of all *C. glabrata* genes changed significantly, with similar numbers of genes up- and downregulated. This is similar to the glucose induced transcriptional response in *S. cerevisiae*, which showed 22-41% of differentially expressed genes in the microarray study of Wang *et al.* (2004). This glucose induced transcriptional response is caused by different signaling cascades, including the glucose repression pathway, the sugar receptor repressor pathway and the cAMP-PKA pathway (Conrad *et al.*, 2014; Van Ende *et al.*, 2019).

In *S. cerevisiae*, glucose addition alters the transcription of genes involved in various cellular processes such as gluconeogenesis, glyoxylate cycle, TCA cycle, respiration and ß-oxidation (Soontorngun *et al.*, 2007). Closer inspection of the *C. glabrata* up- and downregulated genes shows various similarities: *C. glabrata* genes of gluconeogenesis and the glyoxylate cycle were repressed, which in *S. cerevisiae* is mediated by the serine threonine kinase *Sc*Snf1 of the glucose repression pathway. In absence of glucose, *Sc*Snf1 activates the transcriptional activators *Sc*Cat8 and *Sc*Rds2 and inactivates the repressor *Sc*Mig1 (Kayikci and Nielsen, 2015; Soontorngun *et al.*, 2007). In *C. glabrata,* a highly similar homolog of *Sc*Snf1 is present

which can also complement a *Scsnf1*Δ strain, suggesting a similar transcriptional control (Petter and Kwon-Chung, 1996). Fatty acid catabolism generally provides the cell with the generation of energy (ATP) in absence of glucose and our results indeed show this is downregulated upon glucose addition. In *S. cerevisiae*, the expression of *ScFOX2*, encoding the acyl-CoA dehydrogenase of ß-oxidation, is controlled by *Sc*Snf1, by activation of its transcription factor *Sc*Adr1 (Kayikci and Nielsen, 2015). On the other hand, the PKA regulated transcription factors *Sc*Msn2/4 activate the expression of several genes involved in fatty acid oxidation (Rajvanshi *et al.*, 2017). *C. glabrata* contains functional orthologs of *Sc*Msn2/4 which have a similar glucose dependent cellular localization, probably controlled by PKA phosphorylation (Roetzer *et al.*, 2008). Genes involved in aerobic respiration are downregulated, as *C. glabrata* is known to rapidly and efficiently ferment glucose (Calderone and Clancy, 2012). In literature, several transcriptional analyses are performed on macrophage-engulfed *C. glabrata* and *C. albicans* cells, an environment which is typically nutrient-limited and particularly in glucose availability (Kaur *et al.*, 2007; Lorenz *et al.*, 2004). These studies report the upregulation of gluconeogenesis, glyoxylate cycle and ß-oxidation of fatty acids and downregulation of glycolysis and translation of *Candida* cells inside macrophages (Chew *et al.*, 2019).

Other enriched GO categories of downregulated genes upon glucose addition included metabolism of the reserve carbohydrates trehalose and glycogen as well as cellular responses to starvation or oxidative stress. This is probably mediated by cAMP-PKA pathway regulation of the Msn transcription factors affecting the expression of many genes by stress responsive elements in their promoters (discussed in Section 1.3.1.4), as we characterized the *C. glabrata* cAMP-PKA pathway and *C. glabrata* Msn2 and Msn4 contain the PKA phosphorylation sequence (PhD thesis De Brucker, 2011; Roetzer *et al.*, 2008). Roetzer *et al.* (2008) also showed that the environmental stress response profiles of *C. glabrata* and *S. cerevisiae* are similar, including many Msn2-regulated genes. Both genes of *C. glabrata* trehalose and glycogen biosynthesis and degradation were repressed by glucose, which is in line with the expression of the homologous genes in *S. cerevisiae* (Parrou *et al.*, 1999; Winderickx *et al.*, 1996). Yet, there is a discrepancy between the transcriptional and the actual enzymatic trehalase activity, as we showed in Chapter 2 that the addition of glucose does not change the activity of *C. glabrata* Ath1 nor Nth2 but activates Nth1 trehalase activity.

Besides nutrient metabolism, several GO categories of vesicle transport (autophagy, endocytosis, etc.) were downregulated upon addition of glucose. In *S. cerevisiae*, autophagy is controlled at the transcriptional level by several transcription factors including *Sc*Gln3 and *Sc*Msn2/4, providing a simultaneous control by different nutrient signaling pathways. For instance, it is known that the presence of preferred nitrogen sources activates the *S. cerevisiae* conserved target of rapamycin (TOR) kinases and this leads to the repression of genes involved autophagy (Cebollero and Reggiori, 2009). As our data show that glucose also represses *C. glabrata* autophagy at the transcriptional level, this might be controlled via the cAMP-PKA pathway and the transcription factors *C. glabrata* Msn2/4. In *S. cerevisiae*, several endocytosis factors are repressed by the glucose-regulated *Sc*Mig1 in glucose replete conditions (Laidlaw *et al.*, 2021). As the *C. glabrata* homolog of *Sc*Mig1 accumulates in the nucleus after addition of glucose, this suggests a similar regulation (Roetzer *et al.*, 2010).
As glucose is the preferred carbon source, its addition causes *C. glabrata* to start cell growth as the translational machinery including ribosome biogenesis and tRNA synthesis were strongly induced, similar to the *S. cerevisiae* transcriptional response (Wang *et al.*, 2004; Yin *et al.*, 2003).
The results discussed so far indicate similar transcriptional responses of *C. glabrata* and *S. cerevisiae* upon addition of glucose. In contrast, glucose induced the expression of several enzymes involved in heme biosynthesis in *C. glabrata*, while in *S. cerevisiae* the expression of *ScHEM1/2/3/12* is constitutive and unaffected by the carbon source (Zhang and Hach, 1999).

The cAMP-PKA pathway

In *S. cerevisiae*, the cAMP-PKA pathway signals the availability of an optimal growth medium and adapts its cellular expression accordingly (Thevelein and de Winde, 1999). While our data show that the expression of a high number of *C. glabrata* genes is significantly up- or downregulated by glucose, only 114 upregulated and 115 downregulated genes (4.3 % of the genome) showed no significant difference in expression in the *gpr1*Δ strain. This number of genes is lower than expected, as the transcriptome study of Wang *et al.* (2004), which uses similar sampling conditions as our study, shows that in *S. cerevisiae* 161 genes are up- and 314 genes are downregulated by glucose exclusively via PKA (8.1% of the genome). Although it is possible that the discrepancy in number of DE genes is caused by actual differences

in the signaling pathway between the two species, prudence is needed as the *S. cerevisiae* study used a cAMP unresponsive PKA strain: therefore the 8.1% is a result of both *Sc*Ras and *Sc*Gpa2 mediated signaling towards PKA. In addition, the stringency applied to determine differential gene expression is also slightly different (Wang *et al.*, 2004). Our genome-wide expression profile comparison of the wild type with mutant strains tested (Figure 3.4) supports the hypothesis that our glucose-induced transcriptional response depends on redundant signaling pathways. For instance, so far it is not known if *C. glabrata* also signals glucose intracellularly via Ras towards PKA, but this hypothesis serves a possible explanation why few genes were found exclusively controlled by Gpr1 in our analysis. Therefore, we suggest to include a *C. glabrata* attenuated PKA strain for transcriptome analysis in a follow-up experiment. This suggestion is based on the transcriptional study of Wang *et al.* (2004) who also tested a *S. cerevisiae* strain lacking the regulatory PKA subunit and two of the redundant catalytic PKA subunits, with the third catalytic subunit having a low activity present. As this affects PKA directly, we expect to find more differences compared to the wild type transcriptional response using this strain.

Subsequently, the expression profile of several *C. glabrata* homologs of *S. cerevisiae* genes described to be controlled by the PKA pathway were examined, including ribosomal proteins and proteins involved in stress response. *S. cerevisiae* ribosomal protein genes (*ScRPS4, ScRPS13, ScRPL16A; ScRPL28; ScRPL29*) are induced by glucose via the cAMP-PKA pathway and transcription factor *Sc*Rap1 (Klein and Struhl, 1994; Neuman-Silberberg *et al.*, 1995). Unexpectedly, the *C. glabrata* homologs of these specific listed *S. cerevisiae* genes from literature are not significantly induced in our data, in contrast with the glucose-induced genes being clearly enriched in the ribosomal biogenesis (Table 3.1).

On the other hand, genes involved in stress resistance are similarly downregulated in *S. cerevisiae* via PKA (including *ScDDR2*; *ScUBI4* and heat shock proteins *ScHSP12; ScHSP104; SSA3*) (Boorstein and Craig, 1990; Tanaka *et al.*, 1988; Treger *et al.*, 1998; Verghese *et al.*, 2012). Our data also shows repression of the *C. glabrata* homologous genes in all strains tested, indicating again there are probably multiple layers controlling their expression. The expression of *ScCTT1* encoding for the cytosolic catalase is typically repressed by PKA in *S. cerevisiae*, but the *C. glabrata* homolog does not exist (Marchler *et al.*, 1993; Roetzer *et al.*, 2010). *C. glabrata* encodes a single catalase *CTA1*, the ortholog of *S. cerevisiae ScCTA1*, required for

in vitro resistance to H_2O_2 (Cuéllar-Cruz *et al.*, 2008). *C. glabrata* Cta1 is localized in the cytosol and accumulates in peroxisomes during respiration or inside phagocytic cells (Roetzer *et al.*, 2010). *C. glabrata CTA1* expression was found to be induced under carbon source deprivation (Roetzer *et al.*, 2011). Our data shows that *C. glabrata CTA1* is downregulated by the addition of glucose, both in the wild type strain and the *gpr1*Δ strain.

Adhesin transcriptional response

Investigating the expression profile of our list of putative *C. glabrata* adhesins showed that 23% of the ORFs were not transcribed in our conditions. While this significant number of genes is not expressed, still a large number of adhesins were present in our conditions tested, as many are located close to the telomers and are known to be controlled by sub-telomeric silencing (López-Fuentes *et al.*, 2018). Our transcriptome data show that the expression of a large part of adhesins is not differentially affected by addition of glucose in our conditions. As we showed in Chapter 2 that *in vitro* adhesion to polystyrene is reduced by glucose and this is mediated by the cAMP-PKA pathway, we selected adhesins which are differentially up- or downregulated in the wild type strain but not in the *gpr1*Δ strain.

Unpublished research of our lab suggested a possible role for *EPA1* as the downstream target of the cAMP-PKA pathway affecting adherence, as *EPA1* expression was induced around 15-fold by glucose, fructose and sucrose in the wild type strain and this induction was largely absent in the *gpr1*Δ strain (PhD thesis De Brucker, 2011). However, results of this thesis do not support this hypothesis: firstly, our transcriptome data show a $\log_2$ fold change of around 4 upon glucose addition for *EPA1* in the wild type strain, which is in line with the 15-fold induction of the qPCR data, our RNA sequencing data also showed a similar *EPA1* induction in the *gpr1*Δ strain. Secondly, we also showed that *in vitro* adhesion of the *epa1*Δ *epa6*Δ *epa7*Δ strain and the wild type strain were similar (Section 2.2.7). Together, this strongly indicates that Epa1 is not the adhesin involved downstream of the cAMP-PKA pathway affecting adhesion.

Based on our glucose-induced transcriptional profile, we selected a number of adhesin ORFs and tried to construct the respective deletion strains. As homologous recombination is not very efficient in *C. glabrata* and the majority of adhesins are located near the telomeres, we were not able to obtain any correct adhesin deletions

in the wild type strain. Fortunately, several adhesin deletion strains were successfully obtained in the *lig4*Δ background strain, which was previously constructed in our lab and lacks non-homologous end joining thereby increasing the homologous recombination efficiency (Cen *et al.*, 2015). Assessing the adhesion phenotype of the deletion strains shows that adherence is similar in the presence of glucose and galactose in the *aed2*Δ and CAGL0J00253g deletion strains. Both these genes are present in the same group: they were both upregulated by glucose in the wild type strain but not in the *gpr1*Δ strain, which suggests that their expression lowers the affinity of *C. glabrata* towards the abiotic surface. We therefore hypothesized that the deletion of the responsible adhesin would increase adhesion. This hypothesis fits the data of the *aed2*Δ strain. In contrast, the CAGL0J00253g deletion strain shows a low adhesion, suggesting this gene is important for adhesion to the abiotic surface. The extracellular part of this protein shows many serine and threonine residues. These can be glycosylated which also affects the hydrophobicity of the protein and as such adhesion to plastic.

As these two genes give an opposite adhesion phenotype, further research is needed to examine how they affect the cell surface hydrophobicity of the cell wall. Therefore, we suggest to examine if the presence of glucose or galactose affects *C. glabrata* surface hydrophobicity in the wild type strain versus the two adhesin deletion strains in a follow up experiment by atomic force microscopy as described in Valotteau *et al.* (2019). Furthermore, we were not able to construct all deletion strains of the selected list of interesting adhesins from the transcriptome data. Also, as there are many adhesins, it is possible that there is some redundancy or cooperation between adhesins to obtain the observed phenotype, making the identification of the responsible adhesins more challenging.

Galactose response

Upon addition of galactose, the expression of 7.6% of all *C. glabrata* genes changed significantly, with similar numbers of genes up- and downregulated. Compared to the glucose-induced transcriptional response, this percentage is low. It can be explained by the fact that *C. glabrata* lacks the genes encoding galactose transporters and galactose metabolism (galactose utilization pathway and intracellular galactose regulated transcription factors). Therefore, the number of differentially expressed genes is substantial.

Closer investigation of the GO enriched categories of galactose affected genes showed the upregulation of *C. glabrata* aerobic respiration including the TCA cycle and the different complexes of the respiratory electron transport chain: NADH reductase complex (*NDI1*), ubiquinol cytochrome C reductase complex (*QCR6/9*) and cytochrome C (*CYC1*). Also, heme biosynthesis and iron-sulfur cluster assembly categories were enriched. Both heme and iron-sulphur clusters are iron containing prosthetic groups which can be found in the electron transport chain complexes as well as in other proteins, therefore supporting the upregulation of aerobic respiration (Atamna *et al.*, 2002). Closer inspection of the genes involved in iron-sulfur cluster assembly shows mainly the presence of genes of the iron-sulphur cluster (ISC) pathway in the mitochondria (Braymer and Lill, 2017).

Several genes encoding enzymes to detoxify the reactive oxygen species (ROS) hydrogen peroxide (glutathione peroxidase, thioredoxin peroxidase and catalase) were upregulated. ROS are typically generated in phagocytic cells during infection but are also generated in normal aerobic metabolism in the mitochondrial electron transport chain (Cuéllar-Cruz *et al.*, 2014).

Surprisingly, another part of *C. glabrata* metabolism which was upregulated by galactose involves acetate metabolism and lipid synthesis. Acetate can enter the cell via the plasma membrane transporter Ady2 and is then converted into acetyl-CoA which can subsequently enter the TCA cycle, the glyoxylate cycle or function as a building block for lipid synthesis. Our RNA sequencing data shows the induction of genes from the TCA cycle, glyoxylate cycle and lipid biosynthesis, including fatty acid synthesis and phosphatidylcholine synthesis (Henry *et al.*, 2012). Since the TCA cycle occurs in the mitochondria, acetyl-CoA is transported to the mitochondria via the carnitine shuttle: our data shows the upregulation of the carnitine acetyltransferase (*YAT1*) and the carnitine plasma membrane transporter (*HNM1*) (Chen *et al.*, 2015; Chew *et al.*, 2019). In *S. cerevisiae*, the kinase *Sc*Snf1 of the glucose repression pathway plays a major role in cell adaptation to environmental stresses and carbon sources (Abate *et al.*, 2012; Hong and Carlson, 2007). In the absence of glucose, active *Sc*Snf1 phosphorylates and inactivates *Sc*Mig1 leading to the derepression of genes involved in gluconeogenesis and the glyoxylate cycle, while Sc*ADY2* is derepressed via *Sc*Snf1 dependent chromatin remodeling (Abate *et al.*, 2012; Van Ende *et al.*, 2019). A *ScSNF1* homolog exists in *C. glabrata* and is necessary to use trehalose (Petter and Kwon-Chung, 1996). Also, *C. glabrata ADY2* expression was

induced inside macrophages (Kaur *et al.*, 2007). This suggests the involvement of *C. glabrata* Snf1 in the galactose transcriptional response, but further research is needed to prove this hypothesis.

The expression of several *C. glabrata* plasma membrane transporters is also affected by galactose in our results: amino acid and phosphate transporters were upregulated, while several hexose transporters (*HXT1*; *HXT4*; *HXT6/7*; *HXT4/6/7*) were downregulated. In *S. cerevisiae*, the expression of the hexose transporters depends on the extracellular glucose concentration, mainly regulated by the glucose sensors *Sc*Snf3 and *Sc*Rgt2 (Özcan and Johnston, 1999). Similar *C. glabrata* Snf3 and Rgt2 glucose sensors control the expression of *C. glabrata HXT* genes (Ng *et al.*, 2015a; Ng *et al.*, 2015b). *C. albicans Ca*Hgt4 senses both glucose and galactose and controls the transcription of several glucose transporters (*CaHGTs*) via *Ca*Std1 and *Ca*Rgt1 (Brown *et al.*, 2009; Brown *et al.*, 2006). Heterologous expression of *CaHGT4* in *S. cerevisiae* even results in galactose-inducible expression of *ScHXT* genes, indicating *Ca*Hgt4 can similarly transmit a signal downstream (Brown *et al.*, 2009; Van Ende *et al.*, 2019).

Inspection of the protein similarities between these species shows that *C. glabrata* Rgt2 and Snf3 are more closely related to *S. cerevisiae Sc*Rgt2 and *Sc*Sfn3. As *C. albicans Ca*Hgt4 also clusters together with these proteins, one cannot exclude the possibility that *C. glabrata* Snf3 kept the function of sensing galactose, as the *C. glabrata* Snf3/Rgt2 studies so far did not investigate the effect of extracellular galactose as a stimulus.

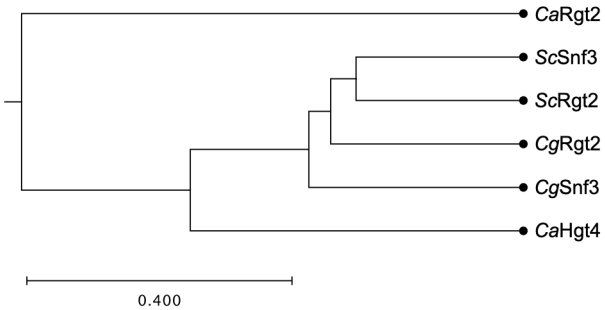

Figure 3.10: Phylogenetic tree of Snf3 and Rgt2 proteins.
The *C. glabrata*, *S. cerevisiae* and *C. albicans* sequences were used to construct the phylogenetic tree. Protein sequences were aligned to construct the tree using the unweighted pair method with arithmetic mean (UPGMA) and the Kimura Protein as a protein distance measure.

So far, many elements of the *C. glabrata* galactose induced transcriptional response can be mirrored to effects seen with *S. cerevisiae* in low glucose conditions, via Rgt2/Snf3 and the kinase Snf1. However, in *S. cerevisiae* both signaling pathways do not signal the presence of galactose. While we cannot exclude that *C. glabrata* Snf3 kept the function to sense galactose during evolution, it is rather unlikely as galactose cannot be used for growth in *C. glabrata*. However, in Chapter 2 we also showed sucrose signaling via Gpr1, which also cannot be used as a carbon source. As the galactose-induced transcriptome includes compelling GO enriched categories, we believe the response is not a random effect, but the cells do signal the extracellular condition to the inside of the cell. But maybe rather than direct signaling of galactose, the effect seen here is due to signaling of a kind of stress. For instance, there are similarities with the transcriptional response seen in *C. glabrata* macrophage-engulfed cells. On the other hand, genes of the core oxidative stress response (e.g. catalase) were induced in our results and similarly, these genes are induced by mild oxidative stress or starvation (Roetzer *et al.*, 2010; Roetzer *et al.*, 2011).

3.4 Materials and methods

Yeast strains and plasmids

Table 3.8: List of *C. glabrata* strains and plasmid used in this chapter

Strain	Genotype	Source
ATCC2001 HTL	*his3Δ::FRT leu2Δ::FRT trp1Δ::FRT*	(Schwarzmüller *et al.*, 2014)
HT631	*gpr1Δ::*NatMX *his3Δ leu2Δ trp1Δ*	Lab collection
HT633	*gpa2Δ::*NatMX *his3Δ leu2Δ trp1Δ*	Lab collection
CgB3	*gpa2Δ*::NatMX *GPA2*^{Q299L} *his3Δ leu2Δ*	This work
AFG1	*lig4Δ::HIS3 trp1Δ::FRT*	(Cen *et al.*, 2015)
CgBAd1	CAGL0B00116gΔ *lig4Δ*	This work
CgBAd2	CAGL0A01584gΔ *lig4Δ*	This work
CgBAd3	*epa6Δ lig4Δ*	This work
CgBAd4	*epa11Δ lig4Δ*	This work
CgBAd5	*aed2Δ lig4Δ*	This work
CgBAd6	*awp3Δ lig4Δ*	This work
CgBAd7	CAGL0J00253gΔ *lig4Δ*	This work
CgBAd8	CAGL0J01463gΔ *lig4Δ*	This work

Plasmid	Relevant genotype	Used for	Source
p*CgACT1*	*TRP1*	Stable centromeric *C. glabrata* plasmid *TRP1* selection marker	(Miyazaki *et al.*, 2010)
p*CgACT1-GPA2*^{Q299L}	*GPA2*^{Q299L}	Expression of constitutively active Gpa2 under own promoter and terminator	This work
pBCAd1	CAGL0B00116g deletion cassette	Construction deletion strain	This work
pBCAd2	CAGL0A01584g deletion cassette	Construction deletion strain	This work
pBCAd3	CAGL0C00110g (*EPA6*) deletion cassette	Construction deletion strain	This work
pBCAd4	CAGL0L13299g (*EPA11*) deletion cassette	Construction deletion strain	This work
pBCAd5	CAGL0K13002g (*AED2*) deletion cassette	Construction deletion strain	This work
pBCAd6	CAGL0J11891g (*AWP3*) deletion cassette	Construction deletion strain	This work
pBCAd7	CAGL0J00253g deletion cassette	Construction deletion strain	This work
pBCAd8	CAGL0J01463g deletion cassette	Construction deletion strain	This work
pBCAd9	CAGL0F09273g deletion cassette	Construction deletion strain	This work
pBCAd10	CAGL0F00105g deletion cassette	Construction deletion strain	This work
pBCAd11	CAGL0I00220g (*EPA23*) deletion cassette	Construction deletion strain	This work

Sampling and RNA isolation

Cells were grown in SC glycerol to mid-exponential phase after which either glucose (2% final concentration) or galactose (2% final concentration) was added. Samples were taken at timepoint zero (just before addition of sugars) and 30 or 60 minutes after addition of glucose or galactose. The wild type ATCC2001 HTL strain, *gpr1*Δ strain and $GPA2^{Q299L}$ strain were used. The harvested cells were washed with sterile water and flash frozen in liquid nitrogen. Total RNA was isolated using the RiboPure Yeast kit (Ambion, Life Technologies, USA), according to manufacturer's instructions. RNA quality was verified using the Nanodrop-1000 (Thermo Scientific) (OD 260/280 between 1.8 and 2.1 and OD 260/230 between 1.8 and 2.0). 100 ng RNA was sent for sequencing to the VIB nucleomics core (Leuven, Belgium), where the quality was checked again with the Bioanalyzer 2100 (Agilent Technologies) to assess RNA integrity of all samples.

RNA sequencing

Library preparation, RNA sequencing and data mapping were performed at the VIB nucleomics core (Leuven, Belgium). All samples were prepared in biological triplicates. The sequencing library was prepared using Illumina TruSeq RNA Library Preparation Kit and single-end 75 bp reads were produced with Illumina NextSeq 500 instrument.

Data analysis

Quality of the sequencing was checked by the yield per sample and the library complexity (e.g. the frequencies for A/T and G/C should be comparable). Afterwards the sequences were processed to remove as much technical artifacts as possible: sequences of low quality (e.g. ends of sequencing) and very short sequences (<35 bp) were removed using FastX (0.0.14). Overall, less than 0.13% of the reads were removed in this step. Secondly, the adapters were removed using Cutadapt (1.7.1) and again very short sequences (<35 bp) were removed. In this step, less than 0.01% of the sequences were removed. Then, polyA-reads, ambiguous reads, overall low-quality reads and artifacts were removed using FastX (0.0.14) and ShortRead (1.24.0), less than 0.4% of the sequences was removed. Finally, using Bowtie (2.2.4) possible contaminants of illumina were removed but this was absent in our samples.

These good quality sequences were subsequently mapped to the reference genome of *Candida glabrata* from the CGD (*Candidaglabrata*CBS138s02m07r06) in three steps: Read mapping using TopHat (v2.0.13), quality filtering and sorting the reads using Samtools (1.1). Overall, less than 2% of the reads could not be mapped and after quality filtering more than 96% of the reads could be mapped. After mapping, again a quality control was performed to remove reads which are ambiguous (mapped to more than one gene), counts were merged with gene annotation and within-sample-normalization was performed. In the meantime, Xu *et al.* (2020) published an updated version of the *C. glabrata* genome. As 5209 genes were identical in protein sequence to the previous version of the genome, we did not redo the complete RNAseq mapping and analysis. However, as we investigated the adhesins and these genes were enriched in sequencing mistakes, we did the reannotation for all predicted adhesins of Xu *et al.* (2020).

For statistical analysis, counts were transformed to log scale (log_2 of indicated ratio) and as we perform multiple testing on the same dataset, p-values were adjusted by Benjamin-Hochberg to control the False Discovery Rate (FDR). Gene ontology (GO) term analysis was performed using FungiFun2 (Priebe *et al.*, 2015). Venn diagrams were made using Venny online freeware (2.1.0). The genome wide transcriptome heatmap and comparison of strains were constructed in R using packages pheatmap and ggplot respectively. The adhesin heatmap was constructed in MeV.

Construction of plasmids

The adhesin deletion cassettes were made in vector PYC44. Promoter and terminator regions were amplified using primers ‘ORF prom-Fw’ plus ‘ORF prom-Rv’ and ‘ORF term-Fw’ plus ‘ORF term-Rv’ respectively (Addendum 3). PYC44 was digested with BamHI and XhoI, after which promoter and terminator were inserted using NEBuilder (New England Biolabs). Correct insertion of the promoter and terminator regions was checked by PCR using primers B4165 and B4166.

Construction of C. glabrata deletion strains

The adhesin deletion strains were generated by insertion of the respective deletion cassettes: therefore, the vectors containing the deletion cassettes were digested with KpnI and SacI and subsequently transformed by electroporation in *C. glabrata*. Correct integration of the cassette was checked by PCR (primers 'ORF control up' and 9064; primers 'ORF control down' and 9065, Addendum 3).

In vitro adhesion to polystyrene

Adhesion to polystyrene was tested as described in Ramage *et al.* (2001). In short, cells were washed twice in phosphate buffered saline (PBS) and diluted to 10^7 cells ml^{-1} in the desired medium. 10^6 cells were added to per well of a 96 well plate and incubated for 90 minutes at 37°C. Non-adherent cells were removed by washing twice with PBS. The quantification of adherent cells was measured using 2,3-bis(2-methoxy-4-nitro-5-sulphophenyl)-2*H*-tetrazolium-5-carboxanilide assay (XTT, Sigma). 100 µl of XTT (1 mg/ml) and 1 µM menadione (Sigma) was added to each well and incubated for one hour at 37°C, after which the optical density at 495 nm was measured.

Chapter 4:
Characterization of *C. glabrata* trehalase enzymes

This chapter is based on the manuscript entitled “The involvement of the *Candida glabrata* trehalase enzymes in stress resistance and gut colonization” which has been published in Virulence. I am shared first author as I helped with the design and optimization of the assays, performed experiments and helped in writing the manuscript. The manuscript has been adapted to match the format and lay-out of this thesis.

4.1 Introduction

As mentioned in Chapter one, in order to survive, micro-organisms need to rapidly adapt to environmental stresses such as nutrient limitation, the immune defence, etc. in the human body. In *C. glabrata*, this activates the general stress response, which includes the induction of genes encoding enzymes involved in trehalose metabolism (Ishchuk *et al.*, 2019). Trehalose is a non-reducing glucose disaccharide with a double role in fungi. It serves as a storage carbon source but is also crucial as a stress protectant molecule by stabilizing proteins and membranes, thereby causing resistance to antifungal drugs, to oxidative stress and to heat stress (Alvarez-Peral *et al.*, 2002; Argüelles, 2014; Eleutherio *et al.*, 1993; Elliott *et al.*, 1996; González-Párraga *et al.*, 2011; Lillie and Pringle, 1980; Tournu *et al.*, 2013).

The trehalose biosynthesis pathway is defined by two main enzymes: trehalose-6-phosphate synthase (Tps1) and trehalose-6-phosphate phosphatase (Tps2). Tps1 converts uridine diphosphate (UDP)-glucose and glucose-6-phosphate into trehalose-6-phosphate (T6P) and UDP, after which Tps2 hydrolyzes T6P into trehalose and free phosphate (Figure 4.1). Trehalose as well as the enzymes linked to its biosynthesis have been described to be involved in virulence and pathogenesis, with functions in infection, biofilm formation, etc. (Argüelles *et al.*, 1999; Fillinger *et al.*, 2001; Ngamskulrungroj *et al.*, 2009; Petzold *et al.*, 2006; Tournu *et al.*, 2013; Van Dijck *et al.*, 2002; Zaragoza *et al.*, 1998; Zhu *et al.*, 2013). Despite their absence in the human body and their long-known role in virulence, still no Tps1 or Tps2 inhibitor has been discovered and brought to clinical trials or to the clinic.

As trehalose accumulates under stress conditions and thereby ‘freezes’ proteins and membranes, a fast hydrolysis of trehalose upon relief of stress is essential to resume growth in *S. cerevisiae* (Singer and Lindquist, 1998; Wera *et al.*, 1999). This hydrolysis is mediated by trehalase enzymes. Fungal species generally have two trehalase enzymes: a neutral and an acid trehalase enzyme. In the yeast model organism *S. cerevisiae*, the neutral trehalase enzyme *Sc*Nth1 is regulated by cAMP-dependent phosphorylation and ensures endogenous trehalose metabolization (Schepers *et al.*, 2012; van der Plaat, 1974; van Solingen and van der Plaat, 1975). It requires divalent cations (Ca^{2+} and Mn^{2+}) and has a pH optimum of 7 (Londesborough and Varimo, 1984; Thevelein, 1984). This neutral trehalase shows higher activity during

exponential growth on fermentable carbon sources and is located in the cytoplasm of the cells (Sánchez-Fresneda *et al.*, 2009). On the other hand, fungal acid trehalase enzymes contain either a transmembrane domain or a signal peptide and are therefore located on the outside of the fungal cell; in the cell membrane, periplasm or cell wall (He *et al.*, 2009; Parrou *et al.*, 2005; Pedreño *et al.*, 2004). The extracellular localization ensures hydrolysis of external trehalose (Nwaka *et al.*, 1996; Pedreño *et al.*, 2004; Zilli *et al.*, 2015). In *S. cerevisiae*, the acid trehalase enzyme is also present in the vacuole (He *et al.*, 2009; Parrou *et al.*, 2005). The acid trehalase enzyme has an optimal pH of 4.5 and is not regulated by cAMP, phosphorylation or divalent cations (Sánchez-Fresneda *et al.*, 2009).

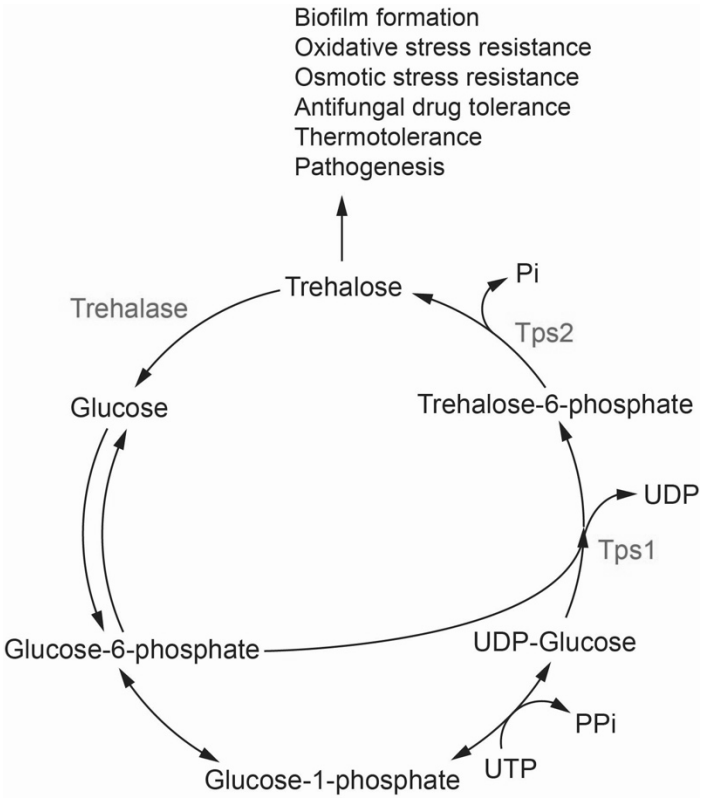

Figure 4.1: Overview of the fungal trehalose metabolism.
Trehalose is synthesized in two steps: Trehalose-6-phosphate (T6P) synthase (Tps1) forms T6P, after which it is converted into trehalose by T6P phosphatase (Tps2). Breakdown of trehalose into two glucose molecules is mediated by the trehalase enzymes. Apart from being a carbon source, trehalose also plays an important role in the stress resistance of fungal cells. This figure is adapted from Thammahong *et al.* (2017).

C. glabrata very rapidly hydrolyzes extracellular trehalose, a feature which is used in the clinic to diagnose *C. glabrata* infections in a quick and cost-effective way (Fenn *et al.*, 1999; Fraser *et al.*, 2012; Freydiere *et al.*, 2003; Land *et al.*, 1996; Lopez *et al.*, 2001; Murray *et al.*, 2005; Willinger *et al.*, 2005). Based on sequence homology with the *S. cerevisiae* trehalase enzymes, the *C. glabrata* genome encodes three trehalase enzymes: Ath1, Nth1 and Nth2. Recently, Ath1 (CAGL0K05137g) was found to be responsible for this extracellular trehalose utilization (Zilli *et al.*, 2015). The Ath1 orthologues in *C. albicans* (*CaATC1)* and *C. parapsilosis* (*CpATC1)* were found to be involved in virulence and stress resistance. The *CaATC1* and *CpATC1* deletion strains showed both an increased thermotolerance and an increased resistance toward oxidative stress (Pedreño *et al.*, 2007; Sánchez-Fresneda *et al.*, 2015; Sánchez-Fresneda *et al.*, 2014). Whereas these results would suggest an increase in virulence, this was not observed using a systemic mouse model, where these deletion strains showed a reduced virulence (Pedreño *et al.*, 2007; Sánchez-Fresneda *et al.*, 2014). The *C. glabrata* neutral trehalases, Nth1 (CAGL0M10439g) and Nth2 (CAGL0C04323g) are considered to be cytosolic trehalases responsible for the hydrolysis of intracellular trehalose. In *C. albicans*, deletion of the neutral trehalase *CaNTC1* does not affect virulence in a mouse model of systemic infection (Eck *et al.*, 1997).

Based on the importance of the trehalose metabolism for virulence in other pathogenic fungi and the observation that *C. glabrata* consumes extracellular trehalose very rapidly, we aimed to characterize the *C. glabrata* trehalase enzymes. Therefore, we first constructed the single, double and triple trehalase deletion strains. These strains were then characterized *in vitro* and finally tested for colonization in the GI tract of mice and for virulence in a mouse model of systemic infection.

4.2 Results

4.2.1 The *C. glabrata* trehalase enzymes are phylogenetically closely related to the *S. cerevisiae* trehalase enzymes

As mentioned before, *C. glabrata* is more related to species within the *Saccharomycetaceae* clade than to *C. albicans* (Gabaldón and Carreté, 2016; Gabaldón *et al.*, 2013). Therefore, we used the *S. cerevisiae* trehalase protein sequences in a BLASTP search to identify the *C. glabrata* trehalase enzymes. In addition, we constructed a phylogenetic tree of different fungal trehalase enzymes and also included the human trehalase enzyme (Figure 4.2A). Even though humans cannot synthesize trehalose, their genome encodes one trehalase. The human trehalase enzyme can be found in the intestines and kidneys but also in the urinary tract (Ishihara *et al.*, 1997; Sacktor, 1968). In the trehalase phylogenetic tree, two main clusters can be distinguished: the neutral trehalases and the acid trehalases (Figure 4.2A).

For the neutral trehalases *Sc*Nth1 (YDR001C) and *Sc*Nth2 (YBR001C), *C. glabrata* Nth1 (CAGL0M10439g) and Nth2 (CAGL0C04323g) were identified as closest orthologs respectively. These proteins are highly conserved to their *S. cerevisiae* orthologs, as reflected by the high percentage of amino acid identity (80% for Nth1 and 68% for Nth2) (Figure 4.2B). As is the case for *S. cerevisiae*, *C. glabrata* Nth1 and Nth2 are highly similar with one another (71% amino acid identity), indicating that these enzymes are most probably the result of the whole genome duplication event (Wolfe and Shields, 1997). *C. glabrata NTH1* encodes a polypeptide of 769 amino acids with a predicted molecular mass of 87.4 kDa, while *NTH2* encodes a polypeptide of 750 amino acids with a predicted molecular mass of 86.5 kDa. Both *C. glabrata* Nth1 and Nth2 amino acid sequences contain neither a transmembrane domain nor a signal sequence (Nielsen, 2017; Omasits *et al.*, 2014). Alignment of *C. glabrata* Nth1 with *Ca*Nth1 (CR_00560W_A) shows 58% amino acid identity, reflecting the more distant phylogenetic relationship between *C. glabrata* and *C. albicans*. Phylogenetically, the human trehalase clusters together with the fungal neutral trehalases (Figure 4.2A). Despite the human trehalase only shows 27% amino acid identity to both Nth1 and Nth2 of *C. glabrata*, the amino acids involved in substrate binding and the active site are conserved (Addendum 4).

For the acid trehalase *Sc*Ath1 (YPR026W), Ath1 (CAGL0K05137g) was found as an ortholog in *C. glabrata,* sharing 67% amino acid identity (Figure 4.2). *C. glabrata ATH1* encodes a polypeptide of 1212 amino acids with a predicted molecular mass of 136.5 kDa. In contrast, alignment of Ath1 with *Ca*Atc1 (C1_06940C_A) showed only 41% amino acid identity. In other organisms, Ath1 was often found on the extracellular side of the cells (He *et al.*, 2009; Jules *et al.*, 2004; Lucio *et al.*, 2000; Nwaka *et al.*, 1996; Pedreño *et al.*, 2004; Sánchez-Fresneda *et al.*, 2014). Hence, the PROTTER and SignalP4.1 algorithms were used to predict a possible transmembrane domain or a signal sequence (Nielsen, 2017; Omasits *et al.*, 2014). No signal peptide was found, but Ath1 is predicted to contain one transmembrane (TMD) domain at the N-terminus (between positions 83 and 103). The orthologous N-terminus and TM domain of *Sc*Ath1 confers the extracellular localization*,* suggesting identical extracellular localization for Ath1 in *C. glabrata* (He *et al.*, 2009).

A

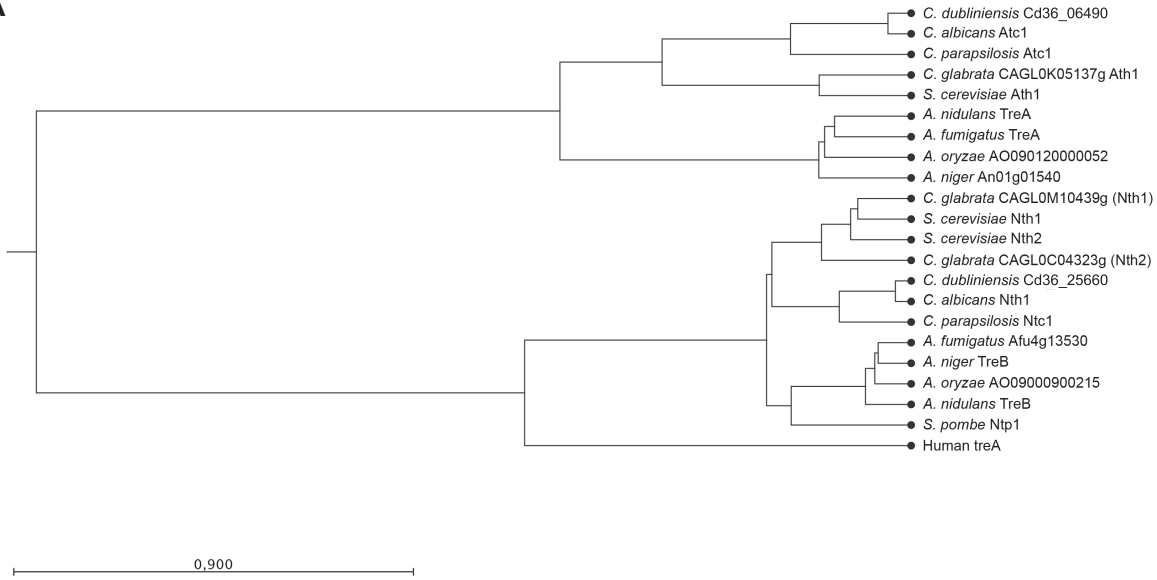

B

C. glabrata trehalase	*S. cerevisiae* trehalase	Percentage identity
Nth1 (CAGL0M10439g)	Nth1 (YDR001C)	80%
Nth2 (CAGL0C04323g)	Nth2 (YBR001C)	68%
Ath1 (CAGL0K05137g)	Ath1 (YPR026W)	67%

Figure 4.2: Phylogenetic tree of fungal trehalases.
Two main clusters can be distinguished: the neutral trehalases and the acid trehalases. The human trehalase enzyme was included and is present in the cluster of neutral trehalase enzymes. Protein sequences were aligned and the phylogenetic tree was constructed using the unweighted pair method with arithmetic mean and the Kimura Protein as a protein distance measure (A). Overview of amino acid identity between the *C. glabrata* and *S. cerevisiae* trehalases (B).

4.2.2 Ath1 is required for growth on trehalose as a carbon source

In order to study the *C. glabrata* trehalase enzymes, the single- double- and triple trehalase deletion strains were generated as described in Materials and Methods in collaboration with Mieke Van Ende. For the *in vitro* characterization of the trehalase mutants, we tested the growth of the strains in minimal medium supplemented with glucose or trehalose, two carbon sources that *C. glabrata* is able to ferment (Rodrigues *et al.*, 2014). All strains grew to the same extent on glucose in both solid and liquid medium (Figure 4.3 A-B). When trehalose was used as external carbon source, all strains lacking *ATH1* had a growth defect in both liquid and solid medium (Figure 4.3 A and C). These results indicate that Ath1 is responsible for the hydrolysis of exogenous trehalose, which led to two hypotheses: either *C. glabrata* transports extracellular trehalose to the inside of the cell by a trehalose transporter and Ath1 hydrolyzes the disaccharide intracellularly, or Ath1 is present at the extracellular side of the cells and hydrolyzes trehalose in the surrounding medium after which glucose is taken up by the glucose transporters. In *S. cerevisiae*, extracellular trehalose is transported by the high-affinity sugar transporter *Sc*Agt1 (Han *et al.*, 1995). Therefore, a BLASTP search was performed using *Sc*Agt1, however no orthologs could be identified in *C. glabrata*. Hence, we measured the concentration of trehalose in the medium over time during the growth on trehalose. We postulated that if Ath1 does indeed hydrolyze trehalose intracellularly after uptake by transporters, a strain deleted for *ATH1* would still show reducing extracellular trehalose levels over time. Yet, for the strains with a deletion of *ATH1,* the trehalose in the medium remained constant (Figure 4.3D). In contrast, the strains with wild type *ATH1* were still able to hydrolyze the extracellular trehalose, which is reflected by a drop of trehalose in the medium (Figure 4.3D). Additionally, coinciding with this decrease in trehalose, a small increase of glucose in the medium was observed confirming extracellular hydrolysis of trehalose in two glucose molecules (Figure 4.3E).

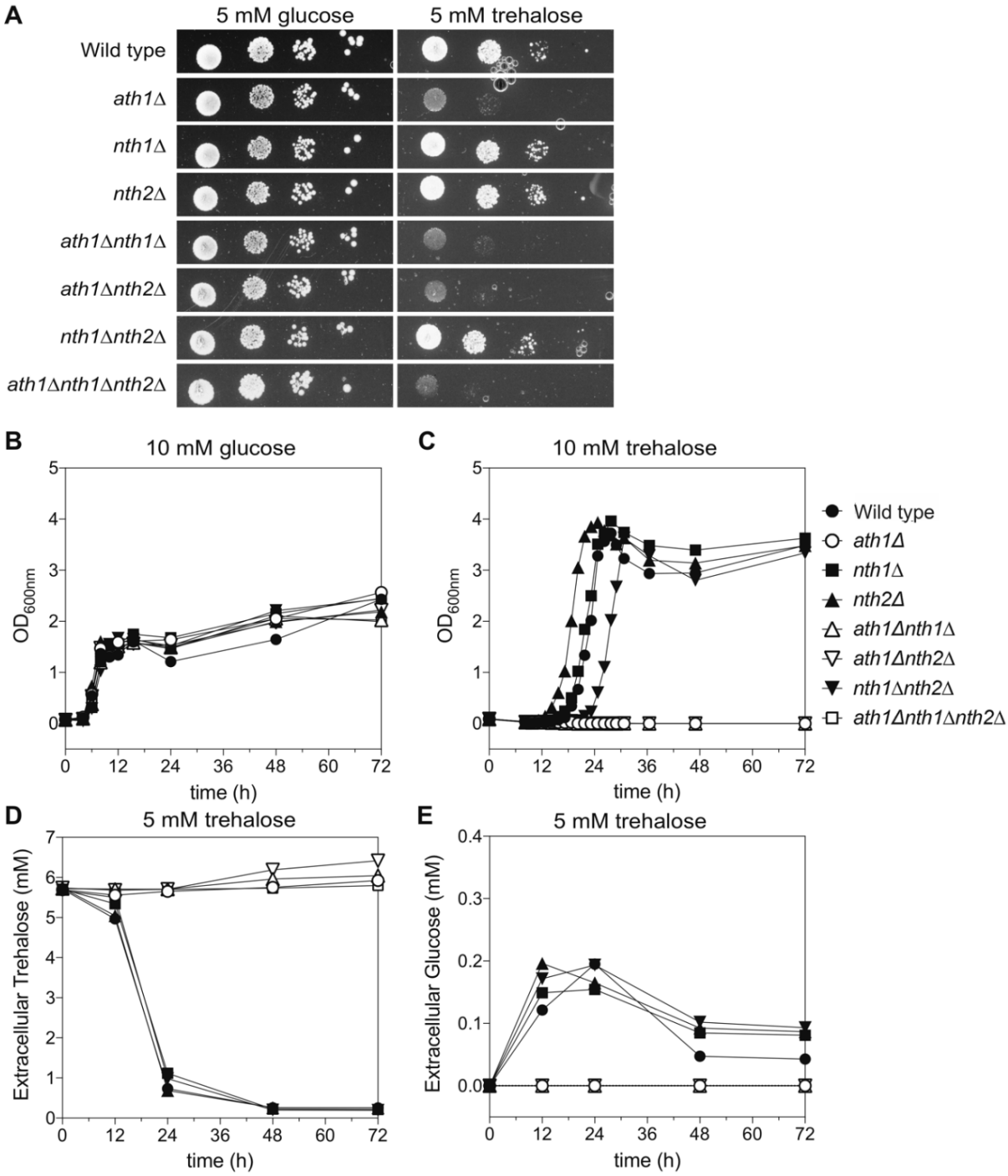

Figure 4.3: Growth of the different trehalase deletion strains.
Cells were grown on solid YNB (A) and in liquid YNB (B-E) medium containing glucose (A-B) or trehalose (A, C-E) as a fermentable carbon source. During growth in YNB trehalose, we also measured the trehalose and glucose concentration in the medium over time (D-E, respectively). The experiments were performed at least twice and average results of three independent transformants are shown.

Taken together, these results suggest that Ath1 hydrolyses extracellular trehalose and thus indicate that Ath1 is present at the cell surface or is secreted. Therefore, we determined its localization by tagging the trehalase enzymes endogenously with the fluorescent protein mCherry (described in Materials and Methods). When *C. glabrata* was grown in glucose-containing medium to the exponential phase, no fluorescence was detected (Figure 4.4), which coincided with a very low trehalase activity measured in exponential phase (less than 5 nmol glucose/min.mg protein). However, when trehalose was used as a carbon source, a fluorescent signal on the border of the cell and a vacuolar signal was observed for the Ath1 tagged strain (Figure 4.5 and Figure 4.6A).

Next, we investigated whether Ath1 is anchored in the plasma membrane as Ath1 contains one predicted TM domain. Therefore, we generated protoplasts of cells grown in glucose or trehalose containing medium and measured the trehalase activity (

Figure 4.6B). Similar to our previous results, trehalase activity of cells grown on glucose was very low and this trehalase activity was not significantly affected by protoplast formation in these cells. When grown on trehalose as a carbon source, a high trehalase activity was observed in the complete cells taken from the growth culture and the untreated cells which did not receive the protoplasting solution, while trehalase activity dropped dramatically in the protoplasts (

Figure 4.6B). In addition, the fluorescent signal of cells with Ath1 fluorescently tagged, observed on the outside of untreated cells, was no longer visible in the protoplasts (

Figure 4.6A). These results indicate that Ath1 is not anchored to the cell membrane but is rather present in the periplasmic space or in the cell wall, similar to the situation in *S. cerevisiae* (He *et al.*, 2009). Zilli and co-workers showed that Ath1 is secreted to the outside of the cells and is released into the medium (Zilli *et al.*, 2015).

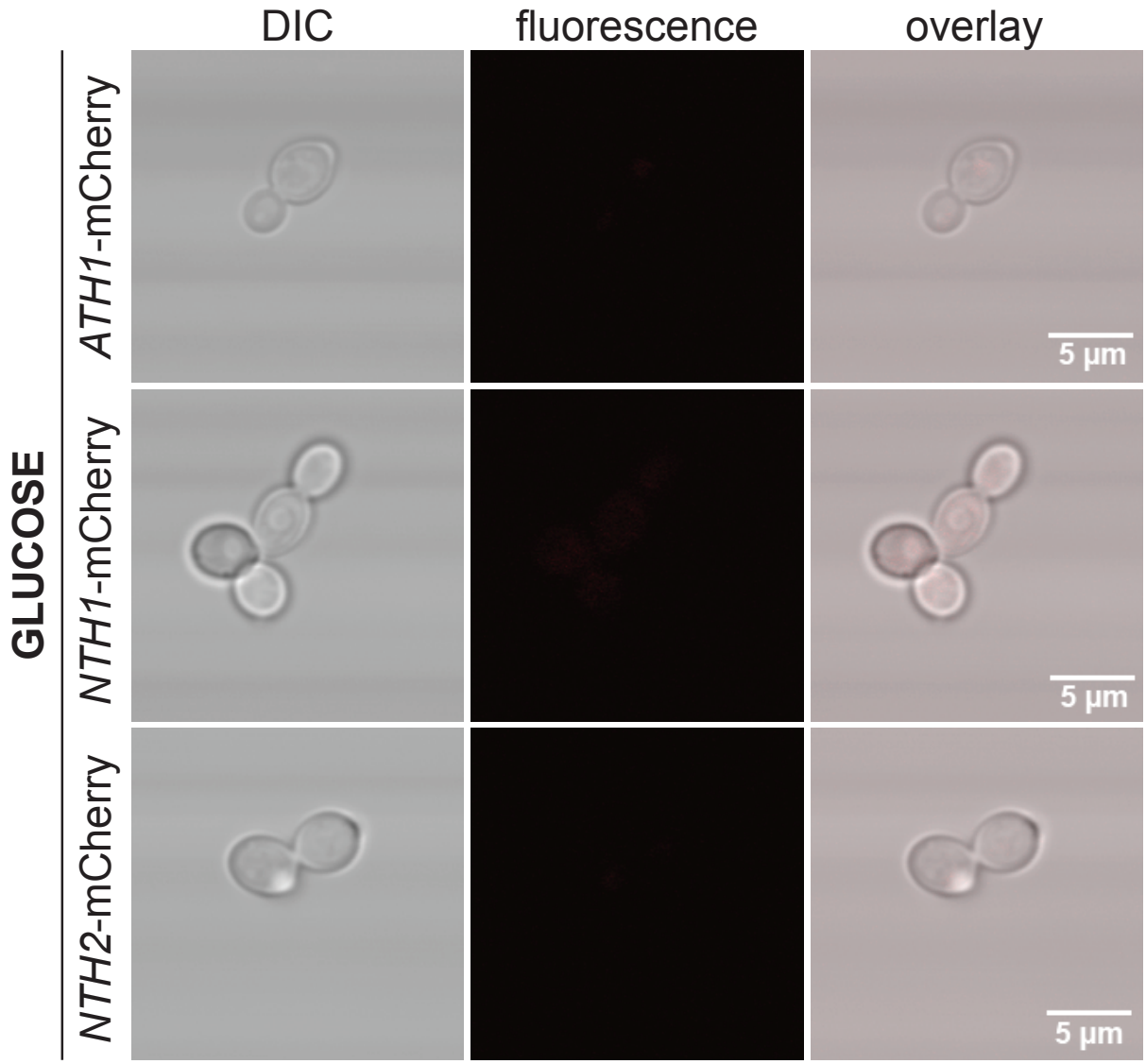

Figure 4.4: Representative microscopy images showing exponential *C. glabrata* cells grown in presence of glucose.
Imaging of the individually tagged trehalases: Ath1-mCherry (top), Nth1-mCherry (middle) and Nth2-mCherry cells, taken with a Fluoview 1000 confocal microscope.

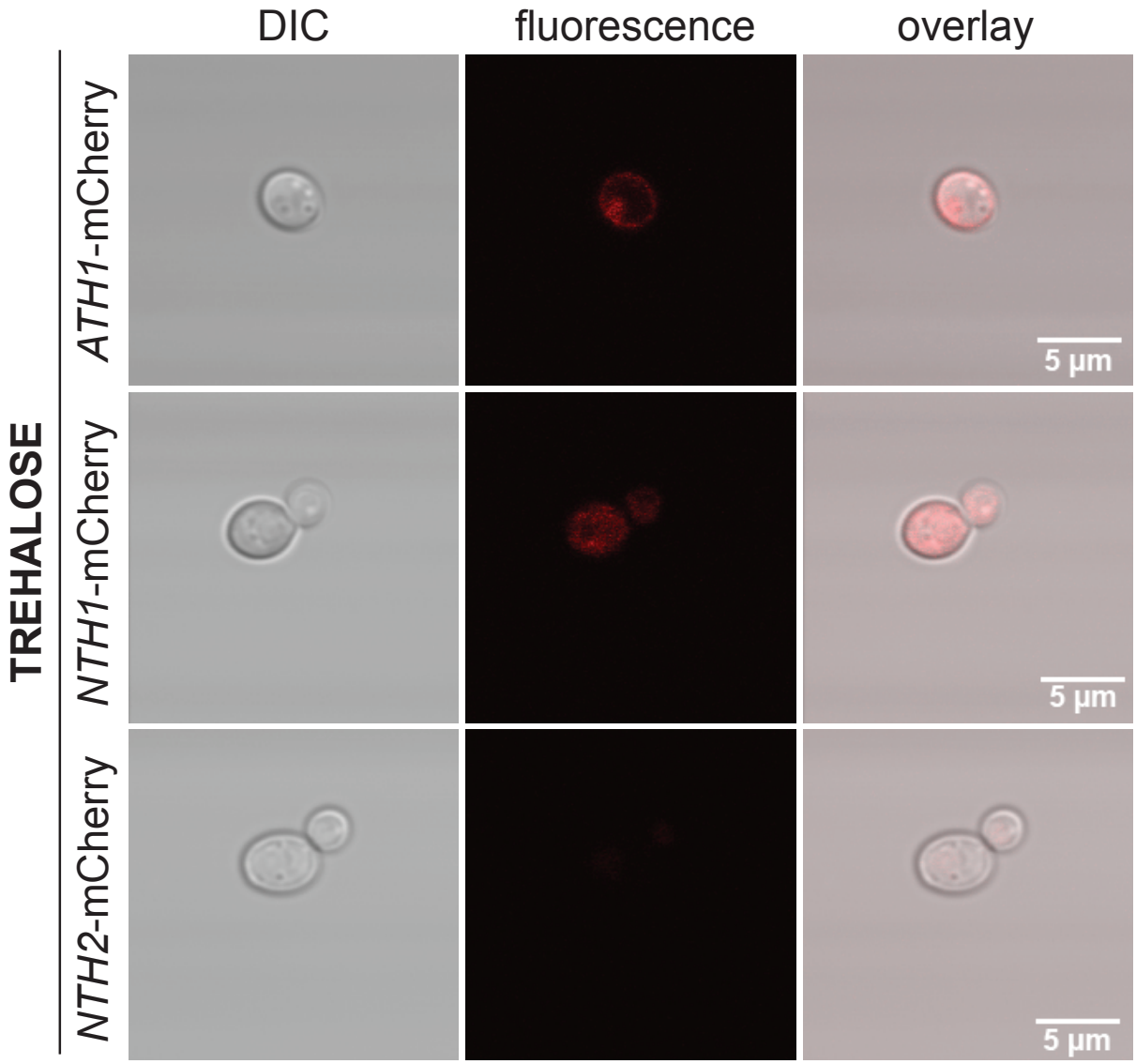

Figure 4.5: Representative microscopy images showing exponential *C. glabrata* cells grown in presence of trehalose.
Imaging of the individually tagged trehalases: Ath1-mCherry (top), Nth1-mCherry (middle) and Nth2-mCherry cells, taken with a Fluoview 1000 confocal microscope.

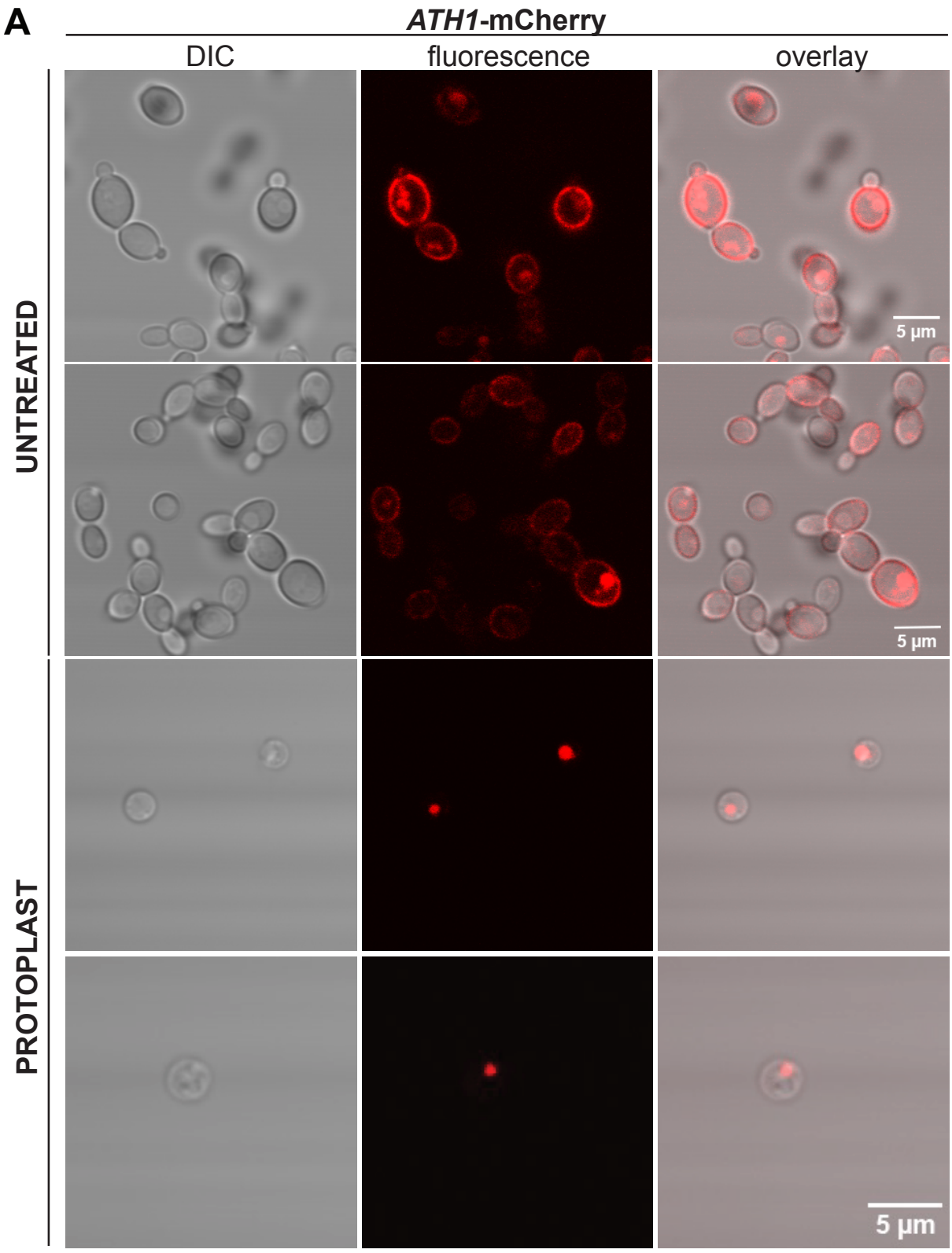
A
ATH1-mCherry
DIC
fluorescence
overlay
UNTREATED
PROTOPLAST
5 µm
5 µm
5 µm

B

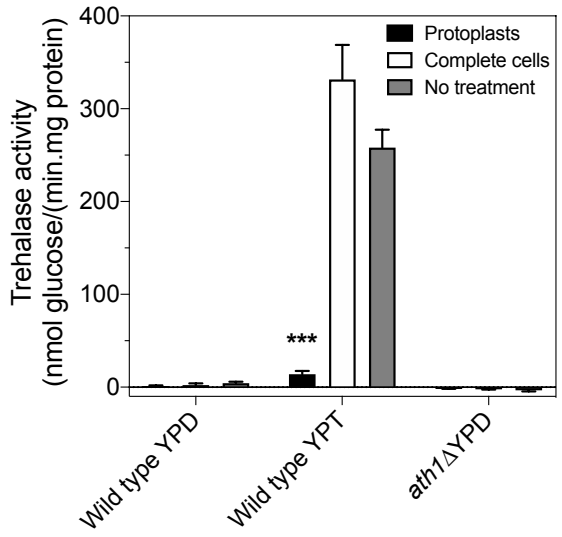

Figure 4.6: Ath1 is present in the periplasm and is responsible for high trehalase activity when cells are grown in presence of trehalose.
Imaging of Ath1-mCherry cells taken with a Fluoview 1000 confocal microscope (A). Cells were grown in presence of trehalose to exponential phase after which protoplasts were made. The upper two panels of A show complete cells (cells taken directly from the growth culture), the lower two panels show protoplasts of Ath1-mCherry. Trehalase activity was measured in complete cells, protoplasts and cells that didn't receive the protoplasting solution after growth on YPD or YPT as indicated (B). Average trehalase activity of at least two experiments is shown with the standard error of the mean (SEM). Statistical Kruskal-Wallis test was used with Dunn's correction for comparing treated and untreated conditions for each strain (*, $P \leq 0,05$; **, $P \leq 0,01$; *** $P \leq 0,001$ and ****, $P \leq 0,0001$). Protoplasts of the cells were made by Mieke Van Ende and trehalase activity was measured by Mieke Van Ende.

4.2.3 Nth1 is important for competition *in vitro* with other micro-organisms

As trehalose serves as both a reserve carbohydrate and a stress protectant molecule, we investigated if these enzymes provide *C. glabrata* a competitional advantage over other micro-organisms when they are cultured together over a longer period of time. To test this hypothesis *in vitro*, we co-cultured *C. glabrata* with another yeast for seven days. Therefore, we first compared the growth of about twenty yeast strains from the lab collection. *S. cerevisiae* strain Bruggeman instant and *S. cerevisiae* strain CNCM-3856 approached the growth rate of *C. glabrata* the most in YPD (Figure 4.7). Furthermore, these strains were also able to use trehalose as a carbon source (Figure 4.7).

In our co-culturing assay, we wanted to distinguish the *C. glabrata* cells from the other yeast species. Unfortunately, despite the small cell size of *C. glabrata*, it was not possible to distinguish untagged *C. glabrata* from the other yeast strain using flowcytometry. Therefore, we labeled the *C. glabrata* strains by genomic introduction of constitutive expressed yellow fluorescent protein (YFP) at the tryptophan locus, as this ORF was deleted in our ATCC2001 HTL background strain. A recent publication also reported the *TRP1* locus is a good candidate for gene complementation, overexpression or modification, as well as reporter gene expression in *C. glabrata* (Sprenger *et al.*, 2020).

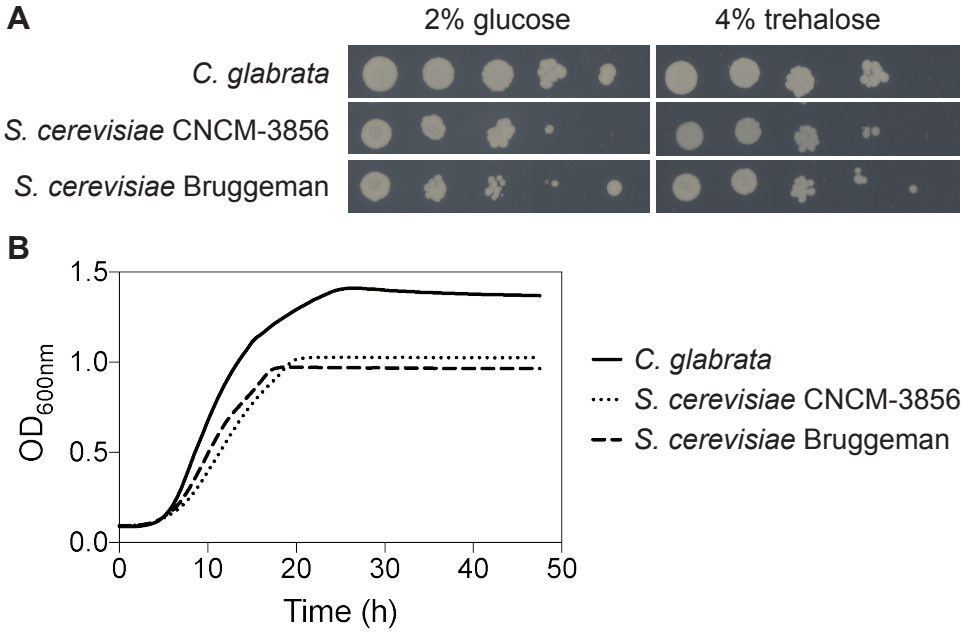

Figure 4.7: *In vitro* growth of *C. glabrata*, *S. cerevisiae* CNCM-3856 and *S. cerevisiae* Bruggeman instant.
The strains were spotted on SC plus glucose or trehalose plates (A) or grown in liquid SC glucose medium (B). Average OD_{600nm} of three independent cultures from one representative experiment is shown and the experiment was performed at least twice (B).

In our growth experiment, the same number of cells of each strain was seeded in complete medium and incubated for seven days. Afterwards, the cultures were analyzed by flow cytometry and gated to distinguish the species from each other. By this, we could determine the percentage of cells of each strain for each of the cultures (Figure 4.8). When wild type *C. glabrata* was co-cultured with *S. cerevisiae* CNCM-3856 or Bruggeman instant, *C. glabrata* clearly outcompeted the other strain (average of 65% and 83% *C. glabrata* cells in the co-cultures with CNCM-3856 and Bruggeman instant respectively). Similar results were seen in co-cultures with a *C. glabrata* strain deleted for the extracellular trehalase *ATH1* (Figure 4.8). In contrast, the co-cultures with *C. glabrata nth1*Δ strain contained significant less *C. glabrata* cells (average of 20% and 40% *C. glabrata* cells with CNCM-3856 and Bruggeman instant respectively), which is similar to the co-cultures of the triple trehalase deletion strain (Figure 4.8). This indicates that the neutral trehalase Nth1, rather than the extracellular trehalase activity of Ath1, is important for growth in presence of other yeast species in our experimental conditions.

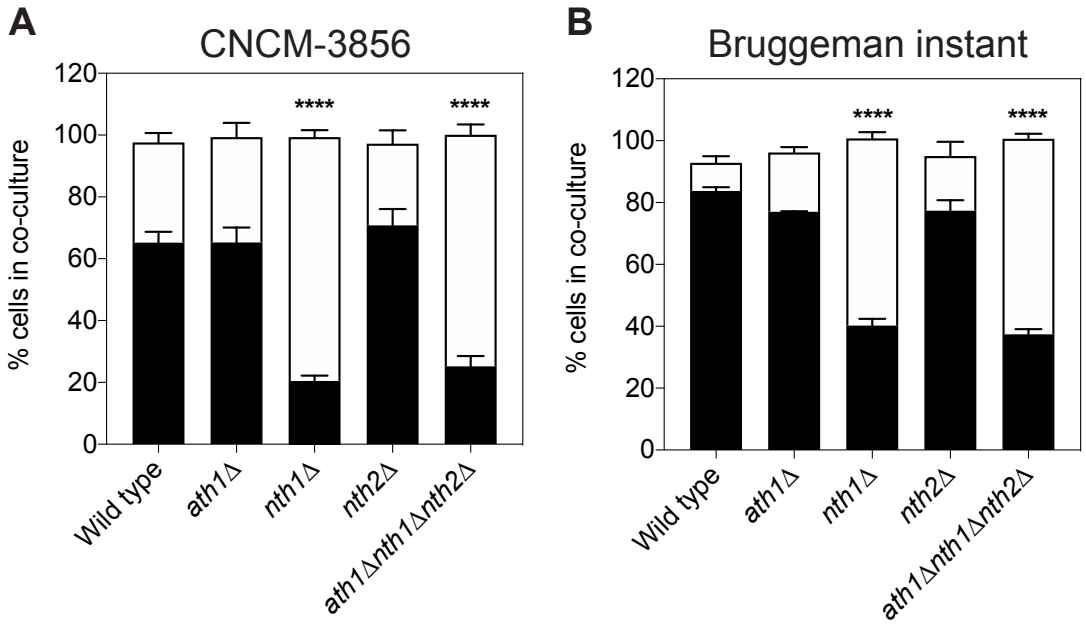

Figure 4.8: *In vitro* competition experiment.
Percentage of cells in the co-cultures of *C. glabrata* (black bars) and *S. cerevisiae* (A) or *S. cerevisiae* (B) (white bars). The co-cultures were grown for seven days in complete medium in presence of glucose (2%). Using flow cytometry, the percentage of cells from each strain in the culture was calculated. Average results of three independent cultures and SEM are shown and the experiment was conducted at least twice. Statistical one-way ANOVA analysis of variance with Bonferroni correction was done (*, P ≤ 0,05; **, P ≤ 0,01; *** P ≤ 0,001 and ****, P ≤ 0,0001).

4.2.4 The triple deletion strain is unable to stably colonize the gut

Humans cannot produce trehalose, while inside the human body trehalose is present in the gut, originating from ingested food or from micro-organisms as a result of production or release after microbial death. Also *Candida* is present in the gastrointestinal (GI) tract as part of the normal microbiota (Underhill and Iliev, 2014). As Ath1 is required for growth on extracellular trehalose, we hypothesized that this enzyme might play a relevant role at this body site. To test this hypothesis, we verified whether the wild type and different trehalase deletion strains were able to colonize the gut over a longer period of time in a mouse model.

To achieve a stable *Candida* colonization in the gut, mice are often treated with antibiotics (Healey *et al.*, 2017; Mason *et al.*, 2012). As we wanted to assess the interaction with these other micro-organisms, we first performed a pilot experiment using non-treated mice (normal drinking water) and mice which received ampicillin in their drinking water (1 mg/ml). These two groups were then infected with wild type *C. glabrata* via oral gavage. The colonization was followed over time by plating dilutions of weighted stool samples for 21 days post infection. Despite the higher colonization in mice receiving ampicillin in the drinking water, we also obtained a stable colonization in mice where microbial perturbation was not induced (Figure 4.9).

Because of the higher relevance of the model without microbial perturbation, we continued the experiments in mice receiving normal drinking water and tested colonization of the trehalase single deletion strains and the triple deletion strain. Similar to the pilot experiment, a stable colonization was obtained for the wild type strain (Figure 4.10A). The main habitat of *C. glabrata* in the GI tract was in the cecum, which had a log(CFU/g) of around 3 (Figure 4.10B). The single trehalase deletion strains showed a similar colonization as the wild type strain (Figure 4.10A). Interestingly, the triple deletion strain was not able to establish a stable colonization of the GI tract, as over 66% of the mice cleared the *C. glabrata* administered at day 21 (Figure 4.10A). Logically, the average colonization of the cecum of mice which were orally infected with the triple deletion strain was significantly lower, as over 66% of the mice showed no colonies (Figure 4.10B). This indicates that trehalase activity is indeed important to achieve persistent colonization, but it is not mediated by Ath1 alone. We also checked whether there was *C. glabrata* in the kidney, as a read out for dissemination, but this was not the case.

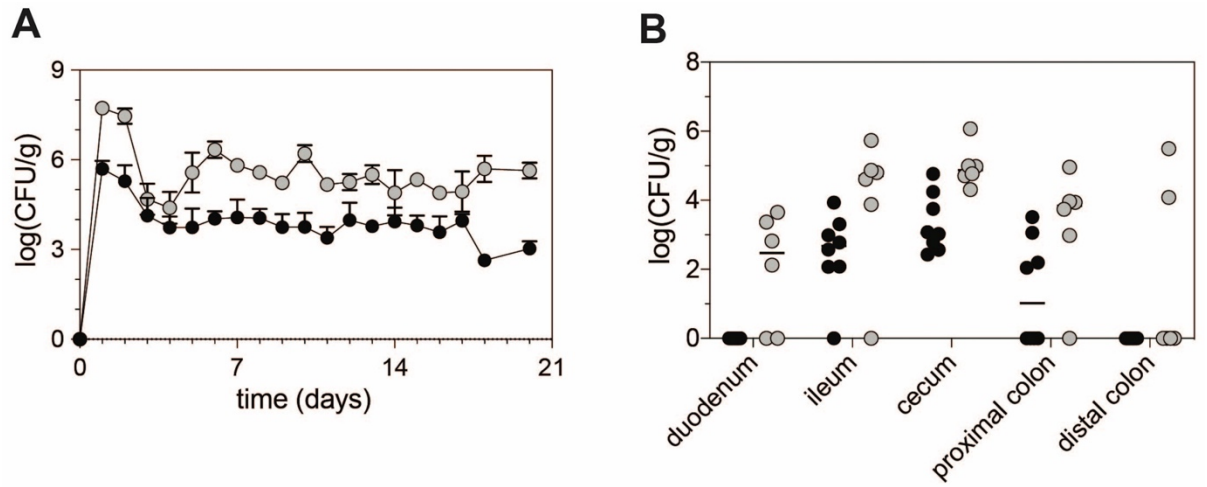

Figure 4.9: Optimization of the *C. glabrata* GI colonization murine model.
Mice received either normal water (black) or ampicillin (1mg/ml) (grey) in their drinking water from four days before gavage. At day 0, mice were orally infected with 10^8 *C. glabrata* cells (gavage). At the indicated days a stool sample was collected from each mouse and plated for CFU counting, for a period of 21 days. Average log transformed CFU/g with SEM of 8 mice per group is shown for the pilot following colonization in time (A). Upon termination of the experiment, mice were sacrificed using cervical dislocation under anaesthesia and different tissues were collected to plate for CFU counting. Fungal burden of the mice in each tissue is shown as log(CFU/g) (B).

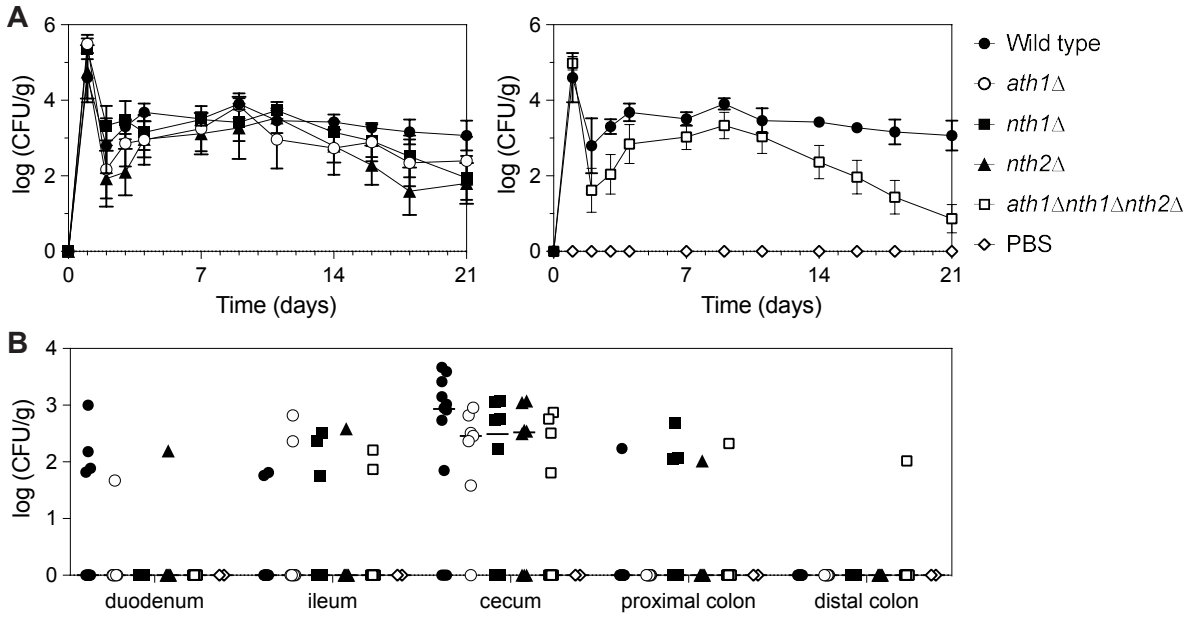

Figure 4.10: Colonization in the GI tract is not maintained in the triple trehalase deletion strain.
At day 0, mice are orally infected with 10^8 *C. glabrata* cells (gavage). Wild type (●), *ath1*Δ (○), *nth1*Δ (■), *nth2*Δ (▲) and *ath1*Δ*nth1*Δ*nth2*Δ (□) or PBS as a control (◇) were tested. At the indicated days a stool sample was collected from each mouse and plated for CFU counting, during 21 days (for each strain, at least 8 mice were used). Average log transformed CFU/g with SEM is shown for the following colonization in time (A). Upon termination of the experiment, mice were sacrificed and different tissues were collected to plate for CFU counting. Fungal burden of the mice in each tissue is shown as log(CFU/g) (B).

4.2.5 Nth1 is involved in regulation of *in vitro* oxidative stress resistance and survival in human macrophages

Inside the human body, fungal pathogens are continuously exposed to different types of environmental stresses (Brown *et al.*, 2014). As trehalose is a disaccharide important for stress resistance, we assessed the growth phenotype of the trehalase deletion strains upon stress treatment, performed by co-author Mieke Van Ende. Therefore, this paragraph indicates the major findings, while all results can be found in our publication (Van Ende and Timmermans *et al.*, 2020). We found that specifically Nth1 is important in presence of oxidative stress, as strains lacking *NTH1* were more sensitive to hydrogen peroxide and showed a decreased survival after acute hydrogen peroxide exposure. Subsequently, the role of the trehalases inside macrophages was investigated as *C. glabrata* encounters oxidative stress, among other stresses, after uptake by macrophages. Therefore, the survival inside macrophages is a *C. glabrata*

virulence trait. The transcriptome of *C. glabrata* cells inside macrophages showed high transcript levels of all trehalases and the trehalase deletion strains all showed a significantly decreased survival inside macrophages after 4 days of incubation, compared to the wild type strain. On the other hand, when macrophage-engulfed *C. glabrata* cells were plated after a short incubation period (3 hours), consistently more *nth1*Δ cells survived the macrophages compared to the wild type strain, although still more repetitions are required to confirm its significance.

4.2.6 Trehalase plays a minor role in the virulence of *C. glabrata* in a mouse model of systemic infection

In order to investigate whether the trehalase enzymes are involved in *C. glabrata* virulence in a mouse model of systemic infection, mice were infected intravenously with the different trehalase deletion strains. Experimental infection of immunocompetent mice with *C. glabrata* generally does not cause mortality (Jacobsen *et al.*, 2010). We confirmed this in a pilot experiment during which we determined the optimal concentration of the immunosuppressant dexamethasone (Figure 4.11). Based on the pilot experiment, 75 mg/kg dexamethasone was chosen to be given to the mice at day -3, 0, 7 and 14.

For each deletion strain, at least 8 mice were included in the experiment (Figure 4.12). The mice infected with the *nth1*Δ strain appeared ill more rapidly and died earlier compared to the wild type (p-value of 0.0184 in log-rank test). The mice infected with the triple deletion strain showed no significant difference in survival compared to mice infected with the wild type strain (p-value 0.0873 in log-rank test). Based on the twice per day monitoring, it was clear that mice infected with the triple deletion mutant did not show disease phenotypes such as ruffled hair, similar to the PBS control mice and different from mice infected with the wild type strain. It should be noted that two mice of the PBS control group died, which is most probably due to the immunosuppression of the mice and the duration of the experiment. The other mice of the PBS control group showed a healthy appearance throughout the experiment.

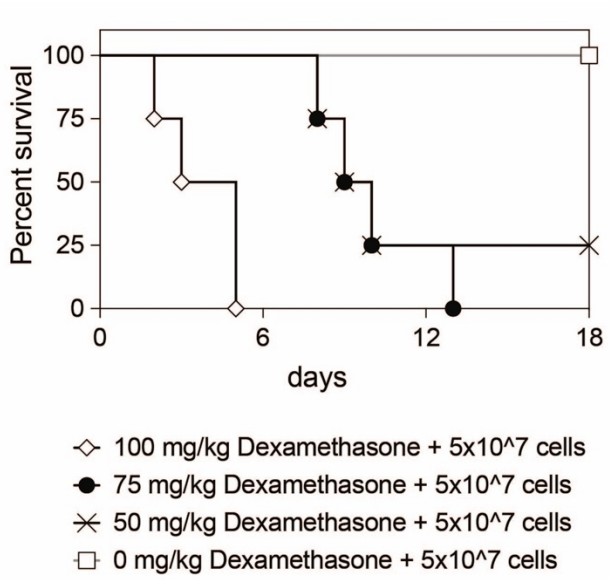

Figure 4.11: Optimization of the *C. glabrata* mouse model of systemic infection. Mice were immunosuppressed with different concentrations of dexamethasone and received no or 5 x 10^7 cells of the indicated *C. glabrata* strain via injection in the lateral tail vain. The mice were monitored two times per day for 18 days (n = 4). When they reached humane endpoints, they were sacrificed. This pilot was executed by Mieke Van Ende.

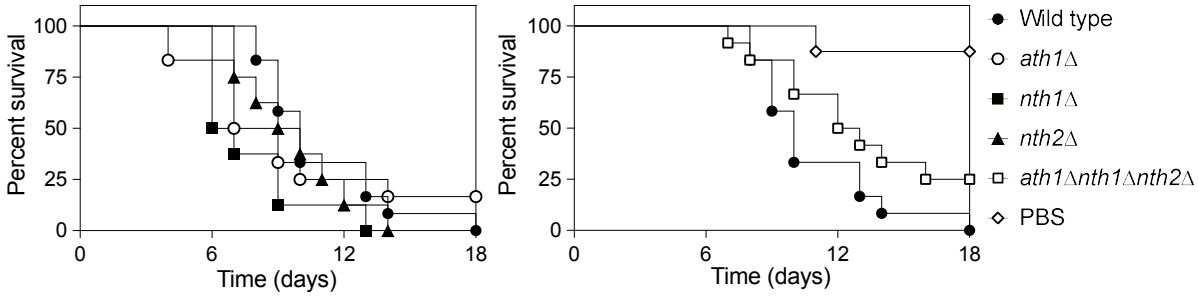

Figure 4.12: Mice survival after systemic infection.
Mice were immunosuppressed with 75 mg/kg dexamethasone and received no or 5 x 10^7 *C. glabrata* cells via injection in the lateral tail vain (for each strain tested, n = 8). Wild type (●), *ath1*Δ (○), *nth1*Δ (■), *nth2*Δ (▲) and *ath1*Δ*nth1*Δ*nth2*Δ (□) or PBS as a control (◇) were tested. The mice were monitored two times per day for 18 days. When they reached humane endpoints, they were sacrificed. Statistical analysis by the use of a log-rank test was performed comparing the deletion strains to the wild type (*, P ≤ 0,05; **, P ≤ 0,01; *** P ≤ 0,001 and ****, P ≤ 0,0001).

4.3 Discussion

Based on the importance of trehalose metabolism for virulence in other pathogenic fungi and the characteristic rapid hydrolysis of trehalose of *C. glabrata*, we aimed to investigate the role of the trehalase enzymes in virulence in *C. glabrata*. Comparison with the *S. cerevisiae* trehalase enzymes resulted in the identification of three trehalase enzymes in *C. glabrata*: Ath1, Nth1 and Nth2. Therefore, we constructed the different single, double and triple trehalase deletion strains and characterized the resulting strains.

We showed that Ath1 is required for the utilization of extracellular trehalose, a phenotype on which the rapid identification of *C. glabrata* in the hospital is based (Fenn *et al.*, 1999; Fraser *et al.*, 2012; Freydiere *et al.*, 2003; Land *et al.*, 1996; Lopez *et al.*, 2001; Murray *et al.*, 2005; Willinger *et al.*, 2005; Zilli *et al.*, 2015). In different fungal species, the acid trehalase is present on the outside of the cells in order to hydrolyze exogenous trehalose (He *et al.*, 2009; Jules *et al.*, 2004; Lucio *et al.*, 2000; Nwaka *et al.*, 1996; Pedreño *et al.*, 2004; Sánchez-Fresneda *et al.*, 2014). Our microscopy data, where Ath1 was tagged to a fluorophore, showed that Ath1 is present both on the outside of the cells as well as in the vacuole. Furthermore, high trehalase activity was measured in complete cells taken from the growth culture, while the trehalase activity was lost upon preparation of protoplasts. At the same time, the fluorescent signal of the labeled Ath1 at the outside of the cells was lost in these protoplasts. This shows that Ath1 is localized in the periplasmic space or cell wall, similar to the situation in *S. cerevisiae* (He *et al.*, 2009). To further elucidate the exact location of *C. glabrata* Ath1, we propose to isolate the cell wall fraction of exponential cells grown in trehalose as a carbon source and measure the trehalase activity. This localization helps the cells to quickly hydrolyze extracellular trehalose to glucose, which is then taken up by the glucose transporters in the plasma membrane (Van Ende *et al.*, 2019). Zilli, *et. al.* showed that *C. glabrata* Ath1 is also secreted to the outside of the cells and is released into the medium (Zilli *et al.*, 2015).

We also grew our *C. glabrata* strains together with another yeast species to investigate if a trehalase plays a role in outcompeting the other yeast. Firstly, we grew *in vitro* microbial co-cultures of *C. glabrata* and one other yeast species for one week. Our results show that wild type *C. glabrata* clearly outcompetes the other yeast strain. At

this timepoint, the deletion of *NTH1* resulted in less *C. glabrata* cells relative to the other yeasts tested. This is in line with high Nth1 trehalase activity in stationary phase cells (unpublished results Mieke Van Ende) and its importance in *C. glabrata* stress tolerance, as the cells are starved for nutrients at seven days of culturing. There was no difference between wild type *C. glabrata* and the *ath1*Δ strain, indicating that the highly active extracellular trehalase does not give the cells a competitional advantage in our conditions. This can be explained as the cells were grown in glucose containing medium and the strains were still in stationary phase. We suggest to test if Ath1 is providing a competitional advantage at later time periods in a future experiment, as at this point microbial death will result in the release of residual trehalose in the growth culture.

Secondly, we investigated the role of the trehalases *in vivo* in a model of GI colonization. In humans, *Candida* is present in the gastrointestinal tract as part of the normal microbiota (Underhill and Iliev, 2014). While *Candida* was present in the GI tract, we did not observe any dissemination to the organs and the animals showed no signs of disease (no weight loss, normal fur and normal moving behavior). Therefore, the GI colonization model we used is no read-out for *Candida* virulence.

Unexpectedly, the single trehalase deletion strains all showed a wild type phenotype in the mouse model of GI colonization. Interestingly, the triple trehalase deletion strain was not able to stably colonize the GI tract. This indicates that trehalase activity is indeed important to achieve persistent colonization, however, any of the enzymes could contribute to this. For future experiments, we propose to investigate the colonization of the GI tract for a longer period, which might expose the contribution of a single trehalase deletion to the phenotype. Or as an alternative experiment, the double deletion strains could be tested. Also, the influence of alterations in the diet of the mice could be tested as this will affect the microbial growth in the GI tract. For instance, trehalose-rich food may cause a larger disadvantage to the *C. glabrata ATH1* deletion strain. Furthermore, *Candida* strains in the GI tract can be tested as an endogenous source to induce a systemic infection, which can be tested by severe immunosuppression of the mice after colonization as described in Healey *et al.* (2017).

We also tested the role of the trehalases in virulence in a mouse model for systemic candidiasis. We chose to use mice as the host for our *in vivo* experiments based on our *in vitro* results: the transcripts of all three trehalases were upregulated inside mouse macrophages and the trehalase deletion strains showed a lower survival inside

the mouse macrophages after 4 days (Section 4.2.5). Otherwise, minihost animal models are commonly used to assay *Candida* mutant strains affecting virulence, including *Galleria mellonella* larvae and *Drosophila melanogaster* flies. As these minimodels are insects, they lack an adaptive immune response. In addition, trehalose is the major sugar in their hemolymph in contrast to mammals. Therefore, insect species have both a soluble (Tre-1) and membrane-bound (Tre-2) trehalase which are expressed in various tissues (Chen *et al.*, 2010; Oliver *et al.*, 1978), while there is only one trehalase in humans, mainly expressed in the gut. Therefore, we chose mice as the animal host to test the role of *C. glabrata* trehalase in virulence.

In *C. albicans* and in *C. parapsilosis*, the acid trehalase Atc1 is a stress-responsive protein and is important for *in vitro* stress resistance. Moreover, mice infected intravenously with *C. albicans* or *C. parapsilosis* cells lacking their acid trehalase enzyme show an increased survival, suggesting a role for *ATC1* in virulence (Pedreño *et al.*, 2004; Sánchez-Fresneda *et al.*, 2014). None of these phenotypes are observed for the acid trehalase of *C. glabrata*, indicating Ath1 is different from its orthologous enzymes in other *Candida* species.

Similar to *S. cerevisiae*, *C. glabrata* Nth1 is important for stress tolerance, specifically toward oxidative stress, which is encountered inside immune cells. Deletion of *NTH1*, as well as the other trehalases, results in a lower survival upon engulfment by macrophages. The small enhanced virulence of the *nth1*Δ strain in the systemic mouse model is unexpected as Nth1 was shown to be important in the oxidative stress response and inside macrophages (Van Ende and Timmermans *et al.*, 2020). However, the deletion of *C. glabrata* Nth1 improves *in vitro* resistance to heat stress and this is associated with elevated intracellular trehalose levels (Van Ende, personal communication). Therefore, the role of *C. glabrata* Nth1 depends on the kind of stress. *In vivo,* the conditions are complex as several stresses are encountered (nutrient limitation, host immune response, etc.). It would be interesting to measure the trehalose level of these *C. glabrata* strains *in vivo* to correlate this with their stress resistance.

The precise role of Nth2 remains unclear, as we could not detect any trehalase activity for this enzyme, but the deletion of *NTH2* does affect the cell survival inside macrophages and the expression of *NTH2* is also rapidly upregulated inside macrophages.

The *ath1*Δ *nth1*Δ *nth2*Δ strain did not show detectable trehalase activity in any growth phase, indicating that these three genes are all the trehalase enzymes present in *C. glabrata.* In general, the triple deletion strain showed results consistent with the single deletion strains. To our knowledge, there are no prior publications in which a mutant lacking all three trehalase enzymes in a pathogenic yeast strain has been characterized.

Based on our animal experiments, we propose to investigate molecules which show a combined inactivation of the three trehalase enzymes, as the triple deletion strain showed a decreased survival in human macrophages and was fully cleared from the murine GI tract. Additionally, the mice infected intravenously with the triple deletion strain appeared more fit (based on our monitoring of their behaviour) compared to the wild type control. As they share trehalose as a substrate, variants of trehalose may cause inhibition of all three enzymes. Structural analogues of trehalose can act as a competitive inhibitor of trehalase (El Nemr and El Ashry el, 2011). Validamycin A, a well-known trehalase inhibitor, is already used in food crops to prevent fungal infections (Asano *et al.*, 1987). This compound showed weak antifungal activity against *C. albicans*, whereas a strong effect was observed against *A. flavus* (Guirao-Abad *et al.*, 2013; Plabutong *et al.*, 2020). *C. glabrata* growth in presence of Validamycin A and trehalose is currently investigated in our lab (personal communication, Mieke Van Ende).

Based on this work, we propose to test different structural analogues of trehalose for their antifungal activity against *C. glabrata*. As mentioned before, the human genome encodes one trehalase. While the amino acid sequence shows low identity, it can't be excluded that a competitive inhibitor would be able to bind to the human trehalase enzyme as the amino acids for substrate binding are conserved. However, a deficiency of the human trehalase causes diarrhea due to an intolerance to trehalose enriched food, but this can be solved by a low trehalose diet. This should be taken into account when looking for the compound.

4.4 Materials and methods

Yeast strains, plasmids and primers

Table 4.1: List of *C. glabrata* strains used in this chapter

Strain	Genotype	Source
	his3Δ:::FRT trp1Δ:::FRT leuΔ:::FRT	(Schwarzmüller *et al.*, 2014)
*Cg*BM1	*ath1*Δ:::FRT	This work
*Cg*BM2	*nth1*Δ:::FRT	This work
*Cg*BM3	*nth2*Δ:::FRT	This work
*Cg*BM4	*ath1*Δ:::FRT *nth1*Δ:::FRT *NTH2*	This work
*Cg*BM5	*ath1*Δ:::FRT *NTH1 nth2*Δ:::FRT	This work
*Cg*BM6	*ATH1 nth1*Δ:::FRT *nth2*Δ:::FRT	This work
*Cg*BM7	*ath1*Δ:::FRT *nth1*Δ:::FRT *nth2*Δ:::FRT	This work
*Cg*BM8	*trp1Δ:::pTEF-YFP*	This work
*Cg*BM9	*ath1Δ:::FRT trp1Δ:::pTEF-YFP*	This work
*Cg*BM10	*nth1*Δ:::FRT *trp1Δ:::pTEF-YFP*	This work
*Cg*BM11	*nth2*Δ:::FRT *trp1Δ:::pTEF-YFP*	This work
CgBM12	*ath1*Δ:::FRT *nth1*Δ:::FRT *nth2*Δ:::FRT *trp1Δ:::pTEF-YFP*	This work

Table 4.2: List of plasmids used in this chapter

Plasmid	Relevant genotype	Used for	Source
pYC44	NatMX cassette flanked by FRT sites	Construction of deletion cassette	(Yáñez-Carrillo *et al.*, 2015)
pYC54	YFP tag, NatMX cassette flanked by FRT sites	Construction of YFP tagged strains	(Yáñez-Carrillo *et al.*, 2015)
pYC56	mCherry, NatMX cassette flanked by FRT sites	Construction of mCherry tagged fusions	(Yáñez-Carrillo *et al.*, 2015)
pLS9	Flippase NatMX	Removal of resistance marker between FRT sites	Kindly provided by Alejandro De Las Peñas & Irene Castaño
pLS10	Flippase hph	Removal of resistance marker between FRT sites	This work
PYC-gRNA-uni-hph	Hygromycin cassette	Amplification hygromycin marker	(Cen and Timmermans *et al.*, 2017)
pYC56-*ATH1*		Construction endogenously tag trehalase-mCherry	This work
pYC56-*NTH1*		Construction endogenously tag trehalase-mCherry	This work
pYC56-*NTH2*		Construction endogenously tag trehalase-mCherry	This work
pBM17	pTEF-YFP flanked by *TRP* promoter and terminator	Construction YFP tagged strains	This work

A list of primers used in this chapter can be found in Addendum 5.

Construction of phylogenetic tree

To create the trehalase phylogenetic tree, protein sequences were retrieved from the *Candida* Genome Database (CGD), *Saccharomyces* Genome Database (SGD), *Aspergillus* Genome Database (AspGD), UniProt and PomBase (Cerqueira GC, 2014; Cherry JM, 2012; Consortium, 2019; Lock A, 2018; Skrzypek MS, 2017). In CLC Main Workbench, protein sequences were aligned and the phylogenetic tree was constructed using the unweighted pair method with arithmetic mean (UPGMA) and the Kimura Protein as a protein distance measure (Qiagen).

Cultivating conditions

Yeast cells were grown in either YP (1% yeast extract, 2% bacteriological peptone), synthetic complete (SC) medium (1.7 g/L Difco yeast nitrogen base without amino acids and without ammonium sulphate, 0.79 g/L complete supplement mixture [CSM; MP Biomedicals], 5 g/L ammonium sulphate), YNB (1.7 g/L Difco yeast nitrogen base without amino acids and without ammonium sulphate, 20 mg/L tryptophan, 20 mg/L histidine, 30 mg/L leucine, 5 g/L ammonium sulphate) or RPMI 1640 medium. These media were supplemented with glucose or trehalose as indicated in the experiment. For solid media, 15 g/L Difco agar granulated was added.

Construction of plasmids

For expression of the flippase enzyme, the nourseothricin cassette of vector pLS9 was replaced by the hygromycin marker resulting in pLS10. The hygromycin marker was amplified using primers C6240 and C6241 from plasmid pgRNA-uni-hph (p58) and subsequently ligated into the NotI digested pLS9. Colonies were checked using primers 7883 and B3220 and verified by sequencing.

For localization experiments, the trehalase enzymes were fused to mCherry. Therefore, open reading frames (ORFs) were amplified using primers D84 and D1728 (*ATH1*), D88 and D89 (*NTH1*) or D92 and D93 (*NTH2*) from wild type genomic DNA. The terminators were amplified using primers D86 and D87 (*ATH1*), D90 and D91 (*NTH1*) or D94 and D95 (*NTH2)* from wild type genomic DNA. The corresponding ORF and terminator fragments were inserted in BamHI and XhoI digested pYC56 vector using NEBuilder (New England Biolabs), resulting in the expression vectors pBM13 (*ATH1*), pBM14 (*NTH1*) and pBM15 (*NTH2*). Correct insertion of the ORF fragments was checked using primers C2950 and A9050, insertion of terminator fragments was checked using primers B1222 and A2047.

Vector pBM17 was constructed for subsequent transformation in *C. glabrata* to acquire labeled strains in the competition experiment. The TRP promoter was amplified from gDNA using primers D1116 and D1117 and inserted into SacI digested pYC54 by NEBuilder assembly (New England Biolabs). Correct insertion was checked using primers B4165 and 9064. Then, the TEF promoter was amplified from vector pBC6 using primers D1093 and D1094, which was inserted into BamHI digested vector. The transformants were checked by PCR using primers B4165 and 9064. A correct transformant was digested again with XhoI for insertion of the TRP terminator,

amplified using primers D1118 and D1119 from gDNA. Insertion of the fragment was checked with primers 9065 and B4166. The resulting plasmid pBM17 was verified by sequencing.

Construction of C. glabrata strains

The trehalase deletion strains were constructed in the ATCC2001 *his3*Δ *trp1*Δ *leu2*Δ background (Schwarzmüller *et al.*, 2014). The wild type strain was transformed by electroporation with the deletion cassette (a nourseothricin cassette flanked by FRT sites and a 100 bp region flanking the targeted gene). The deletion cassettes were PCR amplified from the pYC44 plasmid using primers C6315 and C6316 (*ATH1*), C6317 and C6318 (*NTH1*) or C6319 and C6320 (*NTH2*). Cells were plated on YPD agar medium supplemented with 200 µg/mL nourseothricin. Transformants were checked for insertion of the deletion cassette by PCR using control primers C3177 and C3178 (*ATH1*), C3183 and C3184 (*NTH1*) or C3161 and B3162 (*NTH2*). Correct strains were subsequently transformed with plasmid pLS10 to induce expression of the flippase enzyme (300 µg/ml hygromycin selection). Removal of the nourseothricin cassettes of the transformants was checked by PCR using primers C3177 and C8497 (*ATH1*), C3183 and C3835 (*NTH1*) or C3161 and B2011 (*NTH2*). The pLS10 plasmid was lost by growth on non-selective YPD medium and checked by replating on YPD supplemented with 300 µg/mL hygromycin. The trehalase double and triple mutants were constructed similarly, by transformation of the nourseothricin deletion cassettes mentioned above in the single or double deletion strains respectively, followed by removal of the selective marker by expression of pLS10. The *C. glabrata* trehalase deletion strains were made by Bea Timmermans (single-) and Mieke Van Ende (single-, double- and triple- deletion strains).

Endogenously tagged trehalase strains were constructed by electroporation of the wild type strain with EciI digested plasmid pBM13 (*ATH1*-mCherry), pBM14 (*NTH1*-mCherry) or pBM15 (*NTH2*-mCherry). The resulting transformants were checked using primers C9381 (*ATH1*), C9385 (*NTH1*) or C9388 (*NTH2*) and A9050 (mCherry). *C. glabrata* YFP expressing strains were obtained by insertion of pTEF-YFP construct in the TRP locus. Therefore, vector pBM17 was digested with EciI and subsequently transformed by electroporation in the wild type, *ath1*Δ, *nth1*Δ, *nth2*Δ and triple deletion strains. Resulting transformants were checked by PCR using primers 10058 plus B3067 (upstream) and primers 9065 plus 10053 (downstream).

Growth phenotype

Growth of the strains was followed in time both in liquid and on solid YNB medium over time. Overnight cultures (YNB + 2% glucose) of the different strains were washed three times with sterile milli-Q water and subsequently diluted to an OD_{600} of 0.1. For growth assays in liquid medium, cells were grown in 50 mL YNB containing either 10 mM of glucose or 10 mM of trehalose as the carbon source. The cells were grown at 37°C with continuous shaking at 200 rpm for 72 hours during which the OD_{600} was monitored.

For growth assays on solid medium, a tenfold dilution series of the cultures was spotted on YNB plates containing 5 mM of glucose or 5 mM of trehalose. To investigate the stress response, the cells were spotted on YNB plates supplemented with 100 mM glucose, containing either 6 mM H_2O_2, 1.5 M NaCl or 0.4 mg/mL CFW. The plates were incubated at 37°C for 72 hours during which growth was assessed.

Protoplast preparation

Overnight cultures of the different strains were made in YPD medium. Subsequently, the cultures were grown until mid-exponential phase in YPD (100 mM glucose) or YPT (100 mM trehalose) as indicated in the figure. The cells were collected and washed twice, after which they were incubated for 15 to 45 minutes in the protoplasting solution (600 mM KCl, 800 mM Sorbitol, 41.7 mM K_2HPO_4, 8.3 mM KH_2PO_4, 4.8 units/mL Zymolase, 9.65 mM β-mercapto-ethanol) until the OD_{600} dropped. The cells were collected and washed twice with cold protoplasting buffer (166.8 mM K_2HPO_4, 33.2 mM KH_2PO_4, 800 mM Sorbitol), after which trehalase activity was determined as described below. The protoplast formation was performed by Mieke Van Ende.

Determination of trehalase activity

Trehalase activity was determined as described in Pernambuco *et al.* (1996). In short, crude extracts were incubated with 50 µL of acid trehalose buffer (50 mM trehalose, 200 mM sodium citrate, 2 mM EDTA, pH 4.5). After 30 minutes of incubation at 30°C, the reaction was terminated by boiling for 5 minutes at 90°C. The glucose liberated was determined by the glucose oxidase–peroxidase method. Protein levels were determined by the Lowry method. Trehalase specific activity is expressed as nmol of glucose released per min and mg of protein.

Determination of extracellular glucose and trehalose

Extracellular glucose and trehalose concentrations during growth were analyzed by the Shimadzu HPLC system using an Agilent 87H column at 0.7 mL/min and a RID-20A detector (Shimadzu).

Fluorescence microscopy

The cells were grown in minimal complete medium containing glucose (2%) or trehalose (2%) to exponential phase as indicated in the figure. We used a FluoView FV1000 confocal microscope (Olympus IX81) and its software for localization of Ath1. We visualized mCherry with a 559-nm laser and BA575-675 emission filter. A 60x UPlanSApo (numerical aperture [NA], 1.35) objective lens was used.

Competition assay

All strains were grown overnight in minimal medium plus 100 mM glucose. The cell concentration was determined for each culture using the Guava easyCyte™ 12HT (Luminex). For the competition assay, 10^6 cells of the strains were added to 50 mL of SC medium containing 2% glucose. As a control, also cultures of the strains separately were made with the same number of cells. All cultures were incubated at 30°C shaking (200 rpm). After seven days, all samples were analyzed on a Guava easyCyte™ 12HT (Luminex). Analysis of the samples was done in FlowJo. The settings for gating of each strain were determined using the control samples and was subsequently extrapolated to the competition assay samples.

In vivo mouse model of systemic infection

The virulence of the different strains was assessed in an *in vivo* mouse model of systemic infection in female BALB/c mice (8 weeks old). The mice were housed in groups of four in filter-top cages in a dedicated animal room where temperature, light and humidity were regulated. The animals received a standard *ad libitum* diet and water. At day -3, all mice were immunosuppressed with 75 mg/kg dexamethasone (Fagron) through intraperitoneal injection. After this, the animals received the same amount of immunosuppression on day 0 and from then on, every seven days. On day 0, the mice were injected intravenously via the lateral tail vein with 5 x 10^7 *C. glabrata* cells in 200 µL PBS. After this, the infected mice were monitored daily and when they

reached humane endpoints, they were euthanized by cervical dislocation under anesthesia. The survival assay was terminated at day 18 after infection.

In vivo mouse model of gastrointestinal colonization

The gut colonization capacity of the different strains was determined in an *in vivo* mouse model of gastrointestinal colonization in female c57BL6/J mice (8 weeks old). The mice were housed in groups of four in filter-top cages in a dedicated animal room where temperature, light and humidity were regulated. The animals received a standard *ad libitum* diet and water. At day 0, the mice received 10^8 *C. glabrata* cells via oral gavage. From this day on, stool samples from each mouse were collected during 21 days at the timepoints indicated and plated on CHROMagar™ for CFU counting. The GI colonization is expressed as log(CFU/gram of stool). The gastrointestinal colonization model was terminated at day 21 after gavage. The animals were sacrificed by cervical dislocation under anesthesia and duodenum, ileum, cecum, proximal colon, distal colon, tongue and kidneys were plated for CFU counting on CHROMagar™.

General discussion

The C. glabrata cAMP-PKA pathway

Microorganisms adapt in response to changes in the environment by sensing these changes, then transmit a signal to the inside of the cell and elicit a proper adaptive response. One such condition is the availability of nutrients in the surroundings, which are sensed by nutrient-signaling pathways. In this work, we further elucidated the *C. glabrata* cAMP-PKA pathway which controls several cellular properties including growth, stress tolerance, trehalase activity and adhesion. Our work showed many similarities between the cAMP-PKA pathways of *C. glabrata* and *S. cerevisiae* than for instance to that of *C. albicans*, which can be explained as they are evolutionary more closely related. The cAMP-PKA pathway is present in many fungi and has been subject to rewiring during evolution. In several pathogenic fungi, the cAMP-PKA pathway controls virulence factors, including the yeast-to-hyphal transition in *C. albicans*, capsule production in *Cryptococcus neoformans* and conidia germination in *Aspergillus fumigatus* (Alspaugh *et al.*, 2002; Sudbery, 2011; Zhao *et al.*, 2006).

C. glabrata Gpr1 is a receptor for glucose, fructose and sucrose. While sucrose activates the *C. glabrata* cAMP-PKA pathway, *C. glabrata* can't use sucrose as the invertase is absent in its genome. What is the relevance of sucrose signaling for *C. glabrata* as it can't be metabolized? Gpr1 is a conserved protein with high amino acid identity between *C. glabrata* and *S. cerevisiae*. Therefore, it was present in the common ancestor of *C. glabrata* and *S. cerevisiae* and later, the orthologs further evolved separately. On the other hand, the loss of the gene encoding for the sucrose invertase (and the genes of galactose metabolism) originates at the base of the *Nakaseomyces* group, indicating this was a more recent event in evolution (Gabaldón and Carreté, 2016). The *Nakaseomyces* group also contains nonpathogenic species and probably, pathogenicity emerged twice within the *glabrata* group. Therefore, the invertase (and galactose metabolism) does not coincide with *C. glabrata* becoming pathogenic.

To find the residues involved in ligand binding, we compared the *S. cerevisiae Sc*Gpr1 ligand binding amino acid sequence to *C. glabrata* Gpr1. This shows that many residues in this region are shared between the two species, which is logical as they both have glucose and sucrose as a ligand. On the other hand, the differences in the

amino acid sequence of the ligand binding pocket can explain why *C. glabrata* Gpr1 also signals fructose, while this isn't a ligand of *S. cerevisiae Sc*Gpr1. Our results show that in *C. glabrata* P572 is involved in both glucose, sucrose and fructose sensing. Unfortunately, we were not able to validate other residues involved in sensing sucrose in *C. glabrata* Gpr1. For instance, the results for *Cg*Gpr1 A575C and Q579C were not black and white, which is probably partially due to the low affinity for sucrose. Therefore, we suggest to investigate sugar signaling in these mutants again in the future using the cAMP FRET biosensors as a direct read out (Demuyser *et al.*, 2018). Alternatively, to elucidate which residues are involved in fructose binding in *C. glabrata* Gpr1, the residues of the *Sc*Gpr1 ligand binding pocket can be substituted to the homologous *C. glabrata* residues, such as *Sc*Gpr1 L628C, I631L and G132A, and subsequently tested for fructose-induced cAMP induction.

Furthermore, we investigated two downstream targets of the *C. glabrata* cAMP-PKA pathway: the activation of trehalase and the main virulence factor adhesion.

We showed that the *C. glabrata* neutral trehalase Nth1 is rapidly activated by the cAMP-PKA pathway, which suggests a post-translational activation by PKA phosphorylation, similar to *S. cerevisiae* (Schepers *et al.*, 2012; van der Plaat, 1974). As the amino acid sequence around the phosphorylation site is highly conserved, the phospho-specific antibodies used in *S. cerevisiae* can be tested in a follow-up experiment for use in *C. glabrata* (unpublished results, Mieke Van Ende). Alternatively, the single amino acid substitutions of the homologous *C. glabrata* serine residues can be generated in the *ath1*Δ *nth2*Δ strain, as this strain does not show the high basal activity of Ath1, and tested for trehalase activation after addition of the cAMP-inducing sugars.

On the other hand, we showed that adherence to polystyrene is lowered by sugar signaling via the cAMP-PKA pathway. *C. glabrata* can adhere to biotic surfaces, which is mediated by specific ligand binding of yeast cell wall adhesins to for instance human mucosa, as well as to abiotic surfaces, which is mediated by the yeast cell wall hydrophobicity state. The latter is also affected by the presence of adhesins in the cell wall. For instance, the presence of *C. glabrata* Epa6, which is rich in hydrophobic residues, affects the cell surface hydrophobicity (El-Kirat-Chatel *et al.*, 2015).

To find the adhesin(s) downstream of the cAMP-PKA pathway, we investigated the glucose-induced transcriptome as the *C. glabrata* genome encodes a high number of

predicted adhesins and many of these adhesins are uncharacterized so far (Timmermans *et al.*, 2018). Therefore, we selected the adhesins which showed a different glucose-induced transcriptional response between the wild type and *gpr1*Δ strain for further analysis. Strains deleted for the putative adhesins CAGL0J00253g or *AED2* showed a similar adhesion in presence of glucose and galactose, suggesting that they are downstream of the cAMP-PKA pathway. This needs to be further investigated in the future. Therefore, we propose to test how these deletion strains affect the surface hydrophobicity state of the cell wall by atomic force microscopy. Alternatively, the deletion of these ORFs in the pathway mutants will validate if they are downstream of the pathway. Subsequently, it also needs to be investigated which transcription factor affects the expression of these adhesins downstream of PKA.

Another hurdle in the research of the *C. glabrata* adhesins is that the set of adhesins is highly variable between strains/isolates, because of the high *C. glabrata* genome flexibility. Therefore, we tested the adherence in the presence of glucose in several strains including two clinical isolates. Fortunately, all the strains showed a reduced adhesion in presence of glucose, indicating that the phenotype is common in *C. glabrata*.

Furthermore, we propose to investigate whether the *C. glabrata* cAMP-PKA pathway plays a role in virulence. Unpublished previous research in our lab showed that the *C. glabrata gpr1*Δ strain was as virulent as the wild type strain in a fly infection model (Brunke *et al.*, 2015; PhD thesis De Brucker, 2011). However, the *in vitro* data showed that the *gpr1*Δ strain is highly adherent and it is more tolerant to heat stress (PhD thesis De Brucker, 2011). Instead, we suggest to test a strain expressing the constitutively active allele of Gpa2 in a follow-up experiment, as this strain shows a low adherence phenotype and is sensitive to stress.

The glucose- and galactose-induced transcriptome

To obtain a general overview of how *C. glabrata* responds to the addition of glucose and galactose, we analysed the transcriptome induced by these sugars by RNA sequencing.

The glucose-induced transcriptional response is mediated by several interconnected glucose-dependent signaling pathways. Investigation of the GO enrichment showed many similarities with the glucose-induced response in *S. cerevisiae*: the cells clearly started cell growth, induced fermentation and downregulated autophagy, endocytosis and genes involved in stress tolerance. Unfortunately, comparing the glucose-induced responses of the *gpr1*Δ strain or a strain expressing the constitutively active Gpa2 allele were largely shared with that of the *C. glabrata* wild type strain. The genes which didn't show a glucose-induced differential expression in the *gpr1*Δ strain were also not enriched in GO categories. One can therefore hypothesize that *C. glabrata* Gpr1 is not important for the transcriptional response to glucose. As a follow up experiment, we suggest to test an unresponsive PKA strain, similar to the transcriptional study of Wang *et al.* (2004) in *S. cerevisiae*. As PKA is affected directly in such a strain, instead of upstream signaling through *C. glabrata* Gpr1, one can expect a larger number of genes affected. Inspection of the *C. glabrata* homologs of several genes typically under the control of PKA in *S. cerevisiae*, showed that the genes involved in stress resistance and in reserve carbohydrate metabolism were similarly downregulated. To our surprise, several ribosomal protein genes were not significantly upregulated by glucose, while this was a clearly enriched GO category. Still, 4 out of 5 inspected ribosomal genes were upregulated, although not significantly. One hypothesis is that at a different timepoint, these genes show a higher expression.

In the recent years, the *C. glabrata* genome annotation was updated several times, affecting the transcriptome analysis. This is especially important for our work as we also investigated the adhesin transcriptional response and as half of the *C. glabrata* adhesins are located near the telomeres, a substantial number of these ORFs were reannotated (because of sequencing errors and mapping errors). For instance, we found a high number of predicted adhesin genes which were not expressed in our data but with the update of Xu *et al.* (2020) these ORFs were removed.

On the other hand, we used the addition of galactose as a control as this sugar can't activate the cAMP-PKA pathway. In addition, we did not expect galactose to induce transcriptional changes as this carbohydrate cannot be used as a carbon source by *C. glabrata*. Yet, we found both up- and downregulated GO enriched categories. For instance, respiration was upregulated, and glycolysis was downregulated. As galactose clearly induces a transcriptional response and the genes of galactose metabolism are absent, this raises the question: how is galactose sensed by *C. glabrata* and which signaling pathway is involved? Based on the protein similarity, we propose to investigate if the high affinity glucose receptor *C. glabrata* Snf3 also acts as a galactose receptor, as this protein shows similarity to *Ca*Hgt4 which functions as a galactose receptor in *C. albicans.* We suggest to compare the expression of a selection of genes which are clearly induced or repressed by galactose in the wild type strain to the *C. glabrata SNF3* deletion strain. Alternatively, as was shown that *C. albicans Ca*Hgt4 can induce galactose signaling upon expression in a *S. cerevisiae Scsnf3*Δ strain (Brown *et al.*, 2009), we propose to also express *C. glabrata SNF3* in the *S. cerevisiae Scsnf3*Δ strain and measure galactose induced expression of the *ScHXT* genes. Furthermore, it is not clear which downstream signaling pathway mediates the galactose response. To start, we suggest to investigate into the galactose-induced expression of a selection of galactose up- and downregulated genes in transcription factor mutants from the *C. glabrata* deletion collection, as a follow-up experiment.

The C. glabrata trehalases

The disaccharide trehalose is both a reserve carbohydrate and can serve as a stress protectant molecule in yeast cells. In this work, we generated the *C. glabrata* trehalase deletion strains and characterized these both *in vitro* and *in vivo*.

We showed that the *C. glabrata* acid trehalase Ath1 is essential for growth on trehalose as a carbon source. *C. glabrata* Ath1 is expressed in the periplasm or cell wall in the presence of trehalose as a carbon source, in contrast it is not expressed in the presence of glucose. It is not yet elucidated how *C. glabrata* senses the presence of extracellular trehalose. As a follow-up experiment, the exact location of Ath1 can be investigated by isolating the *C. glabrata* cell walls of the wild type and *ath1*Δ strain, and subsequently measuring the trehalase activity of the cell wall fractions. If *C.*

glabrata Ath1 is a cell wall protein, one cannot exclude it also has another function such as a structural function.

The *C. glabrata* extracellular trehalose hydrolyzation is very fast and is used for its identification in the hospital (Willinger *et al.*, 2005). Yet, in our experiments the effect of the deletion of *C. glabrata ATH1* was limited: unexpectedly, the *C. glabrata ath1*Δ strain showed a wild type phenotype in the GI colonization in mice. There was also no difference in virulence in a mouse model of systemic infection. In contrast, *ATH1* expression was upregulated in macrophage-engulfed cells and the *C. glabrata ath1*Δ strain showed a lower survival inside the macrophages at longer times of incubation (Van Ende *et al.*, 2020). This raises the question: what is the benefit of this high Ath1 activity for *C. glabrata*? *C. glabrata* is considered to be a commensal of humans (and warm-blooded animal hosts), but this is in debate: whole genome comparisons of *C. glabrata* isolates from all over the world showed that there is no apparent geographical origin in the genetic diversity of the sequenced *C. glabrata* genomes (Carreté *et al.*, 2018; Gabaldón and Carreté, 2016). Therefore, they suggest that is more likely that *C. glabrata* resides in nature and humans are a secondary niche (Carreté *et al.*, 2018; Gabaldón and Carreté, 2016). Therefore, the high *C. glabrata* Ath1 activity might not be particularly relevant inside the body, but rather provide a benefit in nature.

We also showed that *C. glabrata* Nth1 is a cytosolic trehalase, therefore responsible for the hydrolysis of intracellular trehalose. We showed that Nth1 activity is regulated by the PKA pathway, possibly by direct phosphorylation as mentioned above. Furthermore, *NTH1* affects the stress tolerance properties of *C. glabrata* cells: a colleague showed that the *nth1*Δ strain is more resistant to heat stress and this correlates with elevated trehalose levels (personal communication, Mieke Van Ende). On the other hand, *nth1*Δ cells were more sensitive to oxidative stress, which is encountered *in vivo* inside macrophages.

Finally, we tested the trehalase deletion strains in two *in vivo* mouse models: colonization of *C. glabrata* in the mouse GI tract and mouse model of systemic infection. In a mouse model of systemic infection, the single trehalase deletion strains and triple deletion strain were not less virulent than the wild type strain. The *nth1*Δ strain was even slightly more virulent, possibly by a higher stress resistance. In a model of GI colonization, the single trehalase mutants showed a similar colonization as the wild type strain. The triple trehalase deletion strain was clearly not able to

establish a stable colonization over time. However, it can't be excluded that when the experiment is prolonged or the mice receive a trehalose-rich diet, the contribution of the single trehalases becomes apparent. While this model doesn't measure the virulence directly, it is a relevant model as *Candida* in the human GI tract is described to be an endogenous source of *Candida* for systemic infections in immunocompromised patients. In the literature, this is tested by the introduction of immunosuppressants after *C. glabrata* GI colonization of the mice.

Antifungal targets

Together, our results indicate that both the *C. glabrata* cAMP-PKA pathway and trehalases are interesting for further investigation to potentially find new molecules to treat *C. glabrata* infections.

Further investigation of the constitutively active Gpa2 allele in an *in vivo* model will show if the cAMP-PKA pathway influences *C. glabrata* virulence. When this *C. glabrata* strain has a reduced ability to establish an infection, then molecules which activate the cAMP-PKA pathway are potentially interesting to treat *C. glabrata.* Importantly, as carbohydrates activate *C. glabrata* Gpr1, it is important to verify the specificity of the molecules towards *C. glabrata,* so prudence is needed for possible side effects in humans.

The *C. glabrata* trehalases are a new potential antifungal target as the *C. glabrata* triple trehalase deletion strain showed promising results *in vivo*. Therefore, we propose to investigate molecules inhibiting all three *C. glabrata* trehalases. As they share the same substrate, structural analogs of trehalose can possibly act as a competitive inhibitor. Since *C. glabrata* Ath1 is present at the cell surface, while Nth1 and Nth2 are intracellular proteins, it is also important that the investigated molecules can be internalized. As there is also a human trehalase, possible side effects of cross-reactivity should be considered. However, as a trehalase deficiency causes diarrhea in these patients when trehalose-rich food is ingested, we do not expect major side effects of such molecules (Bergoz *et al.*, 1982). Also, the discomfort of these patients has been shown to be reduced with a probiotic treatment (Buts *et al.*, 2008).

On the other hand, genes of trehalose biosynthesis have been described to be involved in virulence and pathogenesis in several pathogenic fungi (including *C. albicans*, *A. nidulans* and *C. neoformans*) (Fillinger *et al.*, 2001; Petzold *et al.*, 2006; Van Dijck *et al.*, 2002). As trehalose biosynthesis is absent in the human body, the

trehalose biosynthesis genes also should be considered in the search for new antifungal drug targets. Blocking this pathway should therefore have no or little side effects for the human cells. In fact, the molecule closantel which was found in a screen as an inhibitor of recombinant cryptococcal Tps1, showed *in vitro* antifungal activity against *C. neoformans* and *C. gattii* strains. However, when it was tested in a mouse model, it showed no antifungal activity (Perfect *et al.*, 2017). *C. glabrata* also encodes the genes for trehalose biosynthesis (*TPS1, TPS2, TPS3* and *TSL1*), but so far these genes are not characterized. Therefore, before investigating inhibitors of these enzymes, it needs to be checked whether the deletion of these genes also affects virulence in *C. glabrata.* A new PhD student in the lab started to investigate this.

References

Agarwal, C., Aulakh, K.B., Edelen, K., Cooper, M., Wallen, R.M., Adams, S., Schultz, D.J., and Perlin, M.H. (2013). Ustilago maydis phosphodiesterases play a role in the dimorphic switch and in pathogenicity. Microbiology (Reading) *159*, 857-868.

Ahmad, K.M., Ishchuk, O.P., Hellborg, L., Jørgensen, G., Skvarc, M., Stenderup, J., Jørck-Ramberg, D., Polakova, S., and Piškur, J. (2013). Small chromosomes among Danish *Candida glabrata* isolates originated through different mechanisms. Antonie van Leeuwenhoek *104*, 111-122.

Alspaugh, J.A., Perfect, J.R., and Heitman, J. (1997). *Cryptococcus neoformans* mating and virulence are regulated by the G-protein alpha subunit *GPA1* and cAMP. Genes & development *11*, 3206-3217.

Alspaugh, J.A., Pukkila-Worley, R., Harashima, T., Cavallo, L.M., Funnell, D., Cox, G.M., Perfect, J.R., Kronstad, J.W., and Heitman, J. (2002). Adenylyl cyclase functions downstream of the Galpha protein Gpa1 and controls mating and pathogenicity of *Cryptococcus neoformans*. Eukaryotic cell *1*, 75-84.

Alves, R., Barata-Antunes, C., Casal, M., Brown, A.J.P., Van Dijck, P., and Paiva, S. (2020). Adapting to survive: How Candida overcomes host-imposed constraints during human colonization. PLoS pathogens *16*, e1008478.

Bahn, Y.S., and Sundstrom, P. (2001). *CAP1*, an adenylate cyclase-associated protein gene, regulates bud-hypha transitions, filamentous growth, and cyclic AMP levels and is required for virulence of *Candida albicans*. J Bacteriol *183*, 3211-3223.

Ballou, E.R., Avelar, G.M., Childers, D.S., Mackie, J., Bain, J.M., Wagener, J., Kastora, S.L., Panea, M.D., Hardison, S.E., Walker, L.A., Erwig, L.P., Munro, C.A., Gow, N.A., Brown, G.D., MacCallum, D.M., and Brown, A.J. (2016). Lactate signalling regulates fungal beta-glucan masking and immune evasion. Nat Microbiol *2*, 16238.

Beaussart, A., Alsteens, D., El-Kirat-Chatel, S., Lipke, P.N., Kucharikova, S., Van Dijck, P., and Dufrêne, Y.F. (2012). Single-molecule imaging and functional analysis of Als adhesins and mannans during *Candida albicans* morphogenesis. ACS nano *6*, 10950-10964.

Beullens, M., Mbonyi, K., Geerts, L., Gladines, D., Detremerie, K., Jans, A.W., and Thevelein, J.M. (1988). Studies on the mechanism of the glucose-induced cAMP signal in glycolysis and glucose repression mutants of the yeast *Saccharomyces cerevisiae*. European journal of biochemistry / FEBS *172*, 227-231.

Biswas, S., Van Dijck, P., and Datta, A. (2007). Environmental sensing and signal transduction pathways regulating morphopathogenic determinants of *Candida albicans*. Microbiology and molecular biology reviews : MMBR *71*, 348-376.

Bockmühl, D.P., Krishnamurthy, S., Gerads, M., Sonneborn, A., and Ernst, J.F. (2001). Distinct and redundant roles of the two protein kinase A isoforms Tpk1p and Tpk2p in morphogenesis and growth of *Candida albicans*. Molecular microbiology *42*, 1243-1257.

Bongomin, F., Gago, S., Oladele, R.O., and Denning, D.W. (2017). Global and Multi-National Prevalence of Fungal Diseases-Estimate Precision. J Fungi (Basel) *3*.

Boy-Marcotte, E., Perrot, M., Bussereau, F., Boucherie, H., and Jacquet, M. (1998). Msn2p and Msn4p control a large number of genes induced at the diauxic transition which are repressed by cyclic AMP in Saccharomyces cerevisiae. J Bacteriol *180*, 1044-1052.

Brown, G.D., Denning, D.W., Gow, N.A., Levitz, S.M., Netea, M.G., and White, T.C. (2012). Hidden killers: human fungal infections. Sci Transl Med *4*, 165rv113.

Busti, S., Coccetti, P., Alberghina, L., and Vanoni, M. (2010). Glucose signaling-mediated coordination of cell growth and cell cycle in *Saccharomyces cerevisiae*. Sensors (Basel) *10*, 6195-6240.

Butler, G., Rasmussen, M.D., Lin, M.F., Santos, M.A., Sakthikumar, S., Munro, C.A., Rheinbay, E., Grabherr, M., Forche, A., Reedy, J.L., Agrafioti, I., Arnaud, M.B., Bates, S., Brown, A.J., Brunke, S., Costanzo, M.C., Fitzpatrick, D.A., de Groot, P.W., Harris, D., Hoyer, L.L., Hube, B., Klis, F.M., Kodira, C., Lennard, N., Logue, M.E., Martin, R., Neiman, A.M., Nikolaou, E., Quail, M.A., Quinn, J., Santos, M.C., Schmitzberger, F.F., Sherlock, G., Shah, P., Silverstein, K.A., Skrzypek, M.S., Soll, D., Staggs, R., Stansfield, I., Stumpf, M.P., Sudbery, P.E., Srikantha, T., Zeng, Q., Berman, J., Berriman, M., Heitman, J., Gow, N.A., Lorenz, M.C., Birren, B.W., Kellis, M., and Cuomo, C.A. (2009). Evolution of pathogenicity and sexual reproduction in eight *Candida* genomes. Nature *459*, 657-662.

Calderone, R.A., and Clancy, C.J. (2012). *Candida* and candidiasis. (Washington, DC: ASM Press).

Carolus, H., Pierson, S., Lagrou, K., and Van Dijck, P. (2020). Amphotericin B and Other Polyenes-Discovery, Clinical Use, Mode of Action and Drug Resistance. J Fungi (Basel) *6*.

Carreté, L., Ksiezopolska, E., Pegueroles, C., Gómez-Molero, E., Saus, E., Iraola-Guzmán, S., Loska, D., Bader, O., Fairhead, C., and Gabaldón, T. (2018). Patterns of Genomic Variation in the Opportunistic Pathogen *Candida glabrata* Suggest the Existence of Mating and a Secondary Association with Humans. Current biology : CB *28*, 15-27 e17.

Casadevall, A., Coelho, C., Cordero, R.J.B., Dragotakes, Q., Jung, E., Vij, R., and Wear, M.P. (2019). The capsule of *Cryptococcus neoformans*. Virulence *10*, 822-831.

Castaño, I., Pan, S.J., Zupancic, M., Hennequin, C., Dujon, B., and Cormack, B.P. (2005). Telomere length control and transcriptional regulation of subtelomeric adhesins in *Candida glabrata*. Molecular microbiology *55*, 1246-1258.

Cauchie, M., Desmet, S., and Lagrou, K. (2017). *Candida* and its dual lifestyle as a commensal and a pathogen. Research in microbiology *168*, 802-810.

Cavalheiro, M., and Teixeira, M.C. (2018). Candida Biofilms: Threats, Challenges, and Promising Strategies. Front Med (Lausanne) *5*, 28.

Choi, J., Jung, W.H., and Kronstad, J.W. (2015). The cAMP/protein kinase A signaling pathway in pathogenic basidiomycete fungi: Connections with iron homeostasis. J Microbiol *53*, 579-587.

Choi, W., and Dean, R.A. (1997). The adenylate cyclase gene *MAC1* of *Magnaporthe grisea* controls appressorium formation and other aspects of growth and development. Plant Cell *9*, 1973-1983.

Chowdhary, A., Prakash, A., Sharma, C., Kordalewska, M., Kumar, A., Sarma, S., Tarai, B., Singh, A., Upadhyaya, G., Upadhyay, S., Yadav, P., Singh, P.K., Khillan, V., Sachdeva, N., Perlin, D.S., and Meis, J.F. (2018). A multicentre study of antifungal susceptibility patterns among 350 *Candida auris* isolates (2009-17) in India: role of the ERG11 and FKS1 genes in azole and echinocandin resistance. The Journal of antimicrobial chemotherapy *73*, 891-899.

Colombo, S., Ronchetti, D., Thevelein, J.M., Winderickx, J., and Martegani, E. (2004). Activation state of the Ras2 protein and glucose-induced signaling in *Saccharomyces cerevisiae*. The Journal of biological chemistry *279*, 46715-46722.

Conlan, R.S., and Tzamarias, D. (2001). Sfl1 functions via the co-repressor Ssn6-Tup1 and the cAMP-dependent protein kinase Tpk2. J Mol Biol *309*, 1007-1015.

Conrad, M., Schothorst, J., Kankipati, H.N., Van Zeebroeck, G., Rubio-Texeira, M., and Thevelein, J.M. (2014). Nutrient sensing and signaling in the yeast *Saccharomyces cerevisiae*. FEMS microbiology reviews *38*, 254-299.

Cormack, B.P. (1999). An Adhesin of the Yeast Pathogen *Candida glabrata* Mediating Adherence to Human Epithelial Cells. Science *285*, 578-582.

Cormack, B.P., Ghori, N., and Falkow, S. (1999). An adhesin of the yeast pathogen *Candida glabrata* mediating adherence to human epithelial cells. Science *285*, 578-582.

Coste, A.T., Kritikos, A., Li, J., Khanna, N., Goldenberger, D., Garzoni, C., Zehnder, C., Boggian, K., Neofytos, D., Riat, A., Bachmann, D., Sanglard, D., Lamoth, F., and Fungal Infection Network of, S. (2020). Emerging echinocandin-resistant *Candida albicans* and *glabrata* in Switzerland. Infection *48*, 761-766.

Costerton, J.W., Lewandowski, Z., Caldwell, D.E., Korber, D.R., and Lappin-Scott, H.M. (1995). Microbial biofilms. Annual review of microbiology *49*, 711-745.

Cramer, K.L., Gerrald, Q.D., Nichols, C.B., Price, M.S., and Alspaugh, J.A. (2006). Transcription factor Nrg1 mediates capsule formation, stress response, and pathogenesis in *Cryptococcus neoformans*. Eukaryotic cell *5*, 1147-1156.

D'Souza, C.A., Alspaugh, J.A., Yue, C., Harashima, T., Cox, G.M., Perfect, J.R., and Heitman, J. (2001). Cyclic AMP-dependent protein kinase controls virulence of the fungal pathogen *Cryptococcus neoformans*. Molecular and cellular biology *21*, 3179-3191.

Dagenais, T.R., and Keller, N.P. (2009). Pathogenesis of *Aspergillus fumigatus* in Invasive Aspergillosis. Clin Microbiol Rev *22*, 447-465.

de Groot, P.W., Bader, O., de Boer, A.D., Weig, M., and Chauhan, N. (2013). Adhesins in human fungal pathogens: glue with plenty of stick. Eukaryotic cell *12*, 470-481.

de Groot, P.W., Hellingwerf, K.J., and Klis, F.M. (2003). Genome-wide identification of fungal GPI proteins. Yeast *20*, 781-796.

de Groot, P.W., Kraneveld, E.A., Yin, Q.Y., Dekker, H.L., Gross, U., Crielaard, W., de Koster, C.G., Bader, O., Klis, F.M., and Weig, M. (2008). The cell wall of the human pathogen Candida glabrata: differential incorporation of novel adhesin-like wall proteins. Eukaryotic cell *7*, 1951-1964.

De Las Penas, A., Pan, S.J., Castano, I., Alder, J., Cregg, R., and Cormack, B.P. (2003). Virulence-related surface glycoproteins in the yeast pathogen *Candida glabrata* are encoded in subtelomeric clusters and subject to *RAP1*- and *SIR*-dependent transcriptional silencing. Genes & development *17*, 2245-2258.

Deminoff, S.J., and Santangelo, G.M. (2001). Rap1p requires Gcr1p and Gcr2p homodimers to activate ribosomal protein and glycolytic genes, respectively. Genetics *158*, 133-143.

Deprez, M.A., Eskes, E., Wilms, T., Ludovico, P., and Winderickx, J. (2018a). pH homeostasis links the nutrient sensing PKA/TORC1/Sch9 menage-a-trois to stress tolerance and longevity. Microb Cell *5*, 119-136.

Deprez, M.A., Eskes, E., Winderickx, J., and Wilms, T. (2018b). The TORC1-Sch9 pathway as a crucial mediator of chronological lifespan in the yeast *Saccharomyces cerevisiae*. FEMS yeast research *18*.

Desai, C., Mavrianos, J., and Chauhan, N. (2011). *Candida glabrata* Pwp7p and Aed1p are required for adherence to human endothelial cells. FEMS yeast research *11*, 595-601.

DeZwaan, T.M., Carroll, A.M., Valent, B., and Sweigard, J.A. (1999). *Magnaporthe grisea* pth11p is a novel plasma membrane protein that mediates appressorium differentiation in response to inductive substrate cues. Plant Cell *11*, 2013-2030.

Diderrich, R., Kock, M., Maestre-Reyna, M., Keller, P., Steuber, H., Rupp, S., Essen, L.O., and Mösch, H.U. (2015). Structural Hotspots Determine Functional Diversity of the *Candida glabrata* Epithelial Adhesin Family. The Journal of biological chemistry.

Diekema, D., Arbefeville, S., Boyken, L., Kroeger, J., and Pfaller, M. (2012). The changing epidemiology of healthcare-associated candidemia over three decades. Diagnostic microbiology and infectious disease *73*, 45-48.

Domergue, R., Castaño, I., De Las Peñas, A., Zupancic, M., Lockatell, V., Hebel, J.R., Johnson, D., and Cormack, B.P. (2005). Nicotinic acid limitation regulates silencing of *Candida* adhesins during UTI. Science *308*, 866-870.

Donaton, M.C., Holsbeeks, I., Lagatie, O., Van Zeebroeck, G., Crauwels, M., Winderickx, J., and Thevelein, J.M. (2003). The Gap1 general amino acid permease acts as an amino acid sensor for activation of protein kinase A targets in the yeast *Saccharomyces cerevisiae*. Molecular microbiology *50*, 911-929.

Donlan, R.M., and Costerton, J.W. (2002). Biofilms: survival mechanisms of clinically relevant microorganisms. Clin Microbiol Rev *15*, 167-193.

Drell, T., Lillsaar, T., Tummeleht, L., Simm, J., Aaspõllu, A., Väin, E., Saarma, I., Salumets, A., Donders, G.G., and Metsis, M. (2013). Characterization of the vaginal micro- and mycobiome in asymptomatic reproductive-age Estonian women. PLoS One *8*, e54379.

Dujon, B., Sherman, D., Fischer, G., Durrens, P., Casaregola, S., Lafontaine, I., De Montigny, J., Marck, C., Neuvéglise, C., Talla, E., Goffard, N., Frangeul, L., Aigle, M., Anthouard, V., Babour, A., Barbe, V., Barnay, S., Blanchin, S., Beckerich, J.M., Beyne, E., Bleykasten, C., Boisrame, A., Boyer, J., Cattolico, L., Confanioleri, F., De Daruvar, A., Despons, L., Fabre, E., Fairhead, C., Ferry-Dumazet, H., Groppi, A., Hantraye, F., Hennequin, C., Jauniaux, N., Joyet, P., Kachouri, R., Kerrest, A., Koszul, R., Lemaire, M., Lesur, I., Ma, L., Muller, H., Nicaud, J.M., Nikolski, M., Oztas, S., Ozier-Kalogeropoulos, O., Pellenz, S., Potier, S., Richard, G.F., Straub, M.L., Suleau, A., Swennen, D., Tekaia, F., Wesolowski-Louvel, M., Westhof, E., Wirth, B., Zeniou-Meyer, M., Zivanovic, I., Bolotin-Fukuhara, M., Thierry, A., Bouchier, C., Caudron, B., Scarpelli, C., Gaillardin, C., Weissenbach, J., Wincker, P., and Souciet, J.L. (2004). Genome evolution in yeasts. Nature *430*, 35-44.

Dürrenberger, F., Wong, K., and Kronstad, J.W. (1998). Identification of a cAMP-dependent protein kinase catalytic subunit required for virulence and morphogenesis in *Ustilago maydis*. Proceedings of the National Academy of Sciences of the United States of America *95*, 5684-5689.

ECDC (2018a). *Candida auris* in healthcare settings – Europe. In Rapid Risk Assessment. E.C.f.D.P.a. Control, ed., p. Rapid Risk Assessment.

ECDC (2018b). Healthcare-associated infections acquired in intensive care units. Annual epidemiological report for 2016. (Stockholm: European Centre for Disease Prevention and Control).

ECDC (2018c). Incidence and attributable mortality of healthcare-associated infections in intensive care units in Europe, 2008-2012. In Surveillance report. E.C.f.D.P.a. Control, ed., p. SURVEILLANCE REPORT.

ECDC (2018d). Surgical site infections. Annual epidemiological report for 2016. In Annual Epidemiological Report on Communicable Diseases in Europe (Stockholm: ECDC).

Eichhorn, H., Lessing, F., Winterberg, B., Schirawski, J., Kämper, J., Müller, P., and Kahmann, R. (2006). A ferroxidation/permeation iron uptake system is required for virulence in *Ustilago maydis*. Plant Cell *18*, 3332-3345.

El-Kirat-Chatel, S., Beaussart, A., Derclaye, S., Alsteens, D., Kucharíková, S., Van Dijck, P., and Dufrêne, Y.F. (2015). Force nanoscopy of hydrophobic interactions in the fungal pathogen *Candida glabrata*. ACS nano *9*, 1648-1655.

Fitzpatrick, D.A., Logue, M.E., Stajich, J.E., and Butler, G. (2006). A fungal phylogeny based on 42 complete genomes derived from supertree and combined gene analysis. BMC Evol Biol *6*, 99.

Forsberg, K., Woodworth, K., Walters, M., Berkow, E.L., Jackson, B., Chiller, T., and Vallabhaneni, S. (2019). *Candida auris*: The recent emergence of a multidrug-resistant fungal pathogen. Medical mycology : official publication of the International Society for Human and Animal Mycology *57*, 1-12.

François, J., and Parrou, J.L. (2001). Reserve carbohydrates metabolism in the yeast *Saccharomyces cerevisiae*. FEMS microbiology reviews *25*, 125-145.

Frank, A.T., Ramsook, C.B., Otoo, H.N., Tan, C., Soybelman, G., Rauceo, J.M., Gaur, N.K., Klotz, S.A., and Lipke, P.N. (2010). Structure and function of glycosylated tandem repeats from *Candida albicans* Als adhesins. Eukaryotic cell *9*, 405-414.

Frieman, M.B., McCaffery, J.M., and Cormack, B.P. (2002). Modular domain structure in the *Candida glabrata* adhesin Epa1p, a beta1,6 glucan-cross-linked cell wall protein. Molecular microbiology *46*, 479-492.

Fuller, K.K., Zhao, W., Askew, D.S., and Rhodes, J.C. (2009). Deletion of the protein kinase A regulatory subunit leads to deregulation of mitochondrial activation and nuclear duplication in *Aspergillus fumigatus*. Eukaryotic cell *8*, 271-277.

Gabaldón, T., and Carreté, L. (2016). The birth of a deadly yeast: tracing the evolutionary emergence of virulence traits in *Candida glabrata*. FEMS yeast research *16*, fov110.

Gabaldón, T., Martin, T., Marcet-Houben, M., Durrens, P., Bolotin-Fukuhara, M., Lespinet, O., Arnaise, S., Boisnard, S., Aguileta, G., Atanasova, R., Bouchier, C., Couloux, A., Creno, S., Almeida Cruz, J., Devillers, H., Enache-Angoulvant, A., Guitard, J., Jaouen, L., Ma, L., Marck, C., Neuvéglise, C., Pelletier, E., Pinard, A., Poulain, J., Recoquillay, J., Westhof, E., Wincker, P., Dujon, B., Hennequin, C., and Fairhead, C. (2013). Comparative genomics of emerging pathogens in the *Candida glabrata* clade. BMC Genomics *14*, 623.

Gabaldón, T., Naranjo-Ortíz, M.A., and Marcet-Houben, M. (2016). Evolutionary genomics of yeast pathogens in the Saccharomycotina. FEMS yeast research *16*.

Gallegos-García, V., Pan, S.J., Juárez-Cepeda, J., Ramírez-Zavaleta, C.Y., Martin-del-Campo, M.B., Martinez-Jiménez, V., Castaño, I., Cormack, B., and De Las Peñas, A. (2012). A novel downstream regulatory element cooperates with the silencing machinery to repress *EPA1* expression in *Candida glabrata*. Genetics *190*, 1285-1297.

Ghannoum, M.A., Jurevic, R.J., Mukherjee, P.K., Cui, F., Sikaroodi, M., Naqvi, A., and Gillevet, P.M. (2010). Characterization of the oral fungal microbiome (mycobiome) in healthy individuals. PLoS pathogens *6*, e1000713.

Giots, F., Donaton, M.C., and Thevelein, J.M. (2003). Inorganic phosphate is sensed by specific phosphate carriers and acts in concert with glucose as a nutrient signal for activation of the protein kinase A pathway in the yeast *Saccharomyces cerevisiae*. Molecular microbiology *47*, 1163-1181.

Goemaere, B., Becker, P., Van Wijngaerden, E., Maertens, J., Spriet, I., Hendrickx, M., and Lagrou, K. (2018). Increasing candidaemia incidence from 2004 to 2015 with a shift in epidemiology in patients preexposed to antifungals. Mycoses *61*, 127-133.

Gold, S., Duncan, G., Barrett, K., and Kronstad, J. (1994). cAMP regulates morphogenesis in the fungal pathogen *Ustilago maydis*. Genes & development *8*, 2805-2816.

Gómez-Molero, E., de Boer, A.D., Dekker, H.L., Moreno-Martínez, A., Kraneveld, E.A., Ichsan, Chauhan, N., Weig, M., de Soet, J.J., de Koster, C.G., Bader, O., and de Groot, P.W. (2015). Proteomic analysis of hyperadhesive *Candida glabrata* clinical isolates reveals a core wall proteome and differential incorporation of adhesins. FEMS yeast research *15*.

Görner, W., Durchschlag, E., Martinez-Pastor, M.T., Estruch, F., Ammerer, G., Hamilton, B., Ruis, H., and Schüller, C. (1998). Nuclear localization of the C2H2 zinc finger protein Msn2p is regulated by stress and protein kinase A activity. Genes & development *12*, 586-597.

Görner, W., Durchschlag, E., Wolf, J., Brown, E.L., Ammerer, G., Ruis, H., and Schüller, C. (2002). Acute glucose starvation activates the nuclear localization signal of a stress-specific yeast transcription factor. EMBO J *21*, 135-144.

Gregg, K.S., and Kauffman, C.A. (2015). Invasive Aspergillosis: Epidemiology, Clinical Aspects, and Treatment. Semin Respir Crit Care Med *36*, 662-672.

Grosse, C., Heinekamp, T., Kniemeyer, O., Gehrke, A., and Brakhage, A.A. (2008). Protein kinase A regulates growth, sporulation, and pigment formation in *Aspergillus fumigatus*. Applied and environmental microbiology *74*, 4923-4933.

Guinea, J. (2014). Global trends in the distribution of *Candida* species causing candidemia. Clinical microbiology and infection : the official publication of the European Society of Clinical Microbiology and Infectious Diseases *20 Suppl 6*, 5-10.

Halliwell, S.C., Smith, M.C., Muston, P., Holland, S.L., and Avery, S.V. (2012). Heterogeneous expression of the virulence-related adhesin Epa1 between individual cells and strains of the pathogen *Candida glabrata*. Eukaryotic cell *11*, 141-150.

Harashima, T., and Heitman, J. (2002). The Galpha protein Gpa2 controls yeast differentiation by interacting with kelch repeat proteins that mimic Gbeta subunits. Mol Cell *10*, 163-173.

Hazen, K.C., Plotkin, B.J., and Klimas, D.M. (1986). Influence of growth conditions on cell surface hydrophobicity of *Candida albicans* and *Candida glabrata*. Infection and immunity *54*, 269-271.

Heinekamp, T., Thywißen, A., Macheleidt, J., Keller, S., Valiante, V., and Brakhage, A.A. (2012). *Aspergillus fumigatus* melanins: interference with the host endocytosis pathway and impact on virulence. Front Microbiol *3*, 440.

Hirimburegama, K., Durnez, P., Keleman, J., Oris, E., Vergauwen, R., Mergelsberg, H., and Thevelein, J.M. (1992). Nutrient-induced activation of trehalase in nutrient-starved cells of the yeast *Saccharomyces cerevisiae*: cAMP is not involved as second messenger. Journal of general microbiology *138*, 2035-2043.

Höfs, S., Mogavero, S., and Hube, B. (2016). Interaction of *Candida albicans* with host cells: virulence factors, host defense, escape strategies, and the microbiota. J Microbiol *54*, 149-169.

Hood, M.I., and Skaar, E.P. (2012). Nutritional immunity: transition metals at the pathogen-host interface. Nature reviews. Microbiology *10*, 525-537.

Hoyer, L.L., Fundyga, R., Hecht, J.E., Kapteyn, J.C., Klis, F.M., and Arnold, J. (2001). Characterization of agglutinin-like sequence genes from non-*albicans Candida* and phylogenetic analysis of the *ALS* family. Genetics *157*, 1555-1567.

Hoyer, L.L., Green, C.B., Oh, S.H., and Zhao, X. (2008). Discovering the secrets of the *Candida albicans* agglutinin-like sequence (*ALS*) gene family--a sticky pursuit. Medical mycology : official publication of the International Society for Human and Animal Mycology *46*, 1-15.

Hu, Y., Liu, E., Bai, X., and Zhang, A. (2010). The localization and concentration of the *PDE2*-encoded high-affinity cAMP phosphodiesterase is regulated by cAMP-dependent protein kinase A in the yeast *Saccharomyces cerevisiae*. FEMS yeast research *10*, 177-187.

Huang, J., Reggiori, F., and Klionsky, D.J. (2007). The transmembrane domain of acid trehalase mediates ubiquitin-independent multivesicular body pathway sorting. Molecular biology of the cell *18*, 2511-2524.

Ielasi, F.S., Alioscha-Perez, M., Donohue, D., Claes, S., Sahli, H., Schols, D., and Willaert, R.G. (2016). Lectin-Glycan Interaction Network-Based Identification of Host Receptors of Microbial Pathogenic Adhesins. mBio *7*.

Ielasi, F.S., Decanniere, K., and Willaert, R.G. (2012). The epithelial adhesin 1 (Epa1p) from the human-pathogenic yeast *Candida glabrata*: structural and functional study of the carbohydrate-binding domain. Acta Crystallogr D Biol Crystallogr *68*, 210-217.

Ielasi, F.S., Verhaeghe, T., Desmet, T., and Willaert, R.G. (2014). Engineering the carbohydrate-binding site of Epa1p from Candida glabrata: generation of adhesin mutants with different carbohydrate specificity. Glycobiology *24*, 1312-1322.

Iraqui, I., Garcia-Sanchez, S., Aubert, S., Dromer, F., Ghigo, J.M., d'Enfert, C., and Janbon, G. (2005). The Yak1p kinase controls expression of adhesins and biofilm formation in *Candida glabrata* in a Sir4p-dependent pathway. Molecular microbiology *55*, 1259-1271.

Jones, T., Federspiel, N.A., Chibana, H., Dungan, J., Kalman, S., Magee, B.B., Newport, G., Thorstenson, Y.R., Agabian, N., Magee, P.T., Davis, R.W., and Scherer, S. (2004). The diploid genome sequence of *Candida albicans*. Proceedings of the National Academy of Sciences of the United States of America *101*, 7329-7334.

Juárez-Cepeda, J., Orta-Zavalza, E., Cañas-Villamar, I., Arreola-Gómez, J., Pérez-Cornejo, G.P., Hernández-Carballo, C.Y., Gutiérrez-Escobedo, G., Castaño, I., and De Las Peñas, A. (2015). The *EPA2* adhesin encoding gene is responsive to oxidative stress in the opportunistic fungal pathogen *Candida glabrata*. Current genetics.

Juárez-Reyes, A., Ramírez-Zavaleta, C.Y., Medina-Sánchez, L., De Las Peñas, A., and Castaño, I. (2012). A protosilencer of subtelomeric gene expression in *Candida glabrata* with unique properties. Genetics *190*, 101-111.

Kaffarnik, F., Müller, P., Leibundgut, M., Kahmann, R., and Feldbrügge, M. (2003). PKA and MAPK phosphorylation of Prf1 allows promoter discrimination in *Ustilago maydis*. EMBO J *22*, 5817-5826.

Kang, S.H., Khang, C.H., and Lee, Y.-H. (1999). Regulation of cAMP-dependent protein kinase during appressorium formation in *Magnaporthe grisea*. FEMS microbiology letters *170*, 419-423.

Kankipati, H.N., Rubio-Texeira, M., Castermans, D., Diallinas, G., and Thevelein, J.M. (2015). Sul1 and Sul2 sulfate transceptors signal to protein kinase A upon exit of sulfur starvation. The Journal of biological chemistry *290*, 10430-10446.

Kataoka, T., Powers, S., Cameron, S., Fasano, O., Goldfarb, M., Broach, J., and Wigler, M. (1985). Functional homology of mammalian and yeast *RAS* genes. Cell *40*, 19-26.

Kayikci, O., and Nielsen, J. (2015). Glucose repression in *Saccharomyces cerevisiae*. FEMS yeast research *15*.

Kemp, B.E., Graves, D.J., Benjamini, E., and Krebs, E.G. (1977). Role of multiple basic residues in determining the substrate specificity of cyclic AMP-dependent protein kinase. Journal of Biological Chemistry *252*, 4888-4894.

Klein, C., and Struhl, K. (1994). Protein kinase A mediates growth-regulated expression of yeast ribosomal protein genes by modulating *RAP1* transcriptional activity. Molecular and cellular biology *14*, 1920-1928.

Klosterman, S.J., Perlin, M.H., Garcia-Pedrajas, M., Covert, S.F., and Gold, S.E. (2007). Genetics of morphogenesis and pathogenic development of *Ustilago maydis*. Adv Genet *57*, 1-47.

Klotz, S.A., Drutz, D.J., and Zajic, J.E. (1985). Factors governing adherence of *Candida* species to plastic surfaces. Infection and immunity *50*, 97-101.

Kopp, M., Müller, H., and Holzer, H. (1993). Molecular analysis of the neutral trehalase gene from *Saccharomyces cerevisiae*. The Journal of biological chemistry *268*, 4766-4774.

Kraakman, L., Lemaire, K., Ma, P., Teunissen, A.W., Donaton, M.C., Van Dijck, P., Winderickx, J., de Winde, J.H., and Thevelein, J.M. (1999). A *Saccharomyces cerevisiae* G-protein coupled receptor, Gpr1, is specifically required for glucose activation of the cAMP pathway during the transition to growth on glucose. Molecular microbiology *32*, 1002-1012.

Kraidlova, L., Schrevens, S., Tournu, H., Van Zeebroeck, G., Sychrova, H., and Van Dijck, P. (2016). Characterization of the *Candida albicans* Amino Acid Permease Family: Gap2 Is the Only General Amino Acid Permease and Gap4 Is an S-Adenosylmethionine (SAM) Transporter Required for SAM-Induced Morphogenesis. mSphere *1*.

Kraneveld, E.A., de Soet, J.J., Deng, D.M., Dekker, H.L., de Koster, C.G., Klis, F.M., Crielaard, W., and de Groot, P.W. (2011). Identification and differential gene expression of adhesin-like wall proteins in *Candida glabrata* biofilms. Mycopathologia *172*, 415-427.

Kriel, J., Haesendonckx, S., Rubio-Texeira, M., Van Zeebroeck, G., and Thevelein, J.M. (2011). From transporter to transceptor: signaling from transporters provokes re-evaluation of complex trafficking and regulatory controls: endocytic internalization and intracellular trafficking of nutrient transceptors may, at least in part, be governed by their signaling function. Bioessays *33*, 870-879.

Krom, B.P., and Willems, H.M. (2016). *In Vitro* Models for *Candida* Biofilm Development. Methods Mol Biol *1356*, 95-105.

Kucharíková, S., Neirinck, B., Sharma, N., Vleugels, J., Lagrou, K., and Van Dijck, P. (2015). *In vivo Candida glabrata* biofilm development on foreign bodies in a rat subcutaneous model. The Journal of antimicrobial chemotherapy *70*, 846-856.

Kucharíková, S., Tournu, H., Lagrou, K., Van Dijck, P., and Bujdáková, H. (2011). Detailed comparison of *Candida albicans* and *Candida glabrata* biofilms under different conditions and their susceptibility to caspofungin and anidulafungin. Journal of medical microbiology *60*, 1261-1269.

Kuhn, D.M., Chandra, J., Mukherjee, P.K., and Ghannoum, M.A. (2002). Comparison of biofilms formed by *Candida albicans* and *Candida parapsilosis* on bioprosthetic surfaces. Infection and immunity *70*, 878-888.

Kuhn, D.M., and Vyas, V.K. (2012). The *Candida glabrata* adhesin Epa1p causes adhesion, phagocytosis, and cytokine secretion by innate immune cells. FEMS yeast research *12*, 398-414.

Kumamoto, C.A., Gresnigt, M.S., and Hube, B. (2020). The gut, the bad and the harmless: *Candida albicans* as a commensal and opportunistic pathogen in the intestine. Current opinion in microbiology *56*, 7-15.

Lengeler, K.B., Davidson, R.C., D'Souza, C., Harashima, T., Shen, W.C., Wang, P., Pan, X., Waugh, M., and Heitman, J. (2000). Signal transduction cascades regulating fungal development and virulence. Microbiology and molecular biology reviews : MMBR *64*, 746-785.

Li, F., Svarovsky, M.J., Karlsson, A.J., Wagner, J.P., Marchillo, K., Oshel, P., Andes, D., and Palecek, S.P. (2007). Eap1p, an adhesin that mediates *Candida albicans* biofilm formation *in vitro and in vivo*. Eukaryotic cell *6*, 931-939.

Li, Y., Zhang, X., Hu, S., Liu, H., and Xu, J.R. (2017). PKA activity is essential for relieving the suppression of hyphal growth and appressorium formation by *MoSfl1* in *Magnaporthe oryzae*. PLoS Genet *13*, e1006954.

Liebmann, B., Gattung, S., Jahn, B., and Brakhage, A.A. (2003). cAMP signaling in *Aspergillus fumigatus* is involved in the regulation of the virulence gene pksP and in defense against killing by macrophages. Molecular genetics and genomics : MGG *269*, 420-435.

Liebmann, B., Müller, M., Braun, A., and Brakhage, A.A. (2004). The cyclic AMP-dependent protein kinase a network regulates development and virulence in *Aspergillus fumigatus*. Infection and immunity *72*, 5193-5203.

Linde, J., Duggan, S., Weber, M., Horn, F., Sieber, P., Hellwig, D., Riege, K., Marz, M., Martin, R., Guthke, R., and Kurzai, O. (2015). Defining the transcriptomic landscape of *Candida glabrata* by RNA-Seq. Nucleic acids research *43*, 1392-1406.

Liu, Y., and Filler, S.G. (2011). *Candida albicans* Als3, a multifunctional adhesin and invasin. Eukaryotic cell *10*, 168-173.

Lo, W.S., and Dranginis, A.M. (1998). The cell surface flocculin Flo11 is required for pseudohyphae formation and invasion by *Saccharomyces cerevisiae*. Molecular biology of the cell *9*, 161-171.

Lohse, M.B., and Johnson, A.D. (2009). White-opaque switching in *Candida albicans*. Current opinion in microbiology *12*, 650-654.

Lone, S.A., and Ahmad, A. (2019). *Candida auris*-the growing menace to global health. Mycoses *62*, 620-637.

Lorenz, M.C., and Heitman, J. (1997). Yeast pseudohyphal growth is regulated by *GPA2*, a G protein alpha homolog. EMBO J *16*, 7008-7018.

Lu, A., and Hirsch, J.P. (2005). Cyclic AMP-independent regulation of protein kinase A substrate phosphorylation by Kelch repeat proteins. Eukaryotic cell *4*, 1794-1800.

Luo, G., and Samaranayake, L.P. (2002). *Candida glabrata*, an emerging fungal pathogen, exhibits superior relative cell surface hydrophobicity and adhesion to denture acrylic surfaces compared with *Candida albicans*. APMIS *110*, 601-610.

Ma, P., Wera, S., Van Dijck, P., and Thevelein, J.M. (1999). The *PDE1*-encoded low-affinity phosphodiesterase in the yeast *Saccharomyces cerevisiae* has a specific function in controlling agonist-induced cAMP signaling. Molecular biology of the cell *10*, 91-104.

Maidan, M.M., De Rop, L., Serneels, J., Exler, S., Rupp, S., Tournu, H., Thevelein, J.M., and Van Dijck, P. (2005). The G protein-coupled receptor Gpr1 and the Galpha protein Gpa2 act

through the cAMP-protein kinase A pathway to induce morphogenesis in *Candida albicans*. Molecular biology of the cell *16*, 1971-1986.

Marcet-Houben, M., and Gabaldon, T. (2009). The tree versus the forest: the fungal tree of life and the topological diversity within the yeast phylome. PLoS One *4*, e4357.

Marchler, G., Schüller, C., Adam, G., and Ruis, H. (1993). A *Saccharomyces cerevisiae* UAS element controlled by protein kinase A activates transcription in response to a variety of stress conditions. EMBO J *12*, 1997-2003.

Martínez-Pastor, M.T., Marchler, G., Schüller, C., Marchler-Bauer, A., Ruis, H., and Estruch, F. (1996). The *Saccharomyces cerevisiae* zinc finger proteins Msn2p and Msn4p are required for transcriptional induction through the stress response element (STRE). EMBO J *15*, 2227-2235.

Matsumoto, K., Uno, I., and Ishikawa, T. (1983). Control of cell division in *Saccharomyces cerevisiae* mutants defective in adenylate cyclase and cAMP-dependent protein kinase. Experimental cell research *146*, 151-161.

Mbonyi, K., Beullens, M., Detremerie, K., Geerts, L., and Thevelein, J.M. (1988). Requirement of one functional RAS gene and inability of an oncogenic ras variant to mediate the glucose-induced cyclic AMP signal in the yeast *Saccharomyces cerevisiae*. Molecular and cellular biology *8*, 3051-3057.

Mbonyi, K., van Aelst, L., Argüelles, J.C., Jans, A.W., and Thevelein, J.M. (1990). Glucose-induced hyperaccumulation of cyclic AMP and defective glucose repression in yeast strains with reduced activity of cyclic AMP-dependent protein kinase. Molecular and cellular biology *10*, 4518-4523.

Mehrabi, R., Zhao, X., Kim, Y., and Xu, J.-R. (2009). The cAMP Signaling and MAP Kinase Pathways in Plant Pathogenic Fungi. In Plant Relationships. H.B. Deising, ed. (Berlin, Heidelberg: Springer Berlin Heidelberg), pp. 157-172.

Miranda, L.N., van der Heijden, I.M., Costa, S.F., Sousa, A.P., Sienra, R.A., Gobara, S., Santos, C.R., Lobo, R.D., Pessoa, V.P., Jr., and Levin, A.S. (2009). *Candida* colonisation as a source for candidaemia. J Hosp Infect *72*, 9-16.

Mitchell, T.K., and Dean, R.A. (1995). The cAMP-dependent protein kinase catalytic subunit is required for appressorium formation and pathogenesis by the rice blast pathogen *Magnaporthe grisea*. Plant Cell *7*, 1869-1878.

Moyes, D.L., Richardson, J.P., and Naglik, J.R. (2015). *Candida albicans*-epithelial interactions and pathogenicity mechanisms: scratching the surface. Virulence *6*, 338-346.

Muller, H., Thierry, A., Coppée, J.Y., Gouyette, C., Hennequin, C., Sismeiro, O., Talla, E., Dujon, B., and Fairhead, C. (2009). Genomic polymorphism in the population of *Candida glabrata*: gene copy-number variation and chromosomal translocations. Fungal genetics and biology : FG & B *46*, 264-276.

Naglik, J.R., Moyes, D.L., Wachtler, B., and Hube, B. (2011). *Candida albicans* interactions with epithelial cells and mucosal immunity. Microbes Infect *13*, 963-976.

Nakafuku, M., Obara, T., Kaibuchi, K., Miyajima, I., Miyajima, A., Itoh, H., Nakamura, S., Arai, K., Matsumoto, K., and Kaziro, Y. (1988). Isolation of a second yeast *Saccharomyces cerevisiae* gene (*GPA2*) coding for guanine nucleotide-binding regulatory protein: studies on its structure and possible functions. Proceedings of the National Academy of Sciences of the United States of America *85*, 1374-1378.

Nett, J., Lincoln, L., Marchillo, K., and Andes, D. (2007). Beta -1,3 glucan as a test for central venous catheter biofilm infection. The Journal of infectious diseases *195*, 1705-1712.

Neuman-Silberberg, F.S., Bhattacharya, S., and Broach, J.R. (1995). Nutrient availability and the RAS/cyclic AMP pathway both induce expression of ribosomal protein genes in *Saccharomyces cerevisiae* but by different mechanisms. Molecular and cellular biology *15*, 3187-3196.

Nikawa, J., Sass, P., and Wigler, M. (1987). Cloning and characterization of the low-affinity cyclic AMP phosphodiesterase gene of *Saccharomyces cerevisiae*. Molecular and cellular biology *7*, 3629-3636.

Niranjan, T., Guo, X., Victor, J., Lu, A., and Hirsch, J.P. (2007). Kelch repeat protein interacts with the yeast Galpha subunit Gpa2p at a site that couples receptor binding to guanine nucleotide exchange. The Journal of biological chemistry *282*, 24231-24238.

Nobile, C.J., Fox, E.P., Nett, J.E., Sorrells, T.R., Mitrovich, Q.M., Hernday, A.D., Tuch, B.B., Andes, D.R., and Johnson, A.D. (2012). A recently evolved transcriptional network controls biofilm development in *Candida albicans*. Cell *148*, 126-138.

Nobile, C.J., Schneider, H.A., Nett, J.E., Sheppard, D.C., Filler, S.G., Andes, D.R., and Mitchell, A.P. (2008). Complementary adhesin function in *C. albicans* biofilm formation. Current biology : CB *18*, 1017-1024.

Noble, S.M., Gianetti, B.A., and Witchley, J.N. (2017). *Candida albicans* cell-type switching and functional plasticity in the mammalian host. Nature reviews. Microbiology *15*, 96-108.

Nwaka, S., Kopp, M., and Holzer, H. (1995). Expression and function of the trehalase genes *NTH1* and YBR0106 in *Saccharomyces cerevisiae*. The Journal of biological chemistry *270*, 10193-10198.

O'Meara, T.R., Norton, D., Price, M.S., Hay, C., Clements, M.F., Nichols, C.B., and Alspaugh, J.A. (2010). Interaction of *Cryptococcus neoformans* Rim101 and protein kinase A regulates capsule. PLoS pathogens *6*, e1000776.

Okagaki, L.H., Strain, A.K., Nielsen, J.N., Charlier, C., Baltes, N.J., Chrétien, F., Heitman, J., Dromer, F., and Nielsen, K. (2010). Cryptococcal cell morphology affects host cell interactions and pathogenicity. PLoS pathogens *6*, e1000953.

Özcan, S., and Johnston, M. (1999). Function and regulation of yeast hexose transporters. Microbiology and molecular biology reviews : MMBR *63*, 554-569.

Pande, K., Chen, C., and Noble, S.M. (2013). Passage through the mammalian gut triggers a phenotypic switch that promotes *Candida albicans* commensalism. Nature genetics *45*, 1088-1091.

Pankhurst, C.L. (2013). Candidiasis (oropharyngeal). BMJ Clin Evid *2013*, 1304.

Pappas, P.G., Lionakis, M.S., Arendrup, M.C., Ostrosky-Zeichner, L., and Kullberg, B.J. (2018). Invasive candidiasis. Nat Rev Dis Primers *4*, 18026.

Patil, S., Majumdar, B., Sarode, S.C., Sarode, G.S., and Awan, K.H. (2018). Oropharyngeal Candidosis in HIV-Infected Patients-An Update. Front Microbiol *9*, 980.

Paulitsch, A.H., Willinger, B., Zsalatz, B., Stabentheiner, E., Marth, E., and Buzina, W. (2009). *In-vivo Candida* biofilms in scanning electron microscopy. Medical mycology : official publication of the International Society for Human and Animal Mycology *47*, 690-696.

Peeters, K., Van Leemputte, F., Fischer, B., Bonini, B.M., Quezada, H., Tsytlonok, M., Haesen, D., Vanthienen, W., Bernardes, N., Gonzalez-Blas, C.B., Janssens, V., Tompa, P., Versées, W., and Thevelein, J.M. (2017). Fructose-1,6-bisphosphate couples glycolytic flux to activation of Ras. Nat Commun *8*, 922.

Peeters, T., Louwet, W., Geladé, R., Nauwelaers, D., Thevelein, J.M., and Versele, M. (2006). Kelch-repeat proteins interacting with the Galpha protein Gpa2 bypass adenylate cyclase for direct regulation of protein kinase A in yeast. Proceedings of the National Academy of Sciences of the United States of America *103*, 13034-13039.

Peeters, T., Versele, M., and Thevelein, J.M. (2007). Directly from Galpha to protein kinase A: the kelch repeat protein bypass of adenylate cyclase. Trends in biochemical sciences *32*, 547-554.

Peters, B.M., Ovchinnikova, E.S., Krom, B.P., Schlecht, L.M., Zhou, H., Hoyer, L.L., Busscher, H.J., van der Mei, H.C., Jabra-Rizk, M.A., and Shirtliff, M.E. (2012). *Staphylococcus aureus* adherence to *Candida albicans* hyphae is mediated by the hyphal adhesin Als3p. Microbiology (Reading) *158*, 2975-2986.

Peters, B.M., Yano, J., Noverr, M.C., and Fidel, P.L., Jr. (2014). *Candida* vaginitis: when opportunism knocks, the host responds. PLoS pathogens *10*, e1003965.

Pfaller, M.A., Diekema, D.J., Gibbs, D.L., Newell, V.A., Ellis, D., Tullio, V., Rodloff, A., Fu, W., Ling, T.A., and Global Antifungal Surveillance, G. (2010). Results from the ARTEMIS DISK Global Antifungal Surveillance Study, 1997 to 2007: a 10.5-year analysis of susceptibilities of *Candida* Species to fluconazole and voriconazole as determined by CLSI standardized disk diffusion. J Clin Microbiol *48*, 1366-1377.

Pfaller, M.A., Diekema, D.J., Jones, R.N., Messer, S.A., Hollis, R.J., and Group, S.P. (2002). Trends in antifungal susceptibility of Candida spp. isolated from pediatric and adult patients

with bloodstream infections: SENTRY Antimicrobial Surveillance Program, 1997 to 2000. J Clin Microbiol *40*, 852-856.

Poláková, S., Blume, C., Zárate, J.A., Mentel, M., Jørck-Ramberg, D., Stenderup, J., and Piškur, J. (2009). Formation of new chromosomes as a virulence mechanism in yeast *Candida glabrata*. Proceedings of the National Academy of Sciences of the United States of America *106*, 2688-2693.

Polke, M., Hube, B., and Jacobsen, I.D. (2015). *Candida* survival strategies. Adv Appl Microbiol *91*, 139-235.

Popova, Y., Thayumanavan, P., Lonati, E., Agrochao, M., and Thevelein, J.M. (2010). Transport and signaling through the phosphate-binding site of the yeast Pho84 phosphate transceptor. Proceedings of the National Academy of Sciences of the United States of America *107*, 2890-2895.

Pristov, K.E., and Ghannoum, M.A. (2019). Resistance of Candida to azoles and echinocandins worldwide. Clinical microbiology and infection : the official publication of the European Society of Clinical Microbiology and Infectious Diseases *25*, 792-798.

Ramage, G., Martínez, J.P., and López-Ribot, J.L. (2006). *Candida* biofilms on implanted biomaterials: a clinically significant problem. FEMS yeast research *6*, 979-986.

Ramage, G., Mowat, E., Jones, B., Williams, C., and López-Ribot, J. (2009). Our current understanding of fungal biofilms. Critical reviews in microbiology *35*, 340-355.

Reifenberger, E., Boles, E., and Ciriacy, M. (1997). Kinetic characterization of individual hexose transporters of *Saccharomyces cerevisiae* and their relation to the triggering mechanisms of glucose repression. European journal of biochemistry / FEBS *245*, 324-333.

Reifenberger, E., Freidel, K., and Ciriacy, M. (1995). Identification of novel *HXT* genes in *Saccharomyces cerevisiae* reveals the impact of individual hexose transporters on glycolytic flux. Molecular microbiology *16*, 157-167.

Riera, M., Mogensen, E., d'Enfert, C., and Janbon, G. (2012). New regulators of biofilm development in *Candida glabrata*. Research in microbiology *163*, 297-307.

Rigden, D.J., Mello, L.V., and Galperin, M.Y. (2004). The PA14 domain, a conserved all-beta domain in bacterial toxins, enzymes, adhesins and signaling molecules. Trends in biochemical sciences *29*, 335-339.

Robertson, L.S., and Fink, G.R. (1998). The three yeast A kinases have specific signaling functions in pseudohyphal growth. Proceedings of the National Academy of Sciences of the United States of America *95*, 13783-13787.

Rogers, T.R. (2002). Antifungal drug resistance: does it matter? Int J Infect Dis *6 Suppl 1*, S47-53.

Rolland, F., De Winde, J.H., Lemaire, K., Boles, E., Thevelein, J.M., and Winderickx, J. (2000). Glucose-induced cAMP signalling in yeast requires both a G-protein coupled receptor system

for extracellular glucose detection and a separable hexose kinase-dependent sensing process. Molecular microbiology *38*, 348-358.

Rubio-Texeira, M., Van Zeebroeck, G., Voordeckers, K., and Thevelein, J.M. (2010). *Saccharomyces cerevisiae* plasma membrane nutrient sensors and their role in PKA signaling. FEMS yeast research *10*, 134-149.

Ruis, H., and Schüller, C. (1995). Stress signaling in yeast. Bioessays *17*, 959-965.

Ruiz-Herrera, J., Pérez-Rodriguez, F., and Velez-Haro, J. (2020). The signaling mechanisms involved in the dimorphic phenomenon of the Basidiomycota fungus *Ustilago maydis*. International microbiology : the official journal of the Spanish Society for Microbiology *23*, 121-126.

Rupp, S., Summers, E., Lo, H.J., Madhani, H., and Fink, G. (1999). MAP kinase and cAMP filamentation signaling pathways converge on the unusually large promoter of the yeast *FLO11* gene. EMBO J *18*, 1257-1269.

Sanguinetti, M., Posteraro, B., and Lass-Florl, C. (2015). Antifungal drug resistance among *Candida* species: mechanisms and clinical impact. Mycoses *58 Suppl 2*, 2-13.

Santos, M.A., Keith, G., and Tuite, M.F. (1993). Non-standard translational events in *Candida albicans* mediated by an unusual seryl-tRNA with a 5'-CAG-3' (leucine) anticodon. EMBO J *12*, 607-616.

Santos, R., Costa, C., Mil-Homens, D., Romão, D., de Carvalho, C.C., Pais, P., Mira, N.P., Fialho, A.M., and Teixeira, M.C. (2017). The multidrug resistance transporters *Cg*Tpo1_1 and *Cg*Tpo1_2 play a role in virulence and biofilm formation in the human pathogen *Candida glabrata*. Cellular microbiology *19*.

Sass, P., Field, J., Nikawa, J., Toda, T., and Wigler, M. (1986). Cloning and characterization of the high-affinity cAMP phosphodiesterase of *Saccharomyces cerevisiae*. Proceedings of the National Academy of Sciences of the United States of America *83*, 9303-9307.

Schepers, W., Van Zeebroeck, G., Pinkse, M., Verhaert, P., and Thevelein, J.M. (2012). *In vivo* phosphorylation of Ser21 and Ser83 during nutrient-induced activation of the yeast protein kinase A (PKA) target trehalase. The Journal of biological chemistry *287*, 44130-44142.

Schothorst, J., Zeebroeck, G.V., and Thevelein, J.M. (2017). Identification of Ftr1 and Zrt1 as iron and zinc micronutrient transceptors for activation of the PKA pathway in *Saccharomyces cerevisiae*. Microb Cell *4*, 74-89.

Schrevens, S., Van Zeebroeck, G., Riedelberger, M., Tournu, H., Kuchler, K., and Van Dijck, P. (2018). Methionine is required for cAMP-PKA mediated morphogenesis and virulence of *Candida albicans*. Molecular microbiology *109*, 415-416.

Selvaraj, P., Shen, Q., Yang, F., and Naqvi, N.I. (2017). Cpk2, a Catalytic Subunit of Cyclic AMP-PKA, Regulates Growth and Pathogenesis in Rice Blast. Front Microbiol *8*, 2289.

Seneviratne, C.J., Wang, Y., Jin, L., Abiko, Y., and Samaranayake, L.P. (2010). Proteomics of drug resistance in *Candida glabrata* biofilms. Proteomics *10*, 1444-1454.

Shapiro, R.S., Uppuluri, P., Zaas, A.K., Collins, C., Senn, H., Perfect, J.R., Heitman, J., and Cowen, L.E. (2009). Hsp90 orchestrates temperature-dependent *Candida albicans* morphogenesis via Ras1-PKA signaling. Current biology : CB *19*, 621-629.

Shin, D.Y., Matsumoto, K., Iida, H., Uno, I., and Ishikawa, T. (1987). Heat shock response of *Saccharomyces cerevisiae* mutants altered in cyclic AMP-dependent protein phosphorylation. Molecular and cellular biology *7*, 244-250.

Silva, S., Henriques, M., Martins, A., Oliveira, R., Williams, D., and Azeredo, J. (2009). Biofilms of non-*Candida albicans Candida* species: quantification, structure and matrix composition. Medical mycology : official publication of the International Society for Human and Animal Mycology *47*, 681-689.

Skrzypek, M.S., Binkley, J., Binkley, G., Miyasato, S.R., Simison, M., and Sherlock, G. (2017). The *Candida* Genome Database (CGD): incorporation of Assembly 22, systematic identifiers and visualization of high throughput sequencing data. Nucleic acids research *45*, D592-D596.

Smets, B., Ghillebert, R., De Snijder, P., Binda, M., Swinnen, E., De Virgilio, C., and Winderickx, J. (2010). Life in the midst of scarcity: adaptations to nutrient availability in *Saccharomyces cerevisiae*. Current genetics *56*, 1-32.

Smith, A., Ward, M.P., and Garrett, S. (1998). Yeast PKA represses Msn2p/Msn4p-dependent gene expression to regulate growth, stress response and glycogen accumulation. EMBO J *17*, 3556-3564.

Soontorngun, N., Larochelle, M., Drouin, S., Robert, F., and Turcotte, B. (2007). Regulation of gluconeogenesis in *Saccharomyces cerevisiae* is mediated by activator and repressor functions of Rds2. Molecular and cellular biology *27*, 7895-7905.

Staab, J.F., Bradway, S.D., Fidel, P.L., and Sundstrom, P. (1999). Adhesive and mammalian transglutaminase substrate properties of *Candida albicans Hwp1*. Science *283*, 1535-1538.

Steyfkens, F., Zhang, Z., Van Zeebroeck, G., and Thevelein, J.M. (2018). Multiple Transceptors for Macro- and Micro-Nutrients Control Diverse Cellular Properties Through the PKA Pathway in Yeast: A Paradigm for the Rapidly Expanding World of Eukaryotic Nutrient Transceptors Up to Those in Human Cells. Front Pharmacol *9*, 191.

Sudbery, P.E. (2011). Growth of *Candida albicans* hyphae. Nature reviews. Microbiology *9*, 737-748.

Tamaki, H., Miwa, T., Shinozaki, M., Saito, M., Yun, C.W., Yamamoto, K., and Kumagai, H. (2000). *GPR1* regulates filamentous growth through *FLO11* in yeast *Saccharomyces cerevisiae*. Biochemical and biophysical research communications *267*, 164-168.

Tao, L., Du, H., Guan, G., Dai, Y., Nobile, C.J., Liang, W., Cao, C., Zhang, Q., Zhong, J., and Huang, G. (2014). Discovery of a "white-gray-opaque" tristable phenotypic switching system in *Candida albicans*: roles of non-genetic diversity in host adaptation. PLoS Biol *12*, e1001830.

Tati, S., Davidow, P., McCall, A., Hwang-Wong, E., Rojas, I.G., Cormack, B., and Edgerton, M. (2016). *Candida glabrata* Binding to *Candida albicans* Hyphae Enables Its Development in Oropharyngeal Candidiasis. PLoS pathogens *12*, e1005522.

Thevelein, J.M. (1984). Regulation of trehalose mobilization in fungi. Microbiol Rev *48*, 42-59.

Thevelein, J.M. (1994). Signal transduction in yeast. Yeast *10*, 1753-1790.

Thierry, A., Bouchier, C., Dujon, B., and Richard, G.F. (2008). Megasatellites: a peculiar class of giant minisatellites in genes involved in cell adhesion and pathogenicity in *Candida glabrata*. Nucleic acids research *36*, 5970-5982.

Thierry, A., Dujon, B., and Richard, G.F. (2010). Megasatellites: a new class of large tandem repeats discovered in the pathogenic yeast *Candida glabrata*. Cell Mol Life Sci *67*, 671-676.

Timmermans, B., De Las Peñas, A., Castaño, I., and Van Dijck, P. (2018). Adhesins in *Candida glabrata*. J Fungi (Basel) *4*.

Toda, M., Williams, S.R., Berkow, E.L., Farley, M.M., Harrison, L.H., Bonner, L., Marceaux, K.M., Hollick, R., Zhang, A.Y., Schaffner, W., Lockhart, S.R., Jackson, B.R., and Vallabhaneni, S. (2019). Population-Based Active Surveillance for Culture-Confirmed Candidemia - Four Sites, United States, 2012-2016. MMWR Surveill Summ *68*, 1-15.

Toda, T., Cameron, S., Sass, P., Zoller, M., Scott, J.D., McMullen, B., Hurwitz, M., Krebs, E.G., and Wigler, M. (1987a). Cloning and characterization of *BCY1*, a locus encoding a regulatory subunit of the cyclic AMP-dependent protein kinase in *Saccharomyces cerevisiae*. Molecular and cellular biology *7*, 1371-1377.

Toda, T., Cameron, S., Sass, P., Zoller, M., and Wigler, M. (1987b). Three different genes in *S. cerevisiae* encode the catalytic subunits of the cAMP-dependent protein kinase. Cell *50*, 277-287.

Turner, S.A., and Butler, G. (2014). The *Candida* pathogenic species complex. Cold Spring Harbor perspectives in medicine *4*, a019778.

Underhill, D.M., and Iliev, I.D. (2014). The mycobiota: interactions between commensal fungi and the host immune system. Nat Rev Immunol *14*, 405-416.

Vale-Silva, L., Beaudoing, E., Tran, V.D.T., and Sanglard, D. (2017). Comparative Genomics of Two Sequential *Candida glabrata* Clinical Isolates. G3 (Bethesda) *7*, 2413-2426.

Vale-Silva, L., Ischer, F., Leibundgut-Landmann, S., and Sanglard, D. (2013). Gain-of-function mutations in *PDR1*, a regulator of antifungal drug resistance in *Candida glabrata*, control adherence to host cells. Infection and immunity *81*, 1709-1720.

Vale-Silva, L.A., Moeckli, B., Torelli, R., Posteraro, B., Sanguinetti, M., and Sanglard, D. (2016). Upregulation of the Adhesin Gene *EPA1* Mediated by *PDR1* in *Candida glabrata* Leads to Enhanced Host Colonization. mSphere *1*.

Valotteau, C., Prystopiuk, V., Cormack, B.P., and Dufrêne, Y.F. (2019). Atomic Force Microscopy Demonstrates that *Candida glabrata* Uses Three Epa Proteins To Mediate Adhesion to Abiotic Surfaces. mSphere *4*.

van Aelst, L., Jans, A.W., and Thevelein, J.M. (1991). Involvement of the *CDC25* gene product in the signal transmission pathway of the glucose-induced *RAS*-mediated cAMP signal in the yeast *Saccharomyces cerevisiae*. Journal of general microbiology *137*, 341-349.

Van de Velde, S., and Thevelein, J.M. (2008). Cyclic AMP-protein kinase A and Snf1 signaling mechanisms underlie the superior potency of sucrose for induction of filamentation in *Saccharomyces cerevisiae*. Eukaryotic cell *7*, 286-293.

Van Ende, M., Wijnants, S., and Van Dijck, P. (2019). Sugar Sensing and Signaling in *Candida albicans* and *Candida glabrata*. Front Microbiol *10*, 99.

Van Nuland, A., Vandormael, P., Donaton, M., Alenquer, M., Lourenço, A., Quintino, E., Versele, M., and Thevelein, J.M. (2006). Ammonium permease-based sensing mechanism for rapid ammonium activation of the protein kinase A pathway in yeast. Molecular microbiology *59*, 1485-1505.

Van Zeebroeck, G., Bonini, B.M., Versele, M., and Thevelein, J.M. (2009). Transport and signaling via the amino acid binding site of the yeast Gap1 amino acid transceptor. Nat Chem Biol *5*, 45-52.

Van Zeebroeck, G., Demuyser, L., Zhang, Z., Cottignie, I., and Thevelein, J.M. (2020). Nutrient sensing and cAMP signaling in yeast: G-protein coupled receptor versus transceptor activation of PKA. Microb Cell *8*, 17-27.

Vandamme, J., Castermans, D., and Thevelein, J.M. (2012). Molecular mechanisms of feedback inhibition of protein kinase A on intracellular cAMP accumulation. Cell Signal *24*, 1610-1618.

Versele, M., de Winde, J.H., and Thevelein, J.M. (1999). A novel regulator of G protein signalling in yeast, Rgs2, downregulates glucose-activation of the cAMP pathway through direct inhibition of Gpa2. EMBO J *18*, 5577-5591.

Verstrepen, K.J., Jansen, A., Lewitter, F., and Fink, G.R. (2005). Intragenic tandem repeats generate functional variability. Nature genetics *37*, 986-990.

Vertes, A., Hitchins, V., and Phillips, K.S. (2012). Analytical challenges of microbial biofilms on medical devices. Anal Chem *84*, 3858-3866.

Walker, L.A., Gow, N.A., and Munro, C.A. (2010). Fungal echinocandin resistance. Fungal genetics and biology : FG & B *47*, 117-126.

Weig, M., Jänsch, L., Gross, U., De Koster, C.G., Klis, F.M., and De Groot, P.W. (2004). Systematic identification in silico of covalently bound cell wall proteins and analysis of protein-polysaccharide linkages of the human pathogen *Candida glabrata*. Microbiology *150*, 3129-3144.

Whaley, S.G., Berkow, E.L., Rybak, J.M., Nishimoto, A.T., Barker, K.S., and Rogers, P.D. (2016). Azole Antifungal Resistance in *Candida albicans* and Emerging Non-albicans *Candida* Species. Front Microbiol *7*, 2173.

White, T.C., Marr, K.A., and Bowden, R.A. (1998). Clinical, cellular, and molecular factors that contribute to antifungal drug resistance. Clin Microbiol Rev *11*, 382-402.

Winderickx, J., de Winde, J.H., Crauwels, M., Hino, A., Hohmann, S., Van Dijck, P., and Thevelein, J.M. (1996). Regulation of genes encoding subunits of the trehalose synthase complex in *Saccharomyces cerevisiae*: novel variations of STRE-mediated transcription control? Molecular & general genetics : MGG *252*, 470-482.

Xu, Z., Green, B., Benoit, N., Schatz, M., Wheelan, S., and Cormack, B. (2020). De novo genome assembly of *Candida glabrata* reveals cell wall protein complement and structure of dispersed tandem repeat arrays. Molecular microbiology *113*, 1209-1224.

Xue, C., Bahn, Y.S., Cox, G.M., and Heitman, J. (2006). G protein-coupled receptor Gpr4 senses amino acids and activates the cAMP-PKA pathway in *Cryptococcus neoformans*. Molecular biology of the cell *17*, 667-679.

Xue, Y., Batlle, M., and Hirsch, J.P. (1998). *GPR1* encodes a putative G protein-coupled receptor that associates with the Gpa2p Galpha subunit and functions in a Ras-independent pathway. EMBO J *17*, 1996-2007.

Yang, K., Qin, Q., Liu, Y., Zhang, L., Liang, L., Lan, H., Chen, C., You, Y., Zhang, F., and Wang, S. (2016). Adenylate Cyclase AcyA Regulates Development, Aflatoxin Biosynthesis and Fungal Virulence in *Aspergillus flavus*. Front Cell Infect Microbiol *6*, 190.

Yano, J., Yu, A., Fidel, P.L., Jr., and Noverr, M.C. (2019). *Candida glabrata* Has No Enhancing Role in the Pathogenesis of *Candida*-Associated Denture Stomatitis in a Rat Model. mSphere *4*.

Zajac, D., Karkowska-Kuleta, J., Bochenska, O., Rapala-Kozik, M., and Kozik, A. (2016). Interaction of human fibronectin with *Candida glabrata* epithelial adhesin 6 (Epa6). Acta Biochim Pol *63*, 417-426.

Zaragoza, O., García-Rodas, R., Nosanchuk, J.D., Cuenca-Estrella, M., Rodríguez-Tudela, J.L., and Casadevall, A. (2010). Fungal cell gigantism during mammalian infection. PLoS pathogens *6*, e1000945.

Zeller, C.E., Parnell, S.C., and Dohlman, H.G. (2007). The RACK1 ortholog Asc1 functions as a G-protein beta subunit coupled to glucose responsiveness in yeast. The Journal of biological chemistry *282*, 25168-25176.

Zhang, Q., Tao, L., Guan, G., Yue, H., Liang, W., Cao, C., Dai, Y., and Huang, G. (2016). Regulation of filamentation in the human fungal pathogen *Candida tropicalis*. Molecular microbiology *99*, 528-545.

Zhao, W., Panepinto, J.C., Fortwendel, J.R., Fox, L., Oliver, B.G., Askew, D.S., and Rhodes, J.C. (2006). Deletion of the regulatory subunit of protein kinase A in *Aspergillus fumigatus* alters morphology, sensitivity to oxidative damage, and virulence. Infection and immunity *74*, 4865-4874.

Zheng, Q., Zhang, Q., Bing, J., Ding, X., and Huang, G. (2017). Environmental and genetic regulation of white-opaque switching in *Candida tropicalis*. Molecular microbiology *106*, 999-1017.

Zupancic, M.L., Frieman, M., Smith, D., Alvarez, R.A., Cummings, R.D., and Cormack, B.P. (2008). Glycan microarray analysis of *Candida glabrata* adhesin ligand specificity. Molecular microbiology *68*, 547-559.

Addendum 1: List of primers used in Chapter 2

Primer	Name	Sequence	used for
6973	p*CgACT1* Fw	GCAAGGCGATTAAGTTGGG	control primer in p*CgACT1*
8843	*TPK2* control upstream Fw	CGAGAATTGTCACTTTCACAC	Control primer
8844	*TPK2* control downstream Rv	CAACCTAGTCTCACTAAAGG	Control primer
8845	*TPK1* control upstream Fw	CCTCCATCATATCTGTCGTG	Control primer
8846	*TPK1* control downstream Rv	CCGATATGATTTGCGATTCTGG	Control primer
8863	*TPK2* upstream Fw	GATGTAGACACAAATGCTACCG	Construction deletion strain
8864	*TPK2* upstream Rv	CACGGCGCGCCTAGCAGCGGCATTGCATACAATCTTCTCCGC	Construction deletion strain
8865	*TPK2* downstream Fw	GTCAGCGGCCGCATCCCTGCTAGTAAACACTTTCAAATTGTTTTGG	Construction deletion strain
8866	*TPK2* downstream Rv	GACAAGTATGTTGATCTATCAACC	Construction deletion strain
8867	*TPK1* upstream Fw	GATTGGTAGCAGATAAATTGTGAATAG	Construction deletion strain
8868	*TPK1* upstream Rv	CACGGCGCGCCTAGCAGCGGCATCTGCTGTTGTTGTTCCG	Construction deletion strain
8869	*TPK1* downstream Fw	GTCAGCGGCCGCATCCCTGCTAAAATATTGCCACACATACTCGC	Construction deletion strain
8870	*TPK1* downstream Rv	CTGAAATGTTAGTGACAACCGC	Construction deletion strain
9064	NatMX Rv	CGTCAAGACTGTCAAGGAGGG	control primer inside deletion cassette
9065	NatMX Fw	CATCATCTGCCCAGATGCGAAG	control primer inside deletion cassette
9351	*TEF*p Fw	CCGCTGCTAGGCGCGCCGTGAGCTTGCCTCGTCCCCGC	amplification marker
9356	*TEF*t Rv	GCAGGGATGCGGCCGCTGACCTGGATGGCGGCGTTAGTATCG	amplification marker
A2265	Gpr1-ORF Fw	CATCTAACCATGATGATGACG	control primer in Gpr1 ORF
A2524	Gpr1-Q579C Fw	GCTGACTGTTTATGTTATAACTACGAGGAG	introduction mutation Gpr1 Q579C
A2525	Gpr1-Q579C Rv	CTCCTCGTAGTTATAACATAAACAGTCAGC	introduction mutation Gpr1 Q579C

A2532	Gpr1-A575C Fw	GTTTTCCCTATTATTTGTGACTGTTTACAGTATAAC	introduction mutation Gpr1 A575C
A2533	Gpr1-A575C Rv	GTTATACTGTAAACAGTCACAAATAATAGGGAAAAC	introduction mutation Gpr1 A575C
A2668	Gpr1-P572C Fw	GCGCTTTGGGTTTTCTGTATTATTGCTGACTG	introduction mutation Gpr1 P572C
A2669	Gpr1-P572C Rv	CAGTCAGCAATAATACAGAAAACCCAAAGCGC	introduction mutation Gpr1 P572C
A2674	Gpr1-D576C Fw	GTTTTCCCTATTATTGCTTGCTGTTTACAGTATAACTACG	introduction mutation Gpr1 D576C
A2675	Gpr1-D576C Rv	CGTAGTTATACTGTAAACAGCAAGCAATAATAGGGAAAAC	introduction mutation Gpr1 D576C
A4486	p*CgACT1* Rv	AGCGGATAACAATTTCACACAGG	control primer in p*CgACT1*
B3007	pGpa2 Fw BamHI	CGGGATCCGTGTAGGGAGAAAGAGCTATC	Construction vector p*CgACT1-GPA2*
B3008	tGpa2 Rv BamHI	CGGGATCCATGGCAAATTCGTTGTTCGAG	Construction vector p*CgACT1-GPA2*
B3009	ORF Gpa2-Q299L Rv	TCCATTTCTTACGCTCTGATCTCAATCCACCCACATCATAGATGTG	introduction mutation Gpa2 Q299L
B3010	ORF Gpa2-Q299L Fw	TGGATTGAGATCAGAGCGTAAGAAATGGA	introduction mutation Gpa2 Q299L
B3074	Gpr1-ORF Rv	CTGGTTCCATCAAGGAGC	control primer in Gpr1 ORF
B4165	p*CgACT1* Fw	GTAAAACGACGGCCAGTG	control primer in p*CgACT1*
B4166	p*CgACT1* Rv	GGAAACAGCTATGACCATG	control primer in p*CgACT1*
B6103	p*GPR1* Fw	ACGACGTTGTAAAACGACGGCCAGTCTCACAGCACAAGAAGTTCAACAAG	Construction vector p*CgACT1*-GPR1
B6279	t*GPR1* Rv	TATGACCATGATTACGCCAAGCTTGGTTGCCTTATTCACTCCTGCAATCC	Construction vector p*CgACT1*-GPR1

Addendum 2: Overview of *C. glabrata* adhesins or adhesin-like genes described in literature (strikethrough: previously annotated adhesins which are removed by the recent *de novo* gene assembly by Xu *et al.*, (2018).

Gene ID	Gene Name or Alias	Reference(s)	Description CGD
CAGL0A00099g	***EPA19***	**Xu et al., 2020 (Molecular microbiology)**	**new predicted adhesin like gene**
~~CAGL0A00105g~~	~~CAGL0A00110g.1~~	~~CAGL0A00110g: Family I, de Groot et al., 2008 (Eukaryotic cell); split into 2 ORFs: Linde et al., 2015 (Nucleic Acids Research)~~	~~Protein of unknown function~~
~~CAGL0A00116g~~	~~CAGL0A00110g.2~~	~~CAGL0A00110g: Family I, de Groot et al., 2008 (Eukaryotic cell); split into 2 ORFs: Linde et al., 2015 (Nucleic Acids Research)~~	~~Protein of unknown function~~
CAGL0A01284g	*EPA10*	Family I, de Groot et al., 2008 (Eukaryotic cell)	Putative adhesin-like protein; belongs to adhesin cluster I
CAGL0A01366g	*EPA9*	Family I, de Groot et al., 2008 (Eukaryotic cell)	Putative adhesin; belongs to adhesin cluster I
CAGL0A01584g		Candida Genome Database	Ortholog(s) have cell adhesion molecule binding activity, role in agglutination involved in conjugation with cellular fusion and fungal-type cell wall localization
CAGL0A04851g		**Xu et al., 2020 (Molecular microbiology)**	**new predicted adhesin like gene**
~~CAGL0A04873g~~		~~Family III, de Groot et al., 2008 (Eukaryotic cell)~~	~~Protein with tandem repeats; putative adhesin-like protein; belongs to adhesin cluster III~~
~~CAGL0B00105g~~	~~CAGL0B00110g.1~~	~~CAGL0B00110g: Family V, de Groot et al., 2008 (Eukaryotic cell); split into 2 ORFs: Linde et al., 2015 (Nucleic Acids Research)~~	~~Protein of unknown function~~
~~CAGL0B00116g~~	~~CAGL0B00110g.2~~	~~CAGL0B00110g: Family V, de Groot et al., 2008 (Eukaryotic cell); split into 2 ORFs: Linde et al., 2015 (Nucleic Acids Research)~~	~~Protein of unknown function~~

CAGL0B00154g		**Xu et al., 2020 (Molecular microbiology)**	**new predicted adhesin like gene**
CAGL0B05061g		**Xu et al., 2020 (Molecular microbiology)**	**new predicted adhesin like gene**
~~CAGL0B05093g~~	~~*AWP9*~~	~~Family V, de Groot et al., 2008 (Eukaryotic cell)~~	~~Putative adhesin-like protein; GPI-anchored; belongs to adhesin cluster V; ORF appears artificially broken into fragments due to sequencing errors but the gene is likely protein-coding based on mass spectrometry data~~
~~CAGL0B05126g~~	~~CAGL0B05093g.1~~	~~Family Awp9: Gomez-Molero et al., 2015 (FEMS); split into 3 ORFs: Linde et al., 2015 (Nucleic Acids Research)~~	~~Protein of unknown function~~
~~CAGL0B05137g~~	~~CAGL0B05093g.3~~	~~Family Awp9: Gomez-Molero et al., 2015 (FEMS); split into 3 ORFs: Linde et al., 2015 (Nucleic Acids Research)~~	~~Protein of unknown function~~
~~CAGL0B05148g~~	~~CAGL0B05093g.2~~	~~Family Awp9: Gomez-Molero et al., 2015 (FEMS); split into 3 ORFs: Linde et al., 2015 (Nucleic Acids Research)~~	~~Protein of unknown function~~
CAGL0C00110g	*EPA6*	Family I, de Groot et al., 2008 (Eukaryotic cell)	Sub-telomerically encoded adhesin with a role in cell adhesion; binds to ligands containing a terminal galactose residue; expressed during murine urinary tract infection, biofilm-upregulated; belongs to adhesin cluster I
CAGL0C00209g	*AWP7*	Family IV, de Groot et al., 2008 (Eukaryotic cell)	Putative adhesin-like cell wall protein; belongs to adhesin cluster IV; predicted GPI-anchor
CAGL0C00253g		Family III, de Groot et al., 2008 (Eukaryotic cell)	Putative cell wall adhesin; belongs to adhesin cluster III; predicted GPI anchor; contains 6 tandem repeats
CAGL0C00825g		**Xu et al., 2020 (Molecular microbiology)**	**new predicted adhesin like gene**
CAGL0C00847g	*EPA8*	Family I, de Groot et al., 2008 (Eukaryotic cell)	Putative adhesin-like protein; belongs to adhesin cluster I
CAGL0C00858g		**Xu et al., 2020 (Molecular microbiology)**	**new predicted adhesin like gene**

CAGL0C00968g		Family VII, de Groot et al., 2008 (Eukaryotic cell)	Adhesin-like protein with a predicted role in cell adhesion; belongs to adhesin cluster VII; predicted GPI-anchor
~~CAGL0C01056g~~	~~CAGL0C01067g.1~~	~~CAGL0C01067g: Family VII, de Groot et al., 2008 (Eukaryotic cell); split into 2 ORFs: Linde et al., 2015 (Nucleic Acids Research)~~	~~Protein of unknown function~~
~~CAGL0C01078g~~	~~CAGL0C01067g.2~~	~~CAGL0C01067g: Family VII, de Groot et al., 2008 (Eukaryotic cell); split into 2 ORFs: Linde et al., 2015 (Nucleic Acids Research)~~	~~Protein of unknown function~~
CAGL0C01133g		Family VII, de Groot et al., 2008 (Eukaryotic cell)	Adhesin-like protein; belongs to adhesin cluster VII; predicted GPI anchor
CAGL0C03575g		Weig et al., 2004 (Microbiology)	Predicted GPI-linked protein; putative adhesin-like protein
CAGL0C03872g	*TIR3*	Weig et al., 2004 (Microbiology)	Putative GPI-linked cell wall protein involved in sterol uptake
CAGL0C05643g	*EPA7*	Family I, de Groot et al., 2008 (Eukaryotic cell)	Adhesin-like protein with a predicted GPI-anchor; belongs to adhesin cluster I; strain BG14 encodes the full-length protein, whereas CBS138 contains a stop codon that terminates the ORF at codon 379
~~CAGL0D00105g~~	~~CAGL0D00110g.2~~	~~CAGL0D00110g: Family V, de Groot et al., 2008 (Eukaryotic cell); split into 2 ORFs: Linde et al., 2015 (Nucleic Acids Research)~~	~~Protein of unknown function~~
~~CAGL0D00116g~~	~~CAGL0D00110g.1~~	~~CAGL0D00110g: Family V, de Groot et al., 2008 (Eukaryotic cell); split into 2 ORFs: Linde et al., 2015 (Nucleic Acids Research)~~	~~Protein of unknown function~~
CAGL0D00143g		**Xu et al., 2020 (Molecular microbiology)**	**new predicted adhesin like gene**
CAGL0D06226g		Chaudhuri et al., 2011 (BMC Genomics)	Putative adhesin-like protein

CAGL0D06732g	*EPA21*	Family I, de Groot et al., 2008 (Eukaryotic cell)	Pseudogene with a predicted GPI-anchor sequence; putative adhesin-like protein; belongs to adhesin cluster I
~~CAGL0E00105g~~	~~CAGL0E00110g.1~~	~~CAGL0E00110g: Family III, de Groot et al., 2008 (Eukaryotic cell); split into 3 ORFs: Linde et al., 2015 (Nucleic Acids Research)~~	~~Protein of unknown function~~
~~CAGL0E00116g~~	~~CAGL0E00110g.3~~	~~CAGL0E00110g: Family III, de Groot et al., 2008 (Eukaryotic cell); split into 3 ORFs: Linde et al., 2015 (Nucleic Acids Research)~~	~~Protein of unknown function~~
~~CAGL0E00132g~~	~~CAGL0E00110g.2~~	~~CAGL0E00110g: Family III, de Groot et al., 2008 (Eukaryotic cell); split into 3 ORFs: Linde et al., 2015 (Nucleic Acids Research)~~	~~Protein of unknown function~~
CAGL0E00165g		**Xu et al., 2020 (Molecular microbiology)**	**new predicted adhesin like gene**
CAGL0E00187g		Family IV, de Groot et al., 2008 (Eukaryotic cell)	Putative adhesin-like protein; belongs to adhesin cluster IV
CAGL0E00231g		Family III, de Groot et al., 2008 (Eukaryotic cell)	Putative adhesin-like protein; contains tandem repeats and a predicted GPI-anchor; belongs to adhesin cluster III
CAGL0E00275g	*EPA20*	Family I, de Groot et al., 2008 (Eukaryotic cell)	Putative adhesin; belongs to adhesin cluster I
CAGL0E01661g		Family III, de Groot et al., 2008 (Eukaryotic cell)	Adhesin-like protein with tandem repeats; predicted GPI-anchor; belongs to adhesin cluster III
CAGL0E02915g		Chaudhuri et al., 2011 (BMC Genomics)	Putative adhesin-like protein
CAGL0E06600g		Family V, de Groot et al., 2008 (Eukaryotic cell)	Putative adhesin-like protein; belongs to adhesin cluster V

CAGL0E06644g	*EPA1*	Family I, de Groot et al., 2008 (Eukaryotic cell)	Sub-telomerically encoded adhesin with a role in cell adhesion; GPI-anchored cell wall protein; N-terminal ligand binding domain binds to ligands containing a terminal galactose residue; belongs to adhesin cluster I
CAGL0E06666g	*EPA2*	Family I, de Groot et al., 2008 (Eukaryotic cell)	Epithelial adhesion protein; predicted GPI-anchor; belongs to adhesin cluster I
CAGL0E06688g	*EPA3*	Family I, de Groot et al., 2008 (Eukaryotic cell)	Epithelial adhesion protein; belongs to adhesin cluster I; GPI-anchored
~~CAGL0F00105g~~	~~CAGL0F00110g.2~~	~~CAGL0F00110g: Family V, de Groot et al., 2008 (Eukaryotic cell); split into 2 ORFs: Linde et al., 2015 (Nucleic Acids Research)~~	~~Protein of unknown function~~
~~CAGL0F00116g~~	~~CAGL0F00110g.1~~	~~CAGL0F00110g: Family V, de Groot et al., 2008 (Eukaryotic cell); split into 2 ORFs: Linde et al., 2015 (Nucleic Acids Research)~~	~~Protein of unknown function~~
CAGL0F01463g	*TIR1*	nonenzymatic CWPs, de Groot et al., 2008 (Eukaryotic cell)	Putative GPI-linked cell wall mannoprotein of the Srp1p/Tip1p family
CAGL0F01485g	*TIR2*	Kraneveld et al., 2011 (Mycopathologia); Weig et al., 2004 (Microbiology)	Putative GPI-linked cell wall mannoprotein of the Srp1p/Tip1p family
CAGL0F00077g	***EPA16***	**Xu et al., 2020 (Molecular microbiology)**	**new predicted adhesin like gene**
CAGL0F00099g		**Xu et al., 2020 (Molecular microbiology)**	**new predicted adhesin like gene**
CAGL0F07579g	*CWP1.2*	nonenzymatic CWPs, de Groot et al., 2008 (Eukaryotic cell)	Putative GPI-linked cell wall protein
CAGL0F07601g	*CWP1.1*	nonenzymatic CWPs, de Groot et al., 2008 (Eukaryotic cell)	GPI-linked cell wall protein
CAGL0F08833g		Chaudhuri et al., 2011 (BMC Genomics)	Putative adhesin-like protein
CAGL0F09251g		**Xu et al., 2020 (Molecular microbiology)**	**new predicted adhesin like gene**

~~CAGL0F09273g~~		~~Family V, de Groot et al., 2008 (Eukaryotic cell)~~	~~Putative adhesin-like protein; belongs to adhesin cluster V~~
CAGL0G00099g		**Xu et al., 2020 (Molecular microbiology)**	**new predicted adhesin like gene**
~~CAGL0G00105g~~	~~CAGL0G00110g.2~~	~~CAGL0G00110g: Family III, de Groot et al., 2008 (Eukaryotic cell); split into 2 ORFs: Linde et al., 2015 (Nucleic Acids Research)~~	~~Protein of unknown function~~
~~CAGL0G00121g~~	~~CAGL0G00110g.1~~	~~CAGL0G00110g: Family III, de Groot et al., 2008 (Eukaryotic cell); split into 2 ORFs: Linde et al., 2015 (Nucleic Acids Research)~~	~~Protein of unknown function~~
CAGL0G04125g		Weig et al., 2004 (Microbiology)	Protein with similarity to S. cerevisiae Sag1 agglutinin, involved in cell adhesion; predicted GPI-anchor
CAGL0G05808g		Chaudhuri et al., 2011 (BMC Genomics)	Putative adhesin-like protein
CAGL0G05896g		Chaudhuri et al., 2011 (BMC Genomics)	Putative adhesin-like protein
CAGL0G09537g		Chaudhuri et al., 2011 (BMC Genomics)	Putative adhesin-like protein
CAGL0G09559g		Candida Genome Database	Ortholog(s) have role in adhesion of symbiont to host, cell adhesion, establishment of cell polarity, regulation of transcription, DNA-templated and cellular bud neck, cellular bud tip, mitochondrion, plasma membrane localization
CAGL0G10175g	*AWP6*	Family IV, de Groot et al., 2008 (Eukaryotic cell)	Adhesin-like protein; identified in cell wall extracts by mass spectrometry; belongs to adhesin cluster IV; predicted GPI anchor
CAGL0G10219g	*AWP12*	Family VII, de Groot et al., 2008 (Eukaryotic cell)	Adhesin-like protein with 5 tandem repeats; belongs to adhesin cluster VII; predicted GPI-anchor; similarity to S. cerevisiae flocculins, cell wall proteins that mediate adhesion

~~CAGL0H00110g~~		~~de Groot et al., 2008 (Eukaryotic cell)~~	~~Adhesin-like protein with internal repeats; predicted GPI-anchor; likely a C-terminal fragment of a single ORF with CAGL0H00132g; belongs to adhesin cluster V~~
~~CAGL0H00121g~~	~~CAGL0H00132g.1~~	~~CAGL0H00132g: Family V, de Groot et al., 2008 (Eukaryotic cell); split into 2 ORFs: Linde et al., 2015 (Nucleic Acids Research)~~	~~Protein of unknown function~~
~~CAGL0H00143g~~	~~CAGL0H00132g.2~~	~~CAGL0H00132g: Family V, de Groot et al., 2008 (Eukaryotic cell); split into 2 ORFs: Linde et al., 2015 (Nucleic Acids Research)~~	~~Protein of unknown function~~
CAGL0H00209g		**Xu et al., 2020 (Molecular microbiology)**	**new predicted adhesin like gene**
CAGL0H06413g	*SSR1*	nonenzymatic CWPs, de Groot et al., 2008 (Eukaryotic cell)	Putative GPI-linked cell wall protein
CAGL0H07469g		Chaudhuri et al., 2011 (BMC Genomics)	Putative adhesin-like protein
CAGL0H08844g		Chaudhuri et al., 2011 (BMC Genomics)	Putative adhesin-like protein
CAGL0H10626g	*AWP13*	Family III, de Groot et al., 2008 (Eukaryotic cell)	Predicted cell wall adhesin with a role in adhesion; belongs to adhesin cluster III; predicted GPI anchor; contains tandem repeats
CAGL0I00209g		**Xu et al., 2020 (Molecular microbiology)**	**new predicted adhesin like gene**
~~CAGL0I00105g~~	~~CAGL0I00110g.1~~	~~CAGL0I00110g: Family III, de Groot et al., 2008 (Eukaryotic cell); split into 4 ORFs: Linde et al., 2015 (Nucleic Acids Research)~~	~~Protein of unknown function~~
~~CAGL0I00116g~~	~~CAGL0I00110g.3~~	~~CAGL0I00110g: Family III, de Groot et al., 2008 (Eukaryotic cell); split into 4 ORFs: Linde et al., 2015 (Nucleic Acids Research)~~	~~Protein of unknown function~~

~~CAGL0I00121g~~	~~CAGL0I00110g.4~~	~~CAGL0I00110g: Family III, de Groot et al., 2008 (Eukaryotic cell); split into 4 ORFs: Linde et al., 2015 (Nucleic Acids Research)~~	~~Protein of unknown function~~
~~CAGL0I00143g~~	~~CAGL0I00110g.2~~	~~CAGL0I00110g: Family III, de Groot et al., 2008 (Eukaryotic cell); split into 4 ORFs: Linde et al., 2015 (Nucleic Acids Research)~~	~~Protein of unknown function~~
CAGL0I00220g	*EPA23*	Family I, de Groot et al., 2008 (Eukaryotic cell)	Predicted GPI-linked adhesin-like protein; belongs to adhesin cluster I
CAGL0I06160g	*PIR4*	nonenzymatic CWPs, de Groot et al., 2008 (Eukaryotic cell)	Pir protein family member, putative cell wall component
CAGL0I06182g	*PIR2*	nonenzymatic CWPs, de Groot et al., 2008 (Eukaryotic cell)	Pir protein family member, putative cell wall component
CAGL0I06204g	*PIR1*	nonenzymatic CWPs, de Groot et al., 2008 (Eukaryotic cell)	Pir protein family member, putative cell wall component
CAGL0I07293g		Family V, de Groot et al., 2008 (Eukaryotic cell)	Adhesin-like cell wall protein; predicted GPI-anchor; belongs to adhesin cluster V
CAGL0I10098g	*PWP7*	Family II, de Groot et al., 2008 (Eukaryotic cell)	Cell wall protein that mediates adhesion to endothelial cells; predicted GPI anchor and signal peptide; contains multiple tandem repeats; expressed in stationary growth phase; belongs to adhesin cluster II
CAGL0I10147g	*PWP1*; CAGL0I10197g	Family II, de Groot et al., 2008 (Eukaryotic cell)	Protein with 32 tandem repeats; putative adhesin-like protein; belongs to adhesin cluster II
CAGL0I10200g	*PWP3*; CAGL0I10219g	Family II, de Groot et al., 2008 (Eukaryotic cell)	Protein with tandem repeats; putative adhesin-like protein; belongs to adhesin cluster II
~~CAGL0I10211g~~	~~*NP25*~~	~~Linde et al., 2015 (Nucleic Acids Research)~~	~~Protein of unknown function~~
CAGL0I10246g	*PWP2*; CAGL0I10274g	Family II, de Groot et al., 2008 (Eukaryotic cell)	Adhesin-like protein with tandem repeats; contains a PA14 domain; belongs to adhesin cluster II

CAGL0I10340g	*PWP5*	Family II, de Groot et al., 2008 (Eukaryotic cell)	Cell wall adhesin; predicted GPI anchor; contains tandem repeats; belongs to adhesin cluster II
CAGL0I10362g	*PWP4*	Family II, de Groot et al., 2008 (Eukaryotic cell)	Cell wall adhesin; predicted GPI anchor; contains tandem repeats; belongs to adhesin cluster II
CAGL0I11000g		**Xu et al., 2020 (Molecular microbiology)**	**new predicted adhesin like gene**
~~CAGL0I11011g~~		~~Family V, de Groot et al., 2008 (Eukaryotic cell)~~	~~Putative adhesin; belongs to adhesin cluster V~~
~~CAGL0J00105g~~	~~CAGL0J00110g.2~~	~~CAGL0J00110g: Family III, de Groot et al., 2008 (Eukaryotic cell); split into 2 ORFs: Linde et al., 2015 (Nucleic Acids Research)~~	~~Protein of unknown function~~
~~CAGL0J00110g~~		~~Candida Genome Database~~	~~Putative adhesin-like protein; ORF appears artificially broken into fragments due to sequencing errors; belongs to adhesin cluster III~~
~~CAGL0J00116g~~	~~CAGL0J00110g.1~~	~~CAGL0J00110g: Family III, de Groot et al., 2008 (Eukaryotic cell); split into 2 ORFs: Linde et al., 2015 (Nucleic Acids Research)~~	~~Protein of unknown function~~
CAGL0J00253g		Chaudhuri et al., 2011 (BMC Genomics)	Putative adhesin-like protein
CAGL0I11000g		**Xu et al., 2020 (Molecular microbiology)**	**new predicted adhesin like gene**
CAGL0J00132g		**Xu et al., 2020 (Molecular microbiology)**	**new predicted adhesin like gene**
CAGL0J01463g	*CWP1.3*	Weig et al., 2004 (Microbiology)	Putative GPI-linked cell wall protein
CAGL0J01727g		Family VI, de Groot et al., 2008 (Eukaryotic cell)	Putative adhesion protein; predicted GPI-anchor; belongs to adhesin cluster VI
CAGL0J01774g		Family VI, de Groot et al., 2008 (Eukaryotic cell)	Putative adhesin-like protein; has glycine and serine rich repeats; belongs to adhesin cluster VI
CAGL0J01800g		Family VI, de Groot et al., 2008 (Eukaryotic cell)	Putative adhesin-like protein; belongs to adhesin cluster VI

CAGL0J02508g	*AWP1*	Family VI, de Groot et al., 2008 (Eukaryotic cell)	Adhesin-like protein; identified in cell wall extracts by mass spectrometry; belongs to adhesin cluster VI; predicted GPI anchor
CAGL0J02530g		Family VI, de Groot et al., 2008 (Eukaryotic cell)	Putative adhesion protein; predicted GPI-anchor; belongs to adhesin cluster VI
CAGL0J02552g		Family VI, de Groot et al., 2008 (Eukaryotic cell)	Adhesin-like protein; predicted GPI anchor; belongs to adhesin cluster VI
CAGL0J05159g		de Groot et al., 2008 (Eukaryotic cell)	Putative adhesin-like protein
CAGL0J11176g		Chaudhuri et al., 2011 (BMC Genomics)	Putative adhesin-like protein
CAGL0J11902g	**AWP3a**	**Xu et al., 2020 (Molecular microbiology)**	**new predicted adhesin like gene**
CAGL0J11935g	**AWP3b**	**Xu et al., 2020 (Molecular microbiology)**	**new predicted adhesin like gene**
~~CAGL0J11891g~~	~~*AWP3*~~	~~Family VI, de Groot et al., 2008 (Eukaryotic cell)~~	~~Putative adhesin-like protein; identified in cell wall extracts by mass spectrometry; belongs to adhesin cluster VI~~
CAGL0J11968g	*EPA15*	Family I, de Groot et al., 2008 (Eukaryotic cell)	Putative adhesin-like cell wall protein; belongs to adhesin cluster I
~~CAGL0J11979g~~	~~*AWP4.1;* CAGL0J11990g.3~~	~~CAGL0J11990g: Family V, de Groot et al., 2008 (Eukaryotic cell); split into 3 ORFs: Linde et al., 2015 (Nucleic Acids Research)~~	~~Protein of unknown function~~
~~CAGL0J12012g~~	~~*AWP4.2;* CAGL0J11990g.1~~	~~CAGL0J11990g: Family V, de Groot et al., 2008 (Eukaryotic cell); split into 3 ORFs: Linde et al., 2015 (Nucleic Acids Research)~~	~~Protein of unknown function~~
~~CAGL0J12034g~~	~~*AWP4.3;* CAGL0J11990g.2~~	~~CAGL0J11990g: Family V, de Groot et al., 2008 (Eukaryotic cell); split into 3 ORFs: Linde et al., 2015 (Nucleic Acids Research)~~	~~Protein of unknown function~~
CAGL0J12067g		**Xu et al., 2020 (Molecular microbiology)**	**new predicted adhesin like gene**

CAGL0K00110g	*AWP2*	Family V, de Groot et al., 2008 (Eukaryotic cell)	Putative adhesin; identified in cell wall extracts by mass spectrometry; belongs to adhesin cluster V; predicted GPI-anchor
CAGL0K00170g	*EPA22*	Family I, de Groot et al., 2008 (Eukaryotic cell)	Putative adhesin-like protein; belongs to adhesin cluster I
CAGL0K02277g		Candida Genome Database	Ortholog(s) have role in cell adhesion involved in single-species biofilm formation, cell separation after cytokinesis, cell wall organization and cellular response to glucose starvation, more
CAGL0K09130g		Chaudhuri et al., 2011 (BMC Genomics)	Putative adhesin-like protein
CAGL0K10164g		Weig et al., 2004 (Microbiology)	Predicted GPI-linked protein; putative adhesin-like protein
CAGL0K13002g	*AED2/AGA1*	Family III, de Groot et al., 2008 (Eukaryotic cell)	Putative adhesin; predicted GPI-anchor; belongs to adhesin cluster III
CAGL0K13024g	*AWP5 / AED1*	Family III, de Groot et al., 2008 (Eukaryotic cell)	Adhesin-like protein required for adherence to endothelial cells; identified in cell wall extracts by mass spectrometry; belongs to adhesin cluster III; predicted GPI anchor; 6 tandem repeats; expressed more in stationary growth phase
CAGL0L00157g		Family III, de Groot et al., 2008 (Eukaryotic cell)	Putative adhesin-like protein; multiple tandem repeats; predicted GPI-anchor; belongs to adhesin cluster III
CAGL0L00227g		Family V, de Groot et al., 2008 (Eukaryotic cell)	Putative adhesin with glycine and serine rich repeats; belongs to adhesin cluster V
CAGL0L06424g		Weig et al., 2004 (Microbiology)	Predicted GPI-linked adhesin-like protein
CAGL0L09911g		de Groot et al., 2008 (Eukaryotic cell)	Putative adhesin-like cell wall protein; 5 tandem repeats; predicted GPI-anchor

CAGL0L10092g		Family III, de Groot et al., 2008 (Eukaryotic cell)	Putative adhesin-like cell wall protein; multiple tandem repeats; predicted GPI-anchor; belongs to adhesin cluster III
CAGL0L11528g		Candida Genome Database	Ortholog(s) have role in (1->6)-beta-D-glucan biosynthetic process, adhesion of symbiont to host and cellular response to starvation, more
CAGL0L13299g	*EPA11*	Family I, de Groot et al., 2008 (Eukaryotic cell)	Putative adhesin; belongs to adhesin cluster I
CAGL0L13332g	*EPA13*	Family I, de Groot et al., 2008 (Eukaryotic cell)	Sub-telomerically encoded lectin-like adhesin with a role in cell adhesion; contains multiple tandem repeats; predicted GPI-anchor; belongs to adhesin cluster I
~~CAGL0M00110g~~	~~*AWP11*~~	~~Family V, de Groot et al., 2008 (Eukaryotic cell)~~	~~Putative adhesin-like protein; GPI-anchored; belongs to adhesin cluster V; ORF appears artificially broken into fragments due to sequencing errors but the gene is likely protein-coding based on mass spectrometry data~~
CAGL0L13552g	**EPA14a**	**Xu et al., 2020 (Molecular microbiology)**	**new predicted adhesin like gene**
CAGL0M00121g	**AWP4**	**Xu et al., 2020 (Molecular microbiology)**	**new predicted adhesin like gene**
CAGL0M00132g	*EPA12*	Family I, de Groot et al., 2008 (Eukaryotic cell)	Putative adhesin-like cell wall protein; belongs to adhesin cluster I
CAGL0M03773g		Weig et al., 2004 (Microbiology)	Predicted GPI-linked adhesin-like protein
CAGL0M08492g	*PIR3*	nonenzymatic CWPs, de Groot et al., 2008 (Eukaryotic cell)	Pir protein family member, putative cell wall component
CAGL0M08514g	*PIR5*	Weig et al., 2004 (Microbiology)	Pir protein family member, putative cell wall component
CAGL0M09086g		Candida Genome Database	Ortholog(s) have GTP binding, cell adhesion molecule binding activity
CAGL0M11726g		Weig et al., 2004 (Microbiology)	Putative GPI-linked cell wall adhesin-like protein

CAGL0M14069g	*PWP6*	Family II, de Groot et al., 2008 (Eukaryotic cell)	Adhesin-like protein with similarity to S. cerevisiae flocculins, cell wall proteins that mediate adhesion; predicted GPI anchor; belongs to adhesin cluster II
CAGL0M14300g	***EPA14b***	**Xu et al., 2020 (Molecular microbiology)**	**new predicted adhesin like gene**

Addendum 3: List of primers used in Chapter 3

Primer	Name	Sequence	used for
9064	NatMX Rv	CGTCAAGACTGTCAAGGAGGG	Control primer
9065	NatMX Fw	CATCATCTGCCCAGATGCGAAG	Control primer
BT1000	CAGL0B00116g prom-Fw	CGCTCTAGAACTAGTATCTTCACTAGGAGCTAGAG	Construction deletion strain
BT1001	CAGL0B00116g prom-Rv	AAGTATAGGAACTTCGAGCACAGACAAGTTATCTCG	Construction deletion strain
BT1002	CAGL0B00116g term-Fw	AATAGGAACTTCGTCATCCAATAACAAACACAGGC	Construction deletion strain
BT1003	CAGL0B00116g term-Rv	GGTACCGGGCCCCCCGATGGAGCTAAATTTGGTGG	Construction deletion strain
BT1004	CAGL0A01584g prom-Fw	CGCTCTAGAACTAGTCTTAATCGTGCTCTTGACG	Construction deletion strain
BT1005	CAGL0A01584g prom-Rv	AAGTATAGGAACTTCGTTATAGCTATGCTGTTGTCG	Construction deletion strain
BT1006	CAGL0A01584g term-Fw	AATAGGAACTTCGTCACACGGATTTTAGGAACCAG	Construction deletion strain
BT1007	CAGL0A01584g term-Rv	GGTACCGGGCCCCCCGTTTAGTGAGCCTGAGAACG	Construction deletion strain
BT1008	CAGL0C00110g prom-Fw	CGCTCTAGAACTAGTATGAACAGGTACTCTATTCC	Construction deletion strain
BT1009	CAGL0C00110g prom-Rv	AAGTATAGGAACTTCGTATCTTTTAGACCTCACCTC	Construction deletion strain
BT1010	CAGL0C00110g term-Fw	AATAGGAACTTCGTCCCACATTTCCTAAGATAGGG	Construction deletion strain
BT1011	CAGL0C00110g term-Rv	GGTACCGGGCCCCCCTCACAGTACTATATTCCTGC	Construction deletion strain
BT1012	CAGL0F00105g prom-Fw	CGCTCTAGAACTAGTACATACGTCTCCCACATCAC	Construction deletion strain
BT1013	CAGL0F00105g prom-Rv	AAGTATAGGAACTTCGATGGTCTTCCCATCAGAGAC	Construction deletion strain
BT1014	CAGL0F00105g term-Fw	AATAGGAACTTCGTCGTGTACTAGTTCTGTGACTG	Construction deletion strain
BT1015	CAGL0F00105g term-Rv	GGTACCGGGCCCCCCGGTAACTTCGATTGGTCACG	Construction deletion strain
BT1016	CAGL0L13299g prom-Fw	CGCTCTAGAACTAGTTACAATGGCTTATCTTGTCC	Construction deletion strain
BT1017	CAGL0L13299g prom-Rv	AAGTATAGGAACTTCGTTCCAAAAATGAGTCTTTGC	Construction deletion strain
BT1018	CAGL0L13299g term-Fw	AATAGGAACTTCGTCTTCTTTGAAAGACTCAGAGG	Construction deletion strain
BT1019	CAGL0L13299g term-Rv	GGTACCGGGCCCCCCGTTAACAGAAAGTGTCACAC	Construction deletion strain
BT1020	CAGL0G10219g prom-Fw	CGCTCTAGAACTAGTTAATGCCATCAGCAATACTG	Construction deletion strain
BT1021	CAGL0G10219g prom-Rv	AAGTATAGGAACTTCGATTACAAACAAAGTGCTGTC	Construction deletion strain
BT1022	CAGL0G10219g term-Fw	AATAGGAACTTCGTCGTGTACTAGTTCTGTGACTG	Construction deletion strain

BT1023	CAGL0G10219g term-Rv	GGTACCGGGCCCCCCGAATCCATGGTTGACCAAGA	Construction deletion strain
BT1024	CAGL0I00116g prom-Fw	CGCTCTAGAACTAGTTTGTTATGATCGTGGTAGGC	Construction deletion strain
BT1025	CAGL0I00116g prom-Rv	AAGTATAGGAACTTCGTAATACCTGGAGAAGCCGAC	Construction deletion strain
BT1026	CAGL0I00116g term-Fw	AATAGGAACTTCGTCCTCGTAACAATTATCGCCC	Construction deletion strain
BT1027	CAGL0I00116g term-Rv	GGTACCGGGCCCCCCCTGTTGATCTTGGGCAACG	Construction deletion strain
BT1028	CAGL0L00157g prom-Fw	CGCTCTAGAACTAGTTTGACCAAGACTTTCATCCC	Construction deletion strain
BT1029	CAGL0L00157g prom-Rv	AAGTATAGGAACTTCGAATCAGTAGAACACCTGCAC	Construction deletion strain
BT1030	CAGL0L00157g term-Fw	AATAGGAACTTCGTCGTGTACTAGTTCTGTGACTG	Construction deletion strain
BT1031	CAGL0L00157g term-Rv	GGTACCGGGCCCCCCACCGTGCATTATCACATCTC	Construction deletion strain
BT1032	CAGL0F09273g prom-Fw	CGCTCTAGAACTAGTAAGACACCAGTGCAATGTTC	Construction deletion strain
BT1033	CAGL0F09273g prom-Rv	AAGTATAGGAACTTCGTATCCAGTGAATTGTTGGTC	Construction deletion strain
BT1034	CAGL0F09273g term-Fw	AATAGGAACTTCGTCGTTCACTTCCAGTCATGGTG	Construction deletion strain
BT1035	CAGL0F09273g term-Rv	GGTACCGGGCCCCCCTGGTTGACAAATGTCTGGTG	Construction deletion strain
BT1036	CAGL0E06600g prom-Fw	CGCTCTAGAACTAGTTCTGATTAATCCATGCAACC	Construction deletion strain
BT1037	CAGL0E06600g prom-Rv	AAGTATAGGAACTTCGGCTTTACACTAATTCATGGG	Construction deletion strain
BT1038	CAGL0E06600g term-Fw	AATAGGAACTTCGTCATTAGTTATCCTTTGCACTG	Construction deletion strain
BT1039	CAGL0E06600g term-Rv	GGTACCGGGCCCCCCACATCTAGTGGTGAATATGC	Construction deletion strain
BT1040	CAGL0I07293g prom-Fw	CGCTCTAGAACTAGTCCTCAAGTCATCTGCCTAGG	Construction deletion strain
BT1041	CAGL0I07293g prom-Rv	AAGTATAGGAACTTCGGTTTAGATGCAGTCCCCAGG	Construction deletion strain
BT1042	CAGL0I07293g term-Fw	AATAGGAACTTCGTCTGATTCGAAGACCACTTAGC	Construction deletion strain
BT1043	CAGL0I07293g term-Rv	GGTACCGGGCCCCCCTATGCTACTCTGGGATAAGC	Construction deletion strain
BT1044	CAGL0K00110g prom-Fw	CGCTCTAGAACTAGTGAACTTGAGAAAGAGGCTTG	Construction deletion strain
BT1045	CAGL0K00110g prom-Rv	AAGTATAGGAACTTCGATTTGTTTGGTTCCGATGTC	Construction deletion strain
BT1046	CAGL0K00110g term-Fw	AATAGGAACTTCGTCCTTAAGCCGACTATTATCTG	Construction deletion strain
BT1047	CAGL0K00110g term-Rv	GGTACCGGGCCCCCCATGAAATTGAAAGTGTCACC	Construction deletion strain
BT1048	CAGL0I00220g prom-Fw	CGCTCTAGAACTAGTTGTACAACCATGATATTCTG	Construction deletion strain
BT1049	CAGL0I00220g prom-Rv	AAGTATAGGAACTTCGAGAACTATTGACAAAGTTGG	Construction deletion strain
BT1050	CAGL0I00220g term-Fw	AATAGGAACTTCGTCTTAACAGCACCAAATAGCC	Construction deletion strain

BT1051	CAGL0I00220g term-Rv	GGTACCGGGCCCCCCTAGATCAATAGTTGGCTGG	Construction deletion strain
BT1052	CAGL0K13002g prom-Fw	CGCTCTAGAACTAGTATTTGTCCATGTGATTCACC	Construction deletion strain
BT1053	CAGL0K13002g prom-Rv	AAGTATAGGAACTTCGGTCAAACCATAACTTTGTGG	Construction deletion strain
BT1054	CAGL0K13002g term-Fw	AATAGGAACTTCGTCTTGCTAACAATCAGCCATCG	Construction deletion strain
BT1055	CAGL0K13002g term-Rv	GGTACCGGGCCCCCCTGAATGTCAAGAGACCAGAC	Construction deletion strain
BT1056	CAGL0J11891g prom-Fw	CGCTCTAGAACTAGTTATCAATGAATGTTGCTCTC	Construction deletion strain
BT1057	CAGL0J11891g prom-Rv	AAGTATAGGAACTTCGGAAATCATTTGGCTATTGTG	Construction deletion strain
BT1058	CAGL0J11891g term-Fw	AATAGGAACTTCGTCCGACCACCATCATCTTACTG	Construction deletion strain
BT1059	CAGL0J11891g term-Rv	GGTACCGGGCCCCCCTTCCGCAACTTCTTCACTCC	Construction deletion strain
BT1060	CAGL0J00253g prom-Fw	CGCTCTAGAACTAGTTTTAGTGTTCCTGGAGAAGC	Construction deletion strain
BT1061	CAGL0J00253g prom-Rv	AAGTATAGGAACTTCGATAGATCTGTCCCGATACAG	Construction deletion strain
BT1062	CAGL0J00253g term-Fw	AATAGGAACTTCGTCGTGAGTATTACACTATCAGC	Construction deletion strain
BT1063	CAGL0J00253g term-Rv	GGTACCGGGCCCCCCAGGTATAAACATAAACTGGC	Construction deletion strain
BT1064	CAGL0E06688g prom-Fw	CGCTCTAGAACTAGTGTGACATCATAATTACTTGG	Construction deletion strain
BT1065	CAGL0E06688g prom-Rv	AAGTATAGGAACTTCGCGATTATGATGGTTATTCTG	Construction deletion strain
BT1066	CAGL0E06688g term-Fw	AATAGGAACTTCGTCCTGATTTAATTCTGTTCCC	Construction deletion strain
BT1067	CAGL0E06688g term-Rv	GGTACCGGGCCCCCCTGTTGACTGATTAGATACG	Construction deletion strain
BT1068	CAGL0J01463g prom-Fw	CGCTCTAGAACTAGTGTTGTATATCAGCTCTTCTC	Construction deletion strain
BT1069	CAGL0J01463g prom-Rv	AAGTATAGGAACTTCGAGTAAACTTCATTTGATTCC	Construction deletion strain
BT1070	CAGL0J01463g term-Fw	AATAGGAACTTCGTCAACTGATTTTTACCCCATC	Construction deletion strain
BT1071	CAGL0J01463g term-Rv	GGTACCGGGCCCCCCTTCAAGGGATTTGAATAGG	Construction deletion strain
BT1072	CAGL0B00116g control up	GAACCCCTCTGCTGATATCGC	Control PCR deletion strain
BT1073	CAGL0B00116g control down	ATGGGTATCTCTGACACATGG	Control PCR deletion strain
BT1074	CAGL0A01584g control up	ACCTTCTCGAGTCTCTACTGC	Control PCR deletion strain
BT1075	CAGL0A01584g control down	AGCTTAGAGAGGAGCTCAGGC	Control PCR deletion strain
BT1076	CAGL0C00110g control up	CTCTATACAGATGCCTTTCTCC	Control PCR deletion strain
BT1077	CAGL0C00110g control down	CCTTTCCGTACAAGTAGTACC	Control PCR deletion strain

BT1078	CAGL0F00105g control up	GTGGTCTCCAACTCTCGACGG	Control PCR deletion strain
BT1079	CAGL0F00105g control down	TCGTATGATGTGCTGTTGTGG	Control PCR deletion strain
BT1080	CAGL0L13299g control up	CACACAAGTATAACTTCGCGC	Control PCR deletion strain
BT1081	CAGL0L13299g control down	GCATACACAAAACCACAGGGG	Control PCR deletion strain
BT1082	CAGL0G10219g control up	CAATTTGGAAGTGTACTCGCC	Control PCR deletion strain
BT1083	CAGL0G10219g control down	CAATCTTAAACCCACAGGCTC	Control PCR deletion strain
BT1084	CAGL0I00116g control up	AACAGCTGTAATCGTGTGACC	Control PCR deletion strain
BT1085	CAGL0I00116g control down	GACTACAACTTGCCTGATGGC	Control PCR deletion strain
BT1086	CAGL0L00157g control up	GTAATGCTCGCACTTTCGCCC	Control PCR deletion strain
BT1087	CAGL0L00157g control down	TGGGTGCTGAAGTGCGCACTC	Control PCR deletion strain
BT1088	CAGL0F09273g control up	GTAGATATTCCAAGTCATTGG	Control PCR deletion strain
BT1089	CAGL0F09273g control down	TATAGGAAGGAACTTCAACAC	Control PCR deletion strain
BT1090	CAGL0E06600g control up	GAGTAGGTATGATCTGAAGGC	Control PCR deletion strain
BT1091	CAGL0E06600g control down	TTAAGTTGTCAGGAACCCTCG	Control PCR deletion strain
BT1092	CAGL0I07293g control up	CTGTAATGTAAGAAAGCGGAG	Control PCR deletion strain
BT1093	CAGL0I07293g control down	CTTCGTCGATCTATCAACGTC	Control PCR deletion strain
BT1094	CAGL0K00110g control up	ACACGAATGTCTACTTTGTAG	Control PCR deletion strain
BT1095	CAGL0K00110g control down	ATTGATATGGGCAAGAAGGTG	Control PCR deletion strain
BT1096	CAGL0I00220g control up	CCTGATCTCCATTGTAGTCCC	Control PCR deletion strain
BT1097	CAGL0I00220g control down	CCATGAATAACAACAACGTCC	Control PCR deletion strain
BT1098	CAGL0K13002g control up	TAATTTGCTTACATACCAACC	Control PCR deletion strain
BT1099	CAGL0K13002g control down	CATCATATGTTATGAATTCCG	Control PCR deletion strain
BT1100	CAGL0J11891g control up	AACTTTCGGATGGTTACTCTG	Control PCR deletion strain
BT1101	CAGL0J11891g control down	ACCTAAGGTCATACGTGTGGG	Control PCR deletion strain
BT1102	CAGL0J00253g control up	AATGGAAGACGTGGACTTTGC	Control PCR deletion strain
BT1103	CAGL0J00253g control down	TACAGTATTGGTAGAGTTCAC	Control PCR deletion strain
BT1104	CAGL0E06688g control up	TTTGCTACAGCAGTGAGCATG	Control PCR deletion strain
BT1105	CAGL0E06688g control down	GGAAGTACTTCCTGCCAACTG	Control PCR deletion strain

BT1106	CAGL0J01463g control up	TCTACTCAGGAACCCTAGAGC	Control PCR deletion strain
BT1107	CAGL0J01463g control down	CATAGCTACTGCAGGCTGCTG	Control PCR deletion strain

Addendum 4: Alignment of neutral trehalases and human trehalase

Using Swiss model, residues of the active site or involved in substrate binding were searched for all species of the phylogenetic tree. These residues were reported for *S. cerevisiae*, *S. pombe* and *A. nidulans* neutral trehalases. For alignment, we also included *C. glabrata* and the human trehalase enzyme. The amino acid sequences were aligned using Clustal O. Residues of the active site are highlighted in blue, amino acids conferring substrate binding are highlighted in purple.

CLUSTAL O(1.2.4) multiple sequence alignment
AA of active site - AA conferring substrate binding

```
Human_TREH          ------------------------------------------------------------  0
CgNTH2              ----MPTLTFY------------------------------LGADDAVDGGVKSKSMA  24
ScNTH2              MVDFLPKVTEINPPSEGNDGEDNIKPLSSGSEQRPL----KEEGQQGGRRHHRRLSSMHE  56
CgNTH1              ---------MSDPMDEGP--------LGKGAVATPAMVE-KVANESPKKTRPRRLSSLNE  42
ScNTH1              ------------------------------------MSQVNTSQGPVAQGRQRRLSSLSE  24
S_Pombe_Ntp1        ------------------------------------MPSKFSSKYVD--TE---AISND  18
A_nidulans_TreB     ------------------------------MDDSA-LPSNTSNGINGRTAH---RRSSS  25

Human_TREH          ------------------------------------------------------------  0
CgNTH2              FSDPFHKNVKVQSPEPEPVDA--KEKKKLNRTRTMSVFYNVADFKD-DEEIRKHKLKRRA  81
ScNTH2              YFDPFSNAEVYYGPITDPRKQSK--IHRLNRTRTMSVFNKVSDFK---NGMKDYTLKRRG  111
CgNTH1              FYDPFSTAEVYYGPATDPRKQKKS-STKLNRTRTMSVFDNTSIAKT-TASFGQFQLKRRG  100
ScNTH1              FNDPFSNAEVYYGPPTDPRKQKQAKPAKINRTRTMSVFDNVSPFK--KTGFGKLQQTRRG  82
S_Pombe_Ntp1        DDNPFATAKSYYSKDTDLSTR-----VSAGRPRTLSTSMEASAAPTIPE---LKNLRRRG  70
A_nidulans_TreB     GGDPFQHPDIYYGNPESVERI-------KNRRRAFSSSLKSFNRQDFHEMLGDRNT-RRG  77

Human_TREH          ----------------MPGRTWELCL------------------LLLLGLGLGSQEALP  25
CgNTH2              SEDDTYISSKGTRRLFVKDVDWTLKELLQNEDTDQNFQITVEDTGPKVIKLGTANSAGYN  141
ScNTH2              SEDDSFLSSQGNRRFYIDNVDLALDELLASEDTDKNHQITIEDTGPKVIKVGTANSNGFK  171
CgNTH1              SEDDSLTASQGNRKFFIEDVDGTLEELLSSEDTDRNYQITIEDTGPKVLKVGTANSGGYK  160
ScNTH1              SEDDTYSSSQGNRRFFIEDVDKTLNELLAAEDTDKNYQITIEDTGPKVLKVGTANSYGYK  142
S_Pombe_Ntp1        SL-D----EHKQPRKFLVDVDKTLNALLESEDTDRNMQITIEDTGPKVVSLGSASSGGYR  125
A_nidulans_TreB     SMDP----TSGNPRKFLIDVDATLHSLLEREDSDRNMQITIEDVGPKVFSLGTAASHGYN  133
                                    : .    *                        :. :* . . .

Human_TREH          PPCESEIYCHGELLNQVQMAKLYQDDKQFVDM------PLSIAPEQVLQ-----------  68
CgNTH2              HIDIRGTYMLSNLLQELTIAHNFGQRQLYLPESRLNENPVHRLKRVIETHFWDGLTRRLD  201
ScNTH2              HVNVRGTYMLSNLLQELTIAKSFGRHQIFLDEARINENPVDRLSRLITTQFWTSLTRRVD  231
CgNTH1              HVNIRGTYMLSNLLQELTIAKSFGRHSIFLDEARINENPVNRLSRLITNQFWNNLTRRID  220
ScNTH1              HINIRGTYMLSNLLQELTIAKSFGRHQIFLDEARINENPVNRLSRLINTQFWNSLTRRVD  202
S_Pombe_Ntp1        LYELRGTYQLSNLLQELTLAKDYGRRYILLDERRLNENPVNRLSRLIKGTFWDALTRRID  185
A_nidulans_TreB     RFDVRGTYMLSNLLQELTIAKDYGRKQIVLDEERLSENPVSRLSRLIKNSFWNSLTRRID  193
                           *  .:**::: :*: :      :        *:    . :

Human_TREH          --TFTELSRDHNHSIPREQLQAFVHEHFQAKGQELQPWTPADWKDSPQFLQKISDAK---  123
CgNTH2              LNTIGEAAQEKKIDTPEAK--------------NPRVYVPYDCPEMYEYFIQASQMNPSV  247
ScNTH2              LYNIAEIARDSKIDTPGAK--------------NPRIYVPYNCPEQYEFYIQASQMNPSL  277
CgNTH1              LNNIGEIASDTKVDTPEAK--------------NPRVYVPYNCPEQYEFYIQASQMNPSM  266
ScNTH1              LNNVGEIAKDTKIDTPGAK--------------NPRIYVPYDCPEQYEFYVQASQMHPSL  248
S_Pombe_Ntp1        ASVLDVICRDTK-DRSGSH--------------VNRIYVPKAEQEMYEYYVRAAKERPYL  230
A_nidulans_TreB     GRNIEVAGRDPK-DWTDDP--------------RPRIYVPPGAPEQLEYYRRIAEEKPEL  238
                       .     : : .                     : :.*    :  ::  : :. .
```

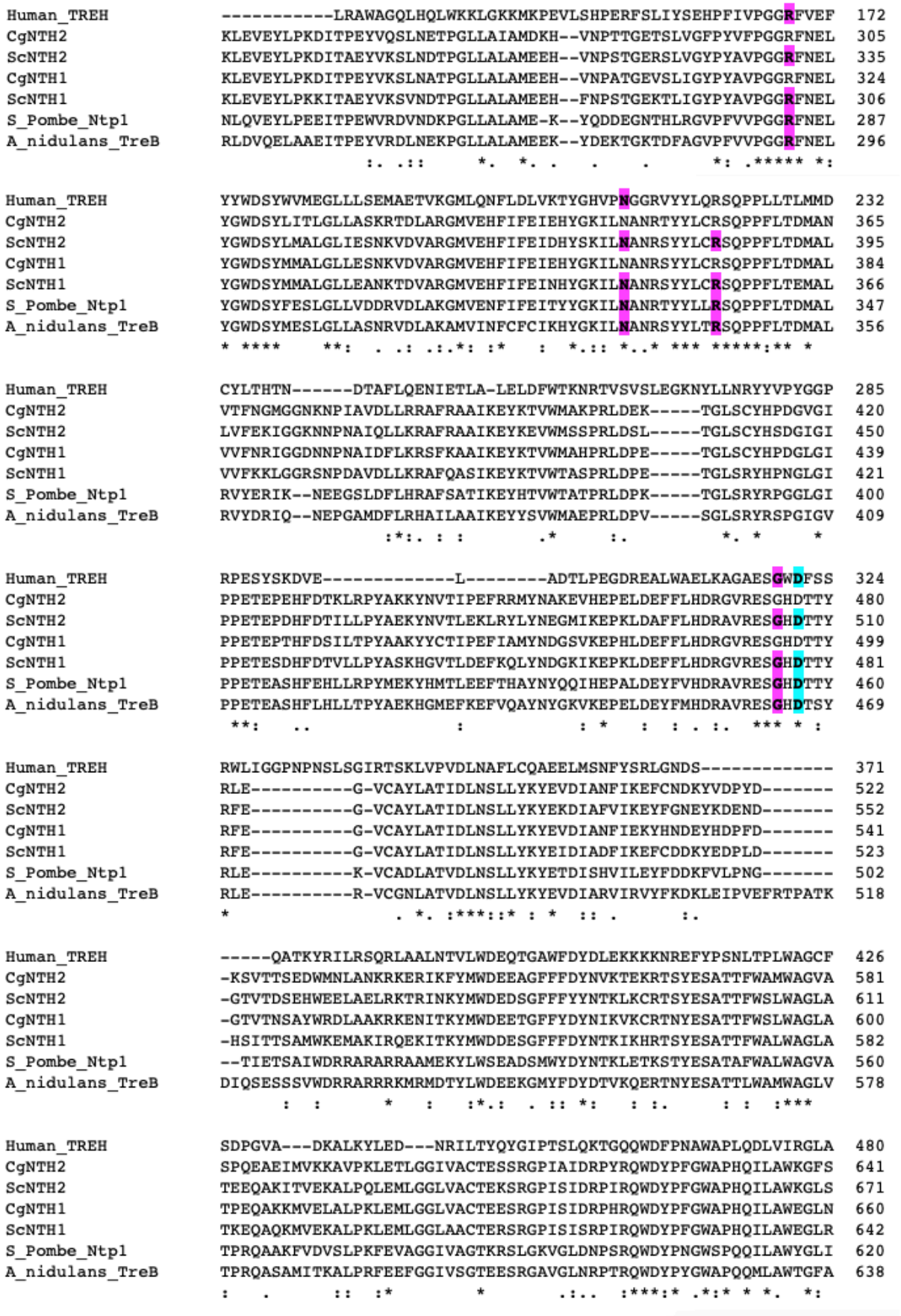
Human_TREH ----------LRAWAGQLHQLWKKLGKKMKPEVLSHPERFSLIYSEHPFIVPGGRFVEF 172
CgNTH2 KLEVEYLPKDITPEYVQSLNETPGLLAIAMDKH--VNPTTGETSLVGFPYVFPGGRFNEL 305
ScNTH2 KLEVEYLPKDITAEYVKSLNDTPGLLALAMEEH--VNPSTGERSLVGYPYAVPGGRFNEL 335
CgNTH1 KLEVEYLPKDITPEYVKSLNATPGLLALAMEEH--VNPATGEVSLIGYPYAVPGGRFNEL 324
ScNTH1 KLEVEYLPKKITAEYVKSVNDTPGLLALAMEEH--FNPSTGEKTLIGYPYAVPGGRFNEL 306
S_Pombe_Ntp1 NLQVEYLPEEITPEWVRDVNDKPGLLALAME-K--YQDDEGNTHLRGVPFVVPGGRFNEL 287
A_nidulans_TreB RLDVQELAAEITPEYVRDLNEKPGLLALAMEEK--YDEKTGKTDFAGVPFVVPGGRFNEL 296
YYWDSYWVMEGLLLSEMAETVKGMLQNFLDLVKTYGHVPNGGRVYYLQRSQPPLLTLMMD 232
YGWDSYLITLGLLASKRTDLARGMVEHFIFEIEHYGKILNANRTYYLCRSQPPFLTDMAN 365
YGWDSYLMALGLIESNKVDVARGMVEHFIFEIDHYSKILNANRSYYLCRSQPPFLTDMAL 395
YGWDSYMMALGLLESNKVDVARGMVEHFIFEIEHYGKILNANRSYYLCRSQPPFLTDMAL 384
YGWDSYMMALGLLEANKTDVARGMVEHFIFEINHYGKILNANRSYYLCRSQPPFLTEMAL 366
YGWDSYFESLGLLVDDRVDLAKGMVENFIFEITYYGKILNANRTYYLLRSQPPFLTDMAL 347
YGWDSYMESLGLLASNRVDLAKAMVINFCFCIKHYGKILNANRSYYLTRSQPPFLTDMAL 356
CYLTHTN------DTAFLQENIETLA-LELDFWTKNRTVSVSLEGKNYLLNRYYVPYGGP 285
VTFNGMGGNKNPIAVDLLRRAFRAAIKEYKTVWMAKPRLDEK-----TGLSCYHPDGVGI 420
LVFEKIGGKNNPNAIQLLKRAFRAAIKEYKEVWMSSPRLDSL-----TGLSCYHSDGIGI 450
VVFNRIGGDNNPNAIDFLKRSFKAAIKEYKTVWMAHPRLDPE-----TGLSCYHPDGLGI 439
VVFKKLGGRSNPDAVDLLKRAFQASIKEYKTVWTASPRLDPE-----TGLSRYHPNGLGI 421
RVYERIK--NEEGSLDFLHRAFSATIKEYHTVWTATPRLDPK-----TGLSRYRPGGLGI 400
RVYDRIQ--NEPGAMDFLRHAILAAIKEYYSVWMAEPRLDPV-----SGLSRYRSPGIGV 409
RPESYSKDVE----------L--------ADTLPEGDREALWAELKAGAESGWDFSS 324
PPETEPEHFDTKLRPYAKKYNVTIPEFRRMYNAKEVHEPELDEFFLHDRGVRESGHDTTY 480
PPETEPDHFDTILLPYAEKYNVTLEKLRYLYNEGMIKEPKLDAFFLHDRAVRESGHDTTY 510
PPETEPTHFDSILTPYAAKYYCTIPEFIAMYNDGSVKEPHLDEFFLHDRGVRESGHDTTY 499
PPETESDHFDTVLLPYASKHGVTLDEFKQLYNDGKIKEPKLDEFFLHDRGVRESGHDTTY 481
PPETEASHFEHLLRPYMEKYHMTLEEFTHAYNYQQIHEPALDEYFVHDRAVRESGHDTTY 460
PPETEASHFLHLLTPYAEKHGMEFKEFVQAYNYGKVKEPELDEYFMHDRAVRESGHDTSY 469
RWLIGGPNPNSLSGIRTSKLVPVDLNAFLCQAEELMSNFYSRLGNDS---------- 371
RLE----------G-VCAYLATIDLNSLLYKYEVDIANFIKEFCNDKYVDPYD------- 522
RFE----------G-VCAYLATIDLNSLLYKYEKDIAFVIKEYFGNEYKDEND------- 552
RFE----------G-VCAYLATIDLNSLLYKYEVDIANFIEKYHNDEYHDPFD------- 541
RFE----------G-VCAYLATIDLNSLLYKYEIDIADFIKEFCDDKYEDPLD------- 523
RLE----------K-VCADLATVDLNSLLYKYETDISHVILEYFDDKFVLPNG------- 502
RLE----------R-VCGNLATVDLNSLLYKYEVDIARVIRVYFKDKLEIPVEFRTPATK 518
-----QATKYRILRSQRLAALNTVLWDEQTGAWFDYDLEKKKKNREFYPSNLTPLWAGCF 426
-KSVTTSEDWMNLANKRKERIKFYMWDEEAGFFFDYNVKTEKRTSYESATTFWAMWAGVA 581
-GTVTDSEHWEELAELRKTRINKYMWDEDSGFFFYYNTKLKCRTSYESATTFWSLWAGLA 611
-GTVTNSAYWRDLAAKRKENITKYMWDEETGFFYDYNIKVKCRTNYESATTFWSLWAGLA 600
-HSITTSAMWKEMAKIRQEKITKYMWDDESGFFFDYNTKIKHRTSYESATTFWALWAGLA 582
--TIETSAIWDRRARARRAAMEKYLWSEADSMWYDYNTKLETKSTYESATAFWALWAGVA 560
DIQSESSSVWDRRARRRKMRMDTYLWDEEKGMYFDYDTVKQERTNYESATTLWAMWAGLV 578
SDPGVA---DKALKYLED---NRILTYQYGIPTSLQKTGQQWDFPNAWAPLQDLVIRGLA 480
SPQEAEIMVKKAVPKLETLGGIVACTESSRGPIAIDRPYRQWDYPFGWAPHQILAWKGFS 641
TEEQAKITVEKALPQLEMLGGLVACTEKSRGPISIDRPIRQWDYPFGWAPHQILAWKGLS 671
TPEQAKKMVELALPKLEMLGGLVACTEESRGPISIDRPHRQWDYPFGWAPHQILAWEGLN 660
TKEQAQKMVEKALPKLEMLGGLAACTERSRGPISISRPIRQWDYPFGWAPHQILAWEGLR 642
TPRQAAKFVDVSLPKFEVAGGIVAGTKRSLGKVGLDNPSRQWDYPNGWSPQQILAWYGLI 620
TPRQASAMITKALPRFEEFGGIVSGTEESRGAVGLNRPTRQWDYPYGWAPQQMLAWTGFA 638


Human_TREH KAPLRRAQEVAFQLAQNWIRTNFDVYS-QKSAMYEKYDVSNGGQPGG----------GGE 529
CgNTH2 NYGY---DNIARRLVYRWLYMMTKAFVDYNGIVVEKYDVTKVTDPHKITAEYGNQGVDFK 698
ScNTH2 AYGY---QQVATRLAYRWLYMITKSFVDYNGMVVEKYDVTRGTDPHRVDAEYGNQGADFK 728
CgNTH1 DYGY---TSVATRLAYRWLFMMTKAFVDYNGIVVEKYDVTRGTDPHRVDAEYGNQGADFK 717
ScNTH1 SYGY---LTVTNRLAYRWLFMMTKAFVDYNGIVVEKYDVTRGTDPHRVEAEYGNQGADFK 699
S_Pombe_Ntp1 RYGY---EEETRRLVYRWLYTITKSFVDFNGIVVEKYDLTRPVDPHRVEAEYGNQGVNIK 677
A_nidulans_TreB RYGY---QEEAERLAYKWLYMITKAFVDFNGVVVEKYDVTRPIDPHRVDAEYGNQGVDFK 695
YEVQEGFGWTNGVVLMLLDRYGDRLTSGAKLAFLEPHCLAATLLPSLLLSLLPW*----- 583
GYAREGFGWVNSSFLLGLQYLDNHAIR----------ALGACIPPKPFLNGLRAKEKARY 748
GVATEGFGWVNTSYLLGLKYMNNHARR----------ALAACSPPLPFFNSLKPSEKKLY 778
GVAKEGFGWVNTSYILGLKFMNSHARR----------ALGACIPPAPFFNSLKDDEKSIY 767
GAATEGFGWVNASYILGLKYMNSHARR----------ALGACIPPISFFSSLRPQERNLY 749
GVAREGFGWVNASYEVGLTFCNSHMRR----------ALGACTTPDVFFAGIKEESLPA- 726
GAPREGFGWVNASYVYGLEMLNAHQRR----------ALGAVTPWETYSKAVSAQGSDTV 745
---------- 583
GL*------- 750
YL*------- 780
GL*------- 769
GL*------- 751
FENLSIHKN* 735
LENRSE*--- 751

Addendum 5: List of primers used in Chapter 4

Primer	Name	Sequence	used for
7883	pLS10-*HPH*-Fw	GACAACGTATACTCATCAGATAACAGCAATA	Checking pLS10 plasmid
9064	NatMx_Rv	cgtcaagactgtcaaggaggg	checking insertion pYC vectors
9065	NatMX_Fw	catcatctgcccagatgcgaag	checking insertion pYC vectors
A2047	vector background Rv	cagctatgaccatgattacg	Checking insertion terminator fragment in pYC56
A9050	mCherry Rv	CTTCACCTTGTAGATGAAC	Checking insertion ORF fragment in pYC56
B1222	NatMX Fw	cgattcgatactaacgcc	Checking insertion terminator fragment in pYC56
B2011	*NTH2* control Rv	CGTGTCTAGTATACAATGCTC	Checking transformants n*th2Δ*
B3220	pLS10-*HPH*-Rev	GTAATACAGTCAAATTGCAGTACTCTGC	Checking pLS10 plasmid
B4165	pYC backbone Fw	GTAAAACGACGGCCAGTG	checking insertion pYC vectors
C2950	vector background Fw	taatacgactcactataggg	Checking insertion ORF fragment in pYC56
C3161	*NTH2* control Fw	CAACGGCAACAACTTCC	Checking transformants n*th2Δ*
C3162	*NTH2* control Rv	TTAGCCTTGATTCTGGC	Checking transformants n*th2Δ*
C3177	*ATH1* control Fw	ACGGATGATTCAAAGGGG	Checking transformants *ath1Δ*
C3178	*ATH1* control Rv	CTTGAGTAAGTGTTCTCACC	Checking transformants *ath1Δ*
C3183	*NTH1* control Fw	CACGAGCTATAGTCCACAG	Checking transformants n*th1Δ*
C3184	*NTH1* control Rv	GGAAGATGGAGTGTCTACC	Checking transformants n*th1Δ*
C3835	*NTH1* control Rv	TGGCCATGACTACCGAAGTC	Checking transformants n*th1Δ*
C6240	*HPH*-Fw-NotI-XhoI	GATCGATGCGGCCGCCTCGAGcacAGATCTGTTTAGCTTGC	Construction pLS10 plasmid
C6241	*HPH*-Rv-NotI	GATCGATGCGGCCGCtCAAaggttaccccagttgg	Construction pLS10 plasmid

C6315	*ATH1*-Fw-del-FRT	CTAAATTTCTGATTATAACACAACACAACACACACACACAA ACTCTGTAAATAATAACAAGACAACACTGCAAGTAGCGAG GTCTGGAAAGAGAAGTACAgctctagaactagtggatcc	Construction deletion cassette *ATH1*
C6316	*ATH1*-Rv-del-FRT	AATATTGTAAGTAATTTCAGATTTTTTTATCCAGATTATAA AAAATAAACTAATTACTCTGCCAAGTAATTATGTGTAGATA TGAGCTAGATCCCCAGTTggaacaaaagctgggtacc	Construction deletion cassette *ATH1*
C6317	*NTH1*-Fw-del-FRT	ATCAACTCCCATAAATTACTAGTGAAAACCCTCTCGCTGAA GGAAAACTAAATCTAAATCTAAATCTAAATCCAAAACTCAC CAAAAAAATAGTGCAATAgctctagaactagtggatcc	Construction deletion cassette *NTH1*
C6318	*NTH1*-Rv-del-FRT	GATCTTTTCTCAATAGAATCATAAAATTATTCTAGACAGCA TTGTGAATATTTTAAATACACTACATATCATCTGGAATATA AAGATAAAGAGTCTCAATggaacaaaagctgggtacc	Construction deletion cassette *NTH1*
C6319	*NTH2*-Fw-del-FRT	CAGGCAAAACTTGAAAATAATAACCGAAACTAAATTAAAT AATTTAACTTACATCAAAATAACATAATAACAAAAGTACAC ATTACACATTACACTCGCGgctctagaactagtggatcc	Construction deletion cassette *NTH2*
C6320	*NTH2*-Rv-del-FRT	AAATCGAACAGTCCGTAGAGTCATCTTTAAATATGTAATT GACGTGCCAAAAATTTCAAATGCCTTACGAGATGATTAAT ATCTAAAAACGTCGAGCAATggaacaaaagctgggtacc	Construction deletion cassette *NTH2*
C8497	*ATH1* control Rv	GTCCTGTGTTCGATCCAC	Checking transformants *ath1Δ*
C9381	ORF ATH1	GGTGGAGATAAACCGATC	checking insertion mCherry tag genome
C9385	ORF NTH1	CCATTGATCTCAACTCAC	checking insertion mCherry tag genome
C9388	ORF NTH2	CTTCATGACCGAGGTGTG	checking insertion mCherry tag genome
D1728	CgATH1-mCherry_Rv	GCCCTTGCTCACCATTAGGATCCCTTCTTGAAGGACAATTT CCTTGATGG	Construction pBM13
D84	CgATH1-ORF_Fw_EciI	gccgctctagaactagtGGGCGGACGCATTGGCAACCATTCG	Construction pBM13
D86	CgATH1-t_Fw	TCctcgagggggggcccggtaccAACTGGGGATCTAGCTCA	Construction pBM13
D87	CgATH1-t_Rv_EciI	aaagggaacaaaagctgGGCGGAGTCTATGGACGCTCAACT	Construction pBM13

D88	CgNTH1-ORF_Fw_EciI	ggccgctctagaactagtGGCGGACTAACTATGAGTCAGCAACTAC	Construction pBM14
D89	CgNTH1-mCherry_Rv	GCCCTTGCTCACCATTAGGATCCcAAGACCATATATGCTCTTTTCATC	Construction pBM14
D90	CgNTH1-t_Fw	TCctcgaggggggcccggtaccATTCCAGATGATATGTAGTG	Construction pBM14
D91	CgNTH1-t_Rv_EciI	ctaaagggaacaaaagctgGGCGGAAGATTGGAAGTCATTTCTG	Construction pBM14
D92	CgNTH2-ORF_Fw_EciI	ggccgctctagaactagtGGCGGAAGCGTACGTCTTATGAGTCC	Construction pBM15
D93	CgNTH2-mCherry_Rv	GCCCTTGCTCACCATTAGGATCCcTAGGCCATAACGTGCTTTTTC	Construction pBM15
D94	CgNTH2-t_Fw	TCctcgaggggggcccggtaccATTGCTCGACGTTTTTAG	Construction pBM15
D95	CgNTH2-t_Rv_EciI	taaagggaacaaaagctgGGCGGATGTGTTATTGTTTCTCCC	Construction pBM15
B4166	Vector control	GGAAACAGCTATGACCATG	checking insertion pYC vectors